UNIVERSIDADE DE LISBOA

FACULDADE DE CIÊNCIAS

MICROMORPHOLOGY OF THE LABELLUM AND STRUCTURE OF THE OSMOPHORE IN A GROUP OF CLOSELY RELATED SPECIES OF THE SEXUALLY DECEPTIVE ORCHID GENUS *OPHRYS* (ORCHIDACEAE)

Doutoramento em Biologia

Especialidade de Biologia Celular

ANA MARGARIDA COSTA FRANCISCO

Tese orientada pela Professora Doutora Lia Ascensão

Documento especialmente elaborado para a obtenção do grau de doutor

2015

UNIVERSIDADE DE LISBOA

FACULDADE DE CIÊNCIAS

MICROMORPHOLOGY OF THE LABELLUM AND STRUCTURE OF THE OSMOPHORE IN A GROUP OF CLOSELY RELATED SPECIES OF THE SEXUALLY DECEPTIVE ORCHID GENUS *OPHRYS* (ORCHIDACEAE)

Doutoramento em Biologia

Especialidade de Biologia Celular

ANA MARGARIDA COSTA FRANCISCO

Tese orientada pela Professora Doutora Lia Ascensão

Documento especialmente elaborado para a obtenção do grau de doutor

2015

À memória de minha Mãe

Ao meu Pai

Aos meus Irmãos

Ao Pedro

Wonder is the beginning of all science and philosophy.
Aristotle, *Metaphysics*

O espanto é a origem de toda a ciência e filosofia.

Aristóteles, *Metafísica*

AGRADECIMENTOS

À minha orientadora, Professora Doutora Lia Ascensão, pelo acompanhamento e orientação do trabalho, pela excelência dos ensinamentos técnicos, pelo rigor científico que sempre pautou a sua investigação, e pelos momentos de partilha do entusiasmo da descoberta ao microscópio. Agradeço toda a confiança que em mim depositou e o carinho e compreensão durante as fases difíceis por que passei nestes anos. Agradeço ainda o empenho que colocou na aquisição de um novo microscópio óptico com câmara fotográfica digital para o laboratório, sem o qual não teria sido possível imprimir o padrão de qualidade necessário ao trabalho experimental.

Ao Doutor Miguel Porto, pelo acompanhamento e orientação da última etapa do meu trabalho, pela valiosa discussão de ideias, que moveu importantes obstáculos no caminho, e pela forma serena e segura com que me prestou a ajuda crucial nos momentos críticos da escrita da tese. Agradeço o exemplo de profissionalismo, clareza de raciocínio, pragmatismo e a infinita disponibilidade, para além dos ensinamentos técnicos e do auxílio imprescindível na preparação de imagens para publicação.

À Luísa Mota, companheira inseparável de laboratório, pela partilha de tantos e importantes momentos, no trabalho e na vida, pela cumplicidade, disponibilidade, ajuda e amizade preciosa. Aos investigadores do Brasil que passaram temporadas no nosso laboratório, nomeadamente à Professora Marília Moraes de Castro (Universidade Estadual de Campinas, São Paulo), pela boa disposição e partilha da sua vasta experiência laboratorial; à Doutora Ana Paula Lacchia (Universidade Estadual de Campinas, São Paulo), pela agradável companhia e troca de experiências no laboratório e durante o congresso de Viena; à Professora Renata Meira (Universidade Federal de Viçosa, Minas Gerais), pela partilha de bibliografia e do seu amplo conhecimento de anatomia vegetal, pela alegria que deu ao laboratório e pela amizade que perdura; e ao Doutor Carlos André Leitão (Universidade Estadual do Sudoeste da Bahia), pelos conselhos técnicos criativos e bom ambiente de trabalho. À Monya Costa, pela presença constante e amiga ao longo dos anos partilhados de trabalho de laboratório e pela ajuda sempre pronta que me prestou. À Sofia Lima, pelo exemplo de trabalho e de coragem, pela disponibilidade permanente e pela valiosa amizade que fomos consolidando ano após ano.

Ao Sr. Chaveiro e ao Dr. Telmo Nunes, pela secagem e metalização das amostras para microscopia electrónica de varrimento e pelo empenho na resolução de problemas técnicos dos microscópios. Ao Sr. Chaveiro agradeço ainda a disponibilidade e a boa disposição constantes, a paciência nas re-metalizações, os conselhos técnicos e a utilização do microscópio electrónico de transmissão da Estação Agronómica Nacional, em Oeiras. Ao Eng.º José Paulo Santos e Sousa, pela paciência, disponibilidade e amabilidade que demonstrou em todas as idas ao campo para colheita de orquídeas.

À Professora Teresa Nunes, do Departamento de Ambiente e Ordenamento do Território da Universidade de Aveiro, por me ter recebido no seu laboratório durante alguns meses, e pelo acompanhamento e orientação do trabalho de recolha e análise química dos compostos voláteis. Agradeço também toda a ajuda e disponibilidade do pessoal da Universidade de Aveiro com quem contactei, em particular Sr. Ivo Mateus e Miguel Rocha (do Departamento de Física), Nuno Costa, Eng.ª Lurdes, D.ª Manuela Marques, D.ª Idalina, Professor Mário Cerqueira, e colegas de laboratório, Rita Simões, Ana Sanchez, Nuno Ferreira, Pedro Cascão, Alexandre, Raquel e Ana Catarina Rocha. Ao Professor António Pedro Alves de Matos, por ter facilitado a observação de amostras no microscópio electrónico de transmissão da Secção de Anatomia Patológica do Hospital Curry Cabral, em Lisboa.

Aos professores, investigadores, funcionários e colegas do Departamento de Biologia Vegetal da FCUL que me foram acompanhando ao longo destes anos e que apoiaram de alguma forma o meu trabalho. A todo o pessoal da Secção de Biologia Celular e Biotecnologia Vegetal, em particular à Professora Ana Cristina Figueiredo (permanentemente atenta e prestável), ao Professor Luís Pedro, à Professora Helena Trindade, ao Professor Francisco Carrapiço, ao Professor Rui Malhó, ao Professor José Barroso, e à D.ª Lurdes Lé, pela ajuda que me facultaram sempre que precisei. À Professora Maria Salomé Pais, por me ter dado a oportunidade de estudar orquídeas, ao propor o tema do meu estágio de licenciatura, e à Doutora Helena Cotrim, por me ter ensinado a identificar orquídeas no campo, também durante o estágio. Ao pessoal da Secção de Ecologia, em particular à Professora Otília Correia, à Professora Cristina Cruz, à Patrícia Correia e à Herculana Velez pelo incentivo e pela amabilidade em terem disponibilizado a câmara fotográfica digital da secção para aquisição de imagens à lupa; à Professora Ana Isabel Correia, pelo processamento cuidadoso das folhas de herbário das espécies estudadas; à Professora Amélia Loução, pelo apoio e confiança de longa data; e aos colegas e amigos Pedro Pinho, Carla Gonzalez, Alice Nunes, Teresa Dias, Adelaide Clemente, Ana Corrêa e João Ferreira, pela camaradagem e espírito de entreajuda exemplares. À Professora Filomena Caeiro e à Professora Adalcina Casimiro, por terem apoiado e acompanhado de perto o desenvolvimento do trabalho laboratorial. À D.ª Manuela Lucas, pelo gosto em ajudar e pelo contínuo encorajamento. À Professora Anabela Bernardes da Silva, por toda a disponibilidade, compreensão e confiança, assim como pelo incentivo e ajuda cruciais na última etapa do caminho. À Professora Vanda Brotas, pelo empenho em tornar mais humana a relação entre a instituição e os alunos.

Aos professores e investigadores do Departamento de Biologia Animal da FCUL que contribuíram para o meu trabalho, nomeadamente ao Professor Leonel Gordo, pela amabilidade em ter possibilitado a utilização do microscópio óptico do Centro de Biologia Ambiental e a aquisição de imagens digitais numa fase importante do trabalho; ao Professor Artur Serrano, pelas fotografias de campo e captura da vespa polinizadora (e respectiva

fêmea) de uma das espécies estudadas; ao Doutor Nuno Oliveira, pela identificação das vespas capturadas; e ao Professor Octávio Paulo, pelos ensinamentos durante o curso avançado de filogenética, que permitiram estabelecer o elo entre o estudo micromorfológico das flores e a abordagem filogenética que sempre sonhei realizar. Aos colegas e amigos Luisa Chaves, Ana Luísa Rego, Filipe Ribeiro, Luís da Costa, Paula Chainho e Gilda Silva, pela boa companhia e horas de almoço divertidas. À Luisa Chaves agradeço ainda o exemplo de coragem e de força de vida, que me ajudou a continuar em momentos de desânimo.

Ao Dr. Cláudio Fernandes, pela forma atenta e eficaz com que me acompanhou na última fase deste processo, por me ter ajudado a acolher as minhas dificuldades, a remover importantes obstáculos do caminho e a conseguir avançar.

A todos os meus amigos que permitiram que eu chegasse ao fim desta etapa, agradeço o apoio incondicional, a força, o ânimo e, sobretudo, a confiança que em mim depositaram. À Ana Júlia Pereira e ao Miguel Porto, por toda a dedicação, generosidade e grandeza de coração, por terem cuidado de mim durante os últimos anos e por nunca me fazerem esquecer a beleza e simplicidade da vida. À Elizabete Carmo Silva, a minha amiga Beta, pelo apoio crucial em tantos momentos difíceis, pelas fotografias e ajuda na colheita das orquídeas no campo, e por estar sempre lá quando é preciso, independentemente da distância. Aos meus amigos na Austrália, Cristina Ramalho, David Aragão e Sofia Caria, pela hospitalidade e generosidade com que me acolheram durante a viagem inesquecível ao outro lado do mundo para participar no congresso internacional de botânica. À Cris agradeço ainda a amizade inabalável e o exemplo de determinação e coragem. À Antonieta Pedroso, pelos ensinamentos técnicos sobre preparação e tratamento de imagens digitais, pelo exemplo de disciplina e pelas palavras de encorajamento. À Cátia Pesquita, pelo apoio essencial durante a última etapa do percurso e pelo bonito elo que nos une. Ao Ramiro Magno, pelas discussões científicas estimulantes e pela calma e confiança que sempre me transmitiu. À Isabel Duarte, pelos conselhos preciosos de filogenética e pela partilha de ideias e experiências de vida. À Cristina Tauleigne Gomes, pelos esclarecimentos sobre taxonomia, pela generosidade e disponibilidade para ajudar. Ao Marco Jacinto, pelas conversas enriquecedoras e pela camaradagem de longa data. À Patrícia Pinto da Silva, pela alegria inspiradora, pela bondade e incentivo. Ao Zé Luís Vitorino, pelo entusiasmo com que fala de plantas e motiva os amigos. À Joana Camejo, pelas mensagens positivas e tranquilizadoras que me foi transmitindo durante o caminho. Ao Nuno Cintrão, por continuar a interessar-se e a estar presente. À Luísa Mendonça, à Teresa Mendonça e ao João Miguel Tavares, pela certeza reconfortante de que continuarão a acompanhar-me ao longo da vida. Aos meus professores e amigos do teatro, em especial ao Professor Carlos do Rosário, à Maria Ceia, à Ana Ceia, à Catarina Alfaia, ao Filipe Valentim e à Inês Sequeira, por não me deixarem esquecer das minhas raízes e das flores que fizemos brotar outrora, que continuam a ser fonte inesgotável de força, alento e coragem. À minha Professora Joaquina

Delgado, por todos os ensinamentos e conselhos, por me ter amparado quando mais precisei, e pela ligação profunda que mantemos e que me ajuda a estar em Yoga comigo e com a vida. Às minhas amigas do Yoga, Antonieta, Sofia, Margarida, Mareen, Soraia, Lara, Graça, Laura, Isabel, Rita, Catarina, Filipa e Ana Bonito, pela experiência marcante de crescimento interior que partilhámos. À Ana Marcos, pela ajuda importante numa altura crítica do caminho.

À minha família de Aveiro e Coimbra, Noémia, Rui, Ana, Joana, Vasco e Sara, por me acolherem sempre de braços abertos, por toda a ajuda em tantos momentos, pelo carinho, pela alegria e pela confiança. À minha sobrinha Joana agradeço ainda a motivação que, a cada sorriso, a cada brincadeira, me conseguiu dar, o respeito pelas minhas ausências, e a forma carinhosa como me chama(va) "Ana pequenina".

Aos meus tios e primos, pelo afecto e palavras de estímulo. Um agradecimento especial à minha Tia Guida, pela presença constante e atenta, pelo cuidado e pela ajuda pronta sempre que precisei.

Aos meus pais, irmãos e avós, pelo amor e apoio incondicionais. Ao meu Pai, com quem aprendi a perseverar, por ter sabido respeitar o meu ritmo e ter tornado possível a concretização da minha tese. À minha Mãe, a quem devo a coragem, a força e a eterna dedicação. À minha irmã, ramo firme e vigoroso com quem posso sempre contar ao longo da vida. Ao meu irmão, pela confiança e pelo alento que continuamente me dá e por nunca ter duvidado das minhas capacidades. À minha Avó Júlia, com quem partilhei o gosto pelas plantas. À minha Avó Bia, pelo carinho e pelo cuidado infinito.

Ao Pedro, por percorrer a meu lado pacientemente o meu caminho, por ser âncora, vela e horizonte, e por me ajudar a voar, consigo.

O trabalho de investigação conducente à presente tese foi co-financiado por fundos nacionais do Ministério da Ciência, Tecnologia e Ensino Superior e pelo Fundo Social Europeu, no âmbito do Programa Operacional Ciência e Inovação 2010 (POCI 2010) do III Quadro Comunitário de Apoio (2000-2006), através da Bolsa de Investigação com a referência SFRH/BD/18823/2004, concedida pela Fundação para a Ciência e a Tecnologia.

The experimental work leading to the present PhD Thesis was co-financed by Portuguese funds from Ministério da Ciência, Tecnologia e Ensino Superior and by European Social Fund, under the POCI 2010 programme from the III European Community Support Framework, through the research grant SFRH/BD/18823/2004 granted by the Fundação para a Ciência e a Tecnologia.

RESUMO

O estudo da micromorfologia das flores é crucial para compreender o complexo processo de polinização e a relação íntima que é estabelecida entre as flores e os seus polinizadores. A interacção planta-polinizador constitui um factor-chave para a diversificação e evolução das angiospérmicas e é especialmente estreita nas plantas polinizadas por engano sexual. Este tipo de polinização altamente específico ocorre quase exclusivamente nas Orchidaceae, que constituem a maior família de plantas com flor, com mais de 27000 espécies.

As orquídeas do género *Ophrys*, cuja área de distribuição geográfica se centra principalmente na Bacia do Mediterrâneo, são polinizadas por engano sexual, atraindo apenas os machos de uma única espécie de insecto, ou poucas espécies afins, principalmente abelhas solitárias. Esta relação altamente específica deve-se ao elevado grau de mimetismo químico, visual e táctil que o labelo (a pétala média modificada característica da flor das orquídeas) apresenta relativamente às fêmeas dos insectos polinizadores, mimetizando de modo quase perfeito a forma, as dimensões, os padrões de côr e brilho e a textura do corpo e, sobretudo, o odor específico da feromona sexual. Os insectos-macho são atraídos a longa distância pelo odor floral das *Ophrys*, durante os seus habituais voos de patrulha de fêmeas, sendo levados a pousar no labelo e a efectuar tentativas de cópula com ele (pseudocópula). Durante estes movimentos, as polinídias (i.e. agregados de grãos de pólen munidos de um disco pegajoso) aderem à cabeça ou à extremidade do abdómen do insecto que, ao ser enganado novamente por uma segunda flor de *Ophrys* da mesma espécie, as deposita na superfície estigmática dessa flor, efectuando assim a polinização.

Uma vez que o odor é o estímulo-chave do processo de atracção dos polinizadores, a maior parte da investigação desenvolvida no género *Ophrys* tem sido focada no subconjunto limitado de compostos do *bouquet* floral que mimetizam a feromona sexual das fêmeas, que são o sinal químico específico para atrair os insectos-macho. Estes compostos são, na maioria das espécies de *Ophrys* estudadas até agora, hidrocarbonetos de cadeia longa (alcanos e alcenos) que se encontram nas ceras cuticulares que revestem a superfície do labelo. Este *bouquet* floral é constituído por mais de 100 componentes de natureza química diversa, contendo compostos de maior volatilidade, tais como compostos alifáticos de cadeia curta e derivados terpénicos, que actuam como atractivos de longo alcance para os insectos polinizadores. No entanto, o local de produção do odor das flores de *Ophrys* não é conhecido e as células envolvidas na biossíntese e emissão dos compostos voláteis não foram ainda estudadas. Dada a elevada especialização funcional do labelo, é expectável que o odor seja produzido por uma estrutura especializada (osmóforo) ao invés de ser emitido difusamente pela flor. De igual modo, pouca atenção tem sido dada à micromorfologia do labelo e ao seu papel crucial na polinização das *Ophrys*, ao proporcionar aos insectos polinizadores, por um lado, estímulos visuais que facilitam a aproximação à flor

a curta distância, e por outro, estímulos tácteis associados à existência de diferentes tricomas (pêlos), cruciais para o posicionamento correcto dos machos sobre o labelo de modo a que a polinização ocorra.

Na presente tese, investigou-se a micromorfologia do labelo e a existência de um osmóforo em flores de seis dos 11 *taxa* de *Ophrys* que ocorrem naturalmente em Portugal, nomeadamente *O. bombyliflora*, *O. fusca* subsp. *fusca*, *O. lutea*, *O. speculum* subsp. *lusitanica*, *O. speculum* subsp. *speculum* e *O. tenthredinifera*. Os seis *taxa* estudados, filogeneticamente próximos, pertencem a um dos grandes grupos monofiléticos (clados) em que o género *Ophrys* se divide, embora as relações filogenéticas entre os diferentes *taxa* estejam ainda mal resolvidas. A investigação foi efectuada em flores em três fases de desenvolvimento, utilizando microscopia electrónica de varrimento para descrever a micromorfologia do labelo e microscopia óptica para estudar a anatomia do labelo e a estrutura do osmóforo, bem como caracterizar histoquimicamente as suas células glandulares e o secretado.

A tese compreende seis capítulos. No Capítulo 1, Introdução geral, realça-se o contexto científico em que se insere a temática da tese e indicam-se os seus objectivos específicos. Nos Capítulos 2, 3 e 4, apresenta-se o estudo micromorfológico e anatómico comparativo do labelo dos seis *taxa* de *Ophrys* estudados, caracterizando a localização, estrutura e secreção do osmóforo, bem como a diversidade e o padrão de distribuição das células epidérmicas da superfície adaxial do labelo. Os resultados apresentam-se organizados da seguinte forma: (a) no Capítulo 2, são estudadas *O. fusca* e *O. lutea*, duas espécies representativas da secção *Pseudophrys* polinizadas por machos de abelhas solitárias do género *Andrena*; (b) no Capítulo 3, estudam-se *O. bombyliflora* e *O. tenthredinifera*, duas espécies polinizadas por machos de abelhas solitárias do género *Eucera*; e (c) no Capítulo 4, estuda-se *O. speculum*, uma espécie polinizada por machos de vespas solitárias de *Dasyscolia ciliata*. Neste capítulo, investigam-se as duas subespécies de *O. speculum* que ocorrem em Portugal e realiza-se uma comparação micromorfológica entre o labelo de *O. speculum* e o corpo da fêmea da espécie de vespa polinizadora. No Capítulo 5, todos os resultados obtidos nos Capítulos 2–4 são usados para realizar uma análise filogenética morfológica do clado em estudo, usando dois métodos de inferência filogenética (máxima parcimónia e inferência Bayesiana). Esta análise é feita com base numa matriz de dados que resultou da quantificação de características florais macromorfológicas, micromorfológicas e anatómicas identificadas nesses capítulos. Tal implicou o estudo micromorfológico do labelo e a caracterização da estrutura do osmóforo de uma sétima espécie de *Ophrys*, *O. scolopax*, que foi utilizada como *outgroup* na análise filogenética. Por fim, o Capítulo 6 integra todos os resultados dos capítulos anteriores numa discussão geral desenvolvida à luz do conhecimento actual sobre a ecologia da polinização e a filogenia do género *Ophrys*, terminando com as principais conclusões do trabalho e destacando alguns tópicos que merecem investigação futura.

A presente tese constitui um contributo substancial para a área da Biologia Floral, em particular para o aprofundamento do conhecimento sobre o processo de polinização por engano sexual das *Ophrys*, tendo-se centrado em três grandes temas: (1) estrutura e função do osmóforo; (2) micromorfologia do labelo; e (3) inferência filogenética das relações interespecíficas e das tendências evolutivas das características florais no clado em estudo.

Realçam-se, em seguida, as principais conclusões do trabalho:

1. As flores de todas as espécies de *Ophrys* estudadas apresentam uma estrutura secretora especializada na síntese e na emissão de odor (osmóforo), que sintetiza uma secreção volátil, de natureza lipofílica, rica em compostos terpénicos. O osmóforo ocorre na região apical do labelo, mais especificamente, na margem do labelo e/ou no apêndice apical (quando existe), estendendo-se para a superfície abaxial da região apical do labelo em *O. tenthredinifera*, *O. fusca* e *O. lutea*, e ocupando também a margem inteira do labelo e das pétalas laterais nestas duas últimas espécies.
2. A ocorrência de um osmóforo funcional em todas as espécies estudadas indica que esta estrutura secretora deve desempenhar um papel importante na polinização das *Ophrys*. Propomos, assim, que o osmóforo seja o local de produção de compostos voláteis atractivos dos polinizadores a longa distância, exercendo uma acção complementar à das ceras cuticulares que revestem a superfície adaxial do labelo, contribuindo desta forma para o sucesso da polinização por engano sexual.
3. A superfície adaxial do labelo de cada espécie de *Ophrys* estudada apresenta uma grande diversidade de tipos de células epidérmicas, que variam entre quatro grandes grupos em termos de forma geral, i.e. células planas/lenticulares, papilas em forma de cúpula, tricomas curtos e tricomas longos, cuja superfície pode ser lisa ou apresentar diferentes padrões de estrias cuticulares. O arranjo específico dos diferentes tipos de células proporciona possivelmente um estímulo táctil aos insectos polinizadores, que os leva a realizar tentativas de cópula com o labelo, assegurando deste modo a eficácia da polinização.
4. Uma análise micromorfológica comparativa detalhada permitiu distinguir, de forma objectiva, diferentes regiões no labelo e na cavidade estigmática, que lhe é contígua, das flores de *Ophrys* e assim estabelecer homologias potenciais entre as partes florais de todos os *taxa* estudados.
5. A análise filogenética morfológica do clado de *Ophrys* em estudo, que foi baseada numa matriz de dados construída utilizando critérios objectivos para a selecção das características florais e para a codificação e definição dos seus atributos, mostrou que *O. tenthredinifera* e *O. bombyliflora* não são grupos irmãos e apontou para uma proximidade filogenética entre *O. speculum* e *O. bombyliflora*. Esta hipótese rejeita a única hipótese filogenética morfológica existente para o género *Ophrys* e favorece as

árvores filogenéticas moleculares produzidas com base em dados da região ITS nuclear (analisados separadamente ou combinados com dados de regiões dos genomas plastidial e/ou mitocondrial), mas não aquelas baseadas exclusivamente em dados de regiões plastidiais. Para além disso, a presente análise permitiu traçar as tendências evolutivas de algumas características florais nas orquídeas do género *Ophrys*.

PALAVRAS-CHAVE: células secretoras do osmóforo; micromorfologia do labelo das orquídeas; mimetismo floral; polinização por engano sexual; análise filogenética morfológica.

ABSTRACT

The study of the micromorphology of flowers is crucial to understand the complex process of pollination and the intimate interaction between flowers and pollinators. This plant-pollinator interaction is a key factor to the diversification and evolution of angiosperms and is particularly tight in species pollinated by sexual deception, almost all of which belonging to the orchid family. The highly specific pollination system of the sexually deceptive species is based on a precise mimicry of the visual, tactile and chemical signals exhibited by the females of the pollinator species (usually a single or a few related insect species), thereby attracting males, which, in most cases, perform copulatory attempts with the flower leading to pollination.

In the Euro-Mediterranean sexually deceptive orchid genus *Ophrys*, most research has been focused on the chemical mimicry between certain components of the odour bouquet emitted by the flowers and the female sex pheromone of their specific insect pollinators. In most cases, these compounds were shown to be mainly long-chained hydrocarbons, which are found in the cuticular waxes spread over the surface of the strongly modified median petal typical of orchid flowers – the labellum. However, numerous compounds of higher volatility were shown to act as long-range attractants for male pollinators, although their site of synthesis and emission (presumably an osmophore) remains unknown. Likewise, little is known about the micromorphological features of the labellum and their importance in providing visual and tactile signals for pollinator attraction.

In the present thesis, we investigated the location, structure and secretion of the osmophore and the labellum micromorphology and anatomy of flowers, at three developmental stages, of six closely related *Ophrys* taxa from natural populations occurring in Portugal, using scanning electron microscopy, light microscopy and histochemistry.

We demonstrated the occurrence of an osmophore, which synthesizes a terpene-rich lipophilic secretion, in the apical region of the labellum in the investigated *Ophrys* taxa, located mainly at the labellum margin and/or in an apical appendix exhibited by some species. A great diversity of epidermal cell types was found in the adaxial surface of the labellum, which form well-defined areas with distinct visual and tactile properties. The detailed comparative analysis of these different areas allowed us to establish potential homologies between the labellum areas of the studied taxa.

The *Ophrys* osmophore probably plays an important role in pollination, by synthesizing highly volatile long-range pollinator attractants, which are possibly complementary to the cuticular waxes spread over the labellum surface for the success of pollination by sexual deception.

Findings of the micromorphological and anatomical study were used to build a morpho-anatomical data matrix, using objective criteria, as a basis for a morphological phylogenetic analysis of the unresolved clade of *Ophrys* formed by the six studied taxa, using maximum

parsimony and Bayesian inference. Our phylogenetic hypothesis rejects an earlier morphological hypothesis and favours the existing molecular phylogenetic trees based on nuclear ITS data rather than plastid data. Furthermore, the present analysis brought some insights into the floral trait evolutionary trends in *Ophrys* orchids.

KEYWORDS: flower mimicry; morphological phylogenetic analysis; orchid labellum micromorphology; osmophore secretory cells; pollination by sexual deception.

DECLARAÇÃO

De acordo com o artigo 25º do Regulamento de Estudos de Pós-Graduação da Universidade de Lisboa, aprovado pelo Despacho n.º 2950/2015, a presente tese engloba quatro artigos científicos já publicados, ou submetidos para publicação, em revistas internacionais indexadas, em colaboração com outros autores. A autora da tese declara que foi responsável pelo desenho e execução do trabalho experimental, pela obtenção e análise dos resultados, assim como pela redacção, submissão e revisão de todos os manuscritos enviados para publicação.

In accordance with the 25th article of the *Regulamento de Estudos de Pós-Graduação da Universidade de Lisboa,* approved by the *Despacho n.º 2950/2015*, the present dissertation includes four original scientific papers, which have been either published or submitted for publication in peer-reviewed journals in collaboration with other authors. The author of the present thesis declares that she was responsible for designing and performing the experimental work, for acquiring and analysing the results, as well as for writing, submitting and revising all the manuscripts sent for publication.

Ana Margarida Costa Francisco

Outubro 2015

LIST OF PAPERS

Ascensão L., Francisco A., Cotrim H. and Pais M.S. 2005. Comparative structure of the labellum in *Ophrys fusca* and *O. lutea* (Orchidaceae). *American Journal of Botany*, 92: 1059-1067. [Chapter 2] (*)

Francisco A. and Ascensão L. 2013. Structure of the osmophore and labellum micromorphology in the sexually deceptive orchids *Ophrys bombyliflora* and *Ophrys tenthredinifera* (Orchidaceae). *International Journal of Plant Sciences*, 174: 619-636. [Chapter 3]

Francisco A. and Ascensão L. Osmophore and new micromorphological floral features in the sexually deceptive wasp pollinated orchid *Ophrys speculum* (Orchidaceae). (submitted). [Chapter 4]

Francisco A., Porto M. and Ascensão L. 2015. Morphological phylogenetic analysis of *Ophrys* (Orchidaceae): insights from morpho-anatomical floral traits into the interspecific relationships in an unresolved clade. *Botanical Journal of the Linnean Society*, 179: 454-476. [Chapter 5]

(*) This paper comprises part of the results obtained by the author of the present thesis during the scientific traineeship of her Licentiate Degree, which was supervised by Prof. Dr. Lia Ascensão and Prof. Dr. M. Salomé Pais at Universidade de Lisboa, together with data acquired in the early stage of her PhD project.

TABLE OF CONTENTS

LIST OF FIGURES

LIST OF TABLES

CHAPTER 1

GENERAL INTRODUCTION

GENERAL INTRODUCTION

An understanding of the evolutionary floral changes that underlie the great diversification of angiosperms is one of the biggest and most fascinating challenges of Biology. The orchid family, Orchidaceae, epitomizes such biodiversity, being the largest family of flowering plants, with more than 27000 species (The Plant List, 2013) distributed throughout all continents apart from Antarctica, although the greatest number of species is found in the wet tropical bioclimatic regions, where they are epiphytic (Arditti, 1992). Orchid flowers exhibit an astonishing diversity of forms, colours, sizes and textures, which is partly due to their unique combination of innovative traits resulting in an exceptionally elaborate flower morphology, already recognized by Sprengel (1793) and superbly described by Darwin in his treatise on the fertilization of orchids by insects (Darwin, 1862). The special floral morphological features that together characterize the orchid flowers comprise: (1) the presence of a gynostemium, a compound floral structure resulting from the congenital fusion between stamens and style (Rudall & Bateman, 2002), which is associated with (2) the presence of pollinaria, which comprise pollinia (i.e. aggregation of all pollen grains of a pollen sac) and a translator formed by a caudicle ending with a sticky viscidium that attaches the entire structure to the body of the pollinator (Endress, 2011); (3) the strongest expression of zygomorphy (i.e. bilateral symmetry) among monocots, which resulted from (4) the differentiation of a morphologically distinct labellum from the median petal (Rudall & Bateman, 2002), and (5) the suppression of all three adaxial stamens, which may be accompanied by the reduction of one or two abaxial stamens (the large majority of orchids has a single fertile anther; Rudall & Bateman, 2002); (6) a perianth differentiated into three sepals, two lateral petals and the labellum, which were allowed to evolve as three semi-autonomous 'modules' due to a developmental genetic predisposition unique to orchids (Mondragón-Palomino & Theißen, 2008; Mondragón-Palomino & Theißen, 2009); (7) the occurrence of resupination (i.e. 180° torsion of the pedicel and/or ovary), which reverses the original uppermost position of the labellum, placing it in a position suitable to act as a landing platform for insects (Arditti, 2003); (8) a sterile median stigma lobe modified into the rostellum, a structure located between the fertile anther and the stigmatic surface (Kurzweil, 1987a; Kurzweil, 1987b); and (9) an accentuated inferior ovary (Endress, 2011) which contains, at maturity, thousands of minute seeds that require an obligate mycorrhizal association with fungi to germinate (this mycorrhizal association should persist to assure subsequent seedling establishment; Jacquemyn *et al.*, 2011). The elaborate structure of orchid flowers, which is extremely well adapted to pollination by insects, allowed the evolution of highly specialized pollination systems, such as those based on deception (Darwin, 1862; van der Pijl & Dodson, 1966; Nilsson, 1992; Schiestl & Schlüter, 2009).

POLLINATION BY SEXUAL DECEPTION

Pollination through deception is particularly prevalent in family Orchidaceae (Cozzolino & Widmer, 2005), being estimated that approximately one third of orchid species are deceptive, i.e. do not offer any reward to pollinators, specifically neither nectar, pollen, oils, liquid fragrances for mating courtship, nest-building materials, viable brood-sites nor shelter (van der Pijl & Dodson, 1966; Renner, 2005). Most deceptive orchids are pollinated through food deception, attracting food-foraging insects by imitating general floral signals typical of rewarding flowers (Dafni, 1984; Nilsson, 1992; Jersáková, Johnson & Kindlmann, 2006; Peter & Johnson, 2013). However, numerous orchid species of at least 22 genera (Gaskett, 2011; Vereecken *et al.*, 2012; Phillips *et al.*, 2014) have evolved an even more sophisticated and highly specialized pollination system by sexual deception, in which rewardless flowers render attractive to only males of a single or few related insect species typically by acquiring an insectiform appearance, mimicking the visual pattern, body texture and the species-specific sex pheromone of their conspecific females (Correvon & Pouyanne, 1916; Pouyanne, 1917; Coleman, 1928; Dafni, 1984; Schiestl, 2005; Vereecken, 2009; Gaskett, 2011).

Pollination by sexual deception has evolved almost exclusively within Orchidaceae, although two confirmed cases of sexual mimicry have been documented in other two plant families (Ellis & Johnson, 2010; Vereecken *et al.*, 2012). This highly specialized pollination system is particularly prevalent in Australia, where 11 genera of terrestrial orchids were found to present sexually deceptive species (e.g. *Caladenia*, *Chiloglottis*, *Cryptostylis*, *Drakaea*, *Leporella*, *Pterostylis*; Coleman, 1928; Peakall, 1989; Peakall & Beattie, 1996; Schiestl *et al.*, 2003; Schiestl, Peakall & Mant, 2004; Peakall *et al.*, 2010; Gaskett, 2011; Bohman *et al.*, 2014; Phillips *et al.*, 2014), and in Europe, where it is represented by the diverse terrestrial orchid genus *Ophrys* (Correvon & Pouyanne, 1916; Pouyanne, 1917; Kullenberg, 1961), besides a single species of the generally food-deceptive genus *Orchis* (Bino, Dafni & Meeuse, 1982). A few orchid species occurring in Central and South America (genera *Geoblasta*, *Lepanthes*, *Mormolyca*, *Trigonidium*; Singer, 2002; Singer *et al.*, 2004; Blanco & Barboza, 2005; Ciotek *et al.*, 2006; Flach *et al.*, 2006) and in South Africa (genus *Disa*; Steiner, Whitehead & Johnson, 1994) also present this type of pollination.

Sexually deceptive orchids are exclusively pollinated by male insects, which are mostly solitary rather than social (exception for the Neotropical *Mormolyca ringens*; Singer *et al.*, 2004). The most common pollinators of these orchids are solitary parasitic wasps although bees, flies, fungus gnats, beetles and ants were also found as specific pollinators (Gaskett, 2011). These orchids elicit different sexual behaviours from their pollinators. In the great majority of cases, male pollinators perform copulatory attempts with the flower (i.e. pseudocopulation), as always occur in the European genus *Ophrys* (Kullenberg, 1961), in all Central-South American genera and in a few Australian genera, such as *Cryptostylis*

(Gaskett, 2011). Pollination in this latter orchid genus involves even pollinator ejaculation (Coleman, 1928; Gaskett, Winnick & Herberstein, 2008). In contrast, for the majority of Australian sexually deceptive species, successful pollination requires only pre-copulatory behaviour from the pollinator (Gaskett, 2011). During this process, pollinaria become attached to a part of the body of the sexually deceived pollinator, which needs to be duped for a second time by another deceptive flower of the same species to accomplish pollination (Scopece *et al.*, 2010).

The highly specialized interaction that has evolved between the sexually deceptive orchids and their insect pollinators is clearly asymmetrical, since the adaptation occurs completely from the side of plant (unidirectional adaptation), and hence should not be misunderstood as a co-evolutionary scenario (Dafni, 1984; Vereecken *et al.*, 2011). Given that these orchids are totally dependent upon visits by their specific pollinators for their reproduction and that insects do not receive any reward, sexual deceptive pollination could be regarded as unilateral exploitation of pollinators (Dafni, 1984) or even as parasitism (Vereecken, 2009).

THE KEY ROLE OF THE LABELLUM IN *OPHRYS* POLLINATION

Pollination of the Euro-Mediterranean, sexually deceptive orchid genus *Ophrys* consists in a highly specific interaction between one *Ophrys* species and males of a single or a few related species of insects (Kullenberg, 1961; Paulus & Gack, 1990; Schiestl & Schlüter, 2009), which are mostly solitary bees, although solitary wasps and even beetles were also reported as pollinators of some *Ophrys* species (Paulus & Gack, 1990; Paulus, 2006; Gaskett, 2011). *Ophrys* male pollinators are deceived by a flower-mimic of a conspecific female (Fig. 1), which simulates the shape, size, colour patterning and texture of its body and the very specific odour of its sex pheromone (Kullenberg, 1961; Ågren, Kullenberg & Sensenbaugh, 1984; Schiestl *et al.*, 1999; Paulus, 2006). Stimulated by three kinds of stimuli (chemical, visual, and tactile) provided by the labellum of *Ophrys* flowers, mate-searching male pollinators are led to perform copulatory attempts with the labellum (pseudocopulation), meanwhile removing pollinaria (either with the abdomen or the head; Godfery, 1928; Devillers & Devillers-Terschuren, 1994) and delivering them on the stigmatic surface of another flower during a subsequent deceptive pollination event (Pouyanne, 1917; Kullenberg, 1961).

The labellum constitutes thus the key floral element in the sexual mimicry of *Ophrys* flowers, exhibiting a great diversity of shapes, sizes, colours and textures, which form a characteristic overall pattern easily identifiable in each species or group of species (Kullenberg, 1961; Bradshaw *et al.*, 2010). The morphological diversity displayed by the labellum is due to the occurrence of different cells that differ in height, shape, pigmentation and cuticular ornamentation (Bradshaw *et al.*, 2010), which originate contrasting patches in

the labellum, that provide important visual signals to male pollinators (Kullenberg, 1961; Kullenberg & Bergström, 1976; Paulus, 2006). For instance, the distinctive, highly reflective, central area of *Ophrys* flowers, the speculum, has long been assumed to mimic the crossed wings of an insect (Correvon & Pouyanne, 1916; Kullenberg, 1961; Ågren *et al.*, 1984; Paulus, 2006). Little attention has been given to the role of the visual and tactile stimuli provided by the labellum in *Ophrys* pollination (Kullenberg, 1961; Ågren *et al.*, 1984; Paulus, 2006; Streinzer *et al.*, 2010), in particular to the micromorphology of the labellum of these orchids (Borg-Karlson *et al.*, 1993; Servettaz, Bino Maleci & Grünanger, 1994; Bradshaw *et al.*, 2010).

Figure 1. Protagonists of the mimicry system underlying the pollination by sexual deception of *Ophrys* orchids. A, Female of *Dasyscolia ciliata* wasp (the model) in the field (Serra de Sicó, Portugal). B, Flower of *Ophrys speculum* subsp. *speculum* (the mimic) in its natural habitat (Cabo Espichel, Sesimbra, Portugal). C, Male (on the left) and female (on the right) of *Dasyscolia ciliata* wasp in the field (Serra de Sicó, Portugal). D, Male of *Dasyscolia ciliata* wasp (the duped operator) alighted upon the labellum of a flower of *Ophrys speculum* subsp. *speculum* (Serra de Sicó, Portugal). Note that the male wasp is positioned with its head towards pollinaria (arrow), which will become attached to insect's head during the copulation attempts that the insect pollinator performs with the labellum (cephalic pseudocopulation). Photographs by Artur Serrano (A, C, D) and Elizabete Carmo-Silva (B).

The specific arrangement of the different trichomes (i.e. hairs) in the labellum originates a particular texture that is believed to mimic the tactile sensations of the body of female insects, which is crucial for the correct positioning of male pollinators on the labellum so that the necessary copulatory attempts leading to pollination could be performed (Kullenberg, 1961; Kullenberg & Bergström, 1976; Ågren *et al.*, 1984). The key

tactile stimulus is only effective when accompanied by the primary chemical stimulus provided by the scent (Kullenberg, 1961; Kullenberg & Bergström, 1976), which constitutes the main reproductive isolation barrier among sympatric *Ophrys* species (Stökl *et al.*, 2005; Scopece *et al.*, 2007; Cozzolino & Scopece, 2008; Schiestl & Schlüter, 2009; Xu *et al.*, 2011; Xu *et al.*, 2012a; Xu, Schlüter & Schiestl, 2012b), like in some Australian sexually deceptive orchids (Peakall *et al.*, 2010; Ayasse & Dötterl, 2014; Bohman *et al.*, 2014; Peakall & Whitehead, 2014). However, the tactile stimulation provided by the specific arrangement of trichomes in the labellum constitutes the only isolation barrier between co-occurring *Ophrys* species that attract the same pollinator by guaranteeing the placement of the pollinaria in different parts of the insect body (Kullenberg, 1961; Paulus & Gack, 1990; Schiestl & Schlüter, 2009; Ayasse, Stökl & Francke, 2011), even though it could occasionally fail to prevent hybridization (Cortis *et al.*, 2009; Vereecken, Cozzolino & Schiestl, 2010a). Characterizing the micromorphological pattern of the labellum of *Ophrys* species is thus crucial to identify those features responsible for converting attraction into effective pollination and to more comprehensively understand the process of pollinator-driven speciation of this sexually deceptive orchid genus (Xu *et al.*, 2012b).

Furthermore, the labellum of *Ophrys* flowers emits a multicomponent odour bouquet which contains more than 100 organic compounds of different volatility (Kullenberg, Borg-Karlson & Kullenberg, 1984; Borg-Karlson, 1990; Ayasse *et al.*, 2000; Ayasse *et al.*, 2003), although only a subset of them, called semiochemicals (Mori, 2010), spreads information (i.e. chemical signals) that is similar to that used in the mating communication system of their specific insect pollinators (Ayasse, Paxton & Tengö, 2001; Vereecken & McNeil, 2010; Ayasse *et al.*, 2011). The key attractant semiochemicals emitted by flowers of the majority of *Ophrys* species hitherto investigated were identified as a fraction of common long-chained hydrocarbons (alkanes and alkenes) that usually compose the cuticular waxes occurring over the epidermal cells of the labellum (Schiestl *et al.*, 1999; Schiestl *et al.*, 2000; Schiestl & Ayasse, 2002; Mant *et al.*, 2005; Stökl *et al.*, 2005; Stökl *et al.*, 2008; Stökl *et al.*, 2009; Schlüter *et al.*, 2011; Xu *et al.*, 2011; Xu *et al.*, 2012a). However, besides this small set of behaviourally active long-chain hydrocarbons, which are able to trigger in male insects the mating behaviour that leads them to perform copulatory attempts with the *Ophrys* labellum, the odour bouquet also contains other compounds with higher volatility, which act effectively as long-range attractants for pollinators by triggering their approach flight to the labellum (Kullenberg, 1973; Kullenberg *et al.*, 1984; Borg-Karlson, 1990). This set of highly volatile compounds includes short-chained aliphatic alcohols, esters, aldehydes, and mono- and sesquiterpenes (Kullenberg *et al.*, 1984; Borg-Karlson, 1990), although the site where they are synthesized is still unknown. Given the strong specialization of the labellum of *Ophrys* flowers, it seems plausible that these volatile odour compounds are synthesized in a specialized structure located in the labellum, instead of being diffusely emitted by the flower.

OSMOPHORES AS FRAGRANCE-PRODUCING SECRETORY STRUCTURES

The findings of the research on chemical signals used in *Ophrys* pollination conducted by Kullenberg and colleagues until early 1990s (Kullenberg, 1961; Kullenberg, 1973; Tengö & Bergström, 1975; Kullenberg & Bergström, 1976; Bergström & Tengö, 1978; Tengö, 1979; Kullenberg *et al.*, 1984; Borg-Karlson & Tengö, 1986; Borg-Karlson, 1990; Borg-Karlson *et al.*, 1993) have been apparently neglected since the discovery of the chemical mimicry of the female sex pheromone of *Andrena* bees by *Ophrys* flowers (Schiestl *et al.*, 1999; Schiestl *et al.*, 2000). The attention of researchers was rapidly transferred to the behaviourally-active long-chained hydrocarbons and other fatty-acid derivatives occurring in the cuticular waxes spread over the labellum surface (Schlüter *et al.*, 2011), and since then four new cases of chemical mimicry have been described, two of which involving compounds other than hydrocarbons as the key semiochemicals in pollination (Ayasse *et al.*, 2003; Mant *et al.*, 2005; Stökl *et al.*, 2008; Vereecken & Schiestl, 2008; Gögler *et al.*, 2011). As a result, the site of synthesis of the highly volatile compounds, which were demonstrated to be effective long-range attractants of specific insect pollinators (Kullenberg *et al.*, 1984; Borg-Karlson, 1990), is still unknown.

At the same time that the entomologist Bertil Kullenberg published his comprehensive study on the pollination and chemical ecology of *Ophrys* orchids (Kullenberg, 1961), the floral biologist Stefan Vogel discovered a new type of glandular tissue in plants, the osmophore, which he described as a secretory floral structure specialized in the synthesis and emission of fragrance (Vogel, 1960; Vogel, 1961). Etymologically, the term *osmophore* originated from the Greek words '*osmo*' (odour) and '*-phoros*' (bearing), derived from '*pherein*' (to bear), and thus means "a bearer or producer of scent". This term seems to have been used for the first time by Arcangeli (1883) to refer to the scent-producing spadix of some Araceae. Through his meticulous floral anatomical studies, Vogel pioneered the investigation on osmophores in early 1960s, first in flowers of *Ceropegia* sp. (Apocynaceae: Asclepiadoideae; Vogel, 1961) and later in flowers of several species of other plant families, mainly Araceae and Orchidaceae (Vogel, 1990).

Osmophores are exposed floral secretory areas provided with a secretory epidermis composed of cells with a dense cytoplasm, a large nucleus and thin cell walls, accompanied by a few layers of the subepidermal parenchyma tissue that generally presents reserve materials (starch or lipids), which synthesise volatile compounds for long-range attraction of pollinators (Vogel, 1990). Volatile organic compounds, which present a wide structural diversity based on a hydrocarbon skeleton with atoms of nitrogen, oxygen and sulphur, are typically characterized by their selectivity, which results in a very low detection threshold, and by their relatively high vapour pressure that allows their efficient evaporation and enables their transport through the air to reach their specific biological target (Herrmann, 2010). Osmophore tissues are usually restricted to certain floral portions that favour scent

dispersion, like perianth tips and margins or other prominent portions of the flower (Pridgeon & Stern, 1983; Vogel, 1990; Sazima *et al.*, 1993; Stpiczyńska, 2001; Vogel & Hadacek, 2004; Sanguinetti *et al.*, 2012), and their differentiation as sites of production of specific attractants for a particular group of pollinators is assumed to have evolved from an undifferentiated epidermis emitting a diffuse and non-specific scent that attract a wide range of pollinators, which should learn to associate the odour signal with food (Vogel, 1990). Volatile compounds synthesized in osmophores differ from those diffusely emitted by epidermis in their innate attractive character and chemical specificity (Vogel, 1990).

Osmophores are mainly associated with deceptive pollination systems, occurring particularly in fly-pollinated sapromyiophilous species in several genera of Araceae, Orchidaceae, Apocynaceae (subfamily Asclepiadoideae) and Aristolochiaceae (Pridgeon & Stern, 1983; Pridgeon & Stern, 1985; Vogel, 1990; Skubatz *et al.*, 1996; Vogel & Martens, 2000; Teixeira, Borba & Semir, 2004; Heiduk *et al.*, 2010; Melo, Borba & Paiva, 2010; Płachno, Świątek & Szymczak, 2010; van der Niet, Hansen & Johnson, 2011). Furthermore, osmophores are typically present in the highly specialized fragrance-rewarding system of Euglossini-bee orchids (Stern, Curry & Pridgeon, 1987; Vogel, 1990; Curry *et al.*, 1991; Sazima *et al.*, 1993; Pansarin, Pansarin & Sazima, 2014), as well as in a few nectar-rewarding orchid species pollinated by a particular group of moths or bees (Vogel, 1990; Stpiczyńska, 2001; Peter *et al.*, 2009; Wiemer *et al.*, 2009). The occurrence of an osmophore was also identified in the tips of sepals or lateral petals of the flowers of some orchid species pollinated by sexual deception, in particular in the Australian *Caladenia* spp. (Stoutamire, 1983; Jones, 1991; Peakall & Beattie, 1996; Dickson & Petit, 2006; Salzmann, Brown & Schiestl, 2006), *Chiloglottis* spp. (Jones, 1991; Peakall & Handel, 1993) and *Leporella fimbriata* (Peakall, Beattie & James, 1987; Peakall, 1989), and in the only two sexually deceptive South African orchid species, *Disa atricapilla* and *D. bivalvata* (Steiner *et al.*, 1994). In genus *Ophrys*, an osmophore was also described for three species, namely *O. fuciflora*, *O. fusca* and *O. lutea* (Vogel, 1990), although our knowledge about the location, structure and activity of these osmophores is still scarce. In addition, whether or not an osmophore occurs in the other *Ophrys* species remains to be investigated.

THE STUDIED SPECIES

The genus *Ophrys* presents an area of geographical distribution mostly confined to the Mediterranean Basin, with a few species occurring in Central Europe, and its origin probably occurred in the central-western Mediterranean region (Delforge, 2005; Pedersen & Faurholdt, 2007; Breitkopf *et al.*, 2015). In Portugal, *Ophrys* orchids are distributed mainly throughout the central-western and southern regions of the country (Fig. 2), in meadows, grasslands and clearings in the scrubland or garrigue, occurring predominantly in exposed sites with calcareous soils. Their habitat was classified as a priority target of biodiversity

conservation by the Council Directive 92/43/EEC (Habitats Directive, Annex I), being part of Natura 2000, the network of nature protection areas in the territory of the European Union. Among the major threats to *Ophrys* orchids is habitat deterioration by urbanization, which is especially significant along the Mediterranean coast where tourism is preponderant (Pedersen & Faurholdt, 2007).

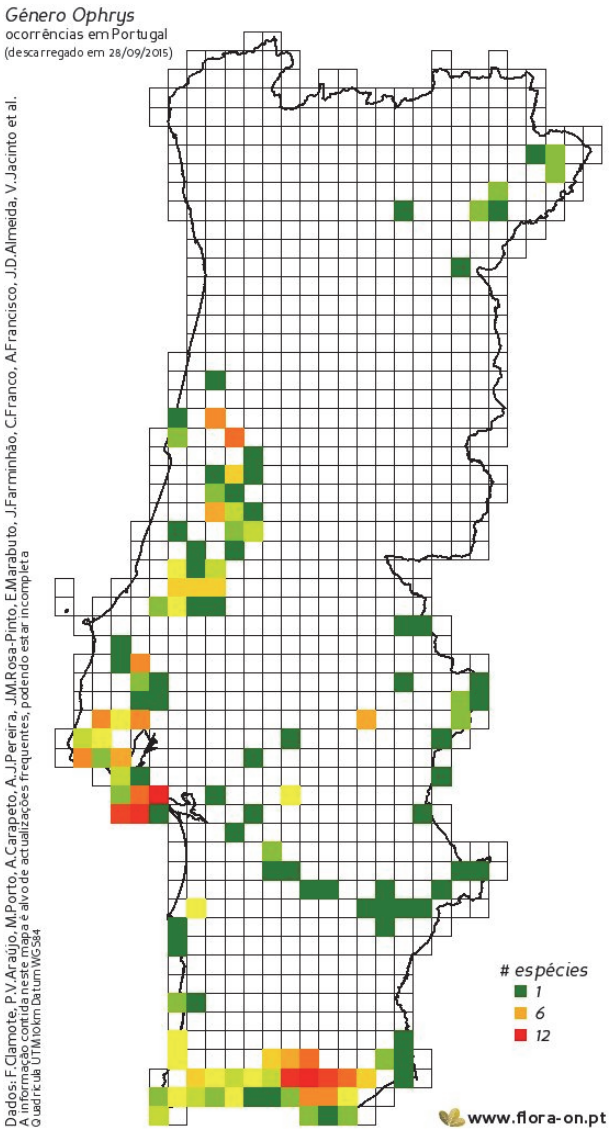

Figure 2. Area of geographical distribution of the eight *Ophrys* species occurring in Portugal, based on the occurrence data recorded in the platform Flora-On (http://www.flora-on.pt/) by Clamote *et al.* (2015). Note that the highest number of species (red-coloured squares) occurs in the Setúbal Peninsula and in Algarve. Map used under the license Creative Commons BY-NC 4.0 International (http://creativecommons.org/licenses/by-nc/4.0/deed.en).

The genus *Ophrys* is represented in Portugal by eight species and 11 taxa, if the infraspecific rank is considered, according to the taxonomic classification by Aldasoro & Sáez (2005), which is the taxonomic classification of the genus adopted in the present thesis. The *Ophrys* species occurring in Portugal (whose common name is given in brackets) are the following: *O. apifera* Huds. (erva-abelha), *O. bombyliflora* Link (erva-mosca), *O. fusca* Link

(moscardo-maior), *O. lutea* Cav. (erva-vespa), *O. scolopax* Cav. (flor-dos-passarinhos), *O. speculum* Link (abelhão), *O. sphegodes* Mill. (erva-aranha) and *O. tenthredinifera* Willd.. According to Aldasoro & Sáez (2005), the species *O. fusca* is composed of three subspecies, namely *O. fusca* Link subsp. *bilunulata* (Risso) Aldasoro & L.Sáez, *O. fusca* Link subsp. *dyris* (Maire) Soó and *O. fusca* Link subsp. *fusca*, whereas the species *O. speculum* comprises two subspecies, namely *O. speculum* Link subsp. *lusitanica* O.Danesch & E.Danesch and *O. speculum* Link subsp. *speculum*.

The taxonomy of the genus *Ophrys* is controversial, with some authors recognizing more than 250 species in the genus (Delforge, 2005) whereas others considering only 19 species, most of which comprising several subspecies (Pedersen & Faurholdt, 2007). This discrepancy results primarily from a disagreement on the diagnostic characters used for species delineation, in particular on the taxonomic value assigned to some floral morphological differences (Devey *et al.*, 2008; Bateman, 2009; Bateman *et al.*, 2010; Vereecken, Dafni & Cozzolino, 2010b; Bateman *et al.*, 2011; Vereecken *et al.*, 2011). Although high variability in flower morphology is easily observed within and among natural populations (Paulus, 2006; Vereecken *et al.*, 2010b), only weak genetic differentiation was detected between most *Ophrys* taxa by means of molecular analytical techniques, which might be caused by their recent origin (Devey *et al.*, 2008). The molecular phylogenetic analyses by Devey *et al.* (2008) showed that only 10 consistent groups of species were able to be genetically distinguished in the genus *Ophrys*, which could be due to the recent diversification of this genus, estimated to have occurred approximately between 4.6 and 4.8 million years ago (Inda, Pimentel & Chase, 2012; Breitkopf *et al.*, 2015), the late-diverging groups being estimated to start diversifying only 1.5 million years ago (Breitkopf *et al.*, 2015).

In the present thesis we studied six out of the 11 *Ophrys* taxa occurring in Portugal, namely *O. bombyliflora*, *O. fusca* subsp. *fusca, O. lutea*, *O. speculum* subsp. *lusitanica*, *O. speculum* subsp. *speculum* and *O. tenthredinifera*. These closely related taxa all belong to a major clade of *Ophrys* formed by the species of the monophyletic section *Pseudophrys* (pollinated by abdominal pseudocopulation; Godfery, 1928) plus a few members of the section *Ophrys* (pollinated by cephalic pseudocopulation; Godfery, 1928), which was shown to be paraphyletic in molecular phylogenetic analyses (Soliva, Kocyan & Widmer, 2001; Bateman *et al.*, 2003; Devey *et al.*, 2008). The relationships between the species of this major clade of *Ophrys* are still uncertain (Soliva *et al.*, 2001; Bateman *et al.*, 2003; Devey *et al.*, 2008; Inda *et al.*, 2012). Furthermore, little is known about the micromorphology and anatomy of the labellum of these species, in particular in what concerns the potential occurrence of an osmophore, which was only described for *O. fusca* and *O. lutea* (Vogel, 1990).

OBJECTIVES OF THE THESIS

The general objective of the present thesis is to improve our understanding of the complex structure of the labellum of *Ophrys* flowers, uncovering its significance for the attraction of specific insect pollinators and contributing to our knowledge about floral trait evolution in this sexually deceptive orchid genus. In particular, we investigated flowers of the above six closely related *Ophrys* taxa, at three developmental stages, in order to achieve the following specific aims:

1. Characterize the structure, location and secretion of the osmophore in each *Ophrys* species through an anatomical study of the labellum and histochemical tests, and evaluate the significance of the occurrence of an osmophore in *Ophrys* pollination;
2. Characterize the micromorphology of the labellum and the contiguous stigmatic cavity by describing the epidermal cell types occurring in their adaxial surface in each *Ophrys* species, and establish homologies between floral parts of the different species;
3. Find new micromorphological floral features that could act as close-range visual and tactile signals for pollinators;
4. Identify macro-, micro-morphological, and anatomical floral characters with potential phylogenetic information in the genus *Ophrys*;
5. Help to clarify the phylogenetic relationships between all four well established groups of species that constitute the still unresolved *Ophrys* clade formed by *O. bombyliflora*, *O. speculum*, *O. tenthredinifera* and section *Pseudophrys*, from a morpho-anatomical data matrix;
6. Identify shared morpho-anatomical features which confer support to the groups of *Ophrys* species found in the phylogenetic tree; and
7. Reconstruct the ancestral character states for the investigated clade, thereby contributing to our knowledge about the evolution of floral traits in the genus *Ophrys*.

ORGANIZATION OF THE THESIS

This thesis is divided into six chapters. Besides the present chapter, in which the scientific context of the thesis and its specific aims are provided, the thesis includes four chapters corresponding to original papers that have been either published (Chapters 2, 3 and 5) or submitted for publication (Chapter 4) in peer-reviewed international journals, and ends with a general discussion that integrates and discusses all findings of the previous four chapters in the light of the current knowledge about *Ophrys* pollination and phylogeny (Chapter 6).

The first three specific aims of the thesis are achieved in Chapters 2, 3, and 4, where a comparative micromorphological and anatomical study of the labellum and the characterization of the osmophore in the six closely related *Ophrys* taxa that form the investigated clade are presented, two taxa in each chapter as follows: in Chapter 2, *O. fusca* and *O. lutea*, two representative species of section *Pseudophrys* pollinated by males of solitary bees of genus *Andrena*; in Chapter 3, *O. bombyliflora* and *O. tenthredinifera*, two species pollinated by males of solitary bees of genus *Eucera*; and in Chapter 4, the two subspecies of *O. speculum* occurring in Portugal, a species pollinated by males of solitary wasps of *Dasyscolia ciliata*. In Chapter 4, a micromorphological comparison with the female of the wasp pollinator is also provided.

Chapter 5 addresses the four last specific aims of the present thesis. In this chapter, a morphological phylogenetic analysis of the investigated clade is conducted based on a data matrix of macro-, micro-morphological and anatomical floral characters that have been identified in Chapters 2–4. In order to perform such cladistic analysis, we also studied the labellum micromorphology and the osmophore structure of a seventh *Ophrys* species, *O. scolopax*, which was used as the outgroup.

Lastly, Chapter 6 incorporates all findings presented in the previous chapters into a general discussion that takes into consideration the current knowledge about the pollination ecology and phylogeny of the genus *Ophrys*, finishing with the major conclusions of our study and some directions for future research on this subject.

REFERENCES

Ågren L, Kullenberg B, Sensenbaugh T. 1984. Congruences in pilosity between three species of *Ophrys* (Orchidaceae) and their hymenopteran pollinators. *Nova Acta Regiae Societatis Scientiarum Upsaliensis, Serie V:C* **3:** 15-25.

Aldasoro JJ, Sáez L. 2005. *Ophrys* L. In: Aedo C, Herrero A, eds. *Flora Iberica: plantas vasculares da la Península Ibérica e Islas Baleares, Vol. XXI.* Madrid: Real Jardín Botánico, CSIC, 165-195.

Arcangeli G. 1883. Osservazione sull' impollinazione in alcune Aracee. *Nuovo Giornale Botanico Italiano* **15:** 12-97.

Arditti J. 1992. *Fundamentals of orchid biology.* New York: John Wiley & Sons, Inc.

Arditti J. 2003. Resupination. *Lankesteriana* **7:** 95-96.

Ayasse M, Schiestl FP, Paulus HF, Löfstedt C, Hansson B, Ibarra F, Francke W. 2000. Evolution of reproductive strategies in the sexually deceptive orchid *Ophrys sphegodes*: how does flower-specific variation of odor signals influence reproductive success? *Evolution* **54:** 1995-2006.

Ayasse M, Paxton RJ, Tengö J. 2001. Mating behavior and chemical communication in the order Hymenoptera. *Annual Review of Entomology* **46:** 31-78.

Ayasse M, Schiestl FP, Paulus HF, Ibarra F, Francke W. 2003. Pollinator attraction in a sexually deceptive orchid by means of unconventional chemicals. *Proceedings of the Royal Society B: Biological Sciences* **270:** 517-522.

Ayasse M, Stökl J, Francke W. 2011. Chemical ecology and pollinator-driven speciation in sexually deceptive orchids. *Phytochemistry* **72:** 1667-1677.

Ayasse M, Dötterl S. 2014. The role of preadaptations or evolutionary novelties for the evolution of sexually deceptive orchids. *New Phytologist* **203:** 710-712.

Bateman RM, Hollingsworth PM, Preston J, Yi-Bo L, Pridgeon AM, Chase MW. 2003. Molecular phylogenetics and evolution of Orchidinae and selected Habenariinae (Orchidaceae). *Botanical Journal of the Linnean Society* **142:** 1-40.

Bateman RM. 2009. Evolutionary classification of European orchids: the crucial importance of maximising explicit evidence and minimising authoritarian speculation. *Journal Europäischer Orchideen* **41:** 243–318.

Bateman RM, Devey DS, Malmgren S, Bradshaw E, Rudall PJ. 2010. Conflicting species concepts underlie perennial taxonomic controversies in *Ophrys*. *Cahiers de la Société Française d'Orchidophilie* **7:** 87-101.

Bateman RM, Bradshaw E, Devey DS, Glover BJ, Malmgren S, Sramkó G, Thomas MM, Rudall PJ. 2011. Species arguments: clarifying competing concepts of species delimitation in the pseudo-copulatory orchid genus *Ophrys*. *Botanical Journal of the Linnean Society* **165:** 336-347.

Bergström G, Tengö J. 1978. Linalool in mandibular gland secretion of *Colletes* bees (Hymenoptera: Apoidea). *Journal of Chemical Ecology* **4:** 437-449.

Bino RJ, Dafni A, Meeuse ADJ. 1982. The pollination ecology of *Orchis galilaea* (Bornm. et Schulze) Schltr. (Orchidaceae). *New Phytologist* **90:** 315-319.

Blanco MA, Barboza G. 2005. Pseudocopulatory pollination in *Lepanthes* (Orchidaceae: Pleurothallidinae) by fungus gnats. *Annals of Botany* **95:** 763-772.

Bohman B, Phillips RD, Menz MHM, Berntsson BW, Flematti GR, Barrow RA, Dixon KW, Peakall R. 2014. Discovery of pyrazines as pollinator sex pheromones and orchid semiochemicals: implications for the evolution of sexual deception. *New Phytologist* **203:** 939-952.

Borg-Karlson A-K, Tengö J. 1986. Odor mimetism? Key substances in *Ophrys lutea* - *Andrena* pollination relationship (Orchidaceae: Andrenidae). *Journal of Chemical Ecology* **12:** 1927-1942.

Borg-Karlson A-K. 1990. Chemical and ethological studies of pollination in the genus *Ophrys* (Orchidaceae). *Phytochemistry* **29:** 1359-1387.

Borg-Karlson A-K, Groth I, Ägren L, Kullenberg B. 1993. Form-specific fragrances from *Ophrys insectifera* L. (Orchidaceae) attract species of different pollinator genera. Evidence of sympatric speciation? *Chemoecology* **4:** 39-45.

Bradshaw E, Rudall PJ, Devey DS, Thomas MM, Glover BJ, Bateman RM. 2010. Comparative labellum micromorphology of the sexually deceptive temperate orchid genus *Ophrys*: diverse epidermal cell types and multiple origins of structural colour. *Botanical Journal of the Linnean Society* **162:** 504-540.

Breitkopf H, Onstein RE, Cafasso D, Schlüter PM, Cozzolino S. 2015. Multiple shifts to different pollinators fuelled rapid diversification in sexually deceptive *Ophrys* orchids. *New Phytologist* **207:** 377-389.

Ciotek L, Giorgis P, Benitez-Vieyra S, Cocucci AA. 2006. First confirmed case of pseudocopulation in terrestrial orchids of South America: pollination of *Geoblasta pennicillata* (Orchidaceae) by *Campsomeris bistrimacula* (Hymenoptera, Scoliidae). *Flora* **201:** 365-369.

Clamote F, Araújo PV, Porto M, Carapeto A, Pereira AJ, Rosa-Pinto JM, Marabuto E, Farminhão J, Franco C, Francisco A, Almeida JD, Jacinto V. 2015. Género *Ophrys* -

mapa de distribuição. Flora-On: Flora de Portugal Interactiva. Sociedade Portuguesa de Botânica. http://www.flora-on.pt/#wOphrys. Consulta realizada em 28/09/2015.

Coleman E. 1928. Pollination of an Australian orchid by the male Ichneumonid *Lissopimpla semipunctata*, Kirby. *Transactions of the Royal Entomological Society of London* **76:** 533-539.

Correvon H, Pouyanne M. 1916. Un curieux cas de mimétisme chez les Ophrydées. *Journal de la Société Nationale d'Horticulture de France, ser. 4,* **17:** 29-31; 41-47; 84-85.

Cortis P, Vereecken NJ, Schiestl FP, Lumaga MRB, Scrugli A, Cozzolino S. 2009. Pollinator convergence and the nature of species' boundaries in sympatric Sardinian *Ophrys* (Orchidaceae). *Annals of Botany* **104:** 497-506.

Cozzolino S, Widmer A. 2005. Orchid diversity: an evolutionary consequence of deception? *Trends in Ecology and Evolution* **20:** 487-494.

Cozzolino S, Scopece G. 2008. Specificity in pollination and consequences for postmating reproductive isolation in deceptive Mediterranean orchids. *Philosophical Transactions of the Royal Society B: Biological Sciences* **363:** 3037-3046.

Curry KJ, McDowell LM, Judd WS, Stern WL. 1991. Osmophores, floral features, and systematics of *Stanhopea* (Orchidaceae). *American Journal of Botany* **78:** 610-623.

Dafni A. 1984. Mimicry and deception in pollination. *Annual Review of Ecology and Systematics* **15:** 259-278.

Darwin C. 1862. *On the various contrivances by which British and foreign orchids are fertilised by insects, and on the good effects of intercrossing.* London: John Murray.

Delforge P. 2005. *Guide des orchidées d'Europe, d'Afrique du Nord et du Proche-Orient.* 3rd ed. Paris: Delachaux et Niestlé.

Devey DS, Bateman RM, Fay MF, Hawkins JA. 2008. Friends or relatives? Phylogenetics and species delimitation in the controversial European orchid genus *Ophrys*. *Annals of Botany* **101:** 385-402.

Devillers P, Devillers-Terschuren J. 1994. Essai d'analyse systématique du genre *Ophrys*. *Les Naturalistes belges* **75 (Orchidées 7):** 273-400.

Dickson C, Petit S. 2006. Effect of individual height and labellum colour on the pollination of *Caladenia* (syn. *Arachnorchis*) *behrii* (Orchidaceae) in the northern Adelaide region, South Australia. *Plant Systematics and Evolution* **262:** 65-74.

Ellis AG, Johnson SD. 2010. Floral mimicry enhances pollen export: the evolution of pollination by sexual deceit outside of the Orchidaceae. *The American Naturalist* **176:** E143–E151.

Endress PK. 2011. Evolutionary diversification of the flowers in angiosperms. *American Journal of Botany* **98:** 370-396.

Flach A, Marsaioli AJ, Singer RB, Amaral MCE, Menezes C, Kerr WE, Batista-Pereira LG, Corrêa AG. 2006. Pollination by sexual mimicry in *Mormolyca ringens*: a floral chemistry that remarkably matches the pheromones of virgin queens of *Scaptotrigona* sp. *Journal of Chemical Ecology* **32:** 59-70.

Gaskett AC, Winnick CG, Herberstein ME. 2008. Orchid sexual deceit provokes ejaculation. *The American Naturalist* **171:** E206-E212.

Gaskett AC. 2011. Orchid pollination by sexual deception: pollinator perspectives. *Biological Reviews* **86:** 33-75.

Godfery MJ. 1928. Classification of the genus *Ophrys*. *The Journal of Botany, British and Foreign* **66:** 33-36.

Gögler J, Twele R, Francke W, Ayasse M. 2011. Two phylogenetically distinct species of sexually deceptive orchids mimic the sex pheromone of their single common pollinator, the cuckoo bumblebee *Bombus vestalis*. *Chemoecology* **21:** 243-252.

Heiduk A, Brake I, Tolasch T, Frank J, Jürgens A, Meve U, Dötterl S. 2010. Scent chemistry and pollinator attraction in the deceptive trap flowers of *Ceropegia dolichophylla*. *South African Journal of Botany* **76:** 762-769.

Herrmann A. 2010. Volatiles - an interdisciplinary approach. In: Herrmann A, ed. *The chemistry and biology of volatiles.* Chichester, West Sussex, UK: John Wiley & Sons Ltd, 1-10.

Inda LA, Pimentel M, Chase MW. 2012. Phylogenetics of tribe Orchideae (Orchidaceae: Orchidoideae) based on combined DNA matrices: inferences regarding timing of diversification and evolution of pollination syndromes. *Annals of Botany* **110:** 71-90.

Jacquemyn H, Brys R, Cammue BPA, Honnay O, Lievens B. 2011. Mycorrhizal associations and reproductive isolation in three closely related *Orchis* species. *Annals of Botany* **107:** 347-356.

Jersáková J, Johnson SD, Kindlmann P. 2006. Mechanisms and evolution of deceptive pollination in orchids. *Biological Reviews of the Cambridge Philosophical Society* **81:** 219-235.

Jones DL. 1991. New taxa of Australian Orchidaceae. *Australian Orchid Research* **2:** 1-208.

Kullenberg B. 1961. Studies in *Ophrys* pollination. *Zoologiska Bidrag fran Uppsala* **34:** 1-340.

Kullenberg B. 1973. Field experiments with chemical sexual attractants on aculeate Hymenoptera males. II. *Zoon* **Suppl. 1:** 31-42.

Kullenberg B, Bergström G. 1976. Hymenoptera Aculeata males as pollinators of *Ophrys* orchids. *Zoologica Scripta* **5:** 13-23.

Kullenberg B, Borg-Karlson A-K, Kullenberg A-L. 1984. Field studies on the behaviour of the *Eucera nigrilabris* male in the odour flow from flower labellum extract of *Ophrys tenthredinifera*. *Nova Acta Regiae Societatis Scientiarum Upsaliensis, Serie V:C* **3:** 79-110.

Kurzweil H. 1987a. Developmental studies in orchid flowers I: Epidendroid and vandoid species. *Nordic Journal of Botany* **7:** 427-442.

Kurzweil H. 1987b. Developmental studies in orchid flowers II: Orchidoid species. *Nordic Journal of Botany* **7:** 443-451.

Mant JG, Brändli C, Vereecken NJ, Schulz CM, Francke W, Schiestl FP. 2005. Cuticular hydrocarbons as sex pheromone of *Colletes cunicularius* (Hymenoptera: Colletidae) and the key to its mimicry by the sexually deceptive orchid, *Ophrys exaltata*. *Journal of Chemical Ecology* **31:** 1765-1787.

Melo MC, Borba EL, Paiva EAS. 2010. Morphological and histological characterization of the osmophores and nectaries of four species of *Acianthera* (Orchidaceae: Pleurothallidinae). *Plant Systematics and Evolution* **286:** 141-151.

Mondragón-Palomino M, Theißen G. 2008. MADS about the evolution of orchid flowers. *Trends in Plant Science* **13:** 51-59.

Mondragón-Palomino M, Theißen G. 2009. Why are orchid flowers so diverse? Reduction of evolutionary constraints by paralogues of class B floral homeotic genes. *Annals of Botany* **104:** 583-594.

Mori K. 2010. Pheromones in chemical communication. In: Herrmann A, ed. *The chemistry and biology of volatiles.* Chichester, West Sussex, UK: John Wiley & Sons Ltd., 123-150.

van der Niet T, Hansen DM, Johnson SD. 2011. Carrion mimicry in a South African orchid: flowers attract a narrow subset of the fly assemblage on animal carcasses. *Annals of Botany* **107:** 981-992.

Nilsson LA. 1992. Orchid pollination biology. *Trends in Ecology and Evolution* **7:** 255-259.

Pansarin LM, Pansarin ER, Sazima M. 2014. Osmophore structure and phylogeny of *Cirrhaea* (Orchidaceae, Stanhopeinae). *Botanical Journal of the Linnean Society* **176:** 369-383.

Paulus HF, Gack C. 1990. Pollinators as prepollinating isolation factors: evolution and speciation in *Ophrys* (Orchidaceae). *Israel Journal of Botany* **39:** 43-79.

Paulus HF. 2006. Deceived males - Pollination biology of the Mediterranean orchid genus *Ophrys* (Orchidaceae). *Journal Europäischer Orchideen* **38:** 303-353.

Peakall R, Beattie AJ, James SH. 1987. Pseudocopulation of an orchid by male ants: a test of two hypotheses accounting for the rarity of ant pollination. *Oecologia* **73:** 522-524.

Peakall R. 1989. The unique pollination of *Leporella fimbriata* (Orchidaceae): pollination by pseudocopulating male ants (*Myrmecia urens*, Formicidae). *Plant Systematics and Evolution* **167:** 137-148.

Peakall R, Handel SN. 1993. Pollinators discriminate among floral heights of a sexually deceptive orchid: implications for selection. *Evolution* **47:** 1681-1687.

Peakall R, Beattie AJ. 1996. Ecological and genetic consequences of pollination by sexual deception in the orchid *Caladenia tentactulata*. *Evolution* **50:** 2207-2220.

Peakall R, Ebert D, Poldy J, Barrow RA, Francke W, Bower CC, Schiestl FP. 2010. Pollinator specificity, floral odour chemistry and the phylogeny of Australian sexually deceptive *Chiloglottis* orchids: implications for pollinator-driven speciation. *New Phytologist* **188:** 437-450.

Peakall R, Whitehead MR. 2014. Floral odour chemistry defines species boundaries and underpins strong reproductive isolation in sexually deceptive orchids. *Annals of Botany* **113:** 341-355.

Pedersen HÆ, Faurholdt N. 2007. *Ophrys, the bee orchids of Europe.* Kew, London: Kew Publishing - Royal Botanic Gardens.

Peter CI, Coombs G, Huchzermeyer CF, Venter N, Winkler AC, Hutton D, Papier LA, Dold AP, Johnson SD. 2009. Confirmation of hawkmoth pollination in *Habenaria epipactidea*: leg placement of pollinaria and crepuscular scent emission. *South African Journal of Botany* **75:** 744-750.

Peter CI, Johnson SD. 2013. Generalized food deception: colour signals and efficient pollen transfer in bee-pollinated species of *Eulophia* (Orchidaceae). *Botanical Journal of the Linnean Society* **171:** 713-729.

Phillips RD, Scaccabarozzi D, Retter BA, Hayes C, Brown GR, Dixon KW, Peakall R. 2014. Caught in the act: pollination of sexually deceptive trap-flowers by fungus gnats in *Pterostylis* (Orchidaceae). *Annals of Botany* **113:** 629-641.

van der Pijl L, Dodson CH. 1966. *Orchids flowers, their pollination and evolution.* Coral Gables, Florida: University of Miami Press.

Płachno BJ, Świątek P, Szymczak G. 2010. Can a stench be beautiful? – Osmophores in stem-succulent stapeliads (Apocynaceae-Asclepiadoideae-Ceropegieae-Stapeliinae). *Flora* **205:** 101-105.

Pouyanne M. 1917. La fécondation des *Ophrys* par les insectes. *Bulletin de la Société d'Histoire Naturelle de l'Afrique du nord* **8:** 6-7.

Pridgeon AM, Stern WL. 1983. Ultrastructure of osmophores in *Restrepia* (Orchidaceae). *American Journal of Botany* **70:** 1233-1243.

Pridgeon AM, Stern WL. 1985. Osmophores of *Scaphosepalum* (Orchidaceae). *Botanical Gazette* **146:** 115-123.

Renner SS. 2005. Rewardless flowers in the angiosperms and the role of insect cognition in their evolution. In: Waser NM, Ollerton J, eds. *Plant-pollinator interactions: from specialization to generalization.* Chicago: University of Chicago Press, 123-144.

Rudall PJ, Bateman RM. 2002. Roles of synorganisation, zygomorphy and heterotopy in floral evolution: the gynostemium and labellum of orchids and other lilioid monocots. *Biological Reviews of the Cambridge Philosophical Society* **77:** 403-441.

Salzmann CC, Brown A, Schiestl FP. 2006. Floral scent emission and pollination syndromes: evolutionary changes from food to sexual deception. *International Journal of Plant Sciences* **167:** 1197-1204.

Sanguinetti A, Buzatto CR, Pedron M, Davies KL, Ferreira PMdA, Maldonado S, Singer RB. 2012. Floral features, pollination biology and breeding system of *Chloraea membranacea* Lindl. (Orchidaceae: Chloraeinae). *Annals of Botany* **110:** 1607-1621.

Sazima M, Vogel S, Cocucci AA, Hausner G. 1993. The perfume flowers of *Cyphomandra* (Solanaceae): pollination by euglossine bees, bellows mechanism, osmophores, and volatiles. *Plant Systematics and Evolution* **187:** 51-88.

Schiestl FP, Ayasse M, Paulus HF, Löfstedt C, Hansson BS, Ibarra F, Francke W. 1999. Orchid pollination by sexual swindle. *Nature* **399:** 421-422.

Schiestl FP, Ayasse M, Paulus HF, Löfstedt C, Hansson BS, Ibarra F, Francke W. 2000. Sex pheromone mimicry in the early spider orchid (*Ophrys sphegodes*): patterns of hydrocarbons as the key mechanism for pollination by sexual deception. *Journal of Comparative Physiology A* **186:** 567-574.

Schiestl FP, Ayasse M. 2002. Do changes in floral odor cause speciation in sexually deceptive orchids? *Plant Systematics and Evolution* **234:** 111-119.

Schiestl FP, Peakall R, Mant JG, Ibarra F, Schulz C, Franke S, Francke W. 2003. The chemistry of sexual deception in an orchid-wasp pollination system. *Science* **302:** 437-438.

Schiestl FP, Peakall R, Mant JG. 2004. Chemical communication in the sexually deceptive orchid genus *Cryptostylis*. *Botanical Journal of the Linnean Society* **144:** 199-205.

Schiestl FP. 2005. On the success of a swindle: pollination by deception in orchids. *Naturwissenschaften* **92:** 255-264.

Schiestl FP, Schlüter PM. 2009. Floral isolation, specialized pollination, and pollinator behavior in orchids. *Annual Review of Entomology* **54:** 425-446.

Schlüter PM, Xu S, Gagliardini V, Whittle E, Shanklin J, Grossniklaus U, Schiestl FP. 2011. Stearoyl-acyl carrier protein desaturases are associated with floral isolation in sexually deceptive orchids. *Proceedings of the National Academy of Sciences of the United States of America* **108:** 5696-5701.

Scopece G, Musacchio A, Widmer A, Cozzolino S. 2007. Patterns of reproductive isolation in mediterranean deceptive orchids. *Evolution* **61:** 2623-2642.

Scopece G, Cozzolino S, Johnson SD, Schiestl FP. 2010. Pollination efficiency and the evolution of specialized deceptive pollination systems. *The American Naturalist* **175:** 98-105.

Servettaz O, Bino Maleci L, Grünanger P. 1994. Labellum micromorphology in the *Ophrys bertolinii* agg. and some related taxa (Orchidaceae). *Plant Systematics and Evolution* **189:** 123-131.

Singer RB. 2002. The pollination mechanism in *Trigonidium obtusum* Lindl (Orchidaceae: Maxillariinae): sexual mimicry and trap-flowers. *Annals of Botany* **89:** 157-163.

Singer RB, Flach A, Koehler S, Marsaioli AJ, Amaral MCE. 2004. Sexual mimicry in *Mormolyca ringens* (Lindl.) Schltr. (Orchidaceae: Maxillariinae). *Annals of Botany* **93:** 755-762.

Skubatz H, Kunkel DD, Howald WN, Trenkle R, Mookherjee B. 1996. The *Sauromatum guttatum* appendix as an osmophore: excretory pathways, composition of volatiles and attractiveness to insects. *New Phytologist* **134:** 631-640.

Soliva M, Kocyan A, Widmer A. 2001. Molecular phylogenetics of the sexually deceptive orchid genus *Ophrys* (Orchidaceae) based on nuclear and chloroplast DNA sequences. *Molecular Phylogenetics and Evolution* **20:** 78-88.

Sprengel CK. 1793. Das entdeckte geheimniss der Natur im bau und in der befruchtung der blumen [Discovery of the secret of nature in the structure and fertilization of flowers]. Translated by Peter Haase (1996). In: Lloyd DG, Barrett SCH, eds. *Floral biology: studies on floral evolution in animal-pollinated plants.* New York: Chapman & Hall, 3-43.

Steiner KE, Whitehead VB, Johnson SD. 1994. Floral and pollinator divergence in two sexually deceptive South African orchids. *American Journal of Botany* **81:** 185-194.

Stern WL, Curry KJ, Pridgeon AM. 1987. Osmophores of *Stanhopea* (Orchidaceae). *American Journal of Botany* **74:** 1323-1331.

Stökl J, Paulus HF, Dafni A, Schulz C, Francke W, Ayasse M. 2005. Pollinator attracting odour signals in sexually deceptive orchids of the *Ophrys fusca* group. *Plant Systematics and Evolution* **254:** 105-120.

Stökl J, Twele R, Erdmann DH, Francke W, Ayasse M. 2008. Comparison of the flower scent of the sexually deceptive orchid *Ophrys iricolor* and the female sex pheromone of its pollinator *Andrena morio*. *Chemoecology* **17:** 231-233.

Stökl J, Schlüter PM, Stuessy TF, Paulus HF, Fraberger R, Erdmann D, Schulz C, Francke W, Assum G, Ayasse M. 2009. Speciation in sexually deceptive orchids: pollinator-driven selection maintains discrete odour phenotypes in hybridizing species. *Biological Journal of the Linnean Society* **98:** 439-451.

Stoutamire WP. 1983. Wasp pollination species of *Caladenia* (Orchidaceae) in south-western Australia. *Australian Journal of Botany* **31:** 383-394.

Stpiczyńska M. 2001. Osmophores of the fragrant orchid *Gymnadenia conopsea* L. (Orchidaceae). *Acta Societatis Botanicorum Poloniae* **70:** 91-96.

Streinzer M, Ellis T, Paulus HF, Spaethe J. 2010. Visual discrimination between two sexually deceptive *Ophrys* species by a bee pollinator. *Arthropod-Plant Interactions* **4:** 141-148.

Teixeira SP, Borba EL, Semir J. 2004. Lip anatomy and its implications for the pollination mechanisms of *Bulbophyllum* species (Orchidaceae). *Annals of Botany* **93:** 499-505.

Tengö J, Bergström G. 1975. All-*trans*-farnesyl hexanoate and geranyl octanoate in the Dufour gland secretion of *Andrena* (Hymenoptera: Apidae). *Journal of Chemical Ecology* **1:** 253-268.

Tengö J. 1979. Odour-released behaviour in *Andrena* male bees (Apoidea, Hymenoptera). *Zoon* **7:** 15-48.

The Plant List. 2013. Version 1.1. Published on the Internet: http://www.theplantlist.org/ Consulta realizada em 03/10/2015.

Vereecken NJ, Schiestl FP. 2008. The evolution of imperfect floral mimicry. *Proceedings of the National Academy of Sciences of the United States of America* **105:** 7484-7488.

Vereecken NJ. 2009. Deceptive behavior in plants. I. Pollination by sexual deception in orchids: a host-parasite perspective. In: Baluška F, ed. *Plant-environment*

interactions. From sensory plant biology to active plant behavior. Heidelberg: Springer-Verlag, 203-222.

Vereecken NJ, Cozzolino S, Schiestl FP. 2010a. Hybrid floral scent novelty drives pollinator shift in sexually deceptive orchids. *BMC Evolutionary Biology* **10:** 103.

Vereecken NJ, Dafni A, Cozzolino S. 2010b. Pollination syndromes in mediterranean orchids - implications for speciation, taxonomy and conservation. *The Botanical Review* **76:** 220-240.

Vereecken NJ, McNeil JN. 2010. Cheaters and liars: chemical mimicry at its finest. *Canadian Journal of Zoology* **88:** 725-752.

Vereecken NJ, Streinzer M, Ayasse M, Spaethe J, Paulus HF, Stökl J, Cortis P, Schiestl FP. 2011. Integrating past and present studies on *Ophrys* pollination – a comment on Bradshaw *et al*. *Botanical Journal of the Linnean Society* **165:** 329-335.

Vereecken NJ, Wilson CA, Hötling S, Schulz S, Banketov SA, Mardulyn P. 2012. Pre-adaptations and the evolution of pollination by sexual deception: Cope's rule of specialization revisited. *Proceedings of the Royal Society B: Biological Sciences* **279:** 4786-4794.

Vogel S. 1960. Osmophoren. Über einen neuartigen typus pflanzlichen drüsengewebes. [Osmophores. A new type of glandular tissue in plants]. *Berichte Der Deutschen Botanischen Gesellschaft* **73:** 56-57.

Vogel S. 1961. Die bestäubung der kesselfallen-blüten von *Ceropegia*. [Pollination of the utricle trap flowers of *Ceropegia*]. *Beitrage zur Biologie der Pflanzen* **36:** 159-237.

Vogel S. 1990. *The role of scent glands in pollination: on the structure and function of osmophores.* Rotterdam: A. A. Balkema. [English translation of: Vogel S. 1963. Duftdrüsen im Dienste der Bestäubung: Über Bau und Funktion der Osmophoren. *Akademie der Wissenschaften und der Literatur in Mainz, Abhandlungen der Mathematisch-Naturwissenschaftlichen Klasse* **10**: 600-763].

Vogel S, Martens J. 2000. A survey of the function of the lethal kettle traps of *Arisaema* (Araceae), with records of pollinating fungus gnats from Nepal. *Botanical Journal of the Linnean Society* **133:** 61-100.

Vogel S, Hadacek F. 2004. Contributions to the functional anatomy and biology of *Nelumbo nucifera* (Nelumbonaceae) III. An ecological reappraisal of floral organs. *Plant Systematics and Evolution* **249:** 173-189.

Wiemer AP, Moré M, Benitez-Vieyra S, Cocucci AA, Raguso RA, Sérsic AN. 2009. A simple floral fragrance and unusual osmophore structure in *Cyclopogon elatus* (Orchidaceae). *Plant Biology* **11:** 506-514.

Xu S, Schlüter PM, Scopece G, Breitkopf H, Gross K, Cozzolino S, Schiestl FP. 2011. Floral isolation is the main reproductive barrier among closely related sexually deceptive orchids. *Evolution* **65:** 2606–2620.

Xu S, Schlüter PM, Grossniklaus U, Schiestl FP. 2012a. The genetic basis of pollinator adaptation in a sexually deceptive orchid. *PLoS Genetics* **8:** e1002889. doi:10.1371/journal.pgen.1002889.

Xu S, Schlüter PM, Schiestl FP. 2012b. Pollinator-driven speciation in sexually deceptive orchids. *International Journal of Ecology* **2012, Article ID 285081:** 9 pages. doi:10.1155/2012/285081.

CHAPTER 2

COMPARATIVE STRUCTURE OF THE LABELLUM IN *OPHRYS FUSCA* AND *O. LUTEA* (ORCHIDACEAE)

This chapter was published in *American Journal of Botany*:

Ascensão L., Francisco A., Cotrim H. and Pais M.S. 2005. Comparative structure of the labellum in *Ophrys fusca* and *O. lutea* (Orchidaceae). *American Journal of Botany*, 92: 1059-1067.

COMPARATIVE STRUCTURE OF THE LABELLUM IN *OPHRYS FUSCA* AND *O. LUTEA* (ORCHIDACEAE)

ABSTRACT

The morphology and anatomy of the labellar epidermal cells and the way in which they are arranged are described in an attempt to locate and characterize the osmophore in *Ophrys fusca* and *O. lutea*. The micromorphology of the labellum of these two species is similar. Four types of epidermal cells are present on the adaxial surface of the labellum. Long unicellular trichomes with straight tips cover the basal region of the labellum, whereas short unicellular trichomes with polygonal flattened bases form the reflective median speculum. The apical region of the labellum possesses a villous indumentum of long acuminate trichomes with bent or sinuate tips. Large smooth-walled dome-shaped papillae occur on the margins and on the distal region of the abaxial surface of the labellum. These remarkable papillae have high polarity; the protoplasm at the apex of each cell contains several small vacuoles, while a prominent nucleus surrounded by numerous hypertrophied amyloplasts occurs at the opposite end of the cell. Positive reactions to Vogel's staining test and to Sudan black B enabled us to conclude that the osmophores of both species are composed of these peculiar secretory epidermal cells and by two or three subsecretory layers of parenchyma cells.

KEYWORDS: anatomy; labellum; micromorphology; *Ophrys*; Orchidaceae; osmophore; Portugal; pseudocopulation.

INTRODUCTION

Ophrys orchids have developed a highly specialized pollination system involving sexual deception, a phenomenon regarded as exclusive to Orchidaceae (Nilsson, 1992), but with a few exceptions, such as *Guiera senegalensis* (Combretaceae: Kullenberg, 1961) and *Gilliesia graminea* (Alliaceae: Rudall *et al.*, 2002). *Ophrys* flowers mimic hymenopteran females in terms of shape, pilosity and color patterns and thereby deceive their males for pollination (Kullenberg, 1961; van der Pijl & Dodson, 1966; Borg-Karlson, 1990). In addition to these visual and tactile cues, the flowers also attract pollinators by means of olfactory stimuli involving synthesis of a complex mixture of volatile odoriferous compounds similar to the sex pheromones of the female (Kullenberg, 1961; Borg-Karlson & Tengö, 1986; Borg-Karlson, 1990; Schiestl *et al.*, 1999). Hence, pollination by sexual deceit is highly specific; each *Ophrys* species is pollinated by only one or a few related species of hymenopterans (Kullenberg, 1961; Paulus & Gack, 1981; Schiestl *et al.*, 1999; Schiestl & Ayasse, 2002; Ayasse *et al.*, 2003). Sexually excited male insects alight on an *Ophrys* labellum and try to copulate with it, a phenomenon known as pseudocopulation (Dafni, 1984; Nilsson, 1992; Delforge, 2001). During these pre-copulatory movements, the pollinator touches the column of the flower and may remove pollinaria with the abdomen tip or the head (Kullenberg, 1961; Delforge, 2001). Transfer of pollinaria results in cross-pollination.

Volatiles released by flowers of *Ophrys* species include alkanes, alkenes, aliphatic alcohols, saturated hydroxy and oxo acids, aldehydes, ketones, esters, and oxygenated mono- and sesquiterpenes, combined in varying proportions (Borg-Karlson & Tengö, 1986; Borg-Karlson, 1990; Schiestl *et al.*, 1999; Ayasse *et al.*, 2000; Schiestl *et al.*, 2000; Schiestl & Ayasse, 2002; Ayasse *et al.*, 2003). However, only a small subset of these compounds has been detected in the females of their pollinators and found to be active in stimulating mating behavior in the males (Schiestl *et al.*, 1999; Schiestl *et al.*, 2000; Schiestl & Ayasse, 2002; Ayasse *et al.*, 2003). Despite the recent advances in chemical and ethological research on *Ophrys* pollination, the study of the specific site of biosynthesis and discharge of the volatile secretion has been neglected, and the fine structure of the *Ophrys* labellum has received little attention. Kullenberg (1961) in his excellent and original survey of *Ophrys* pollination compared, even though superficially, the micromorphology of the flowers with that of their pollinator insects. More recently, the labellum micromorphology of six species from the *O. bertolonii* Moretti aggregate and of other related taxa was described (Servettaz, Bino Maleci & Grünanger, 1994).

On the other hand, despite the pioneer studies of Vogel in the 1960s on Orchidaceae, Aristolochiaceae, Araceae and Asclepiadaceae (Vogel, 1990), our knowledge of the anatomy and cytology of the osmophores of *Ophrys* remains poor. In the last 20 years, most research on the anatomy and ultrastructure of orchid osmophores has concentrated on tropical species (Pridgeon & Stern, 1983; Pridgeon & Stern, 1985; Curry, 1987; Stern, Curry &

Pridgeon, 1987; Curry *et al.*, 1991; Curry & Stern, 1991). By contrast, studies of European species are still relatively rare (Stpiczyńska, 1993; Stpiczyńska, 2001).

Within the framework of a wider project involving speciation of *Ophrys* in Portugal, we have undertaken cytological studies on the flower. In this paper, we compare the structure of the labella of *O. fusca* and *O. lutea* and describe the epidermal cell types and their distribution pattern in an attempt to locate and characterize the osmophore.

MATERIALS AND METHODS

Flowers from natural populations of *O. fusca* Link and *O. lutea* (Gouan) Cav. occurring throughout the central-western Portugal were collected. Flowers prior to and at anthesis were fixed for scanning electron microscopy (SEM), with 2.5% glutaraldehyde in 0.1 M sodium phosphate buffer at pH 7.2. Samples were kept in fixative under vacuum at room temperature for 20 min, followed by 48–72 h at 4°C. The material was then washed in the fixative buffer, dehydrated in a graded acetone series, critical-point dried with CO_2 and coated with gold. Observations were carried out on a JEOL T220 scanning electron microscope (JEOL Ltd., Tokyo, Japan) at an accelerating voltage of 15 or 20 kV.

For light microscopy, pieces of labella from buds just before anthesis and flowers at anthesis were processed in two ways. Some were fixed as described for SEM, but after the washes in the fixative buffer and dehydration through an ethanol series, the material was infiltrated with and embedded in Leica Historesin (Leica Microsystems, Nussloch/Heidelberg, Germany). Sections (2 µm thick) were cut using a Leica RM 2155 microtome (Leica Microsystems, Nussloch, Germany) and sequentially stained with periodic acid–Schiff's (PAS) reagent/toluidine blue O (Feder & O'Brien, 1968) for polysaccharides and for general histology. Sections were tested for starch with Lugol's iodine solution (IKI; Johansen, 1940) and for lipids with Sudan black B (Bronner, 1975) using appropriate controls. Other pieces of labella (namely, portions of the margins) were fixed with 2.5% glutaraldehyde in 0.1 M sodium phosphate buffer at pH 7.2 for 12 h at 4°C, rinsed in the fixative buffer, and postfixed with 2% osmium tetroxide in the same buffer for 1 h at room temperature. After washes in distilled water, specimens were dehydrated in a graded acetone series and embedded in Epon-Araldite resin (Electron Microscopy Sciences, Fort Washington, Pennsylvania, USA). Semithin sections (approximately 0.5 µm thick) were cut with a Sorvall MT-1 ultramicrotome (Sorvall Inc., Norwalk, USA) and stained with Sudan black B as described for the sections embedded in Leica Historesin. Sections were observed with a Leitz (Wetzlar, Germany) Dialux microscope.

Vogel's staining method was used for the macroscopic observation of osmophores (Stern, Curry & Whitten, 1986). Whole fresh buds, just prior to anthesis, and flowers at anthesis were immersed in 0.1% (w/v) aqueous neutral red for 2–24 h. After staining, flowers were rinsed in tap water and examined.

RESULTS

LABELLUM MICROMORPHOLOGY

The *Ophrys* labellum has one central lobe flanked by two lateral lobes. The central lobe can be divided along its length into three main regions: basal (near the stigmatic cavity), median, and apical (Fig. 1).

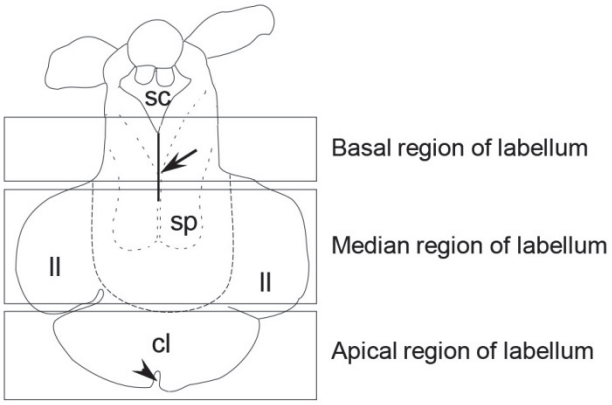

Figure 1. Diagram of the labellum of *Ophrys lutea*. arrow, basal groove; arrowhead, central notch; cl, central lobe; ll, lateral lobes; sp, speculum; sc, stigmatic cavity.

In *O. fusca* and *O. lutea* flowers, each colored patch on the labellum has a particular type of epidermal cell. These cells vary in shape and length according to which colored region of the labellum they occupy, and these variations may also be associated with changes in the fine detail of the cuticle. Four types of epidermal cells can be distinguished on the adaxial surface of the labellum: (1) long trichomes with straight tips occur on the greyish-white portion of the basal part of the labellum; (2) short trichomes with polygonal flattened bases occur on the bluish speculum; (3) long acuminate trichomes with bent or sinuate tips occur on the brown-reddish villous apical part of the labellum, and (4) dome-shaped papillae occur on the yellow margin. Conversely, the abaxial surface of the labellum is entirely glabrous and composed of elongated and flattened epidermal cells, which are replaced by large spherical papillae near the margin, especially towards the apical region of the labellum (Fig. 3F).

The adaxial surface of the basal region is traversed by a longitudinal central groove, which begins in the median region and extends as far as the stigmatic cavity (Fig. 2A, C, E). A dense indumentum occurs on the basal part of the labellum of both species. Long unicellular trichomes, with their straight tips directed towards either the basal groove or the stigmatic cavity, form this zone (Fig. 2A–D), which appears velvety to the naked eye. Indeed, trichomes from the basal part of the labellum of both species are filiform, and the trichome cell wall is rough with thin cuticular striations that run from the base to the apex of the

trichome (Fig. 2B, D). In *O. lutea*, this cuticular pattern in the basal portion of the trichome is less well defined than in *O. fusca*.

The median region of the labella of both these species is almost completely occupied by a bright colored patch, the speculum, which is characterized by a pubescent indumentum of short unicellular trichomes with large polygonal flattened bases (Fig. 2F). The trichome surface, especially at the tips, is covered by a dense reticulate pattern of cuticular ridges. The trichomes of the speculum, on approaching the longitudinal groove, are replaced by hairs with swollen bases and whose tips point toward the groove (Fig. 2E).

A key morphological feature of the apical part of the labellum of *O. fusca* and *O. lutea* is the presence of a central notch (Fig. 3C, E, arrows). In both orchids, the adaxial surface of the apical part of the labellum and lateral lobes is covered to a variable extent by a dense villous indumentum of long acuminate unicellular trichomes with swollen bases and narrow tips that are bent or sinuate (Fig. 3A, B). The trichome cell walls, like those of the other trichomes found in these two species, also show cuticular striations. In *O. fusca*, such a villous indumentum covers the entire portion of the labellum that surrounds the speculum as well as the entire apical portion, with the exception of the glabrous border (Fig. 3C, D). By contrast, in *O. lutea*, the area of the villous indumentum is smaller and is restricted to the proximal zone of the apical part of the labellum and to the lateral lobes, which are in contact with the speculum (Fig. 3E). Otherwise, the distal zone of the labellum is composed of large, smooth, dome-shaped papillae, which strongly resemble the cells of the border and the abaxial epidermal cells from the apical region of the labella of both species (Fig. 3D, F). Furthermore, a marked cell gradient is visible extending from the glabrous margin of the labellum to the area covered by the villous indumentum. The dome-shaped papillae gradually acquire a conical shape with pointed or round tips, which tend to become more hairlike as they approach the villous indumentum (Fig. 3D).

LABELLUM ANATOMY AND HISTOCHEMISTRY

Anatomically, the labella of *O. fusca* and *O. lutea* flowers are similar. They consist of multilayered parenchyma supplied by vascular strands and delimited by an upper and a lower epidermis. These differ from each other and comprise several types of cell depending upon which region is examined. The labellar parenchyma cells range from isodiametric to slightly elongated and are characterized by a large central vacuole and a thin layer of peripheral cytoplasm with relatively few organelles (Fig. 4A–E). Elliptical crystalliferous idioblasts containing raphides of calcium oxalate are frequent among parenchyma cells (Fig. 5E). In close proximity to the border of the labellum, the parenchyma cells, especially those from the subepidermal layer, are less vacuolated and contain abundant small plastids (Figs. 4E, G, 5B, E).

The adaxial epidermis of the labellum consists largely of highly vacuolated cells that have a clear polarity. Such cells possess an apical vacuome consisting of several vacuoles separated by narrow cytoplasmic strands (Figs. 4B, C, 5F). A small, elongated nucleus often occurs at the base of the cell. These cells acquire different shapes along the length of the labellum, as already described (Fig. 4A–E). Remarkably, the adaxial epidermal cells from the distal part of the labellum apex of *O. lutea* are almost circular in transverse section (Fig. 4E).

In both species, the abaxial epidermis of the distal part of the apical region of the labellum has characteristic anatomical features, especially near the central notch. This region comprises smooth-walled large papillae that appear spherical, reniform, or pyriform in section and that have an obvious polarity (Figs. 4F, G, 5A–D). The distal region of the cell possesses several small vacuoles that become confluent, giving rise to a single large vacuole. In contrast, the proximal region of the cell contains dense cytoplasm with a prominent enlarged nucleus, rich in chromatin, surrounded by numerous hypertrophied plastids. These organelles, identified as amyloplasts by PAS and IKI staining, are larger than those observed within parenchyma cells (Fig. 5B). This peculiar papillate epidermis extends throughout the entire border of the labellum, from the apical to the basal region (Fig. 5E, F). In *O. lutea*, this type of epidermis occurs upon the well-defined peripheral area of both the abaxial and adaxial surfaces of the labellum next to the margins and corresponds on the adaxial surface to the glabrous, yellow zone of the labellum.

In semithin sections stained with Sudan black B, the vacuoles of the epidermal and parenchyma cells at the margins of the labellum contain Sudan-positive material (Fig. 5G–J). In the cytoplasm of some epidermal cells are dark blue droplets (Fig. 5I). An exudate that is often present outside the epidermal cell walls is also Sudan-positive (Fig. 5G, I). However, in Leica Historesin sections stained with Sudan black B, only the cuticles gave a positive reaction.

With Vogel's method for locating the osmophores, the labellar margin of both species stained light red. The staining, already visible after only 2 h in neutral red, did not change significantly after 24 h.

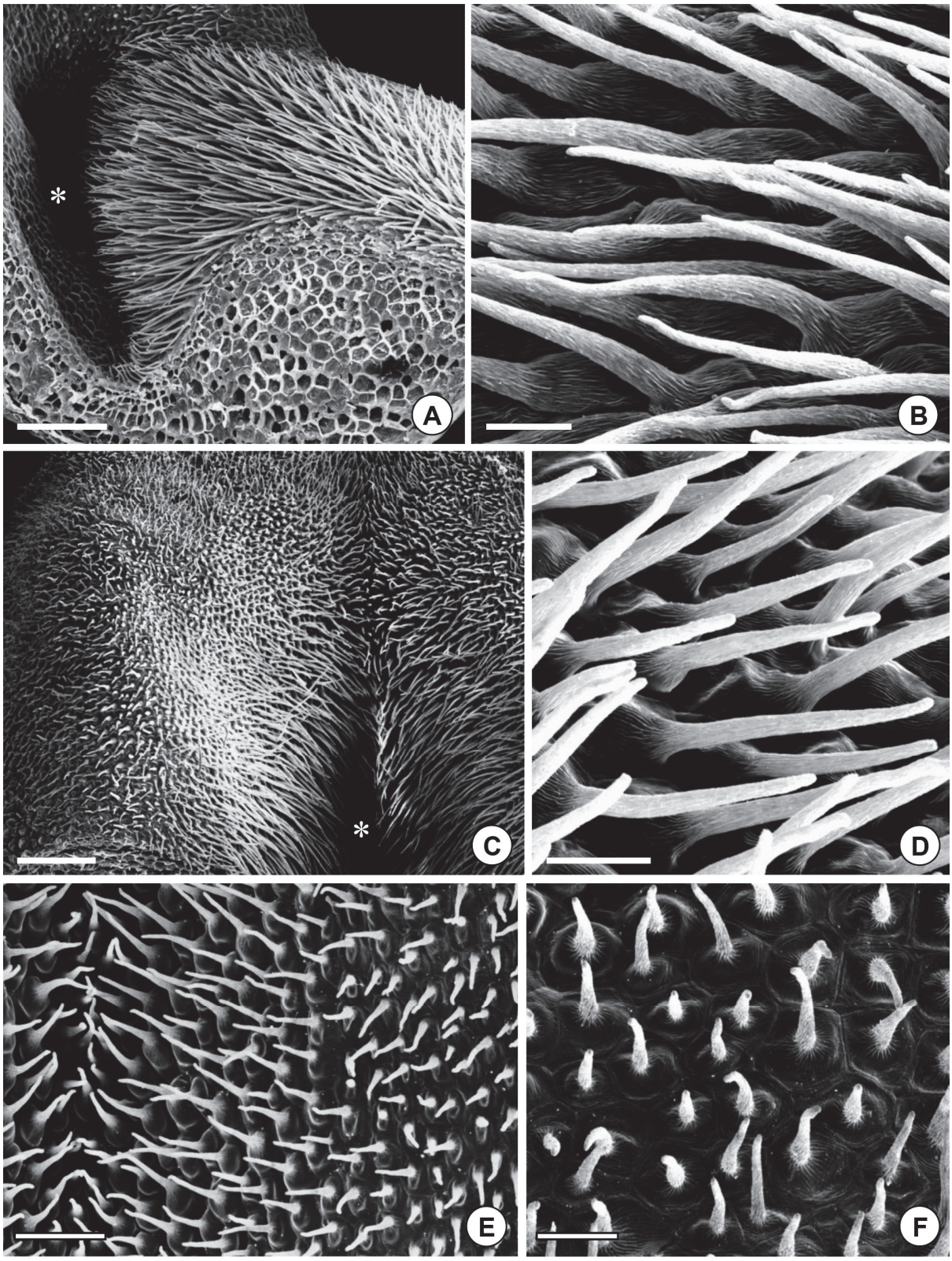

Figure 2. SEM micrographs showing indumentum of adaxial surface of basal and median regions of labellum of *Ophrys fusca* and *Ophrys lutea* at anthesis. A, Basal region of labellum of *O. fusca* cut longitudinally along central groove. Note dense indumentum consisting of long trichomes directed towards the stigmatic cavity (*). B, Detail of long unicellular trichomes present on basal part of labellum of *O. fusca* showing thin, linear cuticular striations on their cell walls. C, Basal part of labellum of *O. lutea* from above. The central longitudinal groove is evident as is the dense indumentum of long filiform trichomes pointing toward the basal groove or to the stigmatic cavity (*). D, Detail of unicellular trichomes with long filiform tips. Thin cuticular striations are present on

trichome cell walls. E, Median part of labellum of *O. fusca* showing transition zone between speculum and basal groove (on the left). In this region, the short trichomes of the speculum are replaced by long acuminate trichomes directed toward the basal groove. F, Enlargement of short unicellular trichomes of speculum. Note large polygonal flattened bases and the cuticular striations that occur on trichome cell wall and that extends from base to apex. Scale bars: 500 μm (A, C); 50 μm (B, D, F); 150 μm (E).

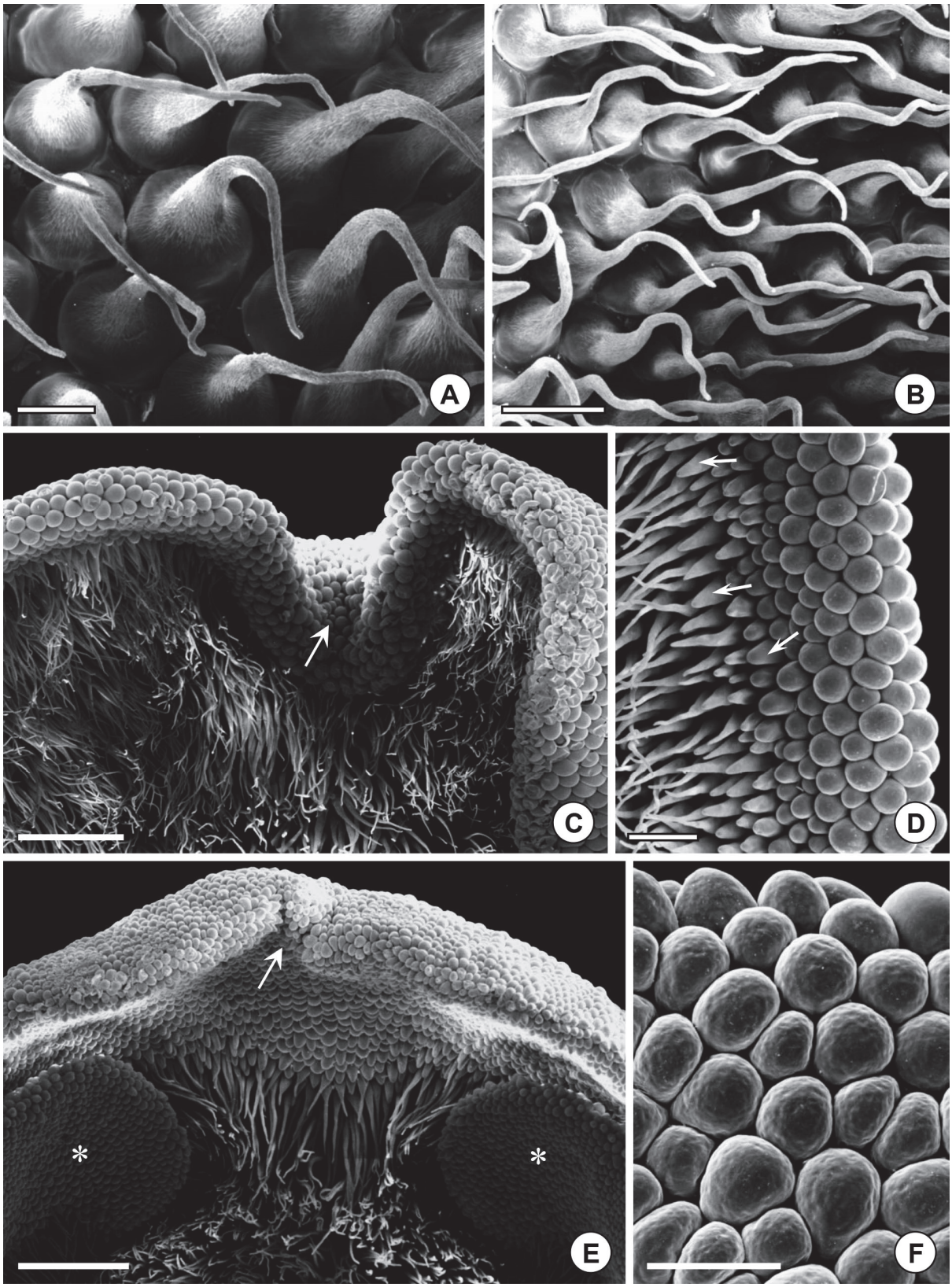

Figure 3. SEM micrographs showing the distribution and the type of epidermal cell that occurs on the adaxial surface of the apical region of the labellum of *Ophrys fusca* and *Ophrys lutea* at anthesis (A, B) and pre-anthesis (C–F). A, B, Long acuminate unicellular trichomes densely packed on typical villous indumentum of apical labellum of *O. fusca* (A) and *O. lutea* (B). Note the bent or sinuate form of trichome tips and the thin reticulate pattern defined by cuticular striations on trichome cell walls. C, Labellum apex of *O. fusca* showing central notch (arrow). A villous indumentum of long acuminate trichomes entirely covers this region except for the thin glabrous borders of the labellum. D, Detail

of glabrous margin of the labellum of *O. fusca* with characteristic dome-shaped papillae. Note that these epidermal cells become conical as they approach the villous indumentum (arrows). E, Apical part of the labellum of a floral bud of *O. lutea* in which the lateral lobes are not yet completely expanded (*). The central notch (arrow) and the villous indumentum covering only the proximal part of the apical portion of the labellum are apparent. Papillae similar to those occurring on the margins are present distally on the adaxial surface of the labellum. F, Dome-shaped papillae typically found at the margins and upon the abaxial surface of the apical labellum of *O. lutea*. Scale bars: 50 μm (A); 150 μm (B, D, F); 500 μm (C, E).

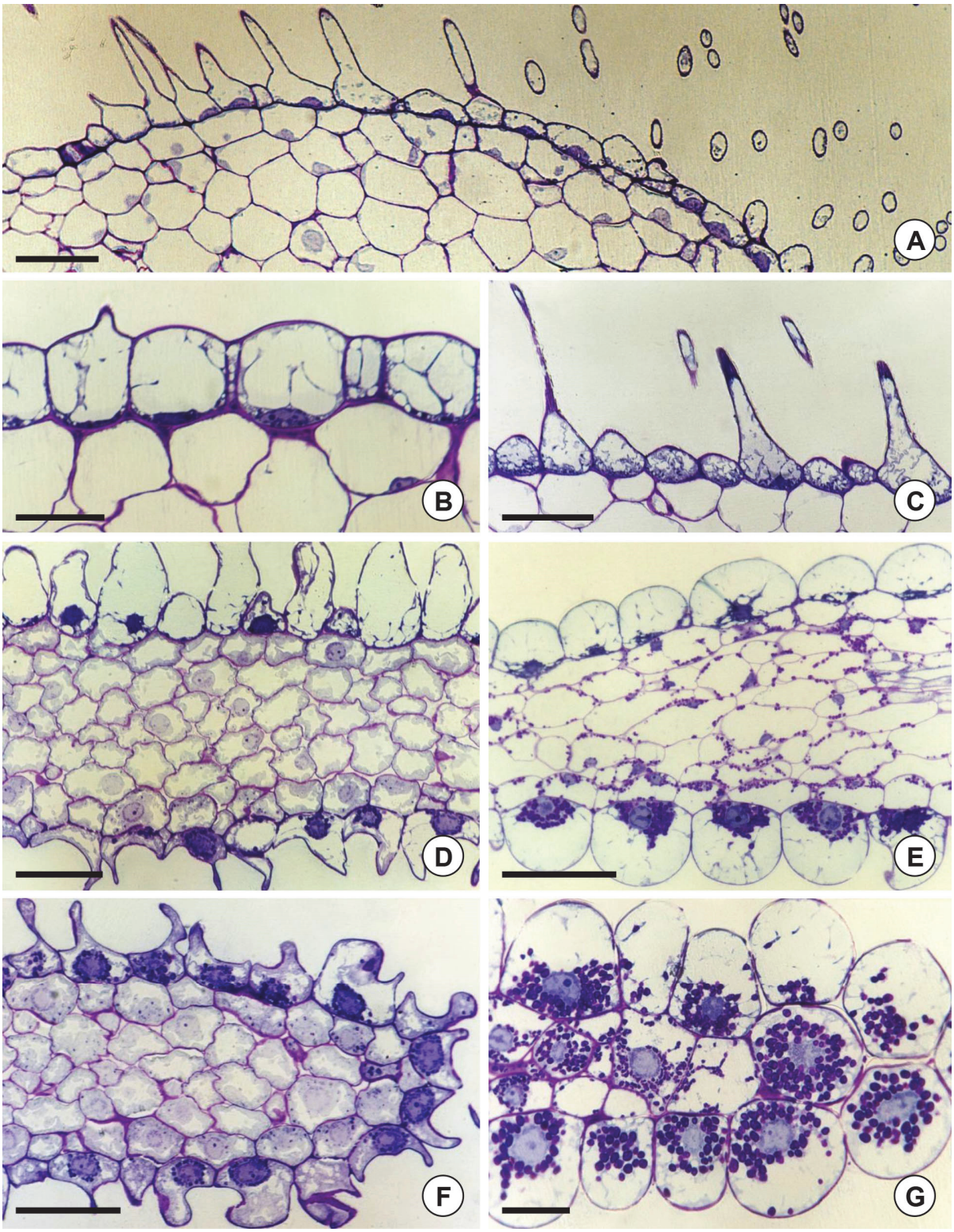

Figure 4. Light micrographs of sections from basal, median and apical regions of the labellum of *Ophrys fusca* and *Ophrys lutea*, sequentially stained with periodic acid–Schiff's reagent/toluidine blue. A, Transverse section of labellum basal region of *O. lutea* flower at anthesis, bearing unicellular trichomes of the basal groove oriented toward the stigmatic cavity (left). B, Transverse section of median portion of labellum of *O. fusca* at anthesis, clearly showing the adaxial speculum. Note the polarity exhibited by these epidermal cells. C, Transverse section of apical labellum of *O. lutea*, showing the adaxial, long acuminate unicellular trichomes of the villous indumentum. D, E, Transverse sections of distal part of the apical region of labellum of *O. fusca* (D) and *O. lutea* (E). F, Transverse section of border of apical part of labellum of *O. fusca* close to the central notch.

Papillose epidermal cells that appear reniform in section and contain dense cytoplasm are visible. G, Paradermal section of the margin of apical region of labellum of *O. lutea*. Large dome-shaped papillae, with abundant hypertrophied starch-rich plastids surrounding the nucleus are present. Scale bars: 100 μm (A, C–F); 50 μm (B, G).

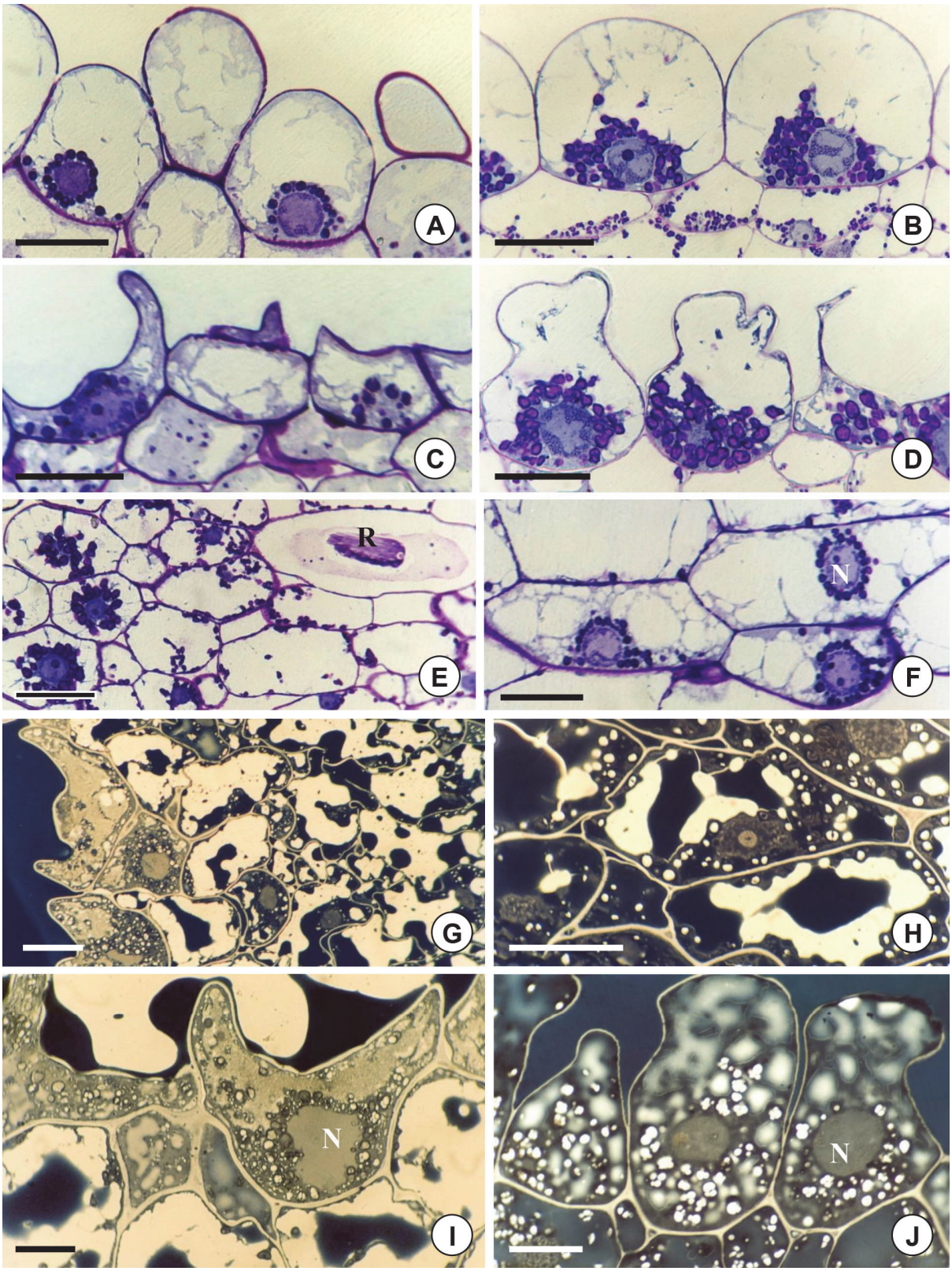

Figure 5. Light micrographs of sections of apical region and lateral lobes of labellum of *Ophrys fusca* and *Ophrys lutea*, sequentially stained with periodic acid–Schiff's reagent /toluidine blue (A–F) and stained with Sudan black B (G–J). A, B, Details of characteristic dome-shaped papillae from abaxial epidermis of apical region of labellum, near the central notch. A, *O. fusca*. B, *O. lutea*. The cells have a considerable degree of polarity and basally contain numerous spherical starch-rich plastids that display a perinuclear distribution. Note in B, the different size of plastids on the dome-shaped papillae and in the subjacent parenchyma cells. C, D, Details of papillae that are reniform to pyriform

in section from the abaxial epidermis near the notch. C, *O. fusca*. D, *O. lutea*. E, Oblique section through lateral lobe of labellum of *O. lutea* flower at pre-anthesis showing the abaxial epidermal and the subjacent parenchyma cells. An elliptical idioblast containing a raphide of calcium oxalate (R) can be seen in the parenchyma. F, Details of paradermal sections on the abaxial epidermis of a lateral lobe of *O. fusca* flower at anthesis. Note numerous small vacuoles fulfilling most part of the cell as well as hypertrophied globular starch-rich plastids surrounding the prominent nucleus (N). G, Transverse section of apical border of labellum of *O. lutea* in pre-anthesis. Reniform epidermal papillae with dense cytoplasm contrast to parenchyma cells that present large vacuoles with black-stained lipid material. H, Detail of parenchyma cells on apical border of *O. fusca* in pre-anthesis. Vacuoles containing lipophilic material are very clear. I, J, Transverse sections on reniform to pyriform epidermal papillae that occur on apical border of labellum of *O. lutea* in pre-anthesis. Several small vacuoles with black-stained interfaces occupy the apex of the cell, whereas numerous amyloplastids are close to the nucleus (N). Note in I, dark blue droplets in the cytoplasm and a Sudan-positive exudate on cell surface. Scale bars: 50 μm (A–G); 25 μm (H–J).

DISCUSSION

LABELLUM MICROMORPHOLOGY AND POLLINATION

The similarity in labellum micromorphology between *O. fusca* and *O. lutea* flowers found in the present study supports the inclusion of both species in section *Pseudophrys*, which was stated by Godfery (1928) and upheld by Devillers & Devillers-Terschuren (1994). Species from this section (*O. fusca, O. lutea* and *O. omegaifera* H. Fleischmann aggregates) differ from the other section, *Euophrys*, in several morphological features of the stigmatic cavity, the structure of the labellum, and the speculum configuration. Also, the type of pseudocopulation performed by the insect pollinators is different in both sections: abdominal in section *Pseudophrys* and cephalic in section *Euophrys* (Godfery, 1928; Devillers & Devillers-Terschuren, 1994; Delforge, 2001). Molecular phylogenetic analysis data also have shown that the *O. fusca–O. lutea* clade is well separated from the other *Ophrys* species (Pridgeon *et al.*, 1997; Soliva, Kocyan & Widmer, 2001). The different position adopted by pollinators upon the labellum during pseudocopulation is probably determined by particular features of the adaxial indumentum. As we have described, this indumentum is composed of unicellular trichomes that vary greatly in shape and size. In contrast, the abaxial part of the labellum, which plays no functional role in insect tactile stimulation, possesses an epidermis of slightly elongated flattened cells that become papillate at the margin, especially in the apical region.

The long trichomes present on the basal part of the labellum of *O. fusca* and *O. lutea* flowers may play a crucial role in the orientation of the excited male on the labellum. These trichomes probably guide the abdomen tip along the basal groove toward the stigmatic cavity (Kullenberg, 1961; Devillers & Devillers-Terschuren, 1994).

The well-defined speculum occurring on the central median region of the labellum of *Ophrys* may provide a secondary stimulus as insects approach the labellum, reinforcing the effect of the odor that acts as the primary attractive factor (Kullenberg, 1961). Indeed, the color and intense brightness of the speculum contrast with the darker background of the

adjacent regions of the labellum so that it resembles the wings of an insect (Moore, 1980; Delforge, 2001). The short unicellular trichomes of the speculum of *O. fusca* and *O. lutea* are similar to those observed on the speculum of *O. garganica* O.Danesch & E.Danesch and *O. promontorii* O.Danesch & E.Danesch, species included in *O. sphegodes* Miller aggregate (Servettaz *et al.*, 1994). Their large flattened bases and short tips with cuticular striations running from base to apex may explain, at least partially, the intense brightness of the speculum. In fact, the expanded bases of the speculum cells may act as a planar epidermis, which reflects most incident radiation. In addition, cuticular striations on lateral walls of trichomes may scatter emergent light, thereby increasing and maintaining the brightness of the speculum, regardless of the direction of viewing and the angle of incident light, as occurs on petal papillate cells (Kay, Daoud & Stirton, 1981).

The border of the labellum of both species and the entire distal part of the apical region of the labellum of *O. lutea* are considered to be the main sites of light reflection due to the presence of large, smooth, spherical papillae. Such remarkable epidermal papillae, already reported by Pais (1976), are similar to those described for the deflexed edge of the labellum of *O. garganica* and other related taxa (Servettaz *et al.*, 1994).

Ophrys fusca and *O. lutea* attract and seems to be pollinated by *Andrena* male bees in general (Kullenberg, 1961; van der Pijl & Dodson, 1966; Borg-Karlson & Tengö, 1986). However, in a recent paper, Schiestl & Ayasse (2002) reported *A. nigroaenea* as the specific pollinator of *O. fusca*. The micromorphological similarities between the *O. fusca* and *O. lutea*'s labella allow us to conclude, as did Kullenberg (1961), that the ability to stimulate the insect males, sexually excited by the odor, by means of tactile cues is probably similar in both species. As a result, the biologically isolating key factor between these two *Ophrys* species may be differences in the scent that they produce, which were identified by Borg-Karlson (1990).

LABELLUM ANATOMY AND HISTOCHEMISTRY

Anatomically, the most remarkable labellar structure in *O. fusca* and *O. lutea* is the border, particularly at the apical region near the central notch, where large spherical to dome-shaped papillae occur. Such cells, besides their high polarity, have features typical of secretory cells, namely, an enlarged nucleus with dense chromatin areas and abundant organelles.

Papillae considered on histochemical grounds to be osmophores (floral scent glands) are often located on the upper surface of the perianth and comprise a single secretory layer of well-differentiated epidermal cells and two to three layers of starch-rich parenchyma, which form a subsecretory tissue (Vogel, 1990). The staining reaction observed when living floral tissue was subjected to Vogel's test enabled us to identify presumed osmophores, although neutral red does not specifically stain this tissue (Stern *et al.*, 1986). The large

dome-shaped papillae on the marginal surface of the labella of *O. fusca* and *O. lutea* fulfill many of the criteria that characterize osmophore cells, such as considerable cell polarity, smooth convex outer tangential walls, large nuclei of the secretory epidermis, and abundant amyloplasts of the subsecretory parenchyma cells. Like the osmophores described for most orchids (Pridgeon & Stern, 1983; Pridgeon & Stern, 1985; Curry, 1987; Stern *et al.*, 1987; Curry *et al.*, 1991; Curry & Stern, 1991; Stpiczyńska, 1993), the osmophores of these two species, apparently comprise a secretory layer of epidermal cells and a subsecretory parenchyma tissue, which are located, in *O. fusca* and *O. lutea*, on both adaxial and abaxial surfaces of margins of the labellum. However, the major quantity of starch-rich plastids is found in epidermal cells, which contrasts with the typical distribution of starch on subepidermal tissue. Similar osmophore structure also occurs in some Ophrydeae spp. (Vogel, 1990).

The presence of lipophilic material inside vacuoles of both epidermal and parenchyma cells in the borders of the labella of *O. fusca* and *O. lutea* provides evidence for the involvement of these tissues in the secretory process, thereby constituting the osmophore in both species. However, some lipoidal material, owing to its low molecular mass and high volatility, is immediately discharged into the atmosphere or easily extracted from its storing sites, the vacuoles, probably following dehydration of the specimens. Black-stained interfaces between small vacuoles occurring in some epidermal cells may be the result of this leaching process. The lipids were not preserved in specimens fixed only with glutaraldehyde and infiltrated with Historesin, a hydrophilic embedding material. More complex lipids with higher molecular masses may accumulate within and even outside the cells, forming an exudate (Vogel, 1990).

The large amount of starch in the numerous amyloplasts in the secretory and subsecretory cells may be used as a source of energy or carbon for the biosynthesis of fragrant metabolites. Generally, following secretion, the osmophores cells develop a larger vacuome, which is accompanied by a marked depletion in starch (Stern *et al.*, 1987). We do not, however, know whether this sequence of cellular events occurs in *O. fusca* and *O. lutea*. Ultrastructural studies are under way to obtain more detailed information on these peculiar osmophores.

In conclusion, the labella of *O. fusca* and *O. lutea* present an adaxial surface consisting of four different types of epidermal cells arranged into well-defined color areas. Unlike the abaxial epidermis, the adaxial indumentum may provide important tactile and visual stimulation to the pollinator insects. Moreover, the entire border and the abaxial surface from the distal part of the apical region of the labellum together constitute the osmophore. In both species, it consists of a secretory papillate epidermis and two or three subsecretory parenchyma layers.

REFERENCES

Ayasse M, Schiestl FP, Paulus HF, Löfstedt C, Hansson B, Ibarra F, Francke W. 2000. Evolution of reproductive strategies in the sexually deceptive orchid *Ophrys sphegodes*: how does flower-specific variation of odor signals influence reproductive success? *Evolution* **54:** 1995-2006.

Ayasse M, Schiestl FP, Paulus HF, Ibarra F, Francke W. 2003. Pollinator attraction in a sexually deceptive orchid by means of unconventional chemicals. *Proceedings of the Royal Society B: Biological Sciences* **270:** 517-522.

Borg-Karlson A-K, Tengö J. 1986. Odor mimetism? Key substances in *Ophrys lutea* - *Andrena* pollination relationship (Orchidaceae: Andrenidae). *Journal of Chemical Ecology* **12:** 1927-1942.

Borg-Karlson A-K. 1990. Chemical and ethological studies of pollination in the genus *Ophrys* (Orchidaceae). *Phytochemistry* **29:** 1359-1387.

Bronner R. 1975. Simultaneous demonstration of lipids and starch in plant tissues. *Stain Technology* **50:** 1-4.

Curry KJ. 1987. Initiation of terpenoid synthesis in osmophores of *Stanhopea anfracta* (Orchidaceae): a cytochemical study. *American Journal of Botany* **74:** 1332-1338.

Curry KJ, McDowell LM, Judd WS, Stern WL. 1991. Osmophores, floral features, and systematics of *Stanhopea* (Orchidaceae). *American Journal of Botany* **78:** 610-623.

Curry KJ, Stern WL. 1991. Osmophore development in *Kegeliella houtteana* (Stanhopeinae - Orchidaceae). *American Journal of Botany* **78 (Supplement):** 22-23.

Dafni A. 1984. Mimicry and deception in pollination. *Annual Review of Ecology and Systematics* **15:** 259-278.

Delforge P. 2001. *Guide des orchidées d'Europe, d'Afrique du Nord et du Proche-Orient.* 2nd ed. Paris: Delachaux et Niestlé S.A.

Devillers P, Devillers-Terschuren J. 1994. Essai d'analyse systématique du genre *Ophrys*. *Les Naturalistes belges* **75 (Orchidées 7):** 273-400.

Feder N, O'Brien TP. 1968. Plant microtechnique: some principles and new methods. *American Journal of Botany* **55:** 123-142.

Godfery MJ. 1928. Classification of the genus *Ophrys*. *The Journal of Botany, British and Foreign* **66:** 33-36.

Johansen DA. 1940. *Plant microtechnique.* New York: McGraw-Hill.

Kay QON, Daoud HS, Stirton CH. 1981. Pigment distribution, light reflection and cell structure in petals. *Botanical Journal of the Linnean Society* **83:** 57-84.

Kullenberg B. 1961. Studies in *Ophrys* pollination. *Zoologiska Bidrag fran Uppsala* **34:** 1-340.

Moore DM. 1980. Orchidaceae. In: Tutin TG, Heywood VH, Burges NA, Moore DM, Valentine DH, Walters SM, Webb DA, eds. *Flora Europaea, Vol. 5.* Cambridge: Cambridge University Press, 325-350.

Nilsson LA. 1992. Orchid pollination biology. *Trends in Ecology and Evolution* **7:** 255-259.

Pais MS. 1976. Quelques données sur la sécrétion chez les Orchidées. *Bulletin de la Societé Botanique de France* **123:** 149-159.

Paulus HF, Gack C. 1981. Neue Beobachtungen zur Bestäubung von *Ophrys* (Orchidaceae) in Südspanien, mit besonderer Berücksichtigung des Formenkreises *Ophrys fusca* agg. *Plant Systematics and Evolution* **137:** 241-258.

van der Pijl L, Dodson CH. 1966. *Orchids flowers, their pollination and evolution.* Coral Gables, Florida: University of Miami Press.

Pridgeon AM, Stern WL. 1983. Ultrastructure of osmophores in *Restrepia* (Orchidaceae). *American Journal of Botany* **70:** 1233-1243.

Pridgeon AM, Stern WL. 1985. Osmophores of *Scaphosepalum* (Orchidaceae). *Botanical Gazette* **146:** 115-123.

Pridgeon AM, Bateman RM, Cox AV, Hapeman JR, Chase MW. 1997. Phylogenetics of the subtribe Orchidinae (Orchidoideae, Orchidaceae) based on nuclear ITS sequences. 1. Intergeneric relationships and polyphyly of *Orchis sensu lato*. *Lindleyana* **12:** 89-109.

Rudall PJ, Bateman RM, Fay MF, Eastman A. 2002. Floral anatomy and systematics of Alliaceae with particular reference to *Gilliesia*, a presumed insect mimic with strongly zygomorphic flowers. *American Journal of Botany* **89:** 1867-1883.

Schiestl FP, Ayasse M, Paulus HF, Löfstedt C, Hansson BS, Ibarra F, Francke W. 1999. Orchid pollination by sexual swindle. *Nature* **399:** 421-422.

Schiestl FP, Ayasse M, Paulus HF, Löfstedt C, Hansson BS, Ibarra F, Francke W. 2000. Sex pheromone mimicry in the early spider orchid (*Ophrys sphegodes*): patterns of hydrocarbons as the key mechanism for pollination by sexual deception. *Journal of Comparative Physiology A* **186:** 567-574.

Schiestl FP, Ayasse M. 2002. Do changes in floral odor cause speciation in sexually deceptive orchids? *Plant Systematics and Evolution* **234:** 111-119.

Servettaz O, Bino Maleci L, Grünanger P. 1994. Labellum micromorphology in the *Ophrys bertolinii* agg. and some related taxa (Orchidaceae). *Plant Systematics and Evolution* **189:** 123-131.

Soliva M, Kocyan A, Widmer A. 2001. Molecular phylogenetics of the sexually deceptive orchid genus *Ophrys* (Orchidaceae) based on nuclear and chloroplast DNA sequences. *Molecular Phylogenetics and Evolution* **20:** 78-88.

Stern WL, Curry KJ, Whitten WM. 1986. Staining fragrance glands in orchid flowers. *Bulletin of the Torrey Botanical Club* **113:** 288-297.

Stern WL, Curry KJ, Pridgeon AM. 1987. Osmophores of *Stanhopea* (Orchidaceae). *American Journal of Botany* **74:** 1323-1331.

Stpiczyńska M. 1993. Anatomy and ultrastructure of osmophores of *Cymbidium tracyanum* Rolfe (Orchidaceae). *Acta Societatis Botanicorum Poloniae* **62:** 5-9.

Stpiczyńska M. 2001. Osmophores of the fragrant orchid *Gymnadenia conopsea* L. (Orchidaceae). *Acta Societatis Botanicorum Poloniae* **70:** 91-96.

Vogel S. 1990. *The role of scent glands in pollination: on the structure and function of osmophores.* Rotterdam: A. A. Balkema. [English translation of: Vogel S. 1963. Duftdrüsen im Dienste der Bestäubung: Über Bau und Funktion der Osmophoren. *Akademie der Wissenschaften und der Literatur in Mainz, Abhandlungen der Mathematisch-Naturwissenschaftlichen Klasse* **10**: 600-763].

CHAPTER 3

STRUCTURE OF THE OSMOPHORE AND LABELLUM MICROMORPHOLOGY IN THE SEXUALLY DECEPTIVE ORCHIDS *OPHRYS BOMBYLIFLORA* AND *OPHRYS TENTHREDINIFERA* (ORCHIDACEAE)

This chapter was published in *International Journal of Plant Sciences*:

Francisco A. and Ascensão L. 2013. Structure of the osmophore and labellum micromorphology in the sexually deceptive orchids *Ophrys bombyliflora* and *Ophrys tenthredinifera* (Orchidaceae). *International Journal of Plant Sciences*, 174: 619-636.

STRUCTURE OF THE OSMOPHORE AND LABELLUM MICROMORPHOLOGY IN THE SEXUALLY DECEPTIVE ORCHIDS *OPHRYS BOMBYLIFLORA* AND *OPHRYS TENTHREDINIFERA* (ORCHIDACEAE)

ABSTRACT

Premise of the research. The insect-like flowers of the *Ophrys* orchids are adapted to sexual deceptive pollination through pseudocopulation, providing chemical, visual, and tactile stimuli for male insects. Although the chemical composition of the odor bouquet of several species has long been identified, the precise site of fragrance production in the labellum remains unknown for most species, and little attention has been given to the visual and tactile signals provided by the labellum for pollinators. Here, the occurrence of an osmophore is investigated and the labellum micromorphology is characterized in detail for *Ophrys bombyliflora* and *Ophrys tenthredinifera*, two closely related species pollinated by *Eucera* bees.

Methodology. Labella of flowers before and at anthesis were studied with scanning electron microscopy, light microscopy, and histochemistry.

Pivotal results. The labellum of *O. bombyliflora* presents a distinctive hidden apical appendix that forms a concavity with a multicelullar protuberance and a tuft of trichomes at the tip. An osmophore occurs in the apical region of the labellum in both species; in *O. bombyliflora* it is confined mostly to the adaxial surface of the appendix, and in *O. tenthredinifera* it comprises the labellum margin and the abaxial surface of both the appendix and the adjacent region of the labellum. A terpene-rich lipophilic secretion likely containing a phenolic fraction was found. The two species have a great diversity of epidermal cell types in the adaxial surface of the labellum and differ mainly in the micromorphology of the basal field, speculum, labellum margins, and appendix.

Conclusions. This study demonstrates for the first time that a specialized secretory structure (osmophore) occurs in the labellum of both species and synthesizes a secretion that probably includes highly volatile long-range attractants for pollinators. This finding seems to suggest that two sources of potential semiochemicals have evolved in the *Ophrys* labellum for pollinator attraction.

KEYWORDS: anatomy; labellum micromorphology; long-range pollinator attraction; *Ophrys*; osmophore; pseudocopulation.

INTRODUCTION

Pollination by sexual deception is one of the most remarkable specialized pollination systems in angiosperms, in which rewardless flowers lure mate-seeking male insects by mimicking the female's attractive signals (Pouyanne, 1917). Sexual mimicry typically implies a highly specific interaction between the plant and one or few closely related pollinator species, since the attraction of male insects to the flowers is primarily mediated by an odor signal identical to the species-specific female sex pheromone (Schiestl *et al.*, 1999; Ayasse *et al.*, 2003; Peakall *et al.*, 2010). The majority of sexually deceptive species are terrestrial orchids occurring in Australia and Europe, although this pollination syndrome, almost exclusive to Orchidaceae (with only two confirmed exceptions, one in Asteraceae and one in Iridaceae; Ellis & Johnson, 2010; Vereecken *et al.*, 2012), has been also reported in some orchid species in South Africa, New Zealand, and Central and South America (Gaskett, 2011, and references therein).

Flowers of the Mediterranean genus *Ophrys* L. (Orchidaceae: Orchidinae), reputedly known for their visual resemblance to insects, are highly adapted to sexual deceptive pollination through pseudocopulation, in which male insects, during copulation attempts with the labellum, remove pollinaria with the head or the abdomen tip and enable cross-pollination by visiting another flower from the same species (Pouyanne, 1917). *Ophrys* orchids are mostly pollinated by bees, but some have wasps or, less frequently, beetles as regular pollinators (Kullenberg, 1961; Paulus, 2006).

The success of the pseudocopulation in *Ophrys* resides predominantly in the special traits of the labellum of the flowers. The distinctive labellar features, totally absent in the flowers of the other genera in the subtribe Orchidinae, turn the *Ophrys* labellum into a suitable mimic of the pollinator's female, providing three categories of stimuli (chemical, visual, and tactile) for their male pollinators (Kullenberg, 1961; Devillers & Devillers-Terschuren, 1994). First, the labellum releases a complex odor bouquet that attracts mate-seeking insects from relatively long distances (Kullenberg, 1961). The floral scent contains a set of semiochemicals identical to the sex pheromone of pollinator's females, which triggers mating behavior in insect males, thereby constituting a highly specific chemical stimulus for pollinators (Schiestl *et al.*, 1999; Mant *et al.*, 2005; Stökl *et al.*, 2008). Second, the shape and color patterns of the labellum are assumed to provide, at least in some *Ophrys* species, close-range visual stimulation for pollinators; the contrasting pigmentation and high reflectivity of its central region, the speculum, make it similar to the insect's wings (Kullenberg, 1961; Paulus, 2006). Third, the strong three-dimensional topology and robustness of the labellum, together with the specific arrangement of diverse stiff trichomes into well-defined areas, offer a crucial tactile stimulus for insect males after they land on the labellum, encouraging them to acquire the correct position for pollination (Kullenberg & Bergström, 1976; Ågren, Kullenberg & Sensenbaugh, 1984).

The floral scent is the key primary stimulus presiding at all stages of the pollination event. Continual chemical stimulation of pollinators is required in long-range attraction and in the approach flight and landing as well as during the tactile stimulation provided by the adaxial surface of the labellum (Kullenberg & Bergström, 1976). Most research in *Ophrys* pollination has been thus focused on the floral scent, giving particular attention to the small set of behaviorally active semiochemicals involved in the chemical mimicry, which are predominantly low-volatile long-chain hydrocarbons (Ayasse, Stökl & Francke, 2011, and references herein) generally found among the common constituents of the cuticular waxes that cover the aerial plant organs (Kunst, Samuels & Jetter, 2005). In most *Ophrys* species investigated so far that are pollinated by males of the solitary bees of genera *Andrena* and *Colletes*, the specificity of the signal is achieved by varying the relative proportions of the different alkenes in the mixture (Mant *et al.*, 2005; Stökl *et al.*, 2008; Stökl *et al.*, 2009; Schlüter *et al.*, 2011). However, in two *Ophrys* species pollinated by males of the eusocial bumblebee *Bombus vestalis*, the compounds considered decisive in pollinator attraction, because they elicit mating behavior in males, were found to be a polar fraction of aliphatic aldehydes, alcohols, fatty acids, and corresponding esters (Gögler *et al.*, 2009; Gögler *et al.*, 2011). Polar compounds, particularly a few uncommon, highly specific oxygenated carboxylic acids, are also the key semiochemicals in *Ophrys speculum*, which is pollinated by a single species of solitary wasp, *Dasyscolia ciliata* (Ayasse *et al.*, 2003). For *Ophrys* species pollinated by other genera of hymenopterans, such as *Eucera* solitary bees, the key attractive scent compounds remain to be identified.

However, behaviorally active semiochemicals are only a small fraction of the multicomponent odor bouquet of *Ophrys* flowers, which encompasses more than 100 organic compounds of different volatility (Borg-Karlson, 1990; Ayasse *et al.*, 2003). For most species investigated, these key attractive compounds are part of the lower-volatile fraction of the bouquet and therefore are expected to be recognized by pollinators at close range or upon contact with the labellum surface (Ayasse *et al.*, 2011). We thus suppose that other components of the floral scent attract pollinators from long distances. Indeed, higher-volatile aliphatic hydrocarbons, alcohols, aldehydes, and esters, as well as oxygenated mono- and sesquiterpenes and a few aromatic compounds, were found to be emitted from the labellum and to act mainly as long-range attractants for pollinators (Kullenberg, Borg-Karlson & Kullenberg, 1984; Borg-Karlson, 1990). Even though the chemical constituents of the odor bouquet have been identified for several *Ophrys* species, the precise site of production of the fragrance has received little attention (Vogel, 1990; Ascensão *et al.*, 2005), and the cells involved in its biosynthesis and emission remain poorly studied. Considering the singular features of the *Ophrys* labellum, we expect that rather than being diffusely emitted, the odor is produced in a specialized secretory structure termed an “osmophore”.

Osmophores are exposed secretory floral structures specialized in the biosynthesis and emission of highly volatile attractants for pollinators (Vogel, 1990). These scent-producing glands, particularly frequent in families Orchidaceae, Araceae and Apocynaceae (Asclepiadoideae) (Stern, Curry & Pridgeon, 1987; Vogel, 1990; Skubatz *et al.*, 1996; Płachno, Świątek & Szymczak, 2010), typically occupy a location in the flower that promotes rapid odor diffusion, and in orchids these are often morphologically well-differentiated regions, restricted to either the long antenniform, club- or brush-shaped appendages at the tips of sepals or petals or to the callus in the basal hypochile of the labellum (Pridgeon & Stern, 1983; Stern *et al.*, 1987; Vogel, 1990; Teixeira, Borba & Semir, 2004). However, undifferentiated osmophores are also found in orchid species and are particularly common in the terrestrial tribe Orchideae, where they cover the entire labellum lamina or only the marginal regions of the labellum or the lateral petals (Vogel, 1990; Steiner, Whitehead & Johnson, 1994; Stpiczyńska, 2001; Ascensão *et al.*, 2005; Peter *et al.*, 2009). In the genus *Ophrys*, osmophores were found in the labella of *O. fusca* and *O. lutea* by Ascensão et al. (2005), confirming the early results obtained by Vogel in the 1960s, who also mentioned an osmophore in the apical appendix of *O. fuciflora* (Vogel, 1990). Whether the other species of the genus present a specialized structure for fragrance emission in the labellum has hitherto remained unknown.

Ophrys bombyliflora Link and *Ophrys tenthredinifera* Willd. belong to the section *Ophrys* (synonym of section *Euophrys* Godfery 1928 nom. nud.), which traditionally comprises all species pollinated by male insects that perform cephalic pseudocopulation with the labellum, removing the pollinaria with the head (Godfery, 1928; Devillers & Devillers-Terschuren, 1994). Unlike the flowers of species included in the other section, *Pseudophrys*, whose pollinaria are placed on the abdomen tip of pollinators, those of the section *Ophrys* present an ornamented stigmatic cavity bearing pseudoeyes and a labellum provided with a distinct basal field and also a particularly diverse speculum (Devillers & Devillers-Terschuren, 1994). An apical appendix in the labellum also occurs in the vast majority of the species of this section, never occurring in the species of the section *Pseudophrys*. In the past decade, molecular phylogenetic analyses revealed that the section *Ophrys* is paraphyletic. *Ophrys bombyliflora*, *O. tenthredinifera*, and *O. speculum* s.l. appear to have a close relationship with each other and with the species belonging to the monophyletic section *Pseudophrys*, together forming a clade in the phylogenetic trees (Soliva, Kocyan & Widmer, 2001; Devey *et al.*, 2008). However, the relative positions of these taxa within the clade are not yet sufficiently clear.

It has long been documented that *O. bombyliflora* and *O. tenthredinifera* are pollinated by different male solitary bees of the genus *Eucera* (Hymenoptera: Apidae) at different locations throughout their distributional geographical areas. Male bees of *Eucera oraniensis*, *E. algira* and *E. eucnemidea* have been recorded as pollinators of *Ophrys bombyliflora* whereas male *E. nigrilabris*, *E. dimidiata*, *E. clypeata*, *E. notata* and *E. longicornis* are

confirmed pollinators of *O. tenthredinifera* (Kullenberg, 1973a; Lara Ruiz, 2010; Gaskett, 2011 and references therein). These *Ophrys-Eucera* pollination relationships remain poorly studied, especially with respect to the chemical signals that regulate male mating behavior (Kullenberg *et al.*, 1984; Borg-Karlson, 1990). Moreover, information about the labellar visual and tactile signals assumed to be crucial for the success of the pseudocopulation by a nearby pollinator is scarce, particularly for these two *Ophrys* species (Ågren *et al.*, 1984; Servettaz, Bino Maleci & Grünanger, 1994; Ascensão *et al.*, 2005; Cortis *et al.*, 2009; Bradshaw *et al.*, 2010). Despite the recent comprehensive comparative labellum micromorphology survey of 32 taxa of the genus *Ophrys* by Bradshaw *et al.* (2010), detailed and more focused studies on particular groups were reported only for some species in the groups of *O. sphegodes* and *O. fusca* (Servettaz *et al.*, 1994; Ascensão *et al.*, 2005).

This study aimed to investigate the occurrence of an osmophore in the labellum of *O. bombyliflora* and *O. tenthredinifera*, which we expect to be the site of synthesis and release of the highly volatile scent compounds responsible for the long-range attraction of pollinators. Furthermore, we characterize in detail the labellum micromorphology of these two species in order to find new characteristics that could act as close-range visual and/or tactile signals for pollinators.

MATERIAL AND METHODS

PLANTS

Inflorescences of *Ophrys bombyliflora* Link and *Ophrys tenthredinifera* Willd. were collected in February and March, between 2005 and 2009, from natural populations occurring throughout the central-western region of Portugal. A voucher specimen of each species was deposited in LISU, the Herbarium of the University of Lisbon Botanical Garden, Portugal (LISU 231243 and LISU 231245).

Three different developmental stages of the flower were investigated in the present study: (1) early bud, buds with dimensions of 5 x 3 to 6 x 4 mm (length x width) in *O. bombyliflora* and 7 x 4 to 8 x 5 mm in *O. tenthredinifera,* corresponding to 3–7 and 4–9 days before the anthesis, respectively; (2) late bud, buds with dimensions of 7 x 4 to 8 x 6 mm (length x width) in *O. bombyliflora* and 8 x 6 to 10 x 7 mm in *O. tenthredinifera*, corresponding to 1–2 and 1–3 days before anthesis, respectively; and (3) freshly opened flower, flowers at the beginning of anthesis.

MICROMORPHOLOGY OF THE LABELLUM AND THE STIGMATIC CAVITY

Five freshly opened flowers and two late buds of each species were fixed for scanning electron microscopy (SEM) with 2.5% glutaraldehyde in 0.1 M sodium phosphate buffer, at pH 7.2. Samples were kept in fixative under vacuum at room temperature for 20 min, followed by 48–72 h at 4^{o}C. The material was then washed in the fixative buffer, dehydrated

in a graded acetone series, critical-point dried with CO_2 and coated with gold. Observations were carried out on a JEOL T220 scanning electron microscope (JEOL, Tokyo) at an accelerating voltage of 15 kV. Images were recorded in a Kodak T-Max 100 professional black-and-white negative film with a MAMIYA 6 x 7 camera.

The terminology used for the external morphological description of the flower follows Devillers & Devillers-Terschuren (1994), whereas the nomenclature of trichomes and indumentum follows the glossary of Payne (1978). The description of the epidermal cell types is based on their surface characteristics, namely, the curvature of the outer cell wall, the cell outline, and the cuticular sculpture, following the terminology of Kay *et al.* (1981) and Koch *et al.* (2008).

LABELLUM VASCULATURE

Two opened flowers of each species, fixed with FAA (formaldehyde : glacial acetic acid : 50% ethanol, 1:1:18, v/v) under vacuum at room temperature for 24 h, were cleared by the method of diaphanization described by Shobe & Lersten (1967). Cleared flowers were stained with 1% ethanol solution of safranin O (w/v) for 30 min. After a washing in ethanol, the flowers were kept immersed in this alcohol and observed using an Olympus SZH-ILLK stereomicroscope (Olympus Optical, Tokyo). Images were recorded digitally with an Olympus C-7070 Wide Zoom digital camera (Olympus Imaging, Tokyo).

OSMOPHORE LOCATION

For the macroscopic identification of fragrance-producing areas in the flowers, elective vital staining with diluted neutral red (Vogel, 1990) was used. Three late buds and six freshly opened flowers of each species were immersed in 0.01% neutral red for 2–5 h. After staining, flowers were rinsed in tap water and examined under the stereomicroscope. Images were recorded digitally.

LABELLUM ANATOMY

To follow the histological and cytological changes during the flower development, pieces of labellum taken from early buds, late buds, and freshly opened flowers of the two *Ophrys* species were processed for anatomical study under light microscopy. Samples were fixed as described for SEM, but after the washing in the fixative buffer and dehydration through an ethanol series, they were infiltrated with and embedded in Leica Historesin. Sections 2 µm thick were cut with a Leica RM-2155 microtome (Leica Microsystems, Nussloch, Germany). Sections were sequentially stained with periodic acid–Schiff (PAS) reagent/toluidine blue O (Feder & O'Brien, 1968) or toluidine blue O with pretreatment with sodium hypochlorite plus post-staining with dilute Lugol (Gutmann, 1995), for general

histology and for total polysaccharides and starch. Sudan black B was used for detection of lipids and tannins (Bronner, 1975; Parham & Kaustinen, 1976), with appropriate controls.

Portions of the apical appendix of the labellum taken from flowers of both species at all three developmental stages were also fixed with 2.5% glutaraldehyde in 0.1 M sodium phosphate buffer at pH 7.2 for 12-16 h at 4^{o}C and post-fixed with 2% osmium tetroxide for 1 h at room temperature. After dehydration in a graded acetone series, samples were embedded in Epon-Araldite resin (Electron Microscopy Sciences, Fort Washington, PA). Semithin sections (≈0.5 µm thick) were obtained on a Sorvall MT-1 ultramicrotome (Sorvall, Norwalk, CT) and stained with Sudan black B for lipids and tannins (Bronner, 1975; Parham & Kaustinen, 1976). Observations were made with a Leica DM-2500 microscope (Leica Microsystems, Wetzlar, Germany), and images were recorded digitally with a Leica DFC-420 camera (Leica Microsystems, Heerbrugg, Switzerland) and the Leica Application Suite software (ver. 2.8.1).

HISTOCHEMISTRY

For the histochemical characterization of the osmophore, transverse and longitudinal hand-cut sections of the apical appendix of labellum were made in fresh late buds and opened flowers from both species. Neutral red was used as a vital stain to locate glandular cells (Vogel, 1990) and as a lipid fluorochrome for detection of lipids under UV and blue light (Kirk, 1970). Sections were tested for total lipids with Sudan IV and Sudan black B (Pearse, 1985), for unsaturated lipids with osmium tetroxide (Ganter & Jollès, 1969), and for terpenoids with Nadi reagent (David & Carde, 1964). Phenolic compounds were detected by their autofluorescence under UV and blue light (Harborne, 1998). Negative control reactions for each histochemical test were carried out simultaneously. Observations under UV and blue wavelengths were made with a Leitz SM-LUX epifluorescence microscope (Leitz-Wetzlar, Wetzlar, Germany) equipped with an HBO 50-W mercury vapor lamp, filter block A (excitation filter BP 340-380, dichroic mirror 450, and barrier filter LP-430), and filter block I2 (excitation filter BP 450-490 and barrier filter LP-515). Images were recorded on Kodak Ultra Gold 400 ASA color slide film with a Leica Wild MPS-52 camera (Leica, Vienna). Otherwise, observations were made with the Leica DM-2500 microscope, and images were recorded digitally.

RESULTS

Ophrys bombyliflora and *Ophrys tenthredinifera* are two morphologically distinct species, easily identifiable by several particular characteristics of their labella. The flower of *O. bombyliflora* bears a small, strongly convex labellum that is subglobular in shape. The labellum is clearly trilobed, having two hirsute, gibbous lateral lobes and a mostly velutinous central labellum lobe that presents a broad glabrous margin, abruptly folded downward.

Most significantly, the central labellum lobe terminates with a unique reflexed, fleshy, thick appendix that is hidden at the back of the labellum when the flower is seen in front view (Figs. 1A, 2A–E). By contrast, the *O. tenthredinifera* labellum is wide and moderately convex, with flattened margins and a subtrapezoidal shape. The labellum is entire or slightly trilobed and typically presents a complete submarginal band covered with a hirsute indumentum and a glabrous reflexed apical appendix turned up in front of the labellum (Figs. 1B, 2G, H).

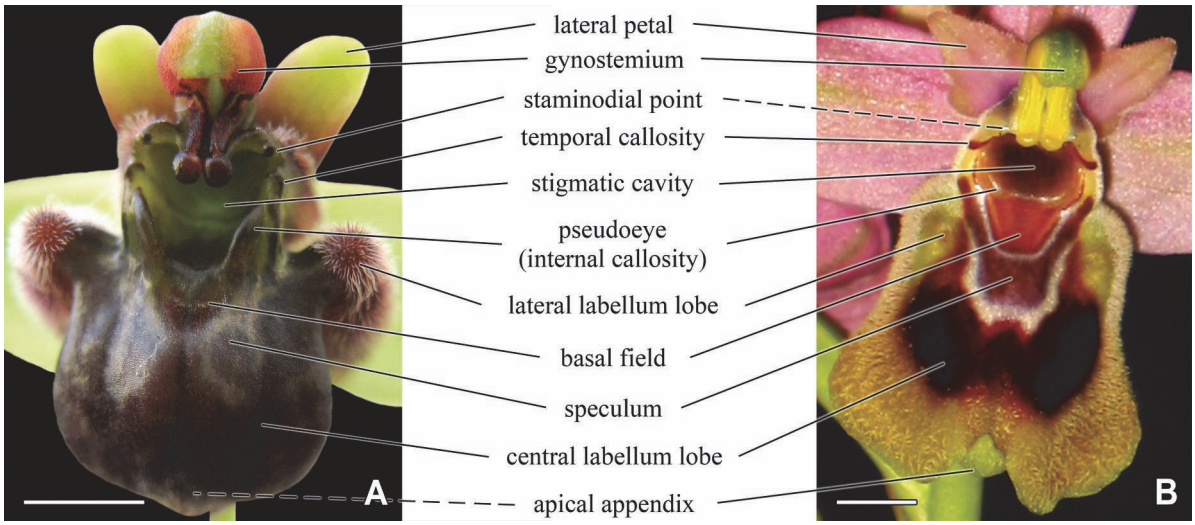

Figure 1. Macrographs of flowers of *Ophrys bombyliflora* (A) and *O. tenthredinifera* (B), illustrating their principal morphological elements (in front view). Scale bars: 3 mm.

MICROMORPHOLOGY OF THE STIGMATIC CAVITY

In the *Ophrys* flower, the fusion of the gynostemium and the labellum results in a distinctive stigmatic cavity provided with several ornamentations that occurs in contiguity with the basal region of the labellum, the stigmatic surface being placed at the ceiling of the cavity. The stigmatic cavities of *O. bombyliflora* and *O. tenthredinifera* differ in structural details. Both species have a glabrous, hemispherical stigmatic cavity comprising a flat floor flanked by two internal labia or crests that constitute the innermost portion of the cavity walls (Fig. 1). Each labium produces a shining globular or elongated protuberance at the tip, the internal callosity, which constitutes the pseudoeye. However, *O. bombyliflora* presents a larger and more robust stigmatic cavity, with protruding internal labia and a markedly concave outline. In the two species, a pair of dark temporal callosities occur at the outermost portion of the cavity walls, and two staminodial points are evident at the uppermost part of the cavity, especially in *O. bombyliflora* (Fig. 1). The stigmatic cavity of the two species is essentially composed of flat or lenticular cells with an elongated polygonal outline, which present a heterogeneous cuticular pattern on their surfaces. Cuticular striations running parallel to the longitudinal axis of the cell occur in the central field of the cell surface, whereas cuticular folds parallel to each other cross the anticlinal field perpendicularly (Figs. 3C, 4B, D, and, available in the online edition of the *International*

Journal of Plant Sciences, Fig. A1D). At the external face of the internal labia in *O. bombyliflora*, very dense and long cuticular depositions over specific sites of the cell walls are occasionally found across adjacent cells (Fig. 3C). The cuticular ornamentation of the floor and walls of the stigmatic cavity varies greatly toward the region occupied by the pseudoeyes. Both species present the tip of the internal callosity (pseudoeye) composed of lenticular cells with smooth, depressed anticlines and fine, diffuse cuticular striations over the outer tangential walls (Fig. 4E). However, the slope that supports the pseudoeye in *O. bombyliflora* is occasionally provided with thick prominent cuticular ridges extended over contiguous cells, which give the region a sulcate texture (Fig. 3B). Likewise, in *O. tenthredinifera*, the surface sculpture is different near the pseudoeye from that elsewhere on floor of the stigmatic cavity (Fig. 4D).

MICROMORPHOLOGY OF THE LABELLUM

The labellum in both species can be divided into three main regions: (1) the basal region comprises the basal field and the lateral lobes; (2) the median region is mostly occupied by the central speculum; and (3) the apical region, covered with a dense indumentum, terminates in the reflexed appendix (Fig. 1). While *O. tenthredinifera* presents a small, well-defined, shield-shaped blue speculum delimited by a narrow whitish-colored contour, *O. bombyliflora* has a frequently larger but less clearly defined bilobed, shield-shaped speculum surrounded by a grayish-colored diffuse area that can extend laterally to the base of lateral lobes (Fig. 1).

Some morphological variation was observed among the individuals examined in this study. In *O. bombyliflora*, variation occurs basically in the extent, coloration, and contrast of the speculum as well as in the size of the basal field. On the other hand, the flowers of *O. tenthredinifera* vary slightly in the shape of both the speculum and the appendix, in the length of the tuft above the appendix, and in the coloration of the submarginal apical pilosity of the labellum.

Scanning electron microscope observations revealed a great diversity of epidermal cell types on the adaxial surface of the labellum in both species. Conversely, the abaxial surface is entirely characterized by typical smooth pavement cells, i.e., elongated tabular or lenticular epidermal cells (Fig. A2F, available in the online edition of the *International Journal of Plant Sciences*), which in *O. tenthredinifera* become larger and dome shaped toward the margin, especially in the apical region of labellum.

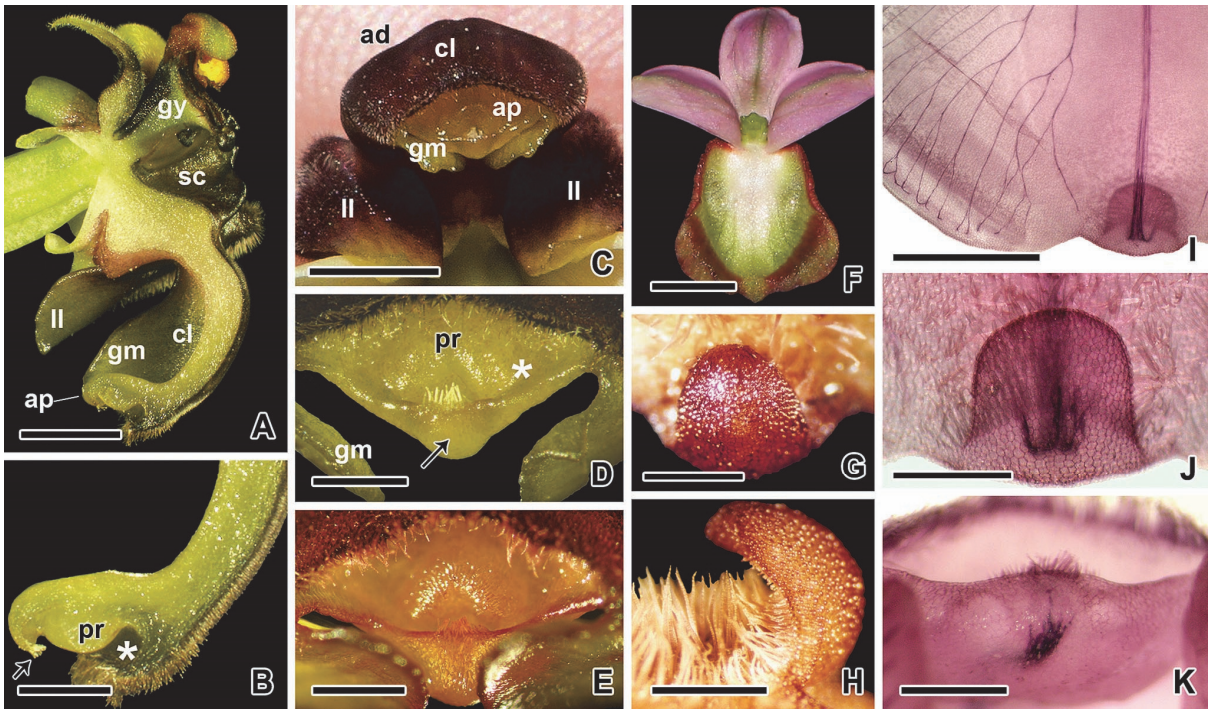

Figure 2. Stereomicrographs of fresh flowers (A–H) and cleared flowers stained with safranin (I–K). A–E, *Ophrys bombyliflora*. A, Longitudinally bisected flower, showing central labellum lobe ending with an apical appendix. B, Enlarged lateral view of the appendix. C, Bottom view of the flower, showing the distal end of central and lateral labellum lobes; the apical appendix and the convex glabrous margins are well seen. D, E, Details of appendix, before (D) and after (E) immersion in neutral red; the outline of the appendix cavity stains red. F–H, *Ophrys tenthredinifera*, after immersion in neutral red. F, Abaxial surface of labellum, showing the red-stained band near the margin. G, H, Close-up of red-stained appendix in front view (G) and in lateral view (H). I, J, Labellum vasculature of *O. tenthredinifera*. I, Abaxial surface, showing central vein branched toward labellum margin. J, Venation of appendix. K, Vein-branched appendix tip of *O. bombyliflora*. In B and D, an arrow indicates the appendix tip with tuft of trichomes, and an asterisk indicates the appendix concavity. ad, adaxial surface of labellum; ap, appendix; cl, central labellum lobe; gm, glabrous margin; gy, gynostemium; ll, lateral labellum lobe; pr, protuberance; sc, stigmatic cavity. Scale bars: 3 mm (A, C, I); 0.5 mm (B); 1 mm (D, E, G, H, J, K); 6 mm (F).

Basal field

The basal field in *O. bombyliflora*, which appears to be interrupted by a glabrous lunular area, presents attenuate to digitiform trichomes (Fig. 3A, F), whereas pulvinate trichomes with smooth, enlarged bases and finely sculptured walls cover the wide basal field in *O. tenthredinifera* (Figs. 4A, F, A2D).

Speculum

The speculum in *O. tenthredinifera* is composed mainly of short, narrow trichomes with flattened bases and prominent, spirally arranged cuticular striations oriented from the anticlines of the cell and concentrated at its apex (Fig. 4I). In this species, the narrow, glabrous lateral areas of the speculum, which occur between the basal field and the hairy basal margins of the labellum, consist of flat, densely striated cells (Figs. 4C, H, A2C). The loose, reticulate aspect of this area is due to the special arrangement of the cuticular

striations on their cell walls (Figs. 4C, H, A2C), which varies gradually toward the central area of the speculum, where short, narrow trichomes occur (Fig. 4I). In some flowers of *O. tenthredinifera*, the glabrous lateral areas of the speculum were found to be larger and composed of small papillae and flat cells (Fig. A2E).

The speculum in *O. bombyliflora* comprises flat or minute papillose cells with wide, polygonal bases and exposed anticlines that present prominent, spirally arranged cuticular striations similar to those exhibited by *O. tenthredinifera* (Figs. 3E and, available in the online edition of the *International Journal of Plant Sciences*, A1F). A large, glabrous area adjacent to the speculum and composed of both smooth and striated papillae usually extends laterally until it reaches the base of lateral lobes in *O. bombyliflora* (Fig. 3D).

Lateral lobes

In sharp contrast with the surrounding areas, the lateral labellum lobes of both species are covered with a hirsute indumentum of long, contorted trichomes. However, whereas in *O. tenthredinifera* the trichomes occur throughout the slightly pronounced lobe, in *O. bombyliflora* the indumentum covers only the basal, highly convex portion of the lobe (Fig. A1A, B); the glabrous apical part presents elongated, flat, polygonal cells with smooth or finely ridged cuticle, similar to the pavement cells of the abaxial surface (Fig. A1C). Contorted trichomes with parallel striations lengthwise and a reticulate cuticular pattern on their bases (Fig. 4G) diverge at the apex of the conical bulge, where they become shorter (Fig. A2A, B).

Apical labellum region

In the median-apical region of the labellum, a velutinous indumentum covers the region around the speculum of *O. bombyliflora*. The short, conical trichomes with depressed bases and globular tips (Fig. 3H) become gradually longer and narrower toward the margins, giving rise to long, attenuate trichomes with smooth bases in the apical indumentum (Fig. A1G). Similar trichomes are present in the homologous regions of the labellum in *O. tenthredinifera* (Fig. A2G, H). A tuft of longer, erect attenuate trichomes with smooth, swollen bases occurs immediately above the reflexed apical appendix in *O. tenthredinifera* (Fig. 4J). By contrast, *O. bombyliflora* presents a shallow longitudinal central groove in the velutinous apical indumentum, and trichomes are found obliquely oriented toward that groove (Fig. 3G). Both species possess a hirsute indumentum of long, contorted, unicellular trichomes near the margins (Fig. A2I). While in *O. bombyliflora* these trichomes border only the apical appendix (Fig. 3J), in *O. tenthredinifera* they form a complete submarginal band throughout labellum, surrounding the narrow to moderate glabrous margin consisting of dome-shaped papillae with a smooth surface (Fig. 4K). Conversely, the glabrous margin of the labellum in *O. bombyliflora* is much wider and is composed of flat cells broadly similar to those occurring on the floor of stigmatic cavity (Figs. 3I, A1I). In this species, a sparse lateral

indumentum of smooth and striate papillae interspersed with attenuate trichomes occurs in the proximity of the glabrous margins (Fig. A1H).

Apical appendix

In both species, a reflexed, glabrous, fleshy appendix is present in the apical region of the labellum. However, whereas in *O. tenthredinifera* the appendix consists of dome-shaped papillae with a smooth surface identical to those from the apical margin (Fig. 4L, M), the thick triangular appendix of *O. bombyliflora* possesses unique micromorphological features, since it forms a wide concavity where a large central protuberance occurs (Figs. 2B, D, 3K). In addition, a tuft of digitiform trichomes with elongated and densely sculptured bases is found in the appendix tip (Fig. 3L). Apart from this small tuft, the appendix is glabrous and consists of smooth to finely ridged lenticular cells with undulated anticlinal cell walls (Fig. 3M).

LOCATION AND STRUCTURE OF THE OSMOPHORE

Ophrys flowers typically emit a faint odor that is most intense in the first days of anthesis. Flowers of *O. bombyliflora*, with a period of anthesis of 6–8 days, are particularly faintly scented, whereas flowers of *O. tenthredinifera* emanate a more intense odor, and present a greater longevity of 9–12 days (A. Francisco, personal observation). Diluted neutral red intensely stained specific areas of freshly opened flowers but failed to stain late flower buds just before anthesis. The apical appendix and the entire glabrous margins of freshly opened flowers of *O. tenthredinifera* stained deeply red after less than 3 h of immersion in neutral red (Fig. 2F–H). Moreover, in most flowers, a narrow red-stained band 3–4 mm in width was seen on the abaxial surface of the apical region of the labellum and was especially intense in the first hours of anthesis (Fig. 2F). Although with weaker intensity, neutral red also stained the appendix in freshly opened flowers of *O. bombyliflora* (Fig. 2D, E).

Anatomical studies carried out on flowers of both species in three developmental stages (early bud, late bud, and freshly opened flowers) showed distinctive histological features in the labellum regions stained by the neutral red: the apical appendix in *O. bombyliflora* and *O. tenthredinifera* and the glabrous margins of the apical labellum in the latter species. Furthermore, cleared flowers of these two species revealed that the labellum is supplied by a central vein composed of several vascular bundles ending at the appendix tip, where they branch intensely (Fig. 2I–K). The central vein is also divided into several secondary veins supplying the margins of the labellum, where further branching occurs, which is especially clear in *O. tenthredinifera* (Fig. 2I).

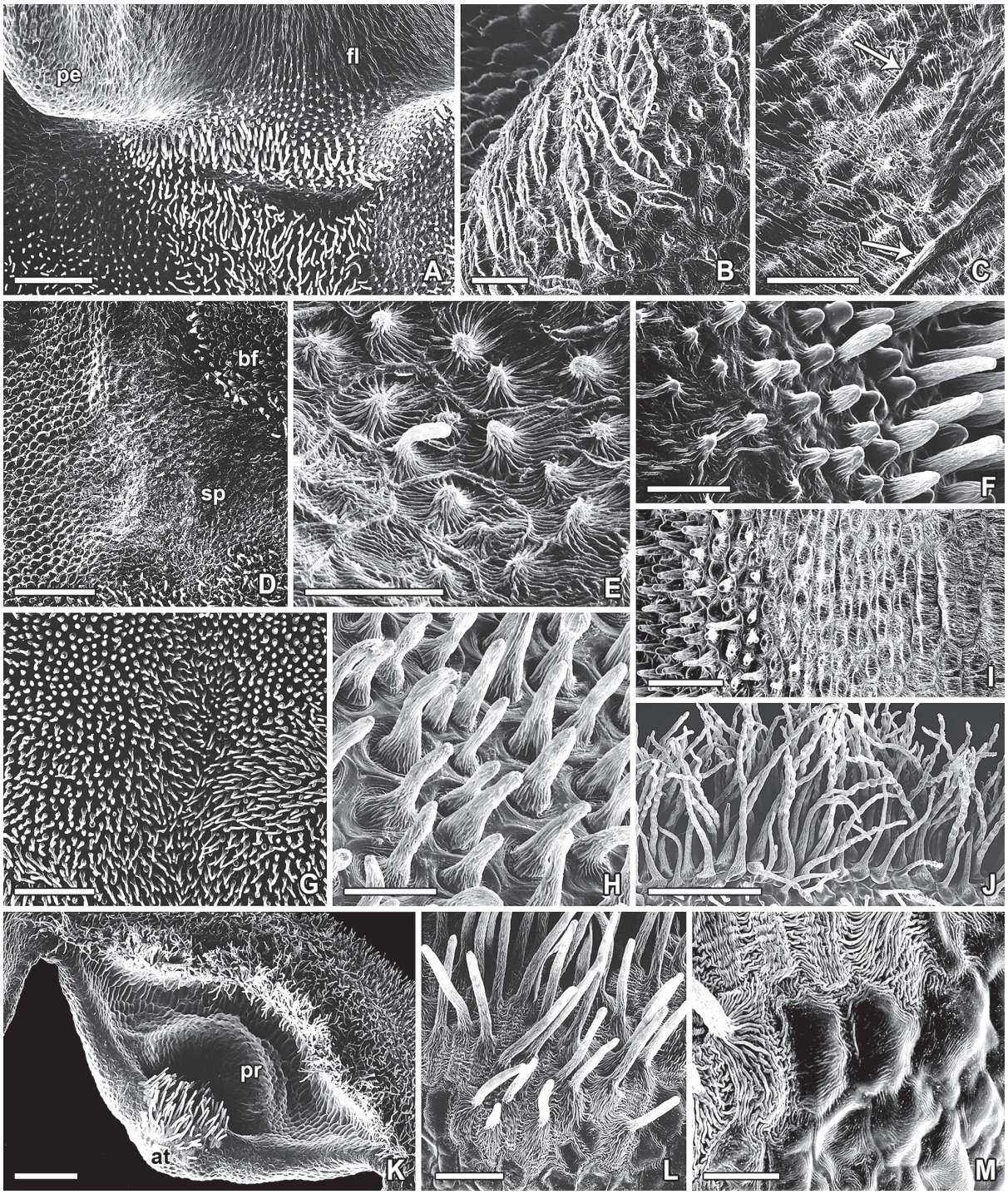

Figure 3. Scanning electron micrographs of adaxial surface of labellum in *Ophrys bombyliflora*. A, Basal region of labellum contiguous to the stigmatic cavity; note that the basal field is interrupted by a glabrous area. B, Pseudoeye slope, with prominent cuticular sculpture. C, External side of the stigmatic cavity wall, showing dense cuticular depositions (arrows). D, Glabrous speculum. E, Detail of speculum, showing minute papillae with spirally arranged cuticular ridges. F, Transition between floor of stigmatic cavity and basal field, where small papillae give rise to attenuate or digitiform trichomes. G, Longitudinal groove in apical indumentum. H, Short conical trichomes of velutinous median indumentum. I, Transition to the convex glabrous margin of the labellum. J, Long, contorted trichomes near the appendix. K, Apical appendix. L, Tuft of digitiform trichomes on appendix tip. M, Detail of appendix tip, showing smooth, lenticular cells with undulated outlines near trichomes of the tuft. fl, floor of stigmatic cavity; pe, pseudoeye; bf, basal field; sp, speculum; at, appendix tip; pr, protuberance. Scale bars: 250 µm (A, D, G, J); 50 µm (B, E, F, H, M); 100 µm (C, I, L); 500 µm (K).

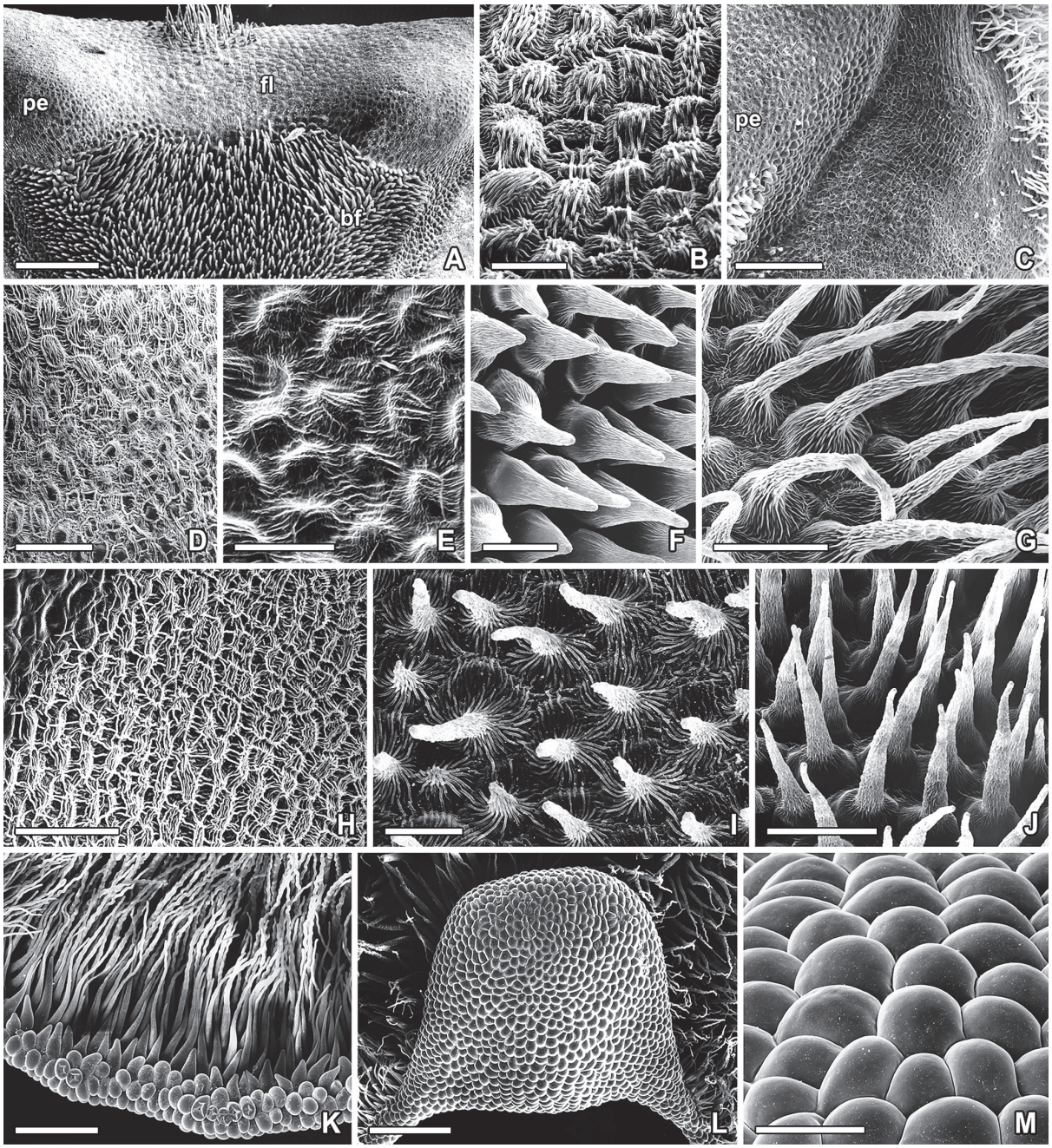

Figure 4. Scanning electron micrographs of adaxial surface of labellum in *Ophrys tenthredinifera*. A, Basal region of labellum contiguous with stigmatic cavity. B, Floor of stigmatic cavity with lenticular, polygonal cells. C, Lateral region of basal labellum near the margin. D, Portion of floor of stigmatic cavity, showing a distinct pattern of cuticular sculpture near pseudoeye (at right). E, Lenticular cells of pseudoeye. F, Pulvinate trichomes of basal field. G, Long, contorted trichomes of lateral labellum lobe. H, Glabrous lateral area of speculum, located between the basal field and labellum margin. I, Central area of speculum, covered with short trichomes with flattened bases and dense, spirally arranged striations. J, Tuft of attenuate trichomes with swollen bases above the appendix. K, Long, contorted trichomes and domed to conical papillae of labellum margin. L, Apical appendix. M, Detail of dome-shaped papillae of appendix. bf, basal field; fl, floor of stigmatic cavity; pe, pseudoeye. Scale bars: 500 µm (A, L); 50 µm (B, E, F, I); 250 µm (C, K); 100 µm (D, G, H, J, M).

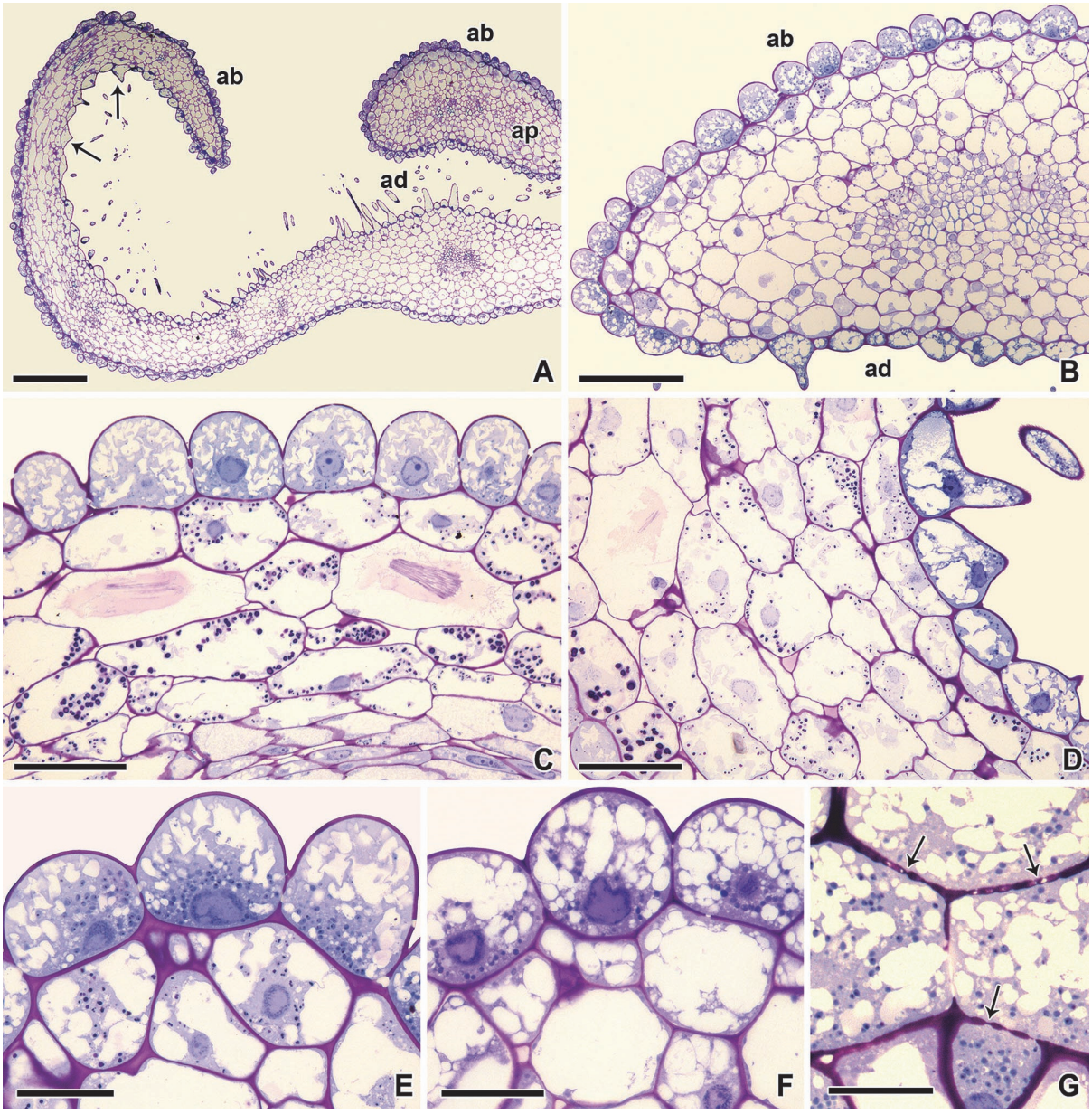

Figure 5. Light micrographs of historesin sections of apical appendix of *Ophrys tenthredinifera*, stained with PAS/toluidine blue (A–E, G) or toluidine blue/Lugol (F). A–C, Early bud. A, Transverse section of apical labellum and appendix; note the large bases of long, contorted trichomes (arrows) near the dome-shaped papillae at the margin. B, Transverse section of appendix, showing the contrast between dome-shaped papillae on abaxial surface and vacuolated conical papillae on adaxial surface. C, Longitudinal section of appendix, showing glandular epidermis and starch-rich parenchyma on abaxial surface. D, Longitudinal section of late bud, showing starch accumulated in subepidermal parenchyma cells on abaxial side. E, F, Transverse sections of secretory tissues on abaxial surface of appendix, showing that the starch content changes from early bud (E) to opened flower (F). G, Opened flower, paradermal section of epidermis of appendix, showing primary pits (arrows) along cell walls. Ab, abaxial surface; ad, adaxial surface; ap, apical appendix. Scale bars: 500 µm (A); 250 µm (B); 100 µm (C, D); 50 µm (E–G).

Osmophore in Ophrys tenthredinifera

Since the central lobe of the labellum of *O. tenthredinifera* ends with an appendix curved up and backward, the labellum in this region exhibits its surfaces inverted; i.e., the abaxial surface of the appendix is actually positioned on the adaxial side of the petal, and

the adaxial surface is hidden, facing the tuft of attenuate trichomes (Figs. 1B, 2H, 3A). Nevertheless, as the appendix is indeed a portion of the labellum, the terminology used for designating the surfaces of the appendix remains the same as that for the labellum itself. The epidermis in the reflexed apical appendix of *O. tenthredinifera* is composed of dome-shaped papillae at the tip and on the abaxial surface and consists of conical papillae on the adaxial surface of this portion of the labellum (Fig. 5B). The appendix presents a multilayered parenchyma, supplied with vascular bundles of xylem and phloem, that consists of highly vacuolated polyhedral cells with starch-rich plastids together with numerous large crystal idioblasts containing calcium oxalate raphides, often located on the abaxial side (Fig. 5B, C). The bulk of starch occurs in the one to three subepidermal parenchyma cell layers on the abaxial surface of the appendix (Fig. 5C, D). In contrast with the more vacuolated epidermal cells from the adaxial surface, the epidermal cells on the abaxial side and at the appendix tip exhibit features typical of secretory cells (Fig. 5D). These dome-shaped papillae are clearly polarized cells with thin walls and dense cytoplasm (Fig. 5E). A large nucleus, surrounded by abundant globular plastids, lies at the base of the cell, whereas several small vacuoles occupy the cell apex (Fig. 5C, E, F). Numerous primary pit fields are found throughout their cell walls (Fig. 5G). Similar papillae occur in the margins and in the abaxial surface of the adjacent apical region of the labellum (Figs. 5A and, available in the online edition of the *International Journal of Plant Sciences*, A3D). Consequently, the osmophore in *O. tenthredinifera* includes not only the tip and the abaxial surface of the appendix, i.e. the dome-shaped papillae together with the one to three layers of starch-rich subepidermal parenchyma cells, but also the margin and the abaxial surface of the apical region of the labellum.

Osmophore in Ophrys bombyliflora

Besides its unique morphological configuration, the apical appendix of *O. bombyliflora* also presents distinctive histological features. The appendix is itself curved upward but, because the strongly convex labellum curves abruptly downwards, it is forced to form a concavity that has a typical multicellular protuberance in the center (Fig. 6A). The protuberance appears to result from the proliferation of the parenchyma cells at the central region of the concavity, with a concomitant elongation of the epidermal cells from the adaxial surface. This peculiar structure is composed of a cluster of hypertrophied parenchyma cells with thin, irregularly sinuate walls (Fig. 6E). Almost all of these cells are raphide idioblasts (Fig. 6A, B). The epidermis of the protuberance comprises secretory lenticular cells with large nuclei, numerous small vacuoles, and abundant globular plastids (Fig. 6D, E). Similar glandular features are exhibited by the epidermal cells of the appendix tip (Fig. 6B). Numerous primary pit fields are found along the walls of these cells (Fig. 6H). In the protuberance, the outer tangential wall of the epidermal cells appears to present helical thickenings at regular intervals (Fig. 7B). More-elongated and more-vacuolated epidermal

cells occur in the proximal region of the appendix concavity (Fig. 6A). Also, apart from the tip, the epidermis on the abaxial surface of the appendix is composed of highly vacuolated cells covered with a thick cuticle, which contrasts with that observed in the glandular cells (Fig. 6C). The parenchyma tissue of the appendix, clearly supplied with vascular bundles, presents a massive amount of starch at the appendix tip, stored in numerous plastids (Fig. 6A, B). In this region, raphide idioblasts are abundant among cytoplasm-rich parenchyma cells (Fig. 6B, F). Furthermore, the appendix tip is provided with a tuft of unicellular digitiform trichomes with striated cell surfaces and phenolic vacuolar inclusions (Figs. 3L, 6B, F). Thus, the osmophore of *O. bombyliflora*, confined to the appendix, comprises the lenticular epidermal cells of the protuberance and the appendix tip, along with the subjacent starch-rich parenchyma of this region.

CYTOLOGICAL CHANGES IN THE LABELLUM DURING FLOWER DEVELOPMENT

In early stages of development, the parenchyma cells of the entire labellum of *O. bombyliflora* are extremely rich in starch (Fig. A4C, available in the online edition of the *International Journal of Plant Sciences*), which disappears completely at the beginning of flower anthesis. By contrast, in the apical appendixes of both species, even though a sharp decrease in starch content is evident as flower development proceeds, some starch is still found in the plastids of their subepidermal parenchyma cells in flowers at anthesis (Figs. 5E, F, 6F, G). Although an increased vacuolization and a concomitant decrease in cytoplasm also occur, the glandular cells of the appendix, particularly those of the epidermis, continue to exhibit secretory features in freshly opened flowers (Figs. 5E, F, 6F, G). Conversely, the epidermal cells of the other regions of the labellum undergo drastic changes in the course of development (Figs. A3A–C, A4A, B, E). In early buds of *O. tenthredinifera*, after staining with PAS/toluidine blue and toluidine blue/Lugol, pink-stained material usually occurs inside the vacuoles of the trichomes throughout the labellum and in the periplasmic space of the contorted and the attenuate trichomes of the tuft (Fig. A3A, E, F). In *O. bombyliflora*, the conical trichomes occurring in the median-apical region of the labellum present several depositions of lipophilic material on their inner periclinal cell walls, which appear dark blue after staining with Sudan black B (Fig. A4D).

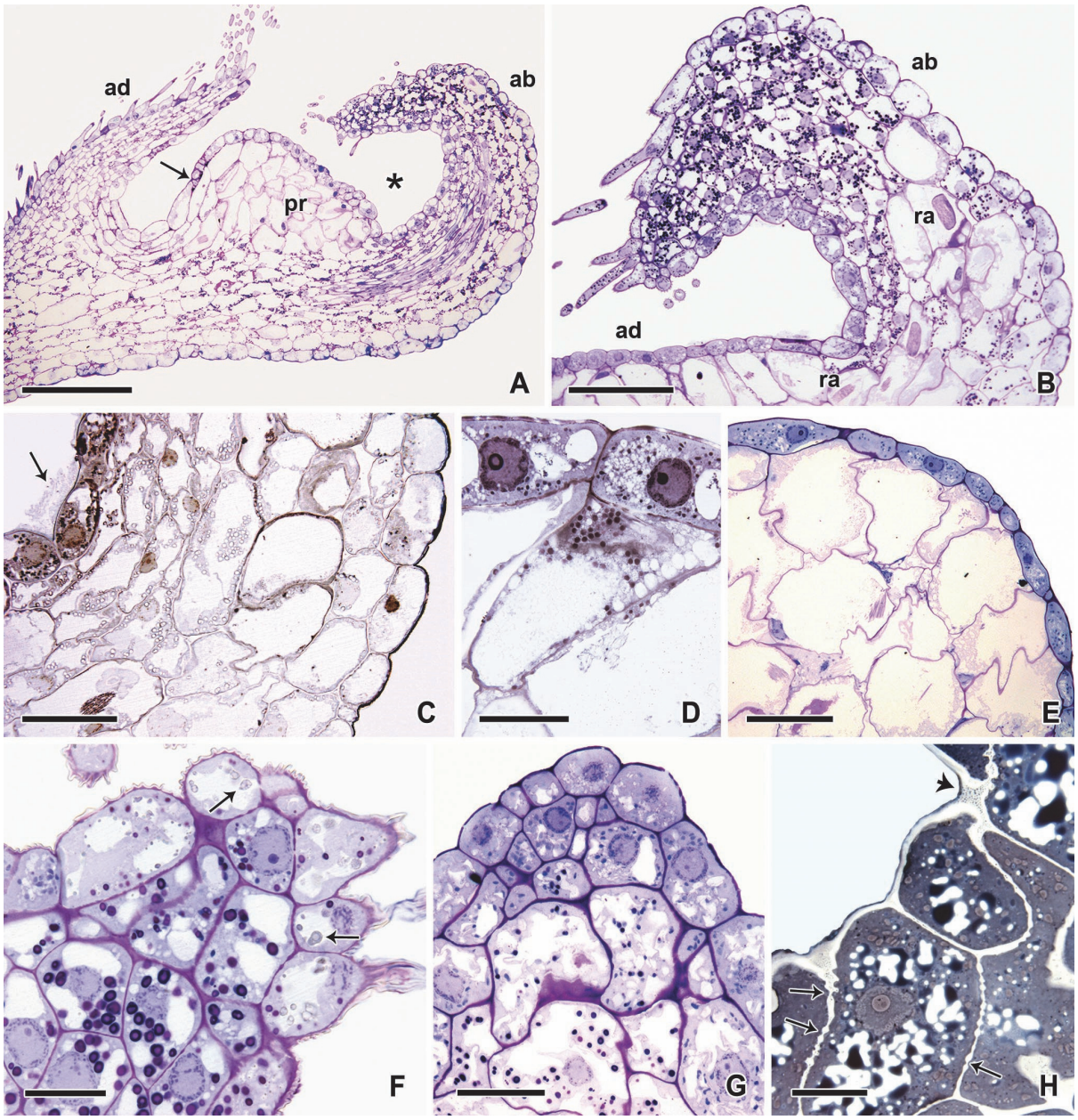

Figure 6. Light micrographs of historesin sections (A–G) and an epoxy section (H) of apical appendix of *Ophrys bombyliflora*. A, B, E–G, Longitudinal sections stained with PAS/toluidine blue. A, Early bud, appendix, showing a concavity (asterisk), a protuberance, and an appendix tip with dense vasculature; the arrow marks the limit of secretory epidermal tissue in the protuberance. B, Early bud, appendix tip; note the starch-rich parenchyma with raphide idioblasts and the secretory epidermal cells bordering the concavity. C, Longitudinal section of appendix of an early bud stained with Sudan black B, showing the contrasting thicknesses of black-stained cuticles in the epidermal cells on adaxial and abaxial surfaces; note also that an unstained presumed exudate (arrow) occurs over some cells. D, E, Protuberance of the appendix of an early bud stained with toluidine blue/Lugol (D) and an opened flower (E). F, G, Appendix tip. F, Early bud, showing starch-rich plastids in subepidermal cells and trichomes of the tuft with phenolic vacuolar inclusions (arrows). G, Opened flower, showing the smaller caliber of starch grains in plastids of subepidermal cells. H, Paradermal epoxy section of the secretory epidermis of an opened flower, stained with Sudan black B; note the primary pits (arrows) along cell walls and also a lipophilic secretion inside vacuoles and in loose walls (arrowhead). Ab, abaxial surface; ad, adaxial surface; pr, protuberance; ra, raphides. Scale bars: 200 µm (A); 100 µm (B, E, G); 50 µm (C); 25 µm (D, F, H).

HISTOCHEMISTRY OF THE SECRETION

Vacuoles of the epidermal cells of the appendix in the two *Ophrys* species studied are rapidly and selectively bright-pink stained with diluted neutral red, which provides a further indication of the glandular nature of these cells, functioning as part of the osmophores (Fig. 7C, M). Under blue light, some epidermal cells of the appendix of *O. bombyliflora* show a yellow-greenish autofluorescence (Fig. 7G, H), probably because of the contents of the vacuoles, which also exhibit a blue autofluorescence under UV light (Fig. 7I), indicating their apparent phenolic nature.

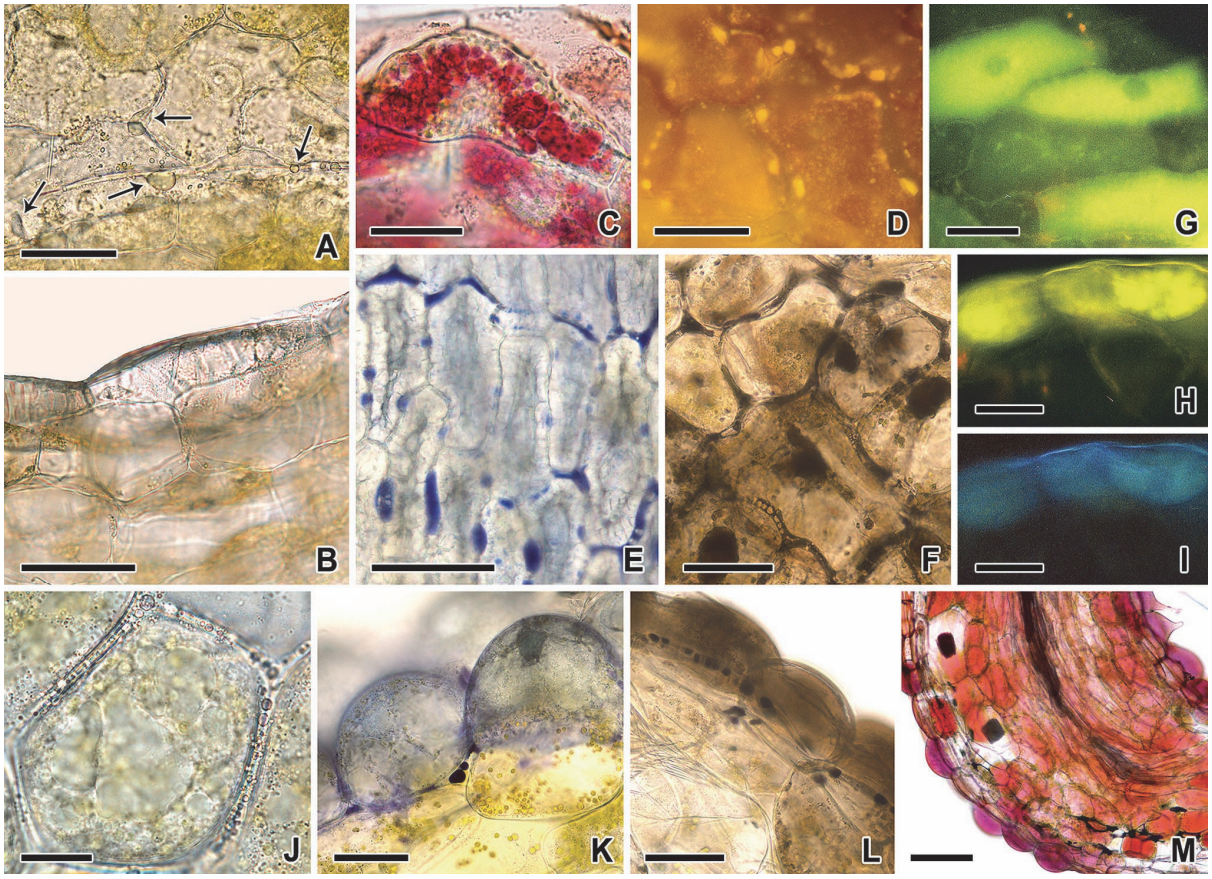

Figure 7. Light micrographs of fresh hand-cut sections of apical appendixes. A–I, Bud just before anthesis (A) and flowers at anthesis (B–I) of *Ophrys bombyliflora*. A, B, Sections without any treatment. A, Paradermal section of appendix, showing translucent droplets (arrows) in the concavity. B, Longitudinal section of protuberance of appendix, showing helical cell wall thickenings in epidermal cells. C, D, Paradermal sections stained with neutral red. C, Protuberance; the diluted stain revealed small vacuoles in epidermal cells. D, Appendix tip; secretion droplets emitted golden-yellow secondary fluorescence under blue light. E, F, Paradermal sections of glandular epidermis. E, Protuberance; secretion stained blue with Nadi reagent. F, Appendix tip after staining with osmium tetroxide. G–I, Autofluorescence of paradermal (G) and longitudinal (H, I) sections of protuberance under blue light (G, H) and ultraviolet light (I). J–M, Flowers of *Ophrys tenthredinifera* at anthesis. J, Unstained paradermal section of epidermis on abaxial side, showing translucent droplets on cell walls. K, Transverse section, showing droplets stained blue or violet with Nadi reagent. L, Transverse section stained with osmium tetroxide. M, Longitudinal section stained with diluted neutral red. Scale bars: 50 µm (A–D, F–I, K, L); 100 µm (E, M); 25 µm (J).

All the histochemical tests performed were consistent in revealing the occurrence of a lipophilic secretion, always detected in low amounts, in the appendix of the two species. The bulk of the secretion was found predominantly in the epidermal cells, although some cytoplasmic Sudan-positive lipid inclusions occur in the subepidermal parenchyma cells of the appendix (not shown). A blue- or violet-stained terpene-rich secretion, revealed with the Nadi reagent, was observed in close association with the epidermal cell walls (Fig. 7E, K). Small droplets seem to fuse with each other to form large secretion deposits, either in the periplasmic space or in the loose cell walls (Fig. 7D–F, J). Translucent droplets were often found in the appendix concavity of *O. bombyliflora*, between the protuberance and the appendix tip, in late buds just before anthesis (Fig. 7A). A presumed exudate was also detected in the same region in historesin sections of the appendix (Fig. 6C). In both species, a black Sudan-positive material was observed in the vacuoles and within the loose walls of the epidermal cells of the appendix in semithin epoxy sections (Fig. 6H).

DISCUSSION

MICROMORPHOLOGY AND POLLINATION

Our micromorphological study reveals new features that might play an important role in the orientation of males of *Eucera* solitary bees on the labella of *Ophrys bombyliflora* and *Ophrys tenthredinifera* in order to perform cephalic pseudocopulation (Godfery, 1928; Devillers & Devillers-Terschuren, 1994). Most remarkably, we clearly demonstrate that an apical appendix always occurs in the labellum of *O. bombyliflora*. Curiously, although this hidden but distinctive appendix had already been noticed almost a century ago (Godfery, 1917), it was overlooked in the recent labellum micromorphology survey of the genus *Ophrys* (Bradshaw *et al.*, 2010), and only in our study is its structure described in detail. The appendix of *O. bombyliflora* is displaced to the back of the labellum and can be perceived only when the flower is seen in bottom view. The strong resemblance of the triangular, glabrous, fleshy appendix of this species to the abdomen tip of a hymenopteran female is astonishing, even to the human eye. Its peculiar concavity, with a central protuberance and a tuft of trichomes at the appendix tip, is unique in the genus *Ophrys*. Also, the appendix of *O. tenthredinifera*, turned up in front of the labellum, may constitute a visual cue for pollinators. According to the observations of Ågren *et al.* (1984), the external appearance of the apical appendix of *Ophrys scolopax* s.l. is similar to that of the last segment of the female's abdomen (the pygidial plate) of the bee *Eucera nigrilabris,* a species reported as a frequent pollinator of *O. tenthredinifera* (Kullenberg, 1973a; Delforge, 2005). Besides their visual role, the appendixes of *O. bombyliflora* and *O. tenthredinifera* should also provide a tactile stimulation for the genitalia of male pollinators, since the smooth texture of their surfaces strongly contrasts with the surrounding hirsute indumentum of the apical region of the labellum. In fact, during copulation attempts with the labellum, some *Eucera* bee males

were observed repeatedly trying to turn their genitalia under the labellum of *O. bombyliflora* (Kullenberg, 1961). The concavity resulting from the folded configuration of the appendix in *O. bombyliflora* may thus have an additional functional role, since males could insert their abdomen tip into the concavity during pseudocopulation. Also, in the tropical sexually deceptive orchid *Lepanthes glicensteinii*, which is pollinated by males of a fungus gnat species, the minute appendix of the labellum, placed in the underside of the flower, seems to mimic the abdominal tip of the pollinator's female and have a pivotal role in pseudocopulation (Blanco & Barboza, 2005).

Another relevant feature is the shallow longitudinal groove that we observed on the apical indumentum of the labellum in *O. bombyliflora*. This groove, reported here for the first time, probably has a guiding function similar to that of the basal groove of the labella in *Ophrys fusca* and *Ophrys lutea* (Kullenberg, 1961; Ascensão *et al.*, 2005), species belonging to the section *Pseudophrys*. Some attenuate trichomes that constitute the apical indumentum of the labellum in *O. bombyliflora* are found to be oriented to the shallow longitudinal groove and may tactilely guide the abdomen tip of *Eucera* male bees into the concavity formed by the appendix. The longer, contorted trichomes that border the appendix in *O. bombyliflora* and the tuft of longer, erect attenuate trichomes in the region above the apical appendix in *O. tenthredinifera* probably enhance tactile mimicry, since hairs on the abdomen of the female bees also lengthen toward the apex (Ågren *et al.*, 1984).

In contrast to the well-defined colored basal field of *O. tenthredinifera*, that of *O. bombyliflora* has a color that does not differ markedly from that of the adjacent dark areas of the labellum. Despite being poorly circumscribed, the basal field of *O. bombyliflora* curiously often presents a central glabrous lunular area with a shape approaching that of a typical basal field, which we suggest resembles the scutellum of a bee. On the other hand, the glabrous stigmatic cavity appears similar to the smooth head of the female bee. The pseudoeyes, usually one of the most reflective areas of the flower, seem to mimic an insect's eyes or the tegulae of its wings (Devillers & Devillers-Terschuren, 1994; Paulus, 2006). Our observations show that the stigmatic cavity of the two species consists of densely striated flat or lenticular polygonal cells and that specifically the pseudoeyes, rather than being smooth, as described by Bradshaw *et al.* (2010), present a diffuse pattern of ridges in their outer cell walls.

Because of its contrasting general bluish pigmentation and higher reflectivity, compared with the surrounding dark areas of the labellum, the speculum has long been considered to mimic the wings of a female insect (Kullenberg, 1961; Ågren *et al.*, 1984; Bradshaw *et al.*, 2010). Our observations show that the flat cells or minute papillae (average length 9 µm) occurring in the speculum of *O. bombyliflora*, even though they parallel roughly the cells found in the narrow lateral areas of the speculum of *O. tenthredinifera*, contrast deeply with the short, narrow trichomes (average length 34 µm) that cover the largest (central) portion

of the speculum in this species. Despite their great difference in length, which determines even the designations of papilla versus trichome, the specular cell types of both species have a flattened polygonal base, in accordance with what seems to be a common characteristic of other *Ophrys* specula (Servettaz *et al.*, 1994; Ascensão *et al.*, 2005; Bradshaw *et al.*, 2010). The trichomes of the speculum of *O. tenthredinifera* resemble those occurring in the speculum of *O. fusca* and *O. lutea* (average length 45 µm), albeit they are shorter and exhibit apparently more prominent cuticular ridges in their bases (Ascensão *et al.*, 2005). As a result, hypotheses arguing, on one hand, that the *O. bombyliflora*, *O. tenthredinifera*, and *Ophrys speculum* species groups could constitute a clade based on the sharing of flat polygonal cells in their specula and, on the other hand, that long specular trichomes (>30 µm) are confined to the species of the section *Pseudophrys* (Bradshaw *et al.*, 2010) could be clearly refuted.

In contrast with our own observations, Bradshaw *et al.* (2010) found that the speculum in *O. tenthredinifera* is composed mainly of smooth, flat (or slightly domed), polygonal cells, although a few striate-papillate or trichomatous cells are clustered in the center. In this regard, the main differences between the two studies reside in the extent of the glabrous area of the speculum and in the degree of cuticular ornamentation of its outer epidermal cell walls. One possible explanation for the discrepancy between our own results concerning the speculum in *O. tenthredinifera* and those reported by Bradshaw *et al.* (2010) may be the different geographical origin (Iberia vs. Sicily and Sardinia) of the specimens analyzed in the two studies. Indeed, several authors assign the morphologically distinct populations of *O. tenthredinifera* occurring in such geographical areas to different species belonging to the group of *O. tenthredinifera*; at least four of these species have been documented for Sicily and Sardinia (Delforge, 2005). Allopatric populations of *O. tenthredinifera* appear to have different species of *Eucera* bees as pollinators (Kullenberg, 1973a; Lara Ruiz, 2010; Gaskett, 2011 and references therein). However, whether the micromorphological variation found in the speculum of this orchid species might be due to the selective pressure by local pollinators, as is evident for the floral scent in other *Ophrys* orchids (Ayasse *et al.*, 2011), remains to be tested.

EPIDERMAL CELL TYPES

Because of the intimate fusion of the orchid gynostemium and labellum, the boundary between the stigmatic cavity and the labellum is imperceptible, and the real nature of the diverse ornamentation of the *Ophrys* stigmatic cavity remains unknown. Yet the pseudoeyes have usually been considered structures belonging to the stigmatic cavity of the flower (Devillers & Devillers-Terschuren, 1994; Delforge, 2005; contra Bradshaw *et al.*, 2010), and here we also adopt this assumption. Our detailed SEM observations revealed a great diversity of epidermal cells in the adaxial surface of the labellum in *O. bombyliflora* and *O.*

tenthredinifera, whereas the stigmatic cavities of both species present a more uniform appearance. According to (1) the cell outline defined by the anticlinal walls and (2) the curvature and (3) the cuticular sculpture of the outer periclinal wall of the epidermal cells (Koch *et al.*, 2008), we distinguish 7 and 10 different cell types in the labella of *O. tenthredinifera* and *O. bombyliflora*, respectively, as well as two types of cells in the stigmatic cavities of both species. The flat or lenticular polygonal cells with a dense cuticular folding pattern that cover most of the stigmatic cavity also occur in certain areas of the labella, whereas the lenticular cells with smooth, depressed anticlines and fine, diffuse cuticular striations characterize exclusively the region of the pseudoeyes. Thus, if the latter cells are added to the cell types occurring in the labellum of each species, we conclude that the total number of different epidermal cell types is 11 for *O. bombyliflora* and 8 for *O. tenthredinifera*.

Compared to the labella of other genera in the subtribe Orchidinae, such as *Gymnadenia* s.l. and *Dactylorhiza*, which have an adaxial surface covered by domed to conical epidermal cells (Box *et al.*, 2008), the *Ophrys* labellum presents a higher level of complexity, recently documented by Bradshaw *et al.* (2010). However, fewer epidermal cell types have been reported by the latter authors in the labella of the two species analyzed in our study. The discrepancy in these numbers, particularly pronounced for *O. bombyliflora* (5 vs. 11 different cell types), originates not only from the disregarding of the characteristic appendix of this species in the survey by Bradshaw *et al.* (2010) but probably also from the different criteria used to define the epidermal cell types.

We anticipate that most micromorphological characters revealed by our study could be useful in helping to clarify the still uncertain phylogenetic relationships between the species in the clade formed by *O. bombyliflora*, *O. tenthredinifera* s.l., *O. speculum* s.l., and the section *Pseudophrys* (Devey *et al.*, 2008). Further detailed micromorphological studies on *O. speculum* s.l. (A. Francisco & L. Ascensão, unpublished manuscript) are also needed for this purpose.

OSMOPHORE LOCATION, STRUCTURE AND PERIOD OF FRAGRANCE EMISSION

Osmophore location and structure

Our study demonstrates for the first time that an osmophore is present in the apical region of the labellum in *O. bombyliflora* and *O. tenthredinifera*. The preliminary indication of this finding was suggested by the rapid absorption of the diluted neutral red by the epidermal cells of certain regions of the labellum. Even though this stain does not have specificity for the glandular cells of the osmophores, it often constitutes a useful indicator of these scent glands if factors such as the color hue and the anatomy are considered (Vogel, 1990; Vogel & Hadacek, 2004). The precise location of the osmophores was confirmed by the anatomical study, which clearly showed that, contrary to the other parts of the flower,

the appendixes of both species, along with the apical margin of the labellum of *O. tenthredinifera*, have histological features comparable to those considered characteristic of the osmophores (Vogel, 1990). The epidermal cells form an exposed glandular epithelium that is assumed to be involved in both the synthesis and the emission of the odoriferous compounds and is supported by one to three layers of starch-rich subepidermal parenchyma cells. The presence of a large nucleus and a relatively dense cytoplasm with Sudan-positive lipophilic droplets of secretion suggests that these parenchyma cells are also involved in the biosynthetic process, especially in *O. bombyliflora*. The numerous primary pit fields located in the cell walls between epidermal and parenchyma cells are preferential sites of translocation of compounds via symplast.

The location of the osmophores of *O. bombyliflora* and *O. tenthredinifera* in the apical appendix of the labellum reflects their function as fragrance-producing organs and matches quite well with that of the other osmophores observed in the genus (Vogel, 1990; Ascensão *et al.*, 2005). In both species, the apical appendix occupies a position homologous to the region of the central notch occurring in the apical labellum of *O. fusca* and *O. lutea*, which was found to be the most important region of the osmophore in these species (Ascensão *et al.*, 2005). The extension of the osmophore of *O. tenthredinifera* to also encompass both the margin and the abaxial surface of the apical region of the labellum is identical to what is observed in *O. fusca* and *O. lutea*. Contrasting with the large majority of the osmophores, which exhibit a glandular adaxial surface (Stern *et al.*, 1987; Melo, Borba & Paiva, 2010; Płachno *et al.*, 2010), the appendix of *O. tenthredinifera* presents the exposed abaxial surface with secretory features, a quality that is known to be shared with only two other orchid genera (Vogel, 1990; Wiemer *et al.*, 2009), in addition to *O. fusca* and *O. lutea*. Conversely, in *O. bombyliflora*, the osmophore is confined exclusively to the apical appendix and presents mostly the adaxial surface as the secretory one. Thus, besides the similar trichomes of the speculum in *O. tenthredinifera*, *O. fusca*, and *O. lutea* (see above), the identical location of their osmophores seems to be an additional character shared between these species.

Starch and period of fragrance emission

Like all the other osmophores described, that of *O. tenthredinifera* exhibits starch-rich plastids in the parenchyma cells instead of in the epidermis, a feature shared with *O. bombyliflora*, and in clear contrast with the osmophores of *O. fusca* and *O. lutea*. Indeed, these latter two species are unique among the osmophore-presenting species in having the bulk of the starch reserve contained in the glandular epidermis rather than in the parenchyma (Vogel, 1990; Ascensão *et al.*, 2005).

In most osmophores, the unusual accumulation of large amounts of starch is believed to be associated with the need for energy and/or carbon to produce a great quantity of secretion within a short period of time, which usually corresponds to the brief period of

anthesis of the flowers of only a few hours or 1–3 days (Pridgeon & Stern, 1983; Vogel, 1990; Skubatz *et al.*, 1996; Heiduk *et al.*, 2010). Depletion in the starch content of the osmophore tissues typically occurs after the cessation of the secretory period (Pridgeon & Stern, 1985; Stern *et al.*, 1987; Vogel, 1990). However, several other osmophore-containing species have flowers with prolonged anthesis that, as in *Ophrys* spp., lasts for one to several weeks (Vogel, 1990; Vogel & Martens, 2000; Melo *et al.*, 2010), and many of these species also contain starch reserves. In *O. bombyliflora* and *O. tenthredinifera*, a decrease in the starch content, accompanied by an increase in vacuolization of both epidermal and subepidermal cells of the osmophores, is observed from the bud to the freshly opened flower stage. Nevertheless, some starch grains remain stored in the parenchyma cells in the osmophores of flowers at anthesis, which together with the detection of a faint odor from the labellum during the anthesis (A. Francisco, personal observation), suggests that the osmophores remain active throughout the entire period of anthesis in these two species. Since the floral buds just before the anthesis do not present any detectable scent and did not stain with diluted neutral red, it is likely that the period of odor emission begins with the opening of the flowers. Fragrance emission seems to have a peak in the first few days of anthesis (A. Francisco, personal observation), a hypothesis that fits, on the one hand, the faster absorption of the diluted neutral red by the epidermal cells of the osmophore in the first hours of anthesis in flowers of *O. tenthredinifera* and, on the other hand, the rapid decline in the starch content from the bud to freshly opened flower stage in both species.

Other osmophore features

The abundance of raphide idioblasts in the parenchyma of the osmophores of these two *Ophrys* species is remarkable, especially in the protuberance of the appendix of *O. bombyliflora*. The occurrence of raphides is frequent in other orchid osmophores (Teixeira *et al.*, 2004; Melo *et al.*, 2010), and in some orchid nectaries (Stpiczyńska, Davies & Gregg, 2004), but the functional significance of these calcium oxalate crystals in secretory tissues is uncertain. One of the major functions assigned to calcium oxalate crystals is the regulation of the calcium levels in the cells, which could be a particularly important phenomenon in species occurring in calcareous soils (Franceschi & Nakata, 2005), such as *Ophrys* spp. The intense venation of the apical appendix in both species is similar to that observed by Vogel (1990) in the apical appendix of *Ophrys fuciflora*, and it could provide an additional supply of water and sugars to the glandular tissues.

SECRETION AND FUNCTION OF THE OSMOPHORE

The low amount of secretion detected in our histochemical study of the osmophores of *O. bombyliflora* and *O. tenthredinifera* fits both the faint floral scent detectable by the human nose, already reported by Kullenberg (1961), and the extremely low odor emission

rate previously found in *Ophrys* flowers (Borg-Karlson, 1990; Schiestl *et al.*, 1997). A terpene-rich lipophilic secretion was found primarily in association with the walls of the epidermal cells of the appendixes. Both the periplasmic space and the loose walls of these cells seem to be transient accumulation sites of the fragrance. Although a continuous synthesis and immediate release of the odoriferous compounds has been assumed to occur in the osmophores (Vogel, 1990), a Sudan-positive lipophilic secretion was detected in the vacuoles of the epidermal cells of the osmophores in the two *Ophrys* species studied, which suggests that some secretory products accumulate temporarily in the cell before being transported through the plasma membrane. Further research is required to elucidate the mode of secretion of the osmophores and their period of activity in these two orchid species.

Our finding that the osmophores of *O. bombyliflora* and *O. tenthredinifera* synthesize a terpene-rich lipophilic secretion containing likely a phenolic fraction fits well with the results of chemical analyses of the floral scent of these two species (Kullenberg *et al.*, 1984; Borg-Karlson, 1990). Fifty out of the 139 compounds detected in the floral odor bouquet of *O. tenthredinifera* were found to be highly volatile compounds released to the headspace, mainly short-chain hydrocarbons, alcohols, and esters as well as mono- and sesquiterpenes, together with a few aromatic compounds (Kullenberg *et al.*, 1984). Despite rarely eliciting copulation attempts by *Eucera* male bees, some of these highly volatile components appeared to be effective in the long-range attraction of pollinators, triggering the approach flight to the labellum when tested in the field (Kullenberg, 1973b; Kullenberg *et al.*, 1984; Borg-Karlson, 1990). We therefore suggest that the osmophores of the two *Ophrys* species investigated are the site of synthesis and emission of the highly volatile long-range attractants for their pollinators.

Furthermore, the odor bouquet of *O. tenthredinifera* also contains, like that of every *Ophrys* species investigated so far (Ayasse *et al.*, 2011), a lower volatile fraction, with mostly long-chain aliphatic compounds, such as saturated and unsaturated hydrocarbons, aldehydes, and esters (Kullenberg *et al.*, 1984). In *O. bombyliflora*, *O. tenthredinifera*, and any other *Ophrys* species pollinated by *Eucera* solitary bees, the key active compounds capable of triggering mating behavior in males have not yet been identified. The sex pheromone produced by *Eucera* females to attract conspecific males also remains unknown.

By contrast, in the *Ophrys* species pollinated by solitary bees of genera *Andrena* and *Colletes*, the key attractive compounds were identified as a set of long-chain cuticular hydrocarbons, especially long-chain alkenes (Schiestl *et al.*, 1999; Mant *et al.*, 2005; Stökl *et al.*, 2008; Stökl *et al.*, 2009), which because of their high molecular mass and chemical properties present low vapor pressure at room temperature, acting at close distances from the labellum or even upon contact (Ayasse *et al.*, 2011). Increased air temperatures, like those occurring in the period of greater activity of the male insects (Kullenberg *et al.*, 1984), could change the biophysical properties of the cuticle (Domínguez, Heredia-Guerrero &

Heredia, 2011), allowing these long-chain hydrocarbons to evaporate and to play their role as short-range semiochemicals. Nevertheless, we presume that higher-volatile compounds are released from the labella of these *Ophrys* species to attract pollinators from long distances. Indeed, the labellum of *Ophrys exaltata*, a species pollinated by *Colletes cunicularius* bees, besides producing the low-volatile key hydrocarbons, also emits small amounts of linalool, a monoterpene alcohol that was found to be part of the female sex pheromone of this bee species, acting as long-range male attractant (Mant *et al.*, 2005). Hymenopteran females typically synthesize, in the mandibular glands, a set of highly volatile short, aliphatic alcohols, esters, aldehydes, and monoterpene and sesquiterpene alcohols that attracts conspecific males at long distances (Borg-Karlson, 1990). Also, in the Neotropical sexually deceptive orchid *Mormolyca ringens* (Epidendroideae: Maxillariinae), while a homologous series of long-chain hydrocarbons acts as short-range elicitor of pseudocopulation by eusocial bee males, the highly volatile 2-heptanol seems to play a role as long-range attractant, acting in a way similar to that of the mixture of 2-alkanols found in the cephalic secretions of the pollinator's virgin females (Flach *et al.*, 2006).

The key finding of our study, that a specialized secretory structure occurs in the labellum of *O. bombyliflora* and *O. tenthredinifera*, provides a wider perspective on the mode of attraction of pollinators in the sexually deceptive genus *Ophrys*. The integration of our finding into current knowledge about the chemical ecology of these orchids implies that two sources of potential chemical attractants have evolved in the *Ophrys* labellum: (1) the cuticular waxes, enriched with low-volatile long-chain hydrocarbons and other fatty-acid derivatives that cover the outer walls of the epidermal cells on the adaxial surface of the labellum, and (2) the osmophore, the secretory structure restricted to the apical region of the labellum, specialized in the biosynthesis and emission of highly volatile compounds (mostly terpenoids and phenylpropanoids).

Considering the diverse volatility of the compounds that constitute the complex odor bouquet released by the *Ophrys* labellum, we could expect that the components of the mixture play different roles, as predicted recently by Steiger *et al.* (2011). A model for the attraction of *Ophrys* pollinators based on the dispersal properties of the attractants was also presented by Kullenberg & Bergstrom (1976). Therefore, we propose that the highly volatile compounds produced by the osmophore capture the attention of the male insects at long distances, guide them during the approach flight to the labellum, and supplement the short-range stimulating effect of the low-volatile components of the cuticular waxes of the labellum. In this regard, we predict that an osmophore will be found in the other species of the genus and that, in *O. exaltata*, the osmophore will be the site of synthesis and emission of the linalool previously reported by Mant *et al.* (2005). Moreover, the occurrence of an osmophore is highly plausible in the flowers of other sexually deceptive orchids that, like *M. ringens* (Flach *et al.*, 2006), produce two types of active semiochemicals that differ in volatility.

ACKNOWLEDGMENTS

We thank M. Porto for assistance with figure preparation and for providing the photograph in Figure 2C. We are grateful to E. Carmo-Silva and C. Pesquita for help in revising the English and to anonymous reviewers for helpful comments on earlier versions of the manuscript. A. Francisco acknowledges Fundação para a Ciência e a Tecnologia (FCT) for financial support through a doctoral grant (SFRH/BD/18823/2004).

REFERENCES

Ågren L, Kullenberg B, Sensenbaugh T. 1984. Congruences in pilosity between three species of *Ophrys* (Orchidaceae) and their hymenopteran pollinators. *Nova Acta Regiae Societatis Scientiarum Upsaliensis, Serie V:C* **3:** 15-25.

Ascensão L, Francisco A, Cotrim H, Pais MS. 2005. Comparative structure of the labellum in *Ophrys fusca* and *O. lutea* (Orchidaceae). *American Journal of Botany* **92:** 1059-1067.

Ayasse M, Schiestl FP, Paulus HF, Ibarra F, Francke W. 2003. Pollinator attraction in a sexually deceptive orchid by means of unconventional chemicals. *Proceedings of the Royal Society B: Biological Sciences* **270:** 517-522.

Ayasse M, Stökl J, Francke W. 2011. Chemical ecology and pollinator-driven speciation in sexually deceptive orchids. *Phytochemistry* **72:** 1667-1677.

Blanco MA, Barboza G. 2005. Pseudocopulatory pollination in *Lepanthes* (Orchidaceae: Pleurothallidinae) by fungus gnats. *Annals of Botany* **95:** 763-772.

Borg-Karlson A-K. 1990. Chemical and ethological studies of pollination in the genus *Ophrys* (Orchidaceae). *Phytochemistry* **29:** 1359-1387.

Box MS, Bateman RM, Glover BJ, Rudall PJ. 2008. Floral ontogenetic evidence of repeated speciation via paedomorphosis in subtribe Orchidinae (Orchidaceae). *Botanical Journal of the Linnean Society* **157:** 429-454.

Bradshaw E, Rudall PJ, Devey DS, Thomas MM, Glover BJ, Bateman RM. 2010. Comparative labellum micromorphology of the sexually deceptive temperate orchid genus *Ophrys*: diverse epidermal cell types and multiple origins of structural colour. *Botanical Journal of the Linnean Society* **162:** 504-540.

Bronner R. 1975. Simultaneous demonstration of lipids and starch in plant tissues. *Stain Technology* **50:** 1-4.

Cortis P, Vereecken NJ, Schiestl FP, Lumaga MRB, Scrugli A, Cozzolino S. 2009. Pollinator convergence and the nature of species' boundaries in sympatric Sardinian *Ophrys* (Orchidaceae). *Annals of Botany* **104:** 497-506.

David R, Carde JP. 1964. Coloration diférentielle des inclusions lipidiques et terpeniques des pseudophylles du *Pin maritime* au moyen du reactif Nadi. *Comptes Rendus de l'Académie des Sciences* **258:** 1338-1340.

Delforge P. 2005. *Guide des orchidées d'Europe, d'Afrique du Nord et du Proche-Orient.* 3rd ed. Paris: Delachaux et Niestlé.

Devey DS, Bateman RM, Fay MF, Hawkins JA. 2008. Friends or relatives? Phylogenetics and species delimitation in the controversial European orchid genus *Ophrys*. *Annals of Botany* **101:** 385-402.

Devillers P, Devillers-Terschuren J. 1994. Essai d'analyse systématique du genre *Ophrys*. *Les Naturalistes belges* **75 (Orchidées 7):** 273-400.

Domínguez E, Heredia-Guerrero JA, Heredia A. 2011. The biophysical design of plant cuticles: an overview. *New Phytologist* **189:** 938–949.

Ellis AG, Johnson SD. 2010. Floral mimicry enhances pollen export: the evolution of pollination by sexual deceit outside of the Orchidaceae. *The American Naturalist* **176:** E143–E151.

Feder N, O'Brien TP. 1968. Plant microtechnique: some principles and new methods. *American Journal of Botany* **55:** 123-142.

Flach A, Marsaioli AJ, Singer RB, Amaral MCE, Menezes C, Kerr WE, Batista-Pereira LG, Corrêa AG. 2006. Pollination by sexual mimicry in *Mormolyca ringens*: a floral chemistry that remarkably matches the pheromones of virgin queens of *Scaptotrigona* sp. *Journal of Chemical Ecology* **32:** 59-70.

Franceschi VR, Nakata PA. 2005. Calcium oxalate in plants: formation and function. *Annual Review of Plant Biology* **56:** 41-71.

Ganter P, Jollès G. 1969. *Histologie normale et pathologique. Volume 1.* Paris: Gauthier-Villars.

Gaskett AC. 2011. Orchid pollination by sexual deception: pollinator perspectives. *Biological Reviews* **86:** 33-75.

Godfery MJ. 1917. The genus *Ophrys*. *The Journal of Botany, British and Foreign* **55:** 329-332.

Godfery MJ. 1928. Classification of the genus *Ophrys*. *The Journal of Botany, British and Foreign* **66:** 33-36.

Gögler J, Stökl J, Sramkova A, Twele R, Francke W, Cozzolino S, Cortis P, Scrugli A, Ayasse M. 2009. Ménage à trois - two endemic species of deceptive orchids and one pollinator species. *Evolution* **63:** 2222-2234.

Gögler J, Twele R, Francke W, Ayasse M. 2011. Two phylogenetically distinct species of sexually deceptive orchids mimic the sex pheromone of their single common pollinator, the cuckoo bumblebee *Bombus vestalis*. *Chemoecology* **21:** 243-252.

Gutmann M. 1995. Improved staining procedures for photographic documentation of phenolic deposits in semithin sections of plant tissue. *Journal of Microscopy* **179:** 277-281.

Harborne JB. 1998. *Phytochemical methods: a guide to modern techniques of plant analysis.* 3rd ed. London: Chapman & Hall.

Heiduk A, Brake I, Tolasch T, Frank J, Jürgens A, Meve U, Dötterl S. 2010. Scent chemistry and pollinator attraction in the deceptive trap flowers of *Ceropegia dolichophylla*. *South African Journal of Botany* **76:** 762-769.

Kay QON, Daoud HS, Stirton CH. 1981. Pigment distribution, light reflection and cell structure in petals. *Botanical Journal of the Linnean Society* **83:** 57-84.

Kirk PW. 1970. Neutral red as a lipid fluorochrome. *Stain Technology* **45:** 1-4.

Koch K, Bhushan B, Barthlott W. 2008. Diversity of structure, morphology and wetting of plant surfaces. *Soft Matter* **4:** 1943-1963.

Kullenberg B. 1961. Studies in *Ophrys* pollination. *Zoologiska Bidrag fran Uppsala* **34:** 1-340.

Kullenberg B. 1973a. New observations on the pollination of *Ophrys* L. (Orchidaceae). *Zoon* **Suppl. 1:** 9-14.

Kullenberg B. 1973b. Field experiments with chemical sexual attractants on aculeate Hymenoptera males. II. *Zoon* **Suppl. 1:** 31-42.

Kullenberg B, Bergström G. 1976. Hymenoptera Aculeata males as pollinators of *Ophrys* orchids. *Zoologica Scripta* **5:** 13-23.

Kullenberg B, Borg-Karlson A-K, Kullenberg A-L. 1984. Field studies on the behaviour of the *Eucera nigrilabris* male in the odour flow from flower labellum extract of *Ophrys tenthredinifera*. *Nova Acta Regiae Societatis Scientiarum Upsaliensis, Serie V:C* **3:** 79-110.

Kunst L, Samuels AL, Jetter R. 2005. The plant cuticle: formation and structure of epidermal surfaces. In: Murphy DJ, ed *Plant lipids: biology, utilisation and manipulation.* Oxford: Blackwell Publishing, 270-302.

Lara Ruiz J. 2010. Polinizadores y visitantes de *Ophrys* L. en la Península Ibérica e Islas Baleares. *Micobotanica-Jaén* **Año V, Nº 3:** http://www.micobotanicajaen.com/Revista/Articulos/JLaraR/Polinizadores/Ophrys.html.

Mant JG, Brändli C, Vereecken NJ, Schulz CM, Francke W, Schiestl FP. 2005. Cuticular hydrocarbons as sex pheromone of *Colletes cunicularius* (Hymenoptera: Colletidae) and the key to its mimicry by the sexually deceptive orchid, *Ophrys exaltata*. *Journal of Chemical Ecology* **31:** 1765-1787.

Melo MC, Borba EL, Paiva EAS. 2010. Morphological and histological characterization of the osmophores and nectaries of four species of *Acianthera* (Orchidaceae: Pleurothallidinae). *Plant Systematics and Evolution* **286:** 141-151.

Parham RA, Kaustinen HM. 1976. Differential staining of tannin in sections of epoxy-embedded plant cells. *Stain Technology* **51:** 237-240.

Paulus HF. 2006. Deceived males - Pollination biology of the Mediterranean orchid genus *Ophrys* (Orchidaceae). *Journal Europäischer Orchideen* **38:** 303-353.

Payne WW. 1978. A glossary of plant hair terminology. *Brittonia* **30:** 239-255.

Peakall R, Ebert D, Poldy J, Barrow RA, Francke W, Bower CC, Schiestl FP. 2010. Pollinator specificity, floral odour chemistry and the phylogeny of Australian sexually deceptive *Chiloglottis* orchids: implications for pollinator-driven speciation. *New Phytologist* **188:** 437-450.

Pearse AGE. 1985. *Histochemistry: theoretical and applied. Volume 2, Analytical technology.* 4th ed. Edinburgh: Churchill-Livingstone.

Peter CI, Coombs G, Huchzermeyer CF, Venter N, Winkler AC, Hutton D, Papier LA, Dold AP, Johnson SD. 2009. Confirmation of hawkmoth pollination in *Habenaria epipactidea*: leg placement of pollinaria and crepuscular scent emission. *South African Journal of Botany* **75:** 744-750.

Płachno BJ, Świątek P, Szymczak G. 2010. Can a stench be beautiful? – Osmophores in stem-succulent stapeliads (Apocynaceae-Asclepiadoideae-Ceropegieae-Stapeliinae). *Flora* **205:** 101-105.

Pouyanne M. 1917. La fécondation des *Ophrys* par les insectes. *Bulletin de la Société d'Histoire Naturelle de l'Afrique du nord* **8:** 6-7.

Pridgeon AM, Stern WL. 1983. Ultrastructure of osmophores in *Restrepia* (Orchidaceae). *American Journal of Botany* **70:** 1233-1243.

Pridgeon AM, Stern WL. 1985. Osmophores of *Scaphosepalum* (Orchidaceae). *Botanical Gazette* **146:** 115-123.

Schiestl FP, Ayasse M, Paulus HF, Erdmann D, Francke W. 1997. Variation of floral scent emission and postpollination changes in individual flowers of *Ophrys sphegodes* subsp. *sphegodes*. *Journal of Chemical Ecology* **23:** 2881-2895.

Schiestl FP, Ayasse M, Paulus HF, Löfstedt C, Hansson BS, Ibarra F, Francke W. 1999. Orchid pollination by sexual swindle. *Nature* **399:** 421-422.

Schlüter PM, Xu S, Gagliardini V, Whittle E, Shanklin J, Grossniklaus U, Schiestl FP. 2011. Stearoyl-acyl carrier protein desaturases are associated with floral isolation in

sexually deceptive orchids. *Proceedings of the National Academy of Sciences of the United States of America* **108:** 5696-5701.

Servettaz O, Bino Maleci L, Grünanger P. 1994. Labellum micromorphology in the *Ophrys bertolinii* agg. and some related taxa (Orchidaceae). *Plant Systematics and Evolution* **189:** 123-131.

Shobe WR, Lersten NR. 1967. A technique for clearing and staining gymnosperm leaves. *Botanical Gazette* **128:** 150-152.

Skubatz H, Kunkel DD, Howald WN, Trenkle R, Mookherjee B. 1996. The *Sauromatum guttatum* appendix as an osmophore: excretory pathways, composition of volatiles and attractiveness to insects. *New Phytologist* **134:** 631-640.

Soliva M, Kocyan A, Widmer A. 2001. Molecular phylogenetics of the sexually deceptive orchid genus *Ophrys* (Orchidaceae) based on nuclear and chloroplast DNA sequences. *Molecular Phylogenetics and Evolution* **20:** 78-88.

Steiger S, Schmitt T, Schaefer HM. 2011. The origin and dynamic evolution of chemical information transfer. *Proceedings of the Royal Society B: Biological Sciences* **278:** 970-979.

Steiner KE, Whitehead VB, Johnson SD. 1994. Floral and pollinator divergence in two sexually deceptive South African orchids. *American Journal of Botany* **81:** 185-194.

Stern WL, Curry KJ, Pridgeon AM. 1987. Osmophores of *Stanhopea* (Orchidaceae). *American Journal of Botany* **74:** 1323-1331.

Stökl J, Twele R, Erdmann DH, Francke W, Ayasse M. 2008. Comparison of the flower scent of the sexually deceptive orchid *Ophrys iricolor* and the female sex pheromone of its pollinator *Andrena morio*. *Chemoecology* **17:** 231-233.

Stökl J, Schlüter PM, Stuessy TF, Paulus HF, Fraberger R, Erdmann D, Schulz C, Francke W, Assum G, Ayasse M. 2009. Speciation in sexually deceptive orchids: pollinator-driven selection maintains discrete odour phenotypes in hybridizing species. *Biological Journal of the Linnean Society* **98:** 439-451.

Stpiczyńska M. 2001. Osmophores of the fragrant orchid *Gymnadenia conopsea* L. (Orchidaceae). *Acta Societatis Botanicorum Poloniae* **70:** 91-96.

Stpiczyńska M, Davies KL, Gregg A. 2004. Nectary structure and nectar secretion in *Maxillaria coccinea* (Jacq.) L.O. Williams ex Hodge (Orchidaceae). *Annals of Botany* **93:** 87-95.

Teixeira SP, Borba EL, Semir J. 2004. Lip anatomy and its implications for the pollination mechanisms of *Bulbophyllum* species (Orchidaceae). *Annals of Botany* **93:** 499-505.

Vereecken NJ, Wilson CA, Hötling S, Schulz S, Banketov SA, Mardulyn P. 2012. Pre-adaptations and the evolution of pollination by sexual deception: Cope's rule of specialization revisited. *Proceedings of the Royal Society B: Biological Sciences* **279:** 4786-4794.

Vogel S. 1990. *The role of scent glands in pollination: on the structure and function of osmophores.* Rotterdam: A. A. Balkema. [English translation of: Vogel S. 1963. Duftdrüsen im Dienste der Bestäubung: Über Bau und Funktion der Osmophoren. *Akademie der Wissenschaften und der Literatur in Mainz, Abhandlungen der Mathematisch-Naturwissenschaftlichen Klasse* **10**: 600-763].

Vogel S, Martens J. 2000. A survey of the function of the lethal kettle traps of *Arisaema* (Araceae), with records of pollinating fungus gnats from Nepal. *Botanical Journal of the Linnean Society* **133:** 61-100.

Vogel S, Hadacek F. 2004. Contributions to the functional anatomy and biology of *Nelumbo nucifera* (Nelumbonaceae) III. An ecological reappraisal of floral organs. *Plant Systematics and Evolution* **249:** 173-189.

Wiemer AP, Moré M, Benitez-Vieyra S, Cocucci AA, Raguso RA, Sérsic AN. 2009. A simple floral fragrance and unusual osmophore structure in *Cyclopogon elatus* (Orchidaceae). *Plant Biology* **11:** 506-514.

SUPPORTING INFORMATION

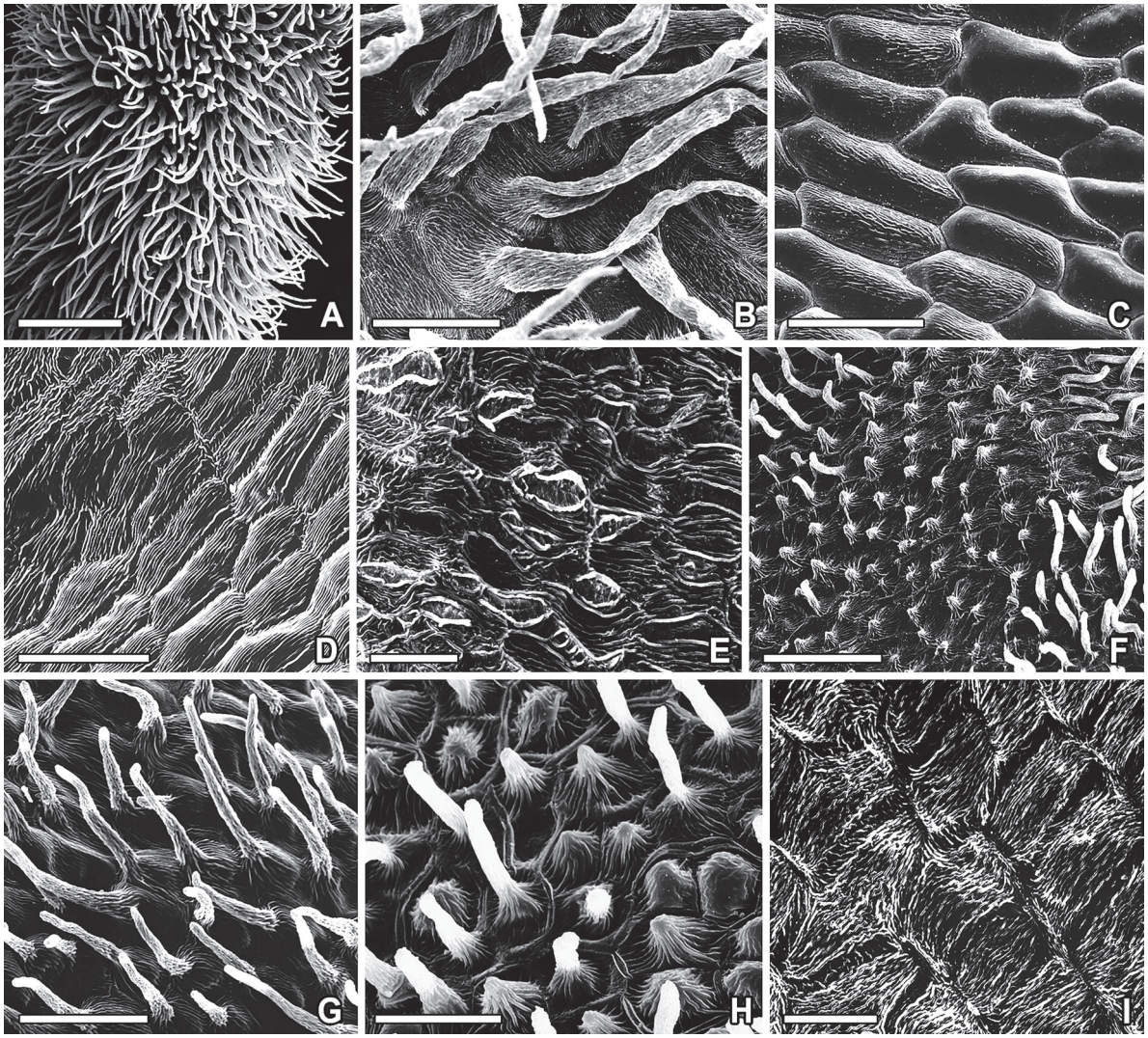

Figure A1. Scanning electron micrographs of adaxial surface of labellum of flowers of *Ophrys bombyliflora*, at anthesis (A, B, D–I) and pre-anthesis (C). A, Hirsute indumentum of lateral labellum lobe. B, Long contorted trichomes on the basal gibbous portion of lateral lobe. C, Glabrous apical portion of lateral lobe. D, Floor of stigmatic cavity at transition area to wall of stigmatic cavity (upper left). E, Detail of pseudoeye slope. F, Glabrous speculum at transition to surrounding indumentum. G, Long attenuate trichomes of apical indumentum. H, Sparse lateral indumentum showing attenuate trichomes among short papillae. I, Flat polygonal cells of broad glabrous labellum margin. Scale bars: 500 µm (A); 100 µm (B–D, F, G); 50 µm (E, H, I).

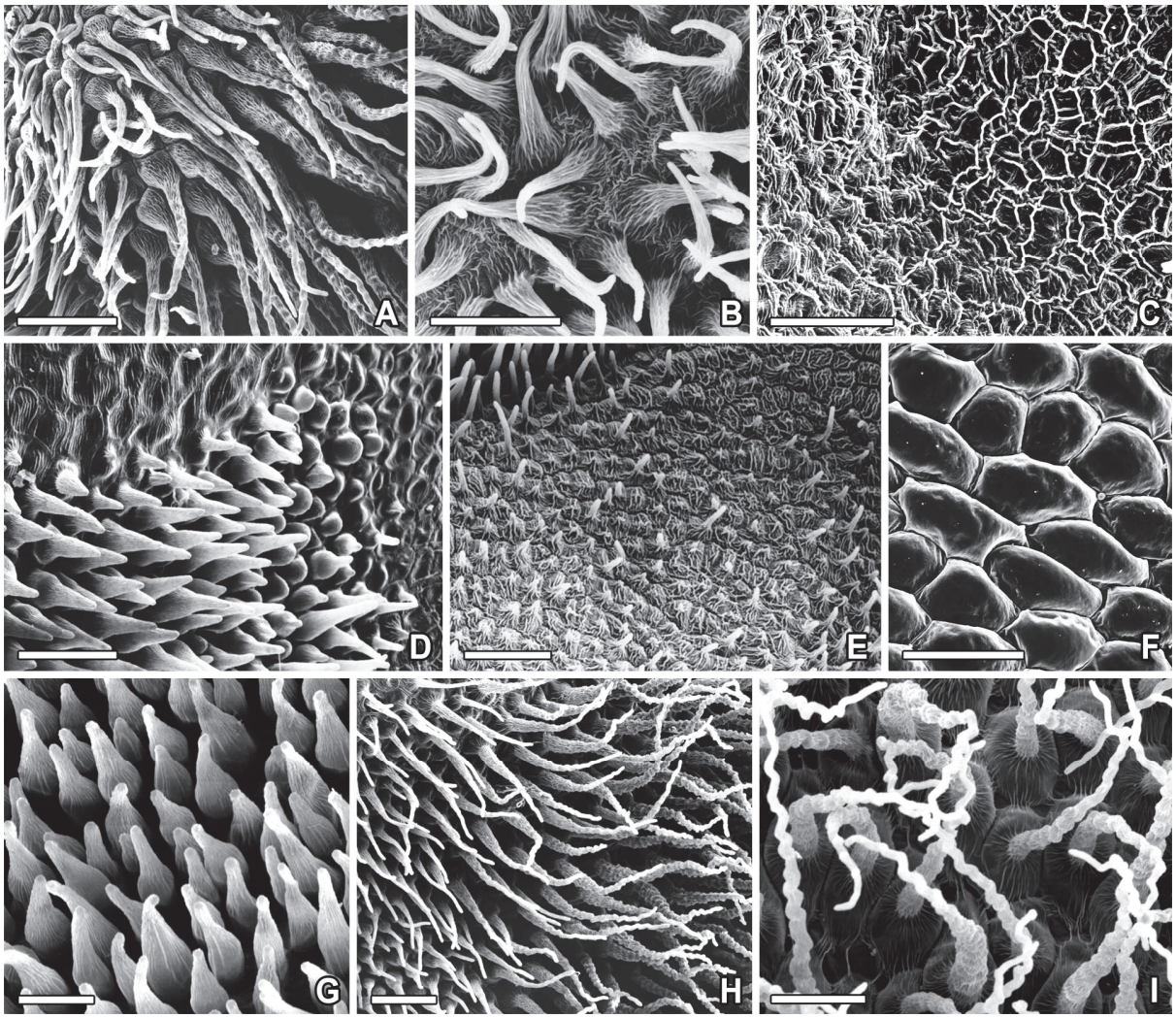

Figure A2. Scanning electron micrographs of labellum of flowers of *Ophrys tenthredinifera*, at pre-anthesis (A, F) and at anthesis (B–E, G–I). A, Long contorted trichomes of lateral labellum lobe. B, Short trichomes diverging from the lateral labellum lobe apex. C, Glabrous lateral area of speculum between basal field and labellum margin. D, Upper right portion of basal field showing transition to glabrous adjacent regions. E, Speculum at transition to basal field (upper left) showing densely striated papillae and flat cells. F, Pavement cells of abaxial surface of apical labellum. G, Short conical trichomes with swollen tips of median indumentum. H, Apical hirsute indumentum showing transition to long contorted trichomes. I, Detail of contorted trichomes with fine sculptured bases and sinuate tips. Scale bars: 150 µm (A, H); 100 µm (B–F, I); 50 µm (G).

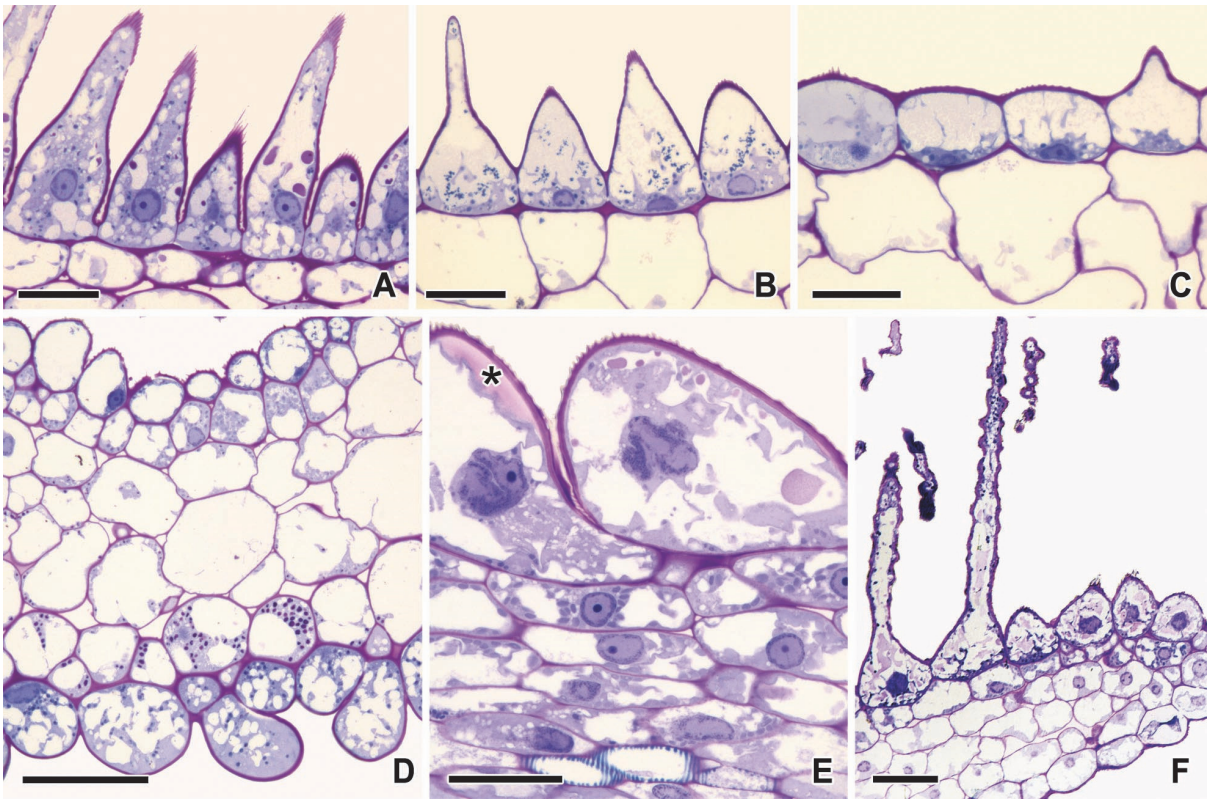

Figure A3. Light micrographs of historesin sections of labellum of *Ophrys tenthredinifera*, stained with PAS/toluidine blue (A–D, F) and toluidine blue/Lugol (E). A, B, Longitudinal sections of median labellum. A, Early bud, vacuoles contain pink-stained deposits. B, Opened flower, conical to attenuate trichomes with green-stained granular vacuolar content. C, Opened flower, longitudinal section of speculum. D, Early bud, transverse section of apical margin near appendix, showing the contrast between adaxial and abaxial surfaces; note that starch-rich plastids are only observed in parenchyma cells on the abaxial side. E, Early bud, longitudinal section of apical labellum, showing a pink-violet-stained material in vacuoles and periplasmic space (asterisk) of the trichome cell. F, Early bud, transverse section of apical labellum near the margin, showing long, contorted trichomes. Scale bars: 50 µm (A–C, E); 100 µm (D, F).

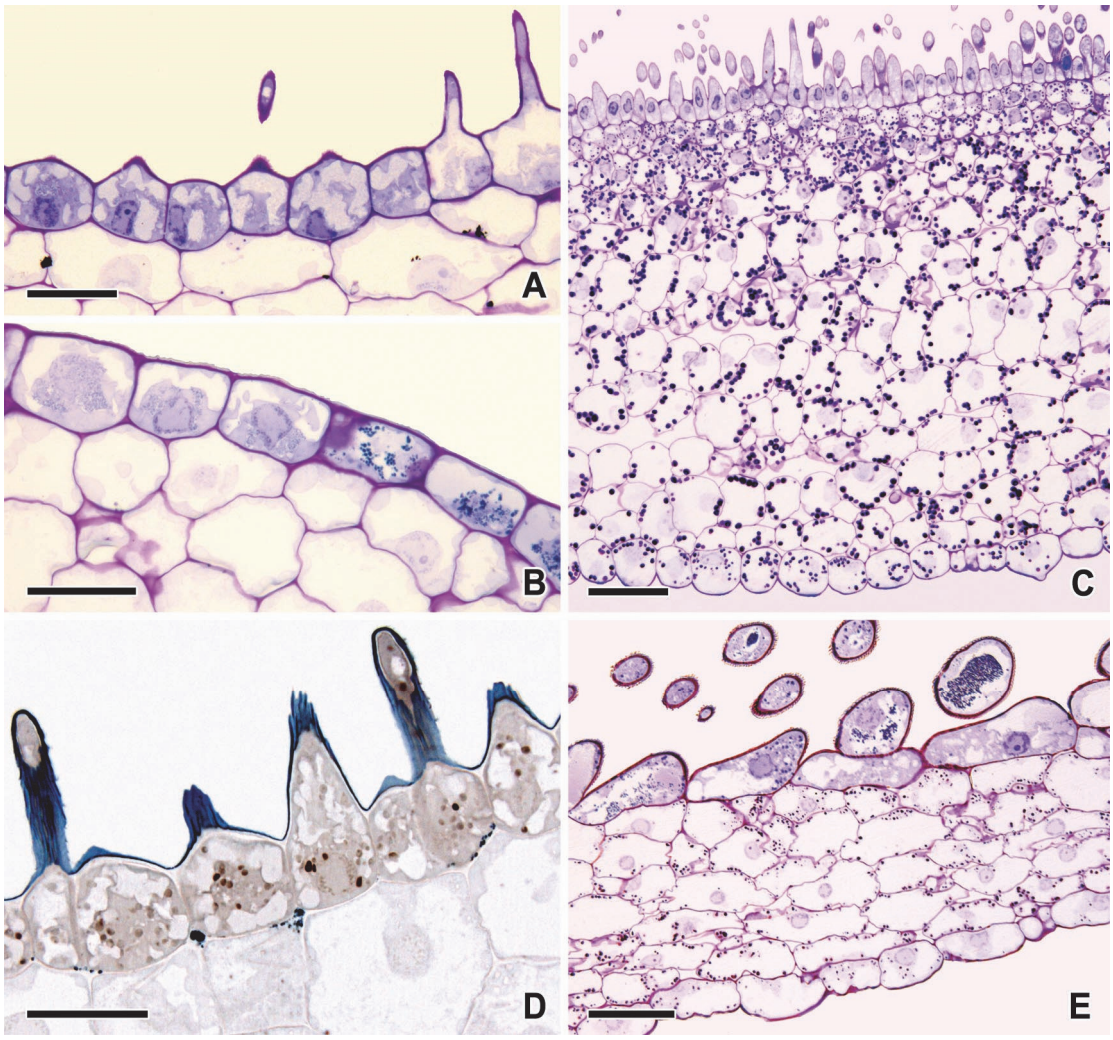

Figure A4. Light micrographs of historesin sections of labellum of *Ophrys bombyliflora*, stained with PAS/toluidine blue (A–C, E) and Sudan black B (D). A, B, Opened flower, transverse sections of median labellum. A, Speculum papillae at the transition area to short trichomes. B, Flat cells of labellum margin with green-stained phenolic vacuolar content. C, Early bud, longitudinal section of median-apical region, showing parenchyma with abundant starch-rich plastids. D, Late bud, transverse section of median labellum, showing short conical trichomes with cutinized outer cell walls and lipophilic material at inner periclinal cell walls. E, Late bud, longitudinal section of lateral labellum lobe, showing dense phenolic vacuolar deposits in trichomes. Scale bars: 50 µm (A–C, E); 25 µm (D).

CHAPTER 4

OSMOPHORE AND NEW MICROMORPHOLOGICAL FLORAL FEATURES IN THE SEXUALLY DECEPTIVE WASP POLLINATED ORCHID *OPHRYS SPECULUM* (ORCHIDACEAE)

This chapter has been submitted for publication in a peer-reviewed international journal:

Francisco A. and Ascensão L. Osmophore and new micromorphological floral features in the sexually deceptive wasp pollinated orchid *Ophrys speculum* (Orchidaceae). (submitted).

OSMOPHORE AND NEW MICROMORPHOLOGICAL FLORAL FEATURES IN THE SEXUALLY DECEPTIVE WASP POLLINATED ORCHID *OPHRYS SPECULUM* (ORCHIDACEAE)

ABSTRACT

Sexually deceptive pollination typically involves highly specific attraction of male insects, primarily by the floral scent, but also by certain morphological floral features. Although the one-to-one liaison between the *Ophrys speculum* orchid and males of the *Dasyscolia ciliata* wasp is essentially due to unusual pheromone-mimicking semiochemicals, the floral odour bouquet contains multiple compounds. A scent-producing gland (osmophore) was described for four closest relatives of *O. speculum* and its occurrence is now investigated for this species. Additionally, since some controversy exists about the labellum configuration in *O. speculum*, here we characterize its micromorphology. Our study revealed that *O. speculum* presents a distinctive basal field which is probably homologous to those of other *Ophrys* species, despite its singular location in the cupuliform concavity occurring between the stigmatic cavity's labia. Furthermore, an osmophore with a vestigial starch content and presumed little activity was found in the apical labellum margin. This osmophore emits a terpene-rich lipophilic secretion with theoretical small relevance for long-range attraction of the specific wasp pollinator of *O. speculum*. However, it could be an important reservoir of semiochemicals to be used in the adaptation to new pollinators, adding flexibility and evolutionary potential to the highly specific pollination system of *Ophrys* orchids.

KEYWORDS: *Dasyscolia ciliata* wasp; floral anatomy; flower morphology; labellum micromorphology; *Ophrys vernixia*; secretory structure; sexual deception; specialized pollination; visual mimicry; volatile secretion.

INTRODUCTION

Unlike most flowering plants, which provide their pollinators with floral rewards such as nectar, pollen, floral oils, liquid fragrances, waxes, or resins, deceptive pollinated species have rewardless flowers that yet simulate the presence of a reward (van der Pijl & Dodson, 1966; Dafni, 1984; Renner, 2005; Schiestl, 2005; Jersáková, Johnson & Kindlmann, 2006). Although pollination through deception has been documented in at least 32 angiosperm families, approximately 87% of the deceptive species are members of the family Orchidaceae (Renner, 2005). It has been estimated that about one third of all orchids, corresponding to 6500 to 8000 species, attracts pollinators by deception (van der Pijl & Dodson, 1966; Renner, 2005). Most deceptive orchids are pollinated through generalized food deception, attracting food-foraging insect pollinators by imitating general floral signals that are characteristic of rewarding flowers (Jersáková *et al.*, 2006; Peter & Johnson, 2013). An even more sophisticated pollination syndrome has evolved in at least 22 genera of orchids (Gaskett, 2011; Vereecken *et al.*, 2012; Phillips *et al.*, 2014), which deceive only male insect pollinators by offering them nothing but an illusion of virgin conspecific females (Pouyanne, 1917; Schiestl, 2005). Sexual deception is typically achieved by a nearly perfect mimic of the female's sex pheromone, visual appearance and body texture provided by the orchid flower, particularly the labellum, i.e. the modified petal of the orchid flower (Kullenberg, 1961; Schiestl *et al.*, 1999; Ciotek *et al.*, 2006; Peakall *et al.*, 2010; Gaskett, 2012). Because insect mating signals are species-specific (Ayasse, Paxton & Tengö, 2001), the flowers of each sexually deceptive species are almost exclusively attractive to males of a single, or a few related, insect species, and a highly specialized pollination interaction is maintained between these orchids and their specific insect pollinators (Kullenberg, 1961; Paulus & Gack, 1990; Schiestl & Schlüter, 2009; Peakall *et al.*, 2010). Strong floral isolation, primarily mediated by the floral scent that underlies the high pollinator specificity, has been reported for most co-occurring sexually deceptive orchids, which have weak or absent postmating barriers and hence rely on the strong prepollination reproductive isolation provided by their labella to prevent hybridization (Scopece *et al.*, 2007; Schiestl & Schlüter, 2009; Xu *et al.*, 2011; Xu *et al.*, 2012a; Xu, Schlüter & Schiestl, 2012b; Peakall & Whitehead, 2014). Despite the primary significance of the floral scent for both pollinator attraction and reproductive isolation in sexually deceptive orchids, floral morphological traits, such as floral shape, colour, size and texture, provide visual and tactile stimuli for male pollinators and play an important role in converting attraction into effective pollination (Kullenberg, 1961; Spaethe, Moser & Paulus, 2007; Benitez-Vieyra, Medina & Cocucci, 2009; Streinzer, Paulus & Spaethe, 2009; Gaskett & Herberstein, 2010; Gaskett, 2012; Phillips *et al.*, 2013). Therefore, characterizing the key floral morphological traits involved in the attraction of specific pollinators is crucial to more comprehensively understand the process of pollinator-

driven speciation that has probably been evolving in sexually deceptive orchids (Ayasse, Stökl & Francke, 2011; Xu *et al.*, 2012b; Peakall & Whitehead, 2014).

The insectiform flowers of the Euro-Mediterranean, sexually-deceptive orchid genus *Ophrys* L. (Orchidaceae: Orchidinae) have long been intriguing naturalists on account of their morphological peculiarity and sophisticated mode of reproduction (Darwin, 1862; Correvon & Pouyanne, 1916; Godfery, 1925; Vereecken & Francisco, 2014). Because of the special properties of their labella, providing chemical, visual, and tactile stimuli for pollinators, *Ophrys* flowers are pollinated through pseudocopulation by mate-searching males of specific insects, predominantly solitary bees, but also solitary parasitic wasps, eusocial bees, and beetles (Kullenberg, 1961; Paulus, 2006; Gaskett, 2011). While performing copulatory attempts with the labellum, male insects remove pollinaria with their head or abdomen tip and thus act as pollen vectors in subsequent visits to *Ophrys* flowers (Pouyanne, 1917; Godfery, 1928).

The process of pollinator attraction to *Ophrys* orchids is triggered by the complex odour bouquet emitted by the labellum, which consists of more than 100 organic compounds of different volatility (Borg-Karlson, 1990) and includes a small set of key semiochemicals that are able to elicit mating behaviour in specific male insects, because of their similarity with the sex pheromones produced by the pollinator´s female (Schiestl *et al.*, 1999; Ayasse *et al.*, 2003; Mant *et al.*, 2005; Stökl *et al.*, 2008; Gögler *et al.*, 2011). In the majority of the *Ophrys* species hitherto investigated, these key behaviourally active compounds are series of low-volatile long-chained hydrocarbons, especially alkenes differing in double-bond position and carbon chain length, which are produced in different proportions according to the species (Stökl *et al.*, 2008; Stökl *et al.*, 2009; Vereecken, Cozzolino & Schiestl, 2010; Xu *et al.*, 2011; Xu *et al.*, 2012a). On the other hand, highly volatile organic compounds, such as short-chained hydrocarbons, alcohols, aldehydes, esters, oxygenated mono- and sesquiterpenes and some aromatic compounds, were proved to be efficient in long-range attraction of male pollinators by triggering their flight approach to the *Ophrys* flowers in field bioassays (Kullenberg, Borg-Karlson & Kullenberg, 1984; Borg-Karlson & Tengö, 1986; Borg-Karlson, 1990; Borg-Karlson *et al.*, 2003; Mant *et al.*, 2005). While the long-chained hydrocarbons are among the common constituents of the plant cuticle (Buschhaus & Jetter, 2011), at least part of the highly volatile components of the odour bouquet is probably synthesised in a floral secretory structure (osmophore) located in the apical region of the *Ophrys* labellum (Francisco & Ascensão, 2013). The occurrence of such a fragrance-producing floral gland was confirmed solely for four closely related *Ophrys* species, namely *Ophrys bombyliflora* Link, *O. fusca* Link, *O. lutea* Cav., and *O. tenthredinifera* Willd. (Vogel, 1990; Ascensão *et al.*, 2005; Francisco & Ascensão, 2013). Molecular phylogenetic analyses performed in the genus *Ophrys* revealed that *O. bombyliflora*, *O. tenthredinifera* and the section *Pseudophrys* Godfery (to which *O. fusca* and *O. lutea* belong) together form a major clade with *O. speculum* Link, although the interspecific relationships within it remain unresolved (Soliva,

Kocyan & Widmer, 2001; Devey *et al.*, 2008). Hence, it is important to know whether the labellum of *O. speculum* also exhibits an osmophore like its closest relatives and to examine floral features in order to find potentially informative micromorphological data that could help clarifying the phylogeny of this clade.

The orchid-pollinator interaction that is established between *O. speculum* and the solitary parasitic wasp *Dasyscolia ciliata* (Hymenoptera: Scoliidae) is particularly remarkable. This rare, highly specific pollination liaison of one-to-one was reported for the first time in the beginning of the twentieth century by Pouyanne, whose field observations on the behaviour of males of this wasp upon the labellum of that particular *Ophrys* species were determinant for the discovery of the pollination by sexual deception (Correvon & Pouyanne, 1916; Pouyanne, 1917). The specificity of this relationship resides predominantly in the unusual chemical mating signals used by the wasp, and mimicked by the orchid, for its reproduction (Ayasse *et al.*, 2003; Ayasse *et al.*, 2011). The behaviourally active compounds were found to be a combination of eight polar saturated (w-1)-hydroxy and (w-1)-oxo carboxylic acids, aldehydes, and ethyl esters, but the fraction considered key is essentially composed of the oxo and hydroxy acids, namely 9-oxodecanoic acid, 9-hydroxydecanoic acid, and 7-hydroxyoctanoic acid, the two latter occurring in specific enantiomeric proportions (Ayasse *et al.*, 2003; Ayasse *et al.*, 2011). Moreover, an especially strong visual resemblance between the flower of *O. speculum* and the female of its pollinator suggests that visual signals may play a significant role in the success of the pseudocopulation (Kullenberg, 1961; Ågren, Kullenberg & Sensenbaugh, 1984; Paulus, 2006). Indeed, the micromorphological characterization of the labellum of several *Ophrys* species and the comparison of the labellum with the body of the female of their pollinators allowed identifying features indicative of visual and tactile mimicry (Ågren *et al.*, 1984; Borg-Karlson, 1990; Borg-Karlson *et al.*, 1993; Servettaz, Bino Maleci & Grünanger, 1994; Ascensão *et al.*, 2005; Cortis *et al.*, 2009; Bradshaw *et al.*, 2010; Vignolini *et al.*, 2012a; Francisco & Ascensão, 2013). Although the general micromorphology of the labellum of *O. speculum* is well documented (Ågren *et al.*, 1984; Devillers & Devillers-Terschuren, 1994; Bradshaw *et al.*, 2010; Vignolini *et al.*, 2012a), a thorough description of the flower structure is needed for this peculiar species, since some controversy exists about the configuration of the stigmatic cavity and the basal region of the labellum (Devillers & Devillers-Terschuren, 1994; Aldasoro & Sáez, 2005; Delforge, 2005; Bradshaw *et al.*, 2010).

Giving continuity to our studies on the labellum micromorphology and anatomy of representative species of the four groups that constitute the clade composed of *O. bombyliflora*, *O. tenthredinifera*, *O. speculum* and the section *Pseudophrys* (Ascensão *et al.*, 2005; Francisco & Ascensão, 2013), here we focus on *O. speculum*, the species for which such detailed information is still missing. The present study aims to investigate the occurrence of an osmophore in the labellum of *O. speculum* and characterize in depth the micromorphology of the labellum and the stigmatic cavity of this species in order to clarify

their structure. In addition, a comparison with the body of the wasp pollinator's female was made with the purpose of finding structural similarities that could constitute new evidences of visual and/or tactile mimicry.

MATERIALS AND METHODS

BIOLOGICAL MATERIAL

Inflorescences of the two subspecies of *O. speculum* co-occurring in the western part of the geographical distributional area of the species, *Ophrys speculum* Link subsp. *lusitanica* O.Danesch & E.Danesch and *Ophrys speculum* Link subsp. *speculum*, were collected in March and April, between 2005 and 2009, from natural populations occurring in Portugal, in the regions of Loures and Sesimbra, respectively. The taxonomic classification adopted here follows Aldasoro & Sáez (2005). A voucher specimen of each taxon was deposited in LISU, the Herbarium of the University of Lisbon Botanical Garden in Portugal (LISU 231242 and LISU 231246).

Flowers at three developmental stages were examined in the present study: (1) early bud – buds with 5 x 3 to 6 x 4 mm (length x width) in *O. speculum* subsp. *lusitanica* and 5 x 3 to 7 x 3 mm (length x width) in *O. speculum* subsp. *speculum*, corresponding to 4–6 days and 3–7 days before the anthesis, respectively; (2) late bud – buds with 7 x 4 to 8 x 6 mm (length x width) in *O. speculum* subsp. *lusitanica* and 7 x 4 to 9 x 6 mm (length x width) in *O. speculum* subsp. *speculum*, corresponding to 1–3 days and 1–2 days before the anthesis, respectively; and (3) freshly opened flower (also referred to as open flower) – flowers at the beginning of the anthesis.

One female wasp of *Dasyscolia ciliata* Fabricius, 1787 (Hymenoptera: Scoliidae) was captured in April 2008 in the vicinity of a population of *O. speculum* subsp. *speculum* in Serra de Sicó, which is located in the central-littoral region of Portugal.

SCANNING ELECTRON MICROSCOPY (SEM)

Four freshly opened flowers and two late buds of each of the two subspecies of *O. speculum* and the sole female wasp were fixed with 2.5% glutaraldehyde in 0.1 M sodium phosphate buffer, at pH 7.2, following the experimental procedure described in Francisco & Ascensão (2013). Observations were carried out on a JEOL T220 scanning electron microscope (JEOL Ltd., Tokyo, Japan) at an accelerating voltage of 15 or 20 kV. Images were recorded in a Kodak T-Max 100 professional black-and-white negative film using a MAMIYA 6 x 7 camera.

Flower morphology was described using the terminology of Devillers and Devillers-Terschuren (1994). Epidermal cell types were defined considering the features of the cell surface, namely, the curvature of the outer cell wall, the cell outline and the cuticular sculpture, following the terminology of Kay *et al.* (1981) and Koch *et al.* (2008).

STEREOMICROSCOPY

Fresh buds and open flowers of the two subspecies of *O. speculum* and the female wasp individual (which was previously fixed and critical-point dried) were examined under an Olympus SZH-ILLK stereomicroscope (Olympus Optical Co., Ltd., Tokyo, Japan). Images were recorded digitally using an Olympus C-7070 Wide Zoom digital camera (Olympus Imaging Corp., Tokyo, Japan).

For detecting macroscopically the osmophore, two intact freshly opened flowers of *O. speculum* subsp*. lusitanica* were immersed in 0.01% neutral red for 2–4 h (Vogel, 1990), rinsed in tap water and examined.

LIGHT MICROSCOPY

For the anatomical characterization of the labellum of *O. speculum*, pieces of labellum taken from early buds, late buds and freshly opened flowers (three flowers at each stage, on average) of each of the two subspecies were fixed as described for SEM and embedded in Leica Historesin, following Francisco & Ascensão (2013). Sections with 2 µm thick were cut using a Leica RM-2155 microtome (Leica Microsystems, Nussloch, Germany). Historesin sections were sequentially stained with periodic acid–Schiff (PAS) reagent / toluidine blue O (Feder & O'Brien, 1968) or toluidine blue O with pre-treatment with sodium hypochlorite plus post-staining with dilute Lugol (Gutmann, 1995) for general histology and for total polysaccharides and starch. Sudan black B (Bronner, 1975; Parham & Kaustinen, 1976) was used for detection of lipids and tannins. Appropriate controls were also performed.

Portions of the apical margin of the labellum from flowers of *O. speculum* subsp. *lusitanica*, at all three developmental stages, were also fixed with glutaraldehyde, post-fixed with osmium tetroxide, and embedded in Epon-Araldite resin (Electron Microscopy Sciences, Fort Washington, Pennsylvania, USA), following the experimental procedure described in Francisco & Ascensão (2013). Semi-thin sections (roughly 0.5 µm thick) were obtained with a Sorvall MT-1 ultramicrotome (Sorvall Inc., Norwalk, USA) and stained with Sudan black B for lipids and tannins (Bronner, 1975; Parham & Kaustinen, 1976).

For the histochemical characterization of the osmophore, transverse and longitudinal hand-cut sections of the glabrous apical margin of the labellum were made in fresh late buds and open flowers of the two subspecies of *O. speculum*. Neutral red was used as a lipid fluorochrome for detecting lipids under ultraviolet and blue light (Kirk, 1970). Sections were tested for total lipids with Sudan black B (Pearse, 1985) and for terpenoids with Nadi reagent (David & Carde, 1964), with negative control reactions being carried out simultaneously. Phenolic compounds were detected by their autofluorescence under ultraviolet and blue light (Harborne, 1998).

Transverse and longitudinal hand-cut sections of the basal and median regions of the labellum were also made in fresh buds and open flowers of the two subspecies of *O. speculum*, and then tested for lipids with Sudan IV (Pearse, 1985).

Observations were made with a Leica DM-2500 microscope (Leica Microsystems, Wetzlar, Germany) and images were recorded digitally with a Leica DFC-420 camera (Leica Microsystems, Heerbrugg, Switzerland) and the Leica Application Suite software (version 2.8.1). For histochemical tests that required observations under ultraviolet and blue wavelengths, a Leitz SM-LUX epifluorescence microscope (Leitz-Wetzlar, Wetzlar, Germany) equipped with a HBO 50 W mercury vapour lamp, a filter block A (excitation filter BP 340-380, dichroic mirror 450, barrier filter LP-430) and a filter block I2 (excitation filter BP 450-490, barrier filter LP-515) was used. Images were recorded in a Kodak Ultra Gold 400 ASA colour slide film, using a Leica Wild MPS-52 camera (Leica, Wien, Austria).

RESULTS

FLOWER MORPHOLOGY

The peculiar flowers of *O. speculum* are easily recognizable by their convex, obovate, trilobed labellum that exhibits a wide, shining, blue speculum delimited by an orange-to-green band and a dense, long submarginal pilosity that hides a broad, glabrous, apical margin provided with a central notch (Fig. 1).

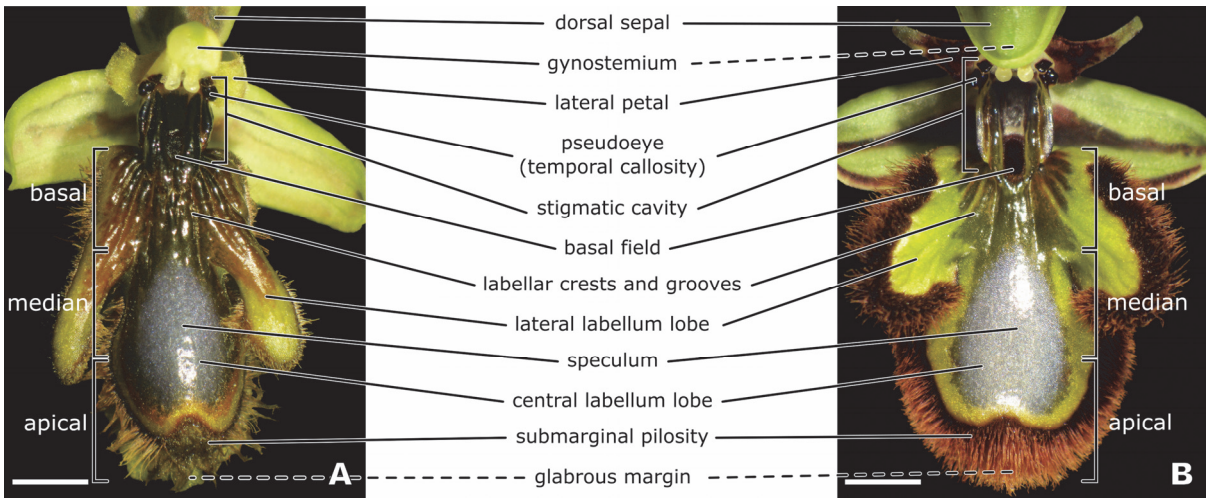

Figure 1. Macrographs of flowers of *Ophrys speculum* subsp. *lusitanica* (A) and *Ophrys speculum* subsp. *speculum* (B), showing the principal morphological floral features. The stigmatic cavity and the three main regions of the labellum (basal, median, apical) are delimited. Scale bars: 2.5 mm.

Stereomicroscopic observations showed that the two investigated subspecies of *O. speculum* differ in some features. The labellum of *O. speculum* subsp. *lusitanica* presents very convex lobes; the central one ends with a wide, light-coloured (usually yellow to greenish-yellow), undulated, glabrous apical margin that often appears folded longitudinally at the central notch, resulting in two halves touching each other (Fig. 2C, E). The two linear-

lanceolate lateral labellum lobes are long, divergent, the tip being directed backwards due to a knee-shaped curvature at the middle (Figs. 1A, 2C, E). By contrast, in *O. speculum* subsp. *speculum* flowers, the central labellum lobe is moderately convex and exhibits a comparatively narrow dark reddish coloured margin (Fig. 2D); the two oval-lanceolate lateral labellum lobes are short, flat, obliquely divergent, pointing the tips forward (Fig. 1B). The two subspecies also exhibit a contrasting colouration in the submarginal pilosity of the labellum and in the lateral petals, which is light and usually yellowish-brown in *O. speculum* subsp. *lusitanica* and dark reddish-brown in *O. speculum* subsp. *speculum* (Fig. 1).

Moreover, the stigmatic cavity of the flowers of *O. speculum* presents an unusually extensive, elevated, flat floor that is framed by two long, protruding labia or crests – one internal and another external – on each of its sides (Fig. 2A, B). The labia are considered to be forward projections of the inferior portion of the walls of the stigmatic cavity flanking its floor (Fig. 2A, B). A pair of shining, black pseudoeyes arises from the temporal callosities, which are located in the upper portion of the stigmatic cavity, immediately below a pair of black staminodial callosities; the stigmatic surface is placed at the ceiling of this cavity, below the pollinaria (Fig. 2A, B).

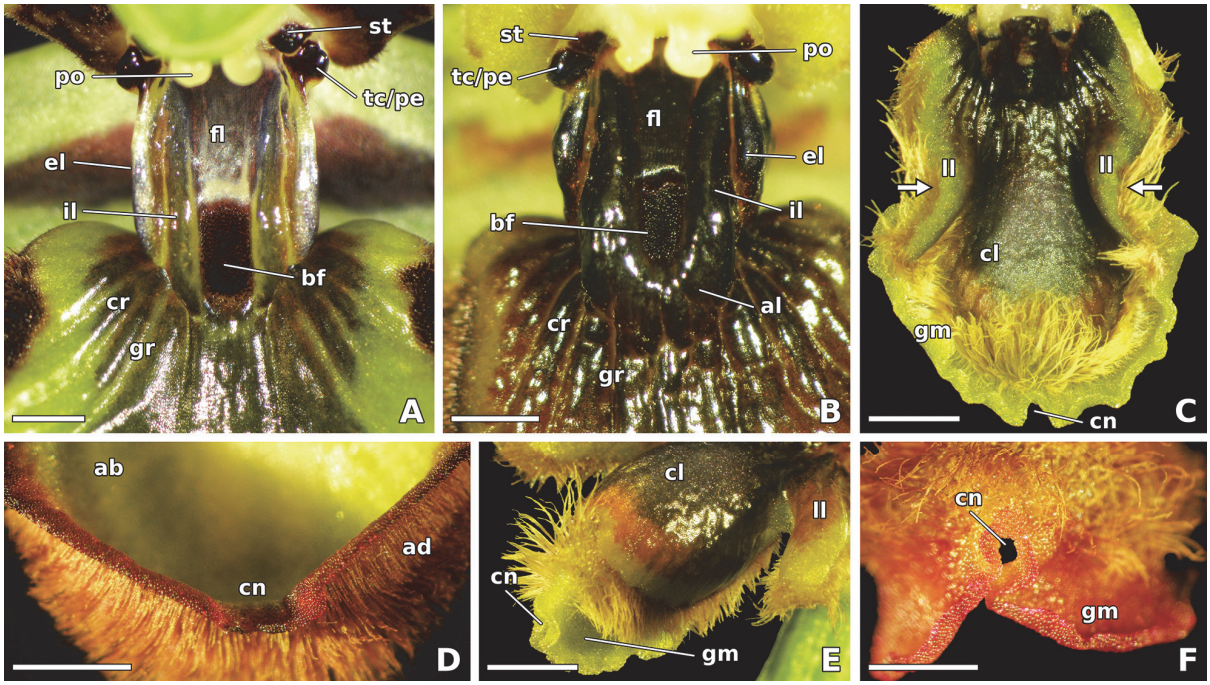

Figure 2. Stereomicrographs of fresh flowers of *Ophrys speculum* subsp. *speculum* (A, D) and *Ophrys speculum* subsp. *lusitanica* (B, C, E, F). A, B, Detail of the stigmatic cavity and the contiguous basal region of the labellum of an open flower of each subspecies, showing their main components. C, Late bud just before the anthesis, showing the not-fully expanded labellum – note the natural yellow pigmentation of the glabrous apical margin of the labellum and the knee-shaped curvature in the lateral labellum lobes (arrows). D, Open flower (in back view), showing the glabrous apical margin of the labellum provided with a central notch – note its natural red pigmentation. E, Open flower (in lateral view), showing the convex central labellum lobe provided with a glabrous margin folded at the central notch. F, Freshly opened flower (in back view) after immersion in diluted neutral red, showing the red-stained apical margin of the labellum. ab, abaxial surface; ad, adaxial surface; al,

augmented portion of labellum; bf, basal field; cl, central labellum lobe; cn, central notch; cr, labellar crest; el, external labium; fl, floor of stigmatic cavity; gm, glabrous margin; gr, labellar groove; il, internal labium; ll, lateral labellum lobe; pe, pseudoeye; po, pollinarium; st, staminodial callosity; tc, temporal callosity. Scale bars: 1 mm (A, B); 2 mm (D, F); 2.5 mm (C, E).

The prominent stigmatic cavity of *O. speculum* seems to join the basal region of the labellum in a singular manner. A confined basal field – a part of the labellum – appears elevated and restricted to a cupuliform concavity, which is located between the distal portions of the internal labia of the stigmatic cavity and is surrounded, in its distal side, by an augmented portion of the labellum fused with these labia (Figs. 2A, B, 3A, B). The area of the labellum immediately below it, which is placed in a lower level, exhibits a sulcate texture due to a series of grooves and crests that diverge radially from the constricted area occurring between the stigmatic cavity and the basal region of the labellum (Figs. 1, 2A, B). The labellum of *O. speculum* subsp. *lusitanica* presents a narrow, oblong to rectangular basal field, which contrasts with the wide, oblong to shield-shaped basal field that typically occurs in *O. speculum* subsp. *speculum* (Figs. 2A, B, 3A, B). This latter subspecies exhibits generally less marked internal labia in the stigmatic cavity and less pronounced grooves and crests in the basal region of the labellum than *O. speculum* subsp. *lusitanica* (Figs. 1, 2A, B). However, some morphological variation was observed among individuals of each subspecies, particularly in what concerns the degree of enlargement of the internal labia, the labellar crests and, especially in *O. speculum* subsp. *lusitanica*, the area of the labellum contiguous to the basal field.

MICROMORPHOLOGY OF THE LABELLUM AND THE STIGMATIC CAVITY

Scanning electron microscopic observations revealed that the flowers of *O. speculum* exhibit seven different epidermal cell types in the adaxial surface of the labellum and the stigmatic cavity. By contrast, the glabrous abaxial surface of the labellum is composed of smooth pavement cells, except for the apical margin, where large dome-shaped papillae occur.

Stigmatic cavity

The unusually extensive floor of the stigmatic cavity of *O. speculum* is composed of (1) flat epidermal cells with elongated, polygonal outline and dense cuticular striations parallel-arranged to the longitudinal axis of the cell on their surface; some striations were found to cross the cell anticlines and to be linked to the striations lain on the outer cell wall of adjacent epidermal cells (Fig. 3C). Apart from the floor, the stigmatic cavity exhibits basically (2) smooth, flat to lenticular cells with isodiametric, polygonal outline, particularly in the pseudoeyes (temporal callosities), staminodial callosities, as well as internal and external labia (Fig. 3A, B, D). In the enlarged, long internal labia and in the augmented portion of the labellum contiguous to the basal field, prominent cuticular ridges were found over the

surface of certain epidermal cells, forming rows that cross each labium perpendicularly to its length (Fig. 3A, B).

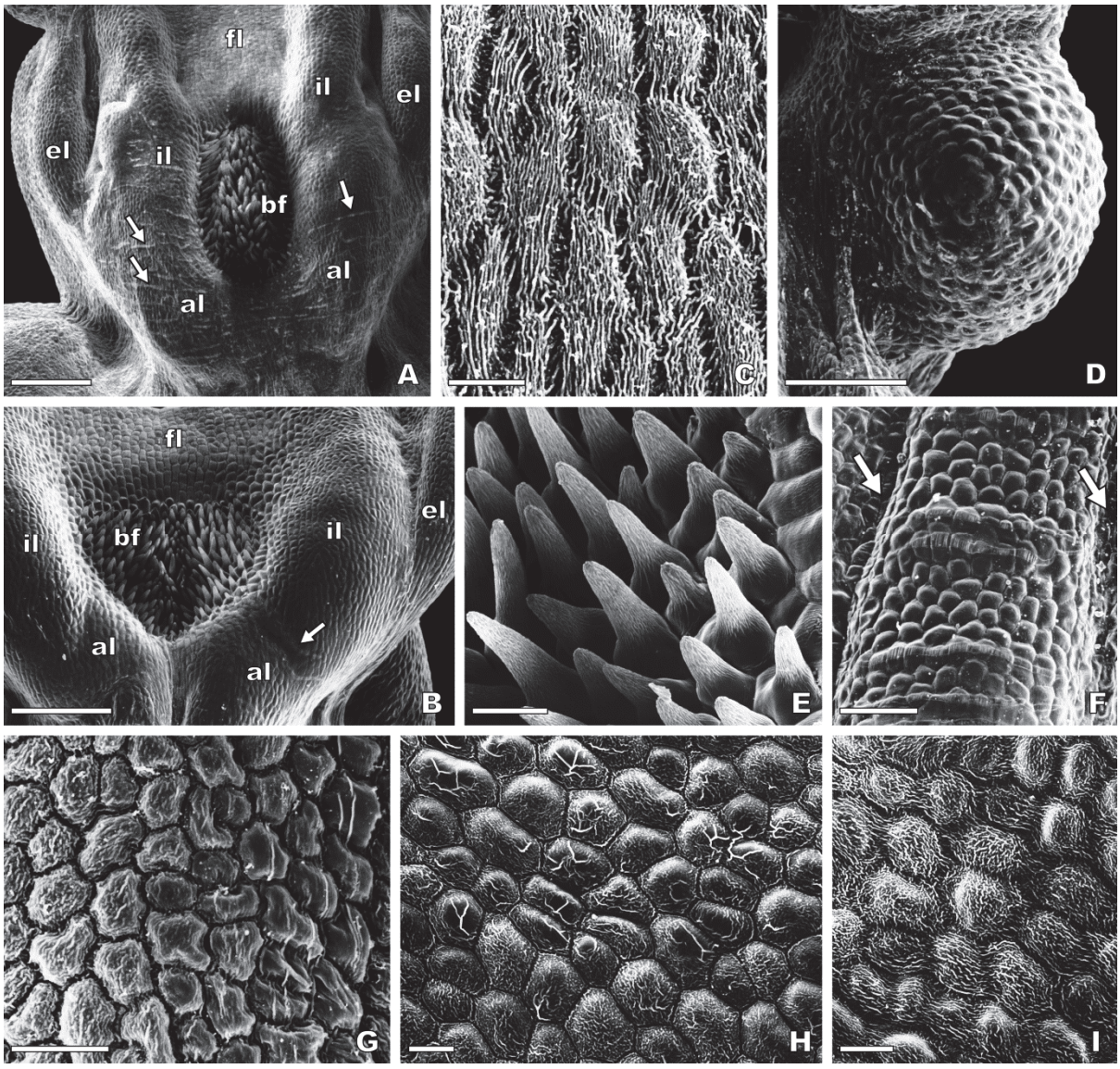

Figure 3. Scanning electron micrographs of the adaxial surface of the stigmatic cavity and the basal region of the labellum in flowers at anthesis of *Ophrys speculum* subsp. *lusitanica* (A, D, F) and *Ophrys speculum* subsp. *speculum* (B, C, E, G–I). A, B, Basal region of the labellum contiguous to the stigmatic cavity of each subspecies – note that the basal field is confined to a cupuliform concavity occurring between the two internal labia of the stigmatic cavity, which are fused distally with an augmented portion of the labellum, where rows of ordered cuticular ridges are evident (arrows). C, Floor of the stigmatic cavity, showing densely striated, elongated, flat epidermal cells. D, Pseudoeye provided with smooth lenticular cells. E, Basal field, showing sub-conical trichomes near the periphery of the cupuliform concavity. F, Labellar crest flanked by grooves (arrows). G, Detail of labellar crest showing the transition between densely striated cells (near the groove) and nearly smooth cells (towards the top of the crest). H, I, Lateral labellum lobe. H, Apical portion, showing lenticular cells with a polygonal outline exhibiting either a reticulate or a heterogeneous cuticular pattern on their surface. I, Basal portion, near the transition to the central labellum lobe – note the diffuse arrangement of the cuticular striations. al, augmented portion of labellum; bf, basal field; el, external labium; fl, floor of stigmatic cavity; il, internal labium. Scale bars: 500 µm (A, B); 250 µm (D); 100 µm (E, F); 30 µm (C, G–I).

Basal region of the labellum

The basal field of the labellum in *O. speculum* consists of mostly (3) sub-conical to attenuate trichomes with fine cuticular striations on their surface, which are restricted to a cupuliform concavity occurring in the area of confluence between the labellum and the stigmatic cavity (Fig. 3A, B, E). Shorter conical trichomes occur in the periphery of the cupuliform concavity (Fig. 3E) and typically longer attenuate trichomes, which have occasionally sinuate tips (especially in *O. speculum* subsp. *lusitanica*), are present in the centre of the basal field.

The sulcate area of labellar crests and grooves that diverge from the constricted area occurring below the basal field extends into the lateral labellum lobes. In *O. speculum* subsp. *lusitanica*, this area is composed of smooth, lenticular cells with a polygonal outline and sometimes it exhibits prominent cuticular ridges similar to those occurring over the surface of the internal labia (Fig. 3F). In contrast, the homologous area of the labellum in *O. speculum* subsp. *speculum* presents (4) lenticular cells with an isodiametric, polygonal outline and a rugose surface, which acquire a nearly smooth appearance towards the top of the crests (Fig. 3G).

Lateral labellum lobes

The lateral lobes of the labellum in *O. speculum* present a wide glabrous surface surrounded by a dense marginal indumentum of (5) long contorted trichomes, similar to those occurring in the sub-marginal indumentum of the central labellum lobe (Fig. 4G). The glabrous portion of the lateral lobes is composed of lenticular cells with an isodiametric, polygonal outline, which are usually smooth or slightly striated in *O. speculum* subsp. *lusitanica* (data not shown) and densely striated in *O. speculum* subsp. *speculum* (Fig. 3H, I), although the degree of cuticular striation was found to vary amongst individuals of each subspecies. Furthermore, the cuticular ornamentation of the cells in *O. speculum* subsp. *speculum* varies according to the area of the lateral lobe in which they occur. Lenticular cells with a reticulate cuticular pattern were found in the apical portion of the lobe and near the margins, whereas those with a diffuse cuticular arrangement occurred in the basal portion, at the transition to the central labellum lobe (Fig. 3H, I). In the apical portion of the lateral lobe, a heterogeneous cuticular pattern consisting of irregular and prominent ridges associated with smooth areas was often found in the surface of some cells (Fig. 3H).

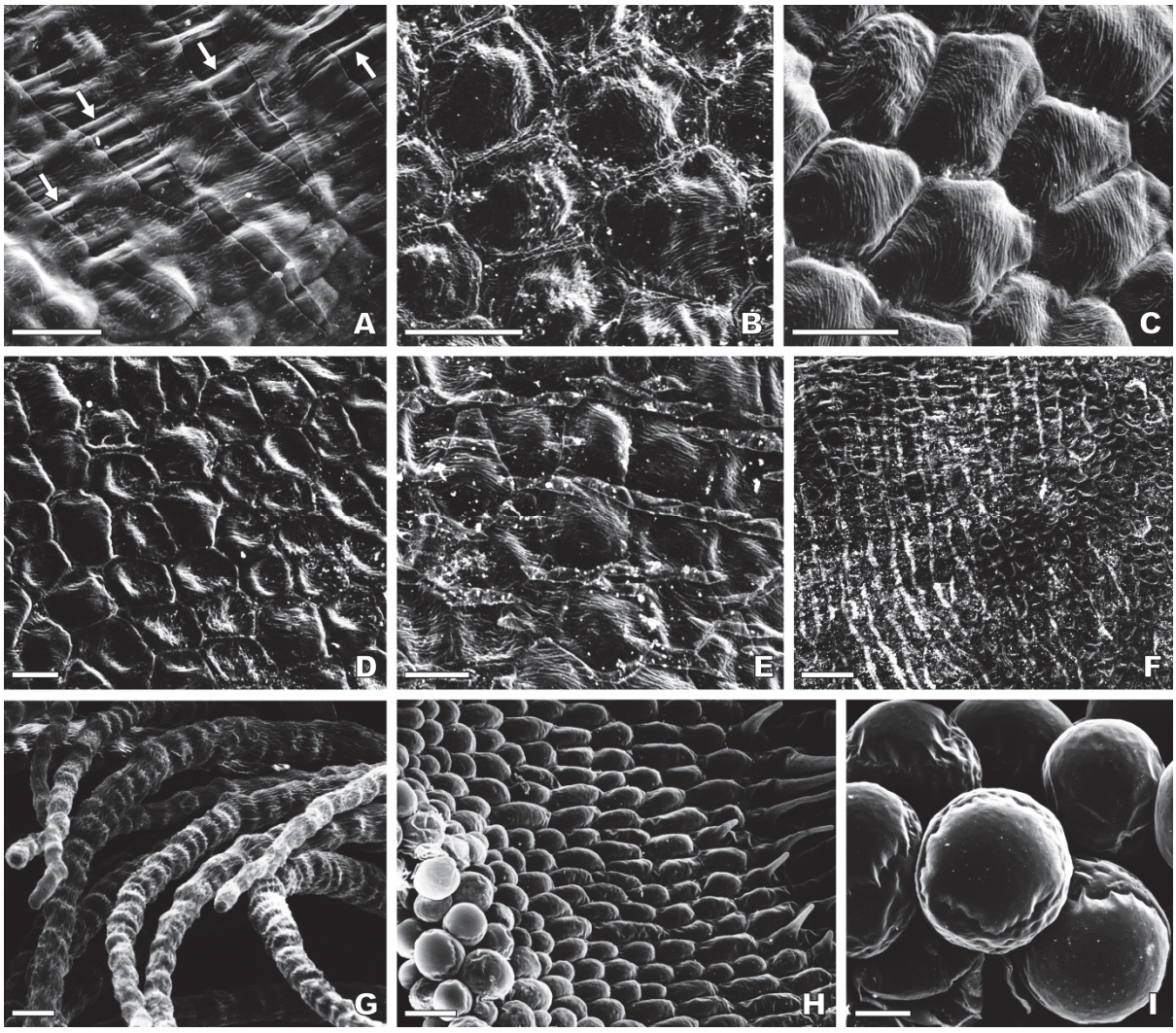

Figure 4. Scanning electron micrographs of the adaxial surface of the median and apical regions of the labellum in flowers at anthesis of *Ophrys speculum* subsp. *speculum* (A, B, G–I) and *Ophrys speculum* subsp. *lusitanica* (C–F). A, Detail of the basal-median region of the labellum, near the beginning of the speculum – a thin film covering the cell surface seems to have been broken into several strips, revealing long and dense cuticular depositions underneath (arrows). B, C, Central area of the speculum of each subspecies, showing flat to lenticular cells with a hexagonal, pentagonal or heptagonal outline – note the fine, parallel-arranged cuticular striations on their surface. D–F, Apical area of the speculum. D, Flat epidermal cells coexist with cells with a central depression. E, Speculum cells with strips of cuticular depositions, near the labellum margin. F, General view of the rows of cuticular depositions that are laid over certain cells near the labellum margin. G, Long contorted trichomes of the submarginal band occurring in the apical labellum. H, Glabrous apical margin of the labellum. I, Detail of dome-shaped papillae of the apical labellum margin. Scale bars: 30 µm (A–E, G, I); 100 µm (F, H).

Central labellum lobe

The major portion of the central labellum lobe in *O. speculum* is occupied with the large speculum that is mostly composed of (6) flat to slightly convex epidermal cells with a hexagonal outline and very fine, parallel cuticular striations on their outer cell wall (Fig. 4B, C). Lenticular cells with flattened anticlinal fields also occur in the speculum (Fig. 4B). Epidermal cells with a pentagonal or heptagonal outline were occasionally found amongst the most common speculum cells with a hexagonal outline (Fig. 4C). In the apical area of the

speculum, several epidermal cells exhibit a central depression on their surface (Fig. 4D) and long, prominent cuticular depositions were found to be laid over certain portions of contiguous cells (Fig. 4E). Rows of such ordered cuticular depositions occur in the speculum of both subspecies, but are particularly extensive in *O. speculum* subsp. *lusitanica*, where they appear parallel arranged to each other near the apical margin (Fig. 4F) and in the beginning of the speculum, near the confluence area between the central and the lateral labellum lobes.

A thin film seems to cover the labellum surface in *O. speculum* subsp. *speculum*. This film appears to have been split into several strips in the area occupied by the labellar grooves and crests, particularly in the central portion of the basal-median region of the labellum, near the beginning of the speculum, revealing the long and dense cuticular depositions that occur underneath (Fig. 4A). Similar strips of a Sudan-positive lipophilic film have been also detected in fresh hand-cut sections of the labellum of that subspecies (Fig. 8H).

The speculum is surrounded by a submarginal band of long contorted trichomes (Fig. 4G) and then by a broad, glabrous apical margin composed of (7) smooth, dome-shaped papillae, which become highly voluminous towards the labellum margin itself (Fig. 4H, I).

MICROMORPHOLOGY OF THE FEMALE WASP

The body and the legs of *Dasyscolia ciliata* female wasp are covered by a brownish-orange-coloured pilosity (Fig. 5A), which consists of long, thin, straight hairs (Fig. 5B, H). The abdominal segments are provided with slightly spiralled hairs grouped in tufts that are arranged into a band around each segment (Fig. 5D–F). A sparse pilosity covers the remaining portion of the surface of the abdominal segments (Fig. 5D, F). By contrast, the two pairs of wings are provided with no hairs on their surface (Fig. 5H, I), except for the proximal area along the costal vein, where sparse, small hairs were found (data not shown). The two crossed forewings, which partially overlap each other, form an inverted V at the apex (Fig. 5A, C) and are provided with several conspicuous veins, particularly prominent at their proximal area (Fig. 5B). The forewings' surface is rippled due to a series of parallel, longitudinal striations (Fig. 5C, I) which are frequently associated with cuticular folds and irregular wrinkles (Fig. 5J, K). A glabrous scale-like sclerite, the tegula, covers the base of the wings near the point of attachment to the thorax (Fig. 5A, B, G). Two distinct areas are visible in the dorsal region of the mesothorax, namely the scutum, a glabrous black-shining area, and the scutellum, a smaller hairy area that presents a pilosity similar to the region occurring immediately below, the metanotum (Fig. 5A, B, H). A hairy inverted triangle appears between the proximal areas of the crossed forewings, showing the pilosity of the portions of the scutellum and the metanotum not hidden by these wings (Fig. 5B, H).

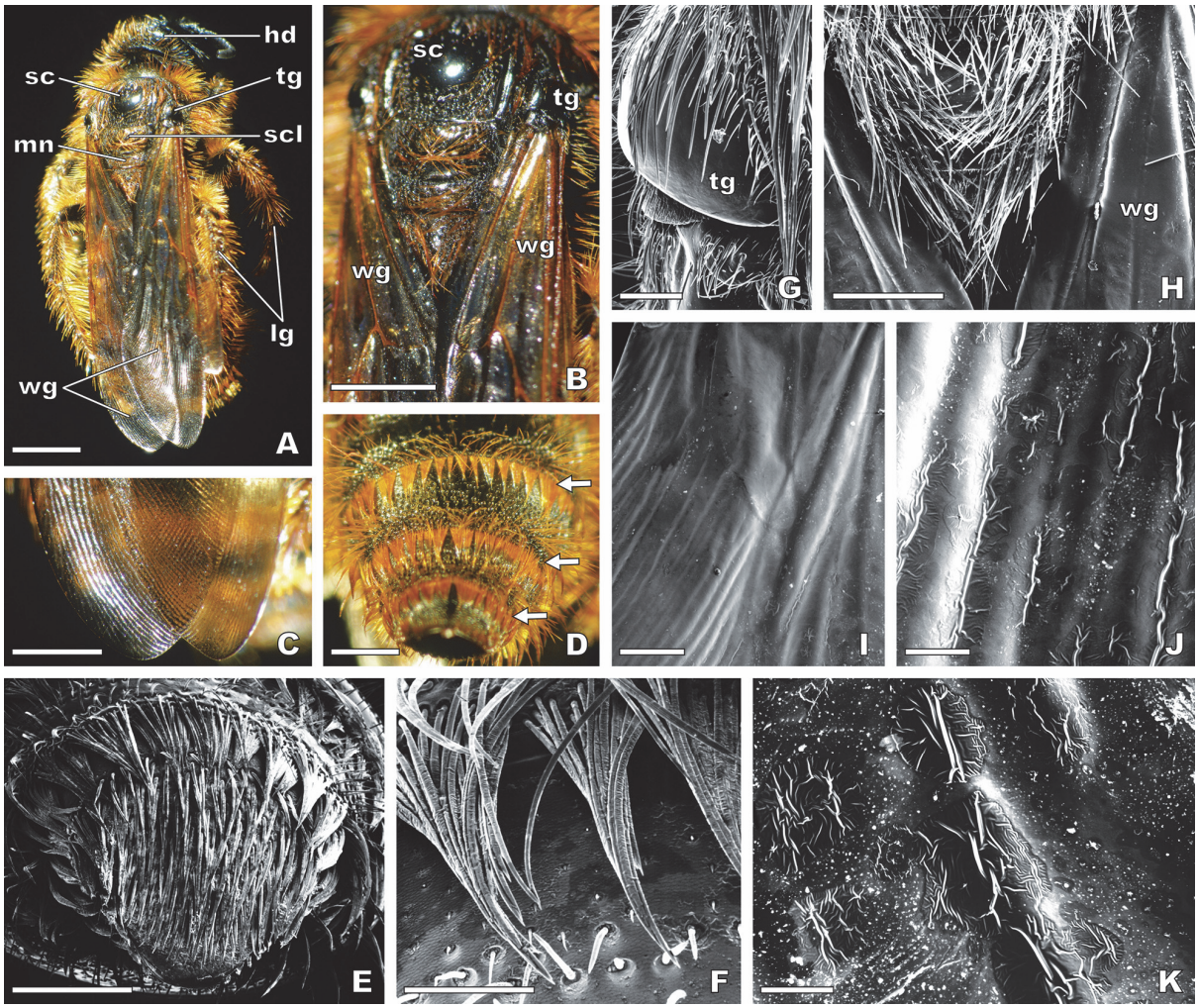

Figure 5. *Dasyscolia ciliata* female wasp. A–D, Stereomicrographs. A, Dorsal surface of the wasp. B, Detail of the dorsal surface of the thorax, showing a triangular area provided with hairs corresponding to the visible portion of the scutellum and the metanotum, which is delimited by the two glabrous forewings with prominent veins – the glabrous scutum and tegulae are also evident. C, Detail of the apex of the crossed wings forming an inverted V – note their rippled texture. D, Ventral surface of the abdomen, showing a band of hair tufts on each segment (arrows). E–K, Scanning electron micrographs. E, Bottom view of the abdomen showing its last segment and the apical bands of hairs. F, Detail of the hairs grouped in tufts on the dorsal surface of the abdomen. G, Glabrous tegula. H, Uncovered portion of the hairy metanotum delimited by the two glabrous forewings. I, Forewing – note the absence of hairs on its rippled surface. J, Detail of the dorsal surface of the forewing, showing parallel arranged cuticular wrinkles. K, Fine cuticular pattern of the forewing. hd, head; lg, leg; mn, metanotum; sc, scutum; scl, scutellum; tg, tegula; wg, forewing. Scale bars: 3 mm (A); 2 mm (B–D); 1 mm (E, H); 500 µm (I); 250 µm (F, G); 100 µm (J, K).

LOCATION, STRUCTURE AND SECRETION OF THE OSMOPHORE

Flowers of the two studied subspecies of *O. speculum* emanate a faint scent and exhibit a long period of anthesis that lasts 12–17 days (A. Francisco, personal observation). The glabrous apical margin of the labellum of freshly opened flowers of *O. speculum* subsp. *lusitanica* stained red after immersion in diluted neutral red (Fig. 2F). The most intense staining appeared in both the adaxial and the abaxial surfaces nearest the labellum margin itself (Fig. 2F). Flowers of *O. speculum* subsp. *speculum* were not tested with diluted neutral

red, since the epidermal cells of the apical labellum margin exhibit a natural magenta-to-red pigmentation (Fig. 2D) due to the presence of anthocyanins in their vacuoles (Fig. 7B), which would interfere with the result of the test.

The quick absorption of the diluted neutral red by the epidermal cells of the apical margin of the labellum in *O. speculum* provided a first indication of their secretory nature, which was subsequently confirmed by the results of the anatomical and histochemical study (Figs. 6, 7). Indeed, the dome-shaped papillae that occur in the apical labellum margin present features typical of secretory cells, i.e. a dense cytoplasm, a large nucleus lying at the base of the cell, numerous plastids, several small vacuoles at the cell apex, and thin cell walls (Figs. 6, 7A). Primary pit fields were also found between epidermal cells (Fig. 6G). The pleiomorphic plastids that occur in the domed papillae exhibit a typical perinuclear distribution (Figs. 6G–I, 7A, E). The absence, in these plastids, of the characteristic red autofluorescence of the chlorophyll pigment under blue light indicates that they are leucoplasts (Fig. 7E). By contrast, large fusiform to oblong chloroplasts abound in the subepidermal parenchyma cells of the apical labellum margin (Figs. 6H, 7A, B, E). In the two-to-three layers of the subepidermal parenchyma cells, few starch grains were found in the plastids, but only at the earliest stage of the flower development (Fig. 6E). Several crystal idioblasts containing raphides often occur in the parenchyma tissue of the labellum margin, which are especially frequent in early buds (Fig. 6A, B).

At the stage of early bud, the labellum of *O. speculum* is composed of cells that present typically a dense cytoplasm and a large nucleus, both in the epidermis and in the parenchyma (Figs. 6B, E, H, 8K–O), and starch-rich plastids occur in the parenchyma cells throughout the labellum (Figs. 6E, 8K, N). The maintenance of these features in later stages of the flower development, which is indicative of the secretory nature of the cells, was observed only in the apical labellum margin, even though an increase in cell vacuolization and a depletion of the starch content had occurred in the epidermal and/or subepidermal parenchyma cells of this labellum portion, from early buds to flowers at anthesis (Fig. 6E, F, H, I). Indeed, other portions of the labellum, such as the area of contorted trichomes that is contiguous to the glabrous margin, exhibit highly vacuolated epidermal cells already in the stage of late bud, in particular on the abaxial surface (Fig. 6C). Therefore, the histological features described above indicate that an osmophore occurs in the glabrous apical margin of the labellum in *O. speculum*, which appears restricted to the portion nearest the margin itself, where hypertrophied dome-shaped papillae occur and where the labellum thickness reaches a maximum of three-to-four layers of parenchyma cells (Fig. 6A, D, F). This finding is consistent with the most intense staining that this area exhibited after immersion in diluted neutral red (Fig. 2F). Thus, the osmophore of *O. speculum* is composed of the generally hypertrophied dome-shaped papillae, together with the underlying two-to-three layers of parenchyma cells, which occur in both the abaxial and the adaxial surfaces of the apical region of the labellum nearest the margin.

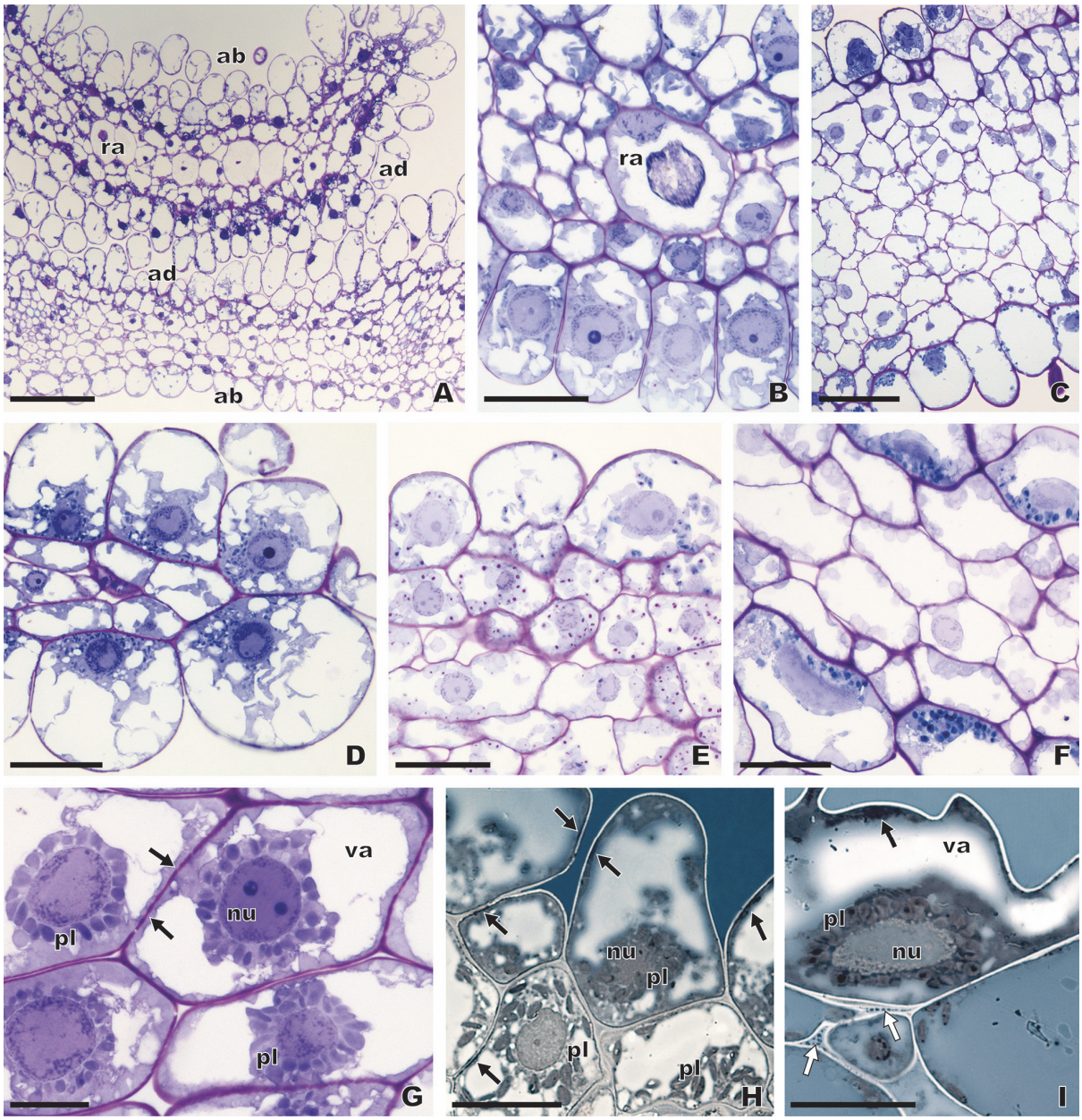

Figure 6. Light micrographs of sections of the apical region of the labellum in *Ophrys speculum* subsp. *lusitanica* (A, C, F–I) and *Ophrys speculum* subsp. *speculum* (B, D, E). A–G, Historesin sections stained with toluidine blue/Lugol (A, G) or PAS/toluidine blue (B–F). A, B, D–G, Transverse, longitudinal (F) or paradermal (G) sections of the glabrous labellum margin. A, Early bud, showing two different portions of the labellum margin – note that the most apical portion (upper half) presents epidermal cells with a denser cytoplasm in both abaxial and adaxial surfaces. B, Early bud, showing secretory epidermal cells on the abaxial surface. D, Labellum margin itself in a late bud, showing hypertrophied secretory dome-shaped papillae. E, Early bud, showing PAS-positive, pink-stained plastids with low starch content in the subepidermal parenchyma cells on the abaxial surface. F, Open flower, showing an absence of starch in the parenchyma and an increased cell vacuolization. G, Paradermal section of epidermal cells in a late bud, showing primary pit fields (arrows) along cell walls and a perinuclear arrangement of plastids. C, Transverse section of the labellum area contiguous to the glabrous margin in a late bud, showing highly vacuolated epidermal cells on the abaxial surface. H, I, Transverse epoxy sections of the secretory tissues of the labellum margin in an early bud (H) and an open flower (I) stained with Sudan Black B – note that a Sudan-positive lipophilic secretion is visible mainly near the outer epidermal cell walls (black arrows) and in

the loose inner cell walls (white arrows). ab, abaxial surface; ad, adaxial surface; nu, nucleus; pl, plastids; ra, raphides; va, vacuole. Scale bars: 150 µm (A); 100 µm (C); 50 µm (B, D–F); 25 µm (G–I).

The histochemical tests performed both in semithin epoxy sections and in fresh hand-cut sections revealed a low amount of a lipophilic secretion associated with the domed papillae at the apical labellum margin of *O. speculum* (Figs. 6H, I, 7C–F). Translucent droplets were often observed on the surface of the domed papillae in fresh material (Fig. 7C). Terpene-rich violet stained droplets, which were revealed with the Nadi reagent, were also found on the surface of the secretory epidermal cells (Fig. 7D). A Sudan-positive secretion was detected either in the periplasmic space or in the cortical cytoplasm of the epidermal cells, as well as in the loose cell walls of the epidermal and subepidermal secretory cells of the labellum margin (Fig. 6H, I). Some lipophilic inclusions located mainly in the cortical cytoplasm of the epidermal cells were revealed by their golden-yellow secondary fluorescence under blue light, after staining with neutral red (Fig. 7F). On the other hand, a green autofluorescence, which is assigned to phenolic compounds, was detected near the outer cell walls of the domed papillae (Fig. 7E).

ANATOMY OF THE BASAL FIELD AND THE SPECULUM

The distinctive basal field of *O. speculum* is composed of densely packed trichomes which are located in a cupuliform concavity occurring between the internal labia of the stigmatic cavity (Fig. 8A, B). These trichomes appeared oblong in transverse and longitudinal sections and exhibited granular phenolic inclusions in their vacuoles, which stained dark greenish-blue with toluidine blue (Fig. 8E–G). In some early buds of *O. speculum* subsp. *lusitanica*, certain trichomes were found to be collapsed, a finding that was shown by the intense dark blue colouration of their protoplast in historesin sections of the basal field stained with toluidine blue (Fig. 8C, D). We did not find any indication of collapsed cells at later stages of flower development in *O. speculum* subsp. *lusitanica* (Fig. 8E) nor did we at early buds, late buds or flowers at anthesis of *O. speculum* subsp. *speculum* (Fig. 8F, G).

An increased cell vacuolization in both the epidermis and the parenchyma, as well as a complete disappearance of the starch content of the plastids in the parenchyma cells, were observed throughout the flower development in the basal field (Fig. 8E–G), labellar crests (Fig. 8I), and speculum (Fig. 8J–O) of *O. speculum* flowers. In the parenchyma tissue of the basal field and the speculum, chloroplasts and raphide-containing idioblasts are frequent, the latter being particularly common in early buds (Fig. 8A).

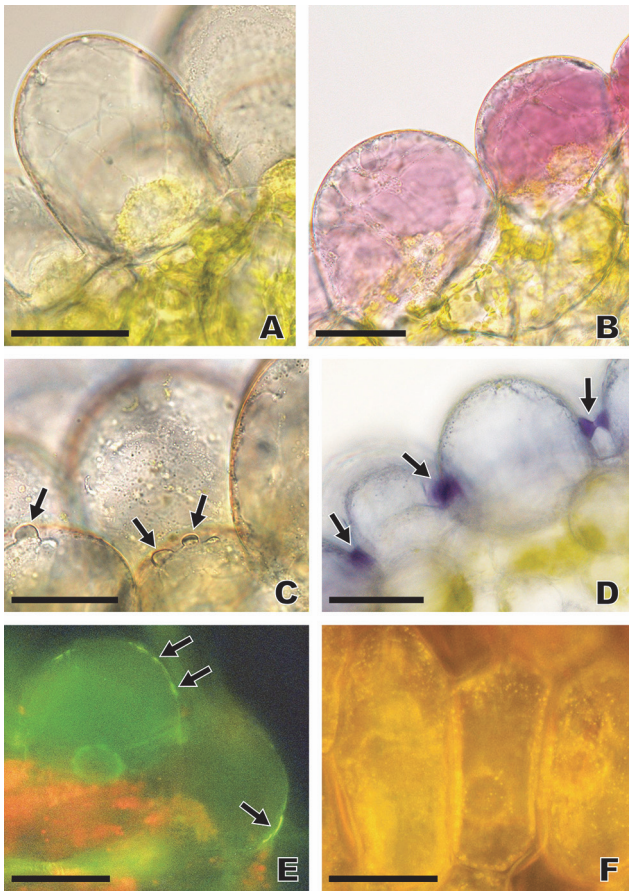

Figure 7. Histochemical characterization of fresh hand-cut sections of the apical margin of the labellum in *Ophrys speculum* subsp. *lusitanica* (A, C–E) and *Ophrys speculum* subsp. *speculum* (B, F). A–C, Transverse sections without any treatment (control). A, Late bud just before the anthesis, showing polarized dome-shaped papillae with a nucleus surrounded by plastids located at the basal portion of the cell and several vacuoles occupying the cell apex. B, Open flower, showing the natural magenta pigmentation of the anthocyanin-rich vacuoles in the epidermal cells. C, Open flower, showing translucent droplets (arrows) visible on the surface of the epidermal cells. D–F, Sections of open flowers. D, Transverse section stained with Nadi reagent, showing violet-stained droplets of secretion (arrows) on the surface of the epidermal cells. E, Autofluorescence of a transverse section seen under blue light – note a green autofluorescence near the outer epidermal cell walls (arrows) and a red autofluorescence of the chloroplasts in the sub-epidermal parenchyma cells. F, Paradermal section of the epidermis stained with neutral red and seen under blue light, showing a golden-yellow secondary fluorescence of lipophilic inclusions occurring mainly in the cortical cytoplasm. Scale bars: 50 µm.

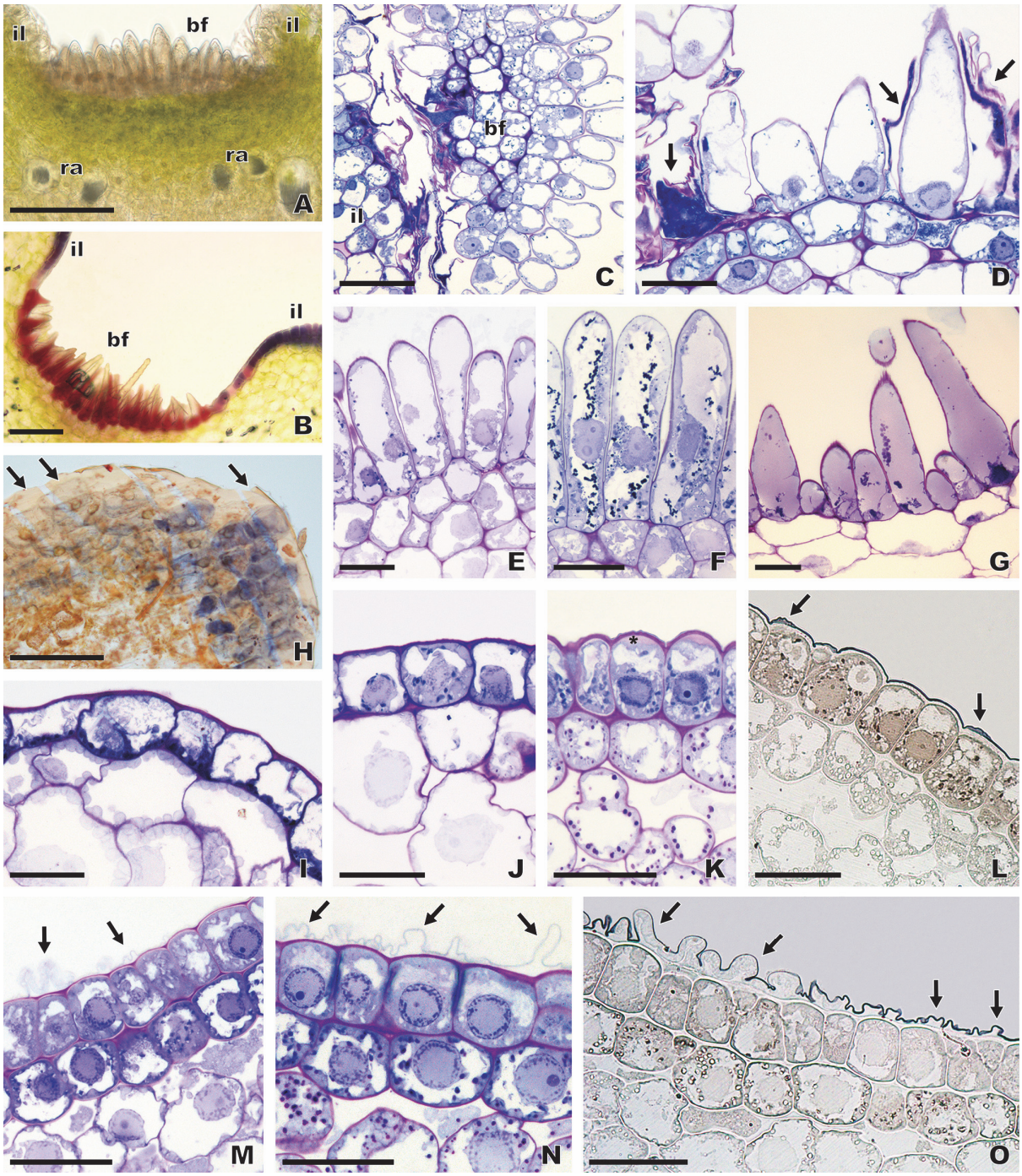

Figure 8. Light micrographs of sections of the basal and median regions of the labellum in *Ophrys speculum* subsp. *lusitanica* (A, C–E, I, K, L) and *Ophrys speculum* subsp. *speculum* (B, F–H, J, M–O). A–G, Basal field of the labellum. A, B, Transverse fresh hand-cut sections in a late bud stained with Sudan IV (A) and a freshly opened flower without any treatment (B), showing the subconical to attenuate trichomes of the basal field occurring in a cupuliform concavity between the internal labia of the stigmatic cavity. C–G, Historesin sections stained with PAS/toluidine blue or toluidine blue/Lugol (E). C, D, Paradermal sections of the basal field in an early bud, showing trichomes in their transverse extent in D – note the intense dark-blue stained content of some collapsed cells (arrows). E–G, Transverse or longitudinal (F) sections of the densely packed trichomes of the basal field in late buds (E, F) and an open flower (G) – note the dark-greenish-blue-stained granular vacuolar inclusions. H, I, Labellar crests near the beginning of the speculum in open flowers. H, Oblique fresh hand-cut section stained with Sudan IV, showing a Sudan-positive, red-stained lipophilic film split into several strips (arrows). I, Transverse historesin section stained with

PAS/toluidine blue, showing highly vacuolated epidermal and parenchyma cells. J–O, Historesin sections of the speculum stained with PAS/toluidine blue (J, K, M, N) or Sudan Black B (L, O). J, Central-median area of the speculum in a late bud, showing a nearly smooth surface of the epidermal cells. K, L, Lateral-median area of the speculum in an early bud, showing a slightly undulated epidermal cell surface – note that a pink-stained material is observed in the periplasmic space (asterisk) and that the cuticle is distended at some places (arrows). M–O, Lateral-apical area of the speculum in an early bud, showing the unusual configuration of the cuticle of certain epidermal cells – note that the cuticle is detached from the outer tangential walls in an irregular way along contiguous cells (arrows) and that a subcuticular space appears underneath. bf, basal field; il, internal labium; ra, raphides. Scale bars: 150 µm (A, B); 100 µm (C, H); 50 µm (D–G, I–O).

The epidermis of the speculum in late buds and open flowers of *O. speculum* consists of highly vacuolated flat to lenticular cells that are quadrangular to rectangular in transverse section, which display a nearly smooth cuticle (Fig. 8J). By contrast, at the early bud stage, the epidermal cells of the speculum, besides presenting a very dense cytoplasm with several plastids and a large nucleus containing a nucleolus (Fig. 8K–O), exhibit a slightly ridged cuticle (Fig. 8K) which acquired occasionally an uncommon configuration in certain areas of the speculum (Fig. 8M–O). Indeed, the lateral portion of the apical area of the speculum in an early bud of *O. speculum* subsp. *speculum* displayed a series of contiguous epidermal cells whose cuticle had been detached from their outer tangential walls, in such a way that irregular cuticular projections had been formed with an underlying subcuticular space, whose content apparently did not stain with any staining procedure used here (Fig. 8M–O). More specifically, this unusual cuticular aspect was observed in the portion of the speculum that is actually folded over itself within the floral bud, and was exclusively found at the early bud stage in *O. speculum* subsp. *speculum* (Fig. 8M–O). We did not find such a cuticular configuration in any flower of *O. speculum* subsp. *lusitanica* (Fig. 8K, L). Conversely, in the lateral portion of the median area of the speculum in an early bud of this latter subspecies, the cuticle of certain epidermal cells was found to be distended at some places due to the deposition of a Sudan-positive lipophilic material in a small subcuticular space (Fig. 8L). Also, some of these epidermal cells exhibited a conspicuous periplasmic space which appeared pink after staining with periodic-acid–Schiff reagent plus toluidine blue (Fig. 8K).

DISCUSSION

THE BASAL FIELD OF *OPHRYS SPECULUM*

The present study shed new light on the configuration of the uncommon stigmatic cavity and labellum of *O. speculum* and is the first to show micromorphological and anatomical evidences for the occurrence of a clear basal field in the labellum of this species. The concept of basal field was defined, and used thereafter, as a differentiated area of the basal region of the labellum in *Ophrys* flowers separating the stigmatic cavity from the speculum, which may have a colouration either contrasting or similar to that exhibited by the adjacent floral areas (Devillers & Devillers-Terschuren, 1994; Delforge, 2005). Such a

differentiated area corresponding to the basal field is easily noticeable in the majority of species of the genus *Ophrys*, being notably absent from the labellum of the species belonging to the section *Pseudophrys*, such as *O. fusca* and *O. lutea* (Godfery, 1928; Devillers & Devillers-Terschuren, 1994; Delforge, 2005). However, the occurrence of a basal field is still controversial for *O. speculum*, despite a distinct circumscribed area has long been documented in the basal region of the labellum of this species (Ågren *et al.*, 1984; Borg-Karlson, 1990; Devillers & Devillers-Terschuren, 1994; Aldasoro & Sáez, 2005; Delforge, 2005; Bradshaw *et al.*, 2010). Some authors considered the basal field of *O. speculum* as absent and replaced by a small shield in the slope that separates the labellum from the floor of the stigmatic cavity (Devillers & Devillers-Terschuren, 1994). One author described it as an (ob)oval to elliptic area provided with callosities (Delforge, 2005), whereas others interpreted it as a smooth, flat area flanked by crests (Aldasoro & Sáez, 2005; Bradshaw *et al.*, 2010). In the present study, we considered that the basal field of *O. speculum* is confined to the distinctive cupuliform concavity provided with trichomes that occurs in the area where the basal region of the labellum joins the stigmatic cavity.

A correct interpretation of the structure of this particular floral part in *O. speculum* demands a detailed micromorphological comparison with other *Ophrys* species, so that the homology between floral parts could be established. Homology assessment is usually based on the following criteria: (1) similarity in relative position; (2) sharing a common special feature; and/or (3) occurrence of intermediate forms (Sattler, 1994; Chin *et al.*, 2013). In this context, and given that the basal field of *Ophrys* flowers is the part of the labellum that separates the floor of the stigmatic cavity from the speculum (Devillers & Devillers-Terschuren, 1994; Francisco & Ascensão, 2013), two lines of evidence emerged from our observations which support a hypothesized homology between the basal field of *O. speculum*, restricted to the trichomes occurring in the cupuliform concavity, and the basal field of other *Ophrys* species. First, in terms of its relative position, the cupuliform concavity of *O. speculum* was found to be located between the unusually extensive floor of the stigmatic cavity and the labellar area of crests and callosities immediately above the speculum. The elongated, flat epidermal cells with a densely ridged surface that were found in the floor of the stigmatic cavity in *O. speculum* are similar to those occurring in the floor of the stigmatic cavity in other *Ophrys* species, particularly its close relatives, *O. bombyliflora* and *O. tenthredinifera*, as well as *O. scolopax* Cav. (Francisco & Ascensão, 2013; Francisco, Porto & Ascensão, 2015). Therefore, there is no reason to interpret the exceptionally long, narrow floor exhibited by *O. speculum*, framed by two pairs of long crests or labia on each side, which are also part of the stigmatic cavity, as a poorly defined, flat basal field (Aldasoro & Sáez, 2005; Bradshaw *et al.*, 2010). By contrast, like in other *Ophrys* species (Francisco & Ascensão, 2013; Francisco *et al.*, 2015), the glabrous portion corresponding to the floor of the stigmatic cavity also occurs in *O. speculum* in contiguity to the basal field, which is represented by the cupuliform concavity in this species. The second

line of evidence is that the cupuliform concavity of *O. speculum* is covered by trichomes, a feature that typically occurs in the basal region of the labellum of *Ophrys* flowers, regardless of forming either a clear or an undefined basal field (Ascensão *et al.*, 2005; Bradshaw *et al.*, 2010; Francisco & Ascensão, 2013; Francisco *et al.*, 2015). Despite trichomes occurring in that labellum region were found to vary in height and shape among *Ophrys* species (Francisco & Ascensão, 2013; Francisco *et al.*, 2015), this finding fulfils the second homology criterion mentioned above.

An additional argument for our hypothesis that the basal field of *O. speculum* is confined to the cupuliform concavity stems from anatomical observations, which were consistent with the idea that the trichomes occurring in the cupuliform concavity are tightly packed into the exiguous space that remained between the enlarged, prominent labia of the stigmatic cavity. We found some of these trichomes collapsed at the early bud stage of flowers of *O. speculum* subsp. *lusitanica*, which is the subspecies with the narrowest floor and with the most inflated internal labia. From this finding we may infer that the cells occurring inside the cupuliform concavity seems to be subjected to great compression and that the collapse of certain cells may occur as a way of gaining extra space for the full development of the basal field trichomes.

Therefore, we propose that the cupuliform concavity of *O. speculum* is an evident basal field which, instead of being absent (Devillers & Devillers-Terschuren, 1994) or being an exclusive structure of this species (Bradshaw *et al.*, 2010), is in fact probably homologous to the basal fields exhibited by the other *Ophrys* species (Francisco & Ascensão, 2013; Francisco *et al.*, 2015). Notwithstanding, the singular location and the special characteristics of the basal field of this species in being confined to the narrow space between the distal portions of the internal labia of the stigmatic cavity, and in being surrounded distally by an augmented labellar portion, seem to be unique in the genus *Ophrys*. On the other hand, despite the peculiar configuration of its stigmatic cavity, we noted that *O. speculum* shares with *O. bombyliflora* the robustness and height of the internal labia (Francisco & Ascensão, 2013; Francisco *et al.*, 2015).

The relevance of a discussion about whether or not *O. speculum* presents a clear basal field in the labellum, which might be regarded apparently as a mere issue of concept, exceeds largely its theoretical dimension. Indeed, elucidating the floral structure of *O. speculum*, through detailed micromorphological characterization and comparison with other *Ophrys* species, allowed the establishment of homologies between floral parts in *Ophrys*, which constitute the necessary basis of any character definition if a morphological phylogenetic analysis is intended to be performed (Kearney & Rieppel, 2006; Nixon & Carpenter, 2012). In effect, the micromorphological and anatomical data on *O. speculum* described in the present study has been recently analysed and combined with equivalent data on its closest relatives (Ascensão *et al.*, 2005; Francisco & Ascensão, 2013) in a

morphological data matrix, which was subsequently used for phylogenetic reconstruction of the still unresolved clade of *O. speculum* (Francisco *et al.*, 2015).

MICROMORPHOLOGY AND POLLINATION

Epidermal cell types

Our micromorphological study revealed that the adaxial surface of the labellum and the stigmatic cavity of *O. speculum* presents seven different epidermal cell types, a cell diversity comparable to that occurring in *O. tenthredinifera* and *O. scolopax*, which exhibit both eight different cell types, in contrast with the 11 cell types exhibited by *O. bombyliflora* and the no more than three cell types occurring in *O. fusca*, *O. lutea*, and other species belonging to section *Pseudophrys* (Ascensão *et al.*, 2005; Bradshaw *et al.*, 2010; Francisco & Ascensão, 2013; Francisco *et al.*, 2015). In the light of the criteria adopted here for defining epidermal cell types, i.e. the curvature of the outer cell wall, the cell outline and the cuticular sculpture (Koch *et al.*, 2008), we noted that, in fact, the labella of *O. fusca* and *O. lutea* present only three different epidermal cell types, rather than four as initially assumed by us, since the long attenuate trichomes with enlarged bases that occur in the basal region of the labellum of these two species are actually rather similar to those covering the apical region of the labellum, regardless of having straight or sinuate tips (Ascensão *et al.*, 2005). Our finding that seven different epidermal cell types occur in the labellum and the stigmatic cavity of *O. speculum* contrasts with the lower cell diversity (of only four cell types) reported for this same species in the comparative micromorphological survey of the genus *Ophrys* carried out by Bradshaw *et al.* (2010). While the latter authors considered that a single cell type, i.e. smooth, non-papillate cells, occurs in the pseudoeyes, in the floor of the stigmatic cavity (which was misinterpreted as a putative basal field in their survey), and in the speculum, our observations showed that each of these floral areas in *O. speculum* exhibits a distinct epidermal cell type. According to our results, only the pseudoeyes exhibit smooth, flat to lenticular cells, whereas the floor of the stigmatic cavity was found to consist of flat, elongated, polygonal cells with a rugose instead of smooth (Bradshaw *et al.*, 2010) surface, like the floor of other *Ophrys* species (Francisco & Ascensão, 2013; Francisco *et al.*, 2015).

Furthermore, the flowers of *O. speculum* observed in our study exhibited a speculum composed of flat to lenticular cells with isodiametric, polygonal outline and very fine, parallel-arranged cuticular striations on their surface. In what concerns cell surface, our finding is somewhat inconsistent with what was described by Bradshaw *et al.* (2010) and Vignolini *et al.* (2012a). Although similar very fine cuticular striations are evident on the surface of the speculum cells in both the scanning and the transmission electron micrographs of the flowers of *O. speculum* subsp. *lusitanica* (synonym: *O. vernixia* Brot.) examined in their study, Bradshaw *et al.* (2010) described these cells as totally smooth, non-striated, non-papillate cells. Likewise, in their subsequent investigation specifically focused

on the speculum of this species (Vignolini *et al.*, 2012a), the authors confirmed the extremely flat and smooth surface of these speculum cells. The discrepancy that seems to exist between our results and those reported by Bradshaw *et al.* (2010) and especially Vignolini *et al.* (2012a) concerning the cuticular striations of the speculum cells may be linked with the different provenance of the plants in the three studies. The flowers examined in the present study came from natural populations whereas those examined in the other two studies came entirely (Vignolini *et al.*, 2012a) or predominantly (Bradshaw *et al.*, 2010) from cultivated plants. Edaphoclimatic conditions such as soil moisture, light intensity, air temperature and air humidity are necessarily different for wild and cultivated plants and could affect the process of cuticular wax deposition and thus cuticle micromorphology (Koch *et al.*, 2006). Independently of considering the speculum cells of *O. speculum* as completely smooth or finely-ridged, it is certain that these cells form a highly reflective, mirror-like surface, which seems to be the major determinant of the glossiness and the strong specular reflection of light reported for the speculum of these flowers (Vignolini *et al.*, 2012a). Rare plant species also present glossy petals, or petal areas, exhibiting a surface formed by smooth, flat cells, such as *Ranunculus repens* L. (Vignolini *et al.*, 2012b), or the sexually deceptive fly-pollinated *Gorteria diffusa* Thunb. (Thomas *et al.*, 2009). The occurrence of flat to lenticular cells in the speculum is also shared with the closely-related *O. bombyliflora* and *O. tenthredinifera* (Bradshaw *et al.*, 2010; Francisco & Ascensão, 2013), although the parallel arrangement of the cuticular striations on the surface of the speculum cells in *O. speculum* appears to be unique in the genus, since it contrasts with the typical spirally arranged pattern of cuticular striations of the other *Ophrys* species (Servettaz *et al.*, 1994; Ascensão *et al.*, 2005; Bradshaw *et al.*, 2010; Francisco & Ascensão, 2013). Besides *O. speculum*, only a few species belonging to the group of *O. bertolonii* Moretti, which are pollinated by wasps of the genus *Chalicodoma* (Delforge, 2005), were found to present exclusively flat epidermal cells in the speculum (Bradshaw *et al.*, 2010).

The thin film that we have detected in the basal region of the labellum in *O. speculum* may be related to the effect of a thin mirror-coating of the speculum surface described by Vignolini *et al.* (2012a) for this species. We could interpret this film as the thin epicuticular wax film that seems to occur in virtually all plant surfaces covered by cuticle (Barthlott *et al.*, 1998; Jetter, Schäffer & Riederer, 2000; Jeffree, 2006; Koch *et al.*, 2008), although it is usually difficult to detect by SEM (Barthlott *et al.*, 1998; Koch *et al.*, 2008). On the other hand, the irregular cuticular projections that we observed on the speculum cell surface in early buds, more precisely in the portion of the speculum that undergoes more drastic distension during the period of labellum expansion preceding the flower anthesis, are likely to distend and disappear to give rise to a nearly smooth cuticular coating over the speculum in open flowers of *O. speculum*. Comparable changes in the cuticle morphology were also observed during the development of the grape berry (Casado & Heredia, 2001).

On the other hand, our finding that the epidermis of the speculum in *O. speculum* consists in an imperfect pattern of cells with a predominantly hexagonal outline intermingled with cells with a pentagonal or a heptagonal outline could be properly comparable to the pattern exhibited by the exoskeleton of an iridescent beetle (Sharma *et al.*, 2009). Indeed, the hexagonal form provides the most efficient utilization of the space on a plane, but adding five- and seven-sided polygons is needed to delineate a curved surface like the convex central lobe of the labellum in *O. speculum*, in which cells with a heptagonal outline are expected to occur in the areas of greater curvature (Sharma *et al.*, 2009).

We also noted a remarkable similarity between the cuticular thickenings found over certain areas of epidermal cells in the basal region of the labellum in *O. speculum* and those occurring in the external labia of the stigmatic cavity in *O. bombyliflora* (Francisco & Ascensão, 2013). Several micromorphological and anatomical features described in the present study were found to have evolutionary significance for the phylogenetic reconstruction of the clade to which *O. speculum* belongs (Francisco *et al.*, 2015).

Visual and tactile mimicry

The present comparative micromorphological study on the labellum and stigmatic cavity of *O. speculum* and on the body of a female of its wasp pollinator, *Dasyscolia ciliata*, provides a fresh view upon the well established visual and tactile mimicry occurring between them (Correvon & Pouyanne, 1916; Pouyanne, 1917; Kullenberg, 1961; Ågren *et al.*, 1984; Paulus, 2006). From a detailed comparison between flower and wasp, we are able to propose new evidences of mimicry, specifically between: (1) the oblong to shield-shaped basal field confined to the cupuliform concavity of *O. speculum* and the hairy area, in the shape of an inverted triangle, corresponding to the pilosity of the metanotum and the scutellum of the wasp (Figs. 2A, B, 3A, B, 5A, B, H); (2) the two pairs of labia of the stigmatic cavity of *O. speculum* and the prominent costal veins of the proximal portion of the crossed forewings of the wasp (Figs. 2A, B, 3A, B, 5B, H); (3) the extensive floor of the stigmatic cavity of *O. speculum* and the glabrous scutum of the wasp (Figs. 2A, B, 3A, B, 5A, B); (4) the series of labellar grooves and crests of the *O. speculum* and the veins of the median portion of the wasp's wings (Figs. 2A, B, 5A, B); (5) the rows of ordered cuticular depositions that appeared parallel to the apical margin of the labellum in *O. speculum* and the rippled surface of the apical portion of the wasp's wings (Figs. 4F, 5C, I); and even (6) the heterogeneous cuticular pattern of the lateral labellum lobes of *O. speculum* and the cuticular wrinkles occurring in the surface of the wasp's wings (Figs. 3H, 5J, K).

Furthermore, our results are consistent with other previously recognized similarities between the flower of *O. speculum* and the female of its specific wasp pollinator (Correvon & Pouyanne, 1916; Kullenberg, 1961; Ågren *et al.*, 1984; Paulus, 2006). For instance, although the dark-coloured pseudoeyes in *O. speculum* are placed at a higher relative position than the black tegulae in the wasp, we propose that the glabrous pseudoeyes of

the flower simulate the shiny tegulae of the wasp (Figs. 2A, B, 3D, 5A, B, G), in accordance with Devillers and Devillers-Terschuren (1994) and Paulus (2006). Additionally, the submarginal band of contorted trichomes that surrounds the labellum of this *Ophrys* species resembles the brownish orange-coloured hairiness of the legs and the abdomen of the female wasp, which is composed of slightly spiralled hairs (Fig. 5A, D–F), as was also described by Ågren *et al.* (1984). Both the submarginal pilosity and the peculiar configuration of the stigmatic cavity and basal region of the labellum of *O. speculum* should provide tactile stimuli to male wasps, which are assumed to imitate the sensations offered by the hairiness of the female, hence guiding them to the correct position upon the labellum so that effective pollination could take place (Correvon & Pouyanne, 1916; Kullenberg, 1961; Ågren *et al.*, 1984; Paulus, 2006). The importance of tactile cues for the success of pseudocopulation in *Ophrys* was also inferred from certain micromorphological details on the labellum of other species (Ågren *et al.*, 1984; Ascensão *et al.*, 2005; Francisco & Ascensão, 2013; Vereecken & Francisco, 2014) and has been tested in the field through choice experiments with their respective male insect pollinators (Kullenberg, 1961; Kullenberg & Bergström, 1976; Kullenberg *et al.*, 1984).

Moreover, our observations corroborate the widely accepted assumption that the speculum of this *Ophrys* flower mimics the crossed wings of a virgin female *Dasyscolia ciliata* wasp (Correvon & Pouyanne, 1916; Kullenberg, 1961; Ågren *et al.*, 1984; Paulus, 2006); even in the detail of the inverted V observed in the apical area of the speculum, which is similar to the one formed by the partial overlapping of the wasp' wings (Figs. 1, 5A, C), a feature also described by Ågren *et al.* (1984). As accurately noted by Pouyanne in the very first description of the pollination by sexual deception of *Ophrys* flowers, the metallic, deep blue reflection from the crossed wings of a female wasp of *Dasyscolia ciliata* standing on the ground is mimicked by the shiny, deep blue speculum of the flower of *O. speculum* (Correvon & Pouyanne, 1916), which owes its special blue colour to a single cyanidin pigment, probably associated with an alkaline pH or metal ions, occurring in the vacuoles of epidermal cells (Vignolini *et al.*, 2012a). Remarkably, the wings of this particular scoliid wasp exhibit a nearly hairless surface, with only sparse hairs found along the proximal area of the costal and median veins (Ågren *et al.*, 1984; Borg-Karlson, 1990; Fig. 5I in the present study). Similar glabrous wings with a rippled surface were also found in other scoliid wasp (Sarrazin *et al.*, 2008). By contrast, the surface of the wings of females of other *Ophrys* insect pollinators is provided with short hairs which display either a uniform distribution along the veins and the wing cells, like in *Argogorytes* wasps and *Andrena* bees, or a more uneven distribution like in *Eucera* bees, where they are more densely found on the veins, forming patches separated from each other by a narrow hairless space (Ågren *et al.*, 1984; Borg-Karlson, 1990). The fact that the wings' surface of that particular scoliid female wasp (the model) is nearly hairless may thus explain why the speculum of *O. speculum* (the mimic) is entirely composed of flat to slightly convex cells, which differ from the papillae and/or short

trichomes with flattened bases that typically occur in the speculum of *Ophrys* species pollinated by *Andrena* bees, *Eucera* bees or *Argogorytes* wasps (Servettaz *et al.*, 1994; Ascensão *et al.*, 2005; Bradshaw *et al.*, 2010; Francisco & Ascensão, 2013; Francisco *et al.*, 2015). Besides mimicking the shape, blue reflection, and glabrous surface of the female wasp's crossed wings, the speculum of this *Ophrys* species also mimics the strong UV-reflectance typical of the wasps' wings, which was found to be a highly attractive visual signal to the male hymenopterans, in contrast with the dark brownish coloured adjacent portions of the labellum, probably difficult to detect by them (Kullenberg, 1961; Paulus, 2006; Gaskett & Herberstein, 2010; Vignolini *et al.*, 2012a; Gaskett, 2014). Consequently, the speculum of flowers of *O. speculum* constitutes a secondary key visual stimulus which, in combination with the primary key odour signal, seems to play a decisive role in the short-range attraction of male insect pollinators to the flower (Kullenberg, 1961; Paulus, 2006). Further field experiments with diverse *Ophrys* species and their respective insect pollinators are yet needed to demonstrate which labellar features act effectively as visual stimuli for pollinators. Moreover, the speculum of *Ophrys* flowers seems to be determinant of the success of the pollination by sexual deception characteristic of the genus, since the loss of the speculum from the labellum of *O. helenae* Renz appeared to constitute the primary phenotypic change necessary to trigger a shift to pollination through shelter mimicry, like in the orchid genus *Serapias* L. (Vereecken *et al.*, 2012).

In the present study, we examined the two subspecies of *O. speculum* that co-occur in the western part of the geographical distributional area of the species, i.e. *O. speculum* subsp. *speculum* (synonym: *O. ciliata* Biv.) and *O. speculum* subsp. *lusitanica* (synonym: *O. vernixia*), following the taxonomic classification adopted by Aldasoro and Sáez (2005). Only the former taxon, which is widespread around the Mediterranean Basin, is consistently pollinated by *Dasyscolia ciliata* male wasps, whose observations had underlain the discovery of the pollination by sexual deception (Correvon & Pouyanne, 1916; Pouyanne, 1917; Kullenberg, 1961; Paulus & Gack, 1990; Pedersen & Faurholdt, 2007). The other studied taxon, *O. speculum* subsp. *lusitanica*, occurs solely in the southwest of the Iberian Peninsula, more specifically in the central-littoral and southern regions of Portugal, and in the region of Andalusia, in the south of Spain (Aldasoro & Sáez, 2005; Delforge, 2005; Pedersen & Faurholdt, 2007). Due to the scarcity of pollination records (Lara Ruiz, 2010), the specific pollinator of this latter subspecies remains unknown. The practically similar flower structure and micromorphology that we found between the two investigated subspecies of *O. speculum*, together with the great resemblance of the flowers of both subspecies to the female wasp of *Dasyscolia ciliata*, suggest that males of this scoliid wasp may be potential pollinators of *O. speculum* subsp. *lusitanica*. However, given the primary role of the scent in the attraction of male pollinators to *Ophrys* flowers (Kullenberg, 1961), only when the composition of the floral odour bouquet of this subspecies of *O. speculum* is characterized and the scent compounds are used in behavioural field tests with males of that particular

scoliid wasp, that hypothesis could be tested. Furthermore, a third taxon, *O. speculum* Link subsp. *regis-ferdinandii* Acht. & Kellerer ex Kuzmanov (synonym: *O. regis-ferdinandii* (Renz) Buttler), is closely-related to the two studied taxa, but its distribution is restricted to the eastern Aegean islands and neighbouring parts of the region of Anatolia, in Turkey (Paulus & Gack, 1990; Delforge, 2005; Pedersen & Faurholdt, 2007). These three closely-related taxa form the so-called '*O. speculum* group' recognized by several authors (Delforge, 2005; Devey *et al.*, 2008; Bradshaw *et al.*, 2010). Although the flower morphology of *O. speculum* subsp. *regis-ferdinandii* appeared not to be quite different from that of the two investigated taxa (Bradshaw *et al.*, 2010), its putative pollinator may be a male of the distantly-related bee-like hoverfly *Merodon velox* (Diptera: Syrphidae; Paulus, 2006).

THE SIGNIFICANCE OF THE OSMOPHORE IN *OPHRYS SPECULUM*

Osmophore location, structure, and secretion

The present study provides anatomical and histochemical evidences for the occurrence of an osmophore, i.e. a fragrance-producing floral gland, in the apical region of the labellum of *O. speculum*. This finding was supported by the peculiar features exhibited by the dome-shaped papillae and the underlying two-to-three layers of parenchyma cells occurring in the apical margin of the labellum, which are comparable to most features considered typical of a secretory structure like an osmophore (Vogel, 1990). The hypertrophied domed papillae that form the epidermis of the labellum margin in *O. speculum* present a high polarity, a dense cytoplasm, a large nucleus at the base of the cell surrounded by numerous plastids, several small vacuoles at the cell apex, and thin cell walls, like the secretory cells of most osmophores described for orchids and several other angiosperm families (Pridgeon & Stern, 1983; Pridgeon & Stern, 1985; Vogel, 1990; Vogel & Hadacek, 2004; Pansarin, Pansarin & Sazima, 2014; Possobom, Guimarães & Machado, 2015). These dome-shaped papillae are also comparable to the secretory cells occurring in the labellum margin and/or in the apical appendix of other *Ophrys* species (Ascensão *et al.*, 2005; Francisco & Ascensão, 2013; Francisco *et al.*, 2015), including its closest relatives *O. bombyliflora*, *O. tenthredinifera*, and species belonging to the section *Pseudophrys* such as *O. fusca* and *O. lutea*, which together form a clade with *O. speculum* in molecular phylogenetic analyses (Soliva *et al.*, 2001; Devey *et al.*, 2008). However, the extent of the secretory tissues in *Ophrys* was found to vary according to the species. The osmophore in *O. speculum* appears to be restricted to the portion of the glabrous apical margin of the labellum nearest the margin itself, occupying both the abaxial and the adaxial surfaces of the labellum. In contrast, in *O. fusca* and *O. lutea*, two species that share the absence of apical appendix in the labellum with *O. speculum*, the osmophore extends to the entire labellum margin and to the abaxial surface of the apical region of the labellum (Ascensão *et al.*, 2005). The osmophores of the other three investigated *Ophrys* species were found in the apical appendix, but in *O. bombyliflora*

it is restricted to the appendix, occurring mainly in its adaxial surface, whereas in *O. scolopax* and *O. tenthredinifera* the osmophore also occupies the apical labellum margin, and in this latter species, it extends further to the abaxial surface of the apical region of the labellum (Francisco & Ascensão, 2013; Francisco *et al.*, 2015). Among the osmophore-containing species, the secretory cells are mostly concentrated on the adaxial surface of the floral organs, generally restricted portions of the perianth segments (Pridgeon & Stern, 1983; Vogel, 1990; Stpiczyńska, 2001; Melo, Borba & Paiva, 2010; Pansarin *et al.*, 2014; Possobom *et al.*, 2015). Furthermore, the location of the osmophores of *O. speculum* and other *Ophrys* species in the apical region of the labellum agrees with the most common location of the scent-producing glands in the flower, i.e. the tips, margins or prominent areas of sepals, petals or labella (Pridgeon & Stern, 1983; Sanguinetti *et al.*, 2012; Pansarin *et al.*, 2014; Possobom *et al.*, 2015), which are exposed surfaces that favour the dispersion of the floral scent. Typically, the osmophores are sites of biosynthesis and emission of highly volatile organic compounds for long-range attraction of pollinators (Vogel, 1990).

Like most *Ophrys* flowers, those of *O. speculum* release a faint scent (Kullenberg, 1961; A. Francisco, personal observation) but their odour bouquet was found to be composed of more than 100 organic compounds of diverse volatility (Borg-Karlson, 1990; Ayasse *et al.*, 2003; Ayasse *et al.*, 2011). Among the highly volatile fraction of odour compounds in *O. speculum* were a series of saturated aliphatic esters, oxygenated carboxylic acids and monoterpene hydrocarbons (Borg-Karlson, 1990; Ayasse *et al.*, 2003; Ayasse *et al.*, 2011). Our finding that a lipophilic terpene-rich secretion is synthesised by the osmophore of *O. speculum* suggests that this fragrance-producing gland is likely the site of biosynthesis and releasing of part of the highly volatile fraction of the odour bouquet of this species, in accordance in what was also proposed for other *Ophrys* species (Francisco & Ascensão, 2013). A low amount of secretion was detected in the osmophore of *O. speculum* in the same sites as in the other *Ophrys* osmophores, particularly, in either the cortical cytoplasm, the periplasmic space, or the loose inner cell walls, although it was not observed in the vacuoles, in contrast to what appears to occur in the osmophores of *O. bombyliflora*, *O. fusca*, and *O. lutea* (Ascensão *et al.*, 2005; Francisco & Ascensão, 2013; Francisco *et al.*, 2015). These findings appear to be consistent with ultrastructural studies of the secretory cells of some orchid osmophores, which revealed osmiophilic droplets temporarily accumulated in the vacuoles and in the periplasmic space (Pridgeon & Stern, 1983; Pridgeon & Stern, 1985; Sanguinetti *et al.*, 2012). Additionally, some secretion droplets were found on the surface of the dome-shaped papillae in *O. speculum*, as seems to also occur in *O. fusca* (A. Francisco, unpubl. data) and in other orchids (Vogel, 1990; Sanguinetti *et al.*, 2012).

However, contrary to what is found in the osmophores of the other *Ophrys* species (Vogel, 1990; Ascensão *et al.*, 2005; Francisco & Ascensão, 2013; Francisco *et al.*, 2015), only vestigial starch was detected in the osmophore of *O. speculum*, even in the early stage of

flower development. The scarce starch content of this osmophore was observed in the two to three layers of parenchyma cells below the glandular epidermis, a location similar to that found in *O. bombyliflora*, *O. tenthredinifera*, and *O. scolopax* (Francisco & Ascensão, 2013; Francisco *et al.*, 2015), but in clear contrast to that of *O. fusca* and *O. lutea*, which exhibit osmophores with a great content in starch accumulated in the plastids of the secretory epidermal cells (Vogel, 1990; Ascensão *et al.*, 2005). No evidence of starch was also noted in the osmophores of some other terrestrial orchids belonging to the subtribes Orchidinae, Chloraeinae, and Spiranthinae (Vogel, 1990; Stpiczyńska, 2001; Wiemer *et al.*, 2009; Sanguinetti *et al.*, 2012), in contrast to most osmophore-containing species, which display considerable amount of starch in the subsecretory tissues (e.g. Pridgeon & Stern, 1983; Vogel & Hadacek, 2004). Starch and lipid reserves in the osmophore tissues are assumed to be an important source of energy and/or structural material for the biosynthesis of the volatile secretion, which needs to be intense and uninterrupted since it is continuously eliminated from the epidermal secretory cells due to its high volatility (Vogel, 1990). Osmophores without starch reserves present usually lipid inclusions in the cytoplasm (Vogel, 1990; Stpiczyńska, 2001; Wiemer *et al.*, 2009; Sanguinetti *et al.*, 2012). Given its virtual absence of starch or other type of reserves, the osmophore of *O. speculum* differ from the other *Ophrys* species, which may indicate a less intense secretory activity.

The role of the osmophore in pollination

Such hypothesis of the occurrence of an osmophore with little activity in *O. speculum* fits well with the fact that the key semiochemicals used by this species for attracting males of its specific *Dasyscolia ciliata* wasp pollinator are three uncommon short-chained oxygenated carboxylic acids, namely 9-oxodecanoic acid, 9-hydroxydecanoic acid, and 7-hydroxyoctanoic acid (Ayasse *et al.*, 2003), which are presumably more volatile than the long-chained hydrocarbons generally used by several *Ophrys* species as primary pollinator attractants (Schiestl *et al.*, 1999; Mant *et al.*, 2005; Stökl *et al.*, 2008; Ayasse *et al.*, 2011). Indeed, despite equivalent series of long-chained alkenes differing in the carbon chain length and in the position of the double-bond were also detected in large amounts in the cuticle solvent extracts of the labellum of *O. speculum*, these compounds did not constitute the behaviourally-active compounds in this species (Ayasse *et al.*, 2003), in contrast to what occurs in the *Ophrys* species pollinated by solitary bees of the genera *Andrena* and *Colletes* (Stökl *et al.*, 2008; Stökl *et al.*, 2009; Vereecken *et al.*, 2010; Xu *et al.*, 2011; Xu *et al.*, 2012a). Because of their physical and chemical properties, most long-chained hydrocarbons have low vapour pressure at room temperature and are non-volatile components of the cuticular waxes, being expected to exert their action only upon contact or at short distances from the labellum, like some contact sex pheromones in insects (Mori, 2010; Ayasse *et al.*, 2011). In those *Ophrys* species that produce hydrocarbons as the key semiochemicals, it is thus plausible that compounds of higher volatility, presumably synthesised in the osmophore,

are responsible for attracting male pollinators from relatively long distances (Francisco & Ascensão, 2013). In contrast, the greater volatility of the highly specific signal provided by the three uncommon (w-1)-hydroxy and (w-1)-oxo carboxylic acids, which occur in minute amounts in the cuticle extracts of the labellum of *O. speculum* (Ayasse *et al.*, 2003), suggests that these compounds could also act as efficient long-range attractants for male wasp pollinators. Therefore, the role of other highly volatile odour compounds, synthesised by the osmophore, in the process of attraction of males of the specific *Dasyscolia ciliata* wasp seems to be redundant in the case of *O. speculum*.

Nevertheless, the labellum of *O. speculum* releases a multitude of volatile organic compounds of diverse chemical origin, i.e. aliphatic and terpenoid compounds along with a few aromatic compounds (Borg-Karlson, 1990; Ayasse *et al.*, 2003), and, as we suggested above, part of the highly volatile compounds is likely synthesised in the osmophore now characterized. Therefore, we deem it reasonable that the osmophore in *O. speculum* be a reservoir of potential semiochemicals that is available to be used in situations that require adaptation to a new pollinator, which uses certainly a different, species-specific mating signal (Ayasse *et al.*, 2001). Such reservoir of compounds is particularly useful in an orchid species that maintains a fixed one-to-one relationship with a wasp pollinator species that evolved an uncommon mating signal consisting of a few unique compounds, and hence is strongly isolated from other scoliid wasps and sympatric insect species (Ayasse *et al.*, 2003; Paulus, 2006). Consequently, a pollinator shift in *O. speculum* may imply a jump to a different taxonomic group of insect pollinators (Vereecken & Francisco, 2014), as might be the case of *O. speculum* subsp. *regis-ferdinandii* if its putative hoverfly pollinator is confirmed (Paulus, 2006). Such scenario of drastic pollinator shifts has indeed occurred in the group of *O. insectifera* L., which consists of three closely-related *Ophrys* species – a widespread taxon plus two other endemic taxa, like in the group of *O. speculum* – each one pollinated by a species of either a wasp, a bee, or a sawfly (Borg-Karlson *et al.*, 1993; Vereecken, 2009; Triponez *et al.*, 2013). In this context, we propose that the *Ophrys* osmophore could maintain a sufficiently diverse odour bouquet upon which natural selective pressures could act, thereby adding flexibility and evolutionary potential to the highly specific sexually deceptive pollination of *Ophrys* orchids.

Osmophores have been also described for some species of the closely related genera of *Ophrys*, such as *Serapias, Himantoglossum* and *Anacamptis*, and even for the more distantly related *Platanthera bifolia* and *Gymnadenia conopsea* (Vogel, 1990; Stpiczyńska, 2001; Barone Lumaga *et al.*, 2012; Kowalkowska *et al.*, 2012), all belonging to the same subtribe Orchidinae (Inda, Pimentel & Chase, 2012). This fact is consistent with the hypothesis that the evolution of a fragrance-producing secretory structure is associated with a certain degree of specialization in diverse pollination interactions, enhancing the specificity of the highly volatile odour signal for long-range attraction of a particular group of insect pollinators (Borg-Karlson, 1990; Vogel, 1990; Huber *et al.*, 2005; Francisco & Ascensão,

2013). Likewise, the presence of n-alkenes in the cuticular waxes covering the labellum surface was also found to be prevalent in the subtribe Orchidinae and may constitute a pre-adaptation to the evolution of sexual deceptive pollination in the genus *Ophrys* (Schiestl & Cozzolino, 2008). Therefore, two complementary sources of chemical information seem to have evolved in the *Ophrys* labellum, playing different functions in *Ophrys* pollination, in accordance with the model of pollinator attraction that we have previously proposed for these orchids (Francisco & Ascensão, 2013): (1) the n-alkene-rich cuticular waxes that spread over the labellum surface, acting mainly at close distance and/or upon contact; and (2) the highly volatile organic compounds synthesised in the osmophore that occurs mostly in the apical labellum region, acting as long-range attractants for males insect pollinators.

ACKNOWLEDGEMENTS

We are grateful to Prof. A. Serrano and Dr. N. Oliveira (University of Lisbon) for capturing and identifying the female wasp, respectively. We thank Prof. O. Correia and Prof. C. Cruz (University of Lisbon) for lending their digital camera for stereomicroscopical image capture. We are also grateful to M. Porto and A. Pedroso for assistance in preparation of figures. This work was partially supported by the Fundação para a Ciência e a Tecnologia through a doctoral grant to A.F. (grant number SFRH/BD/18823/2004).

REFERENCES

Ågren L, Kullenberg B, Sensenbaugh T. 1984. Congruences in pilosity between three species of *Ophrys* (Orchidaceae) and their hymenopteran pollinators. *Nova Acta Regiae Societatis Scientiarum Upsaliensis, Serie V:C* **3:** 15-25.

Aldasoro JJ, Sáez L. 2005. *Ophrys* L. In: Aedo C, Herrero A, eds. *Flora Iberica: plantas vasculares da la Península Ibérica e Islas Baleares, Vol. XXI.* Madrid: Real Jardín Botánico, CSIC, 165-195.

Ascensão L, Francisco A, Cotrim H, Pais MS. 2005. Comparative structure of the labellum in *Ophrys fusca* and *O. lutea* (Orchidaceae). *American Journal of Botany* **92:** 1059-1067.

Ayasse M, Paxton RJ, Tengö J. 2001. Mating behavior and chemical communication in the order Hymenoptera. *Annual Review of Entomology* **46:** 31-78.

Ayasse M, Schiestl FP, Paulus HF, Ibarra F, Francke W. 2003. Pollinator attraction in a sexually deceptive orchid by means of unconventional chemicals. *Proceedings of the Royal Society B: Biological Sciences* **270:** 517-522.

Ayasse M, Stökl J, Francke W. 2011. Chemical ecology and pollinator-driven speciation in sexually deceptive orchids. *Phytochemistry* **72:** 1667-1677.

Barone Lumaga MR, Pellegrino G, Bellusci F, Perrotta E, Perrotta I, Musacchio A. 2012. Comparative floral micromorphology in four sympatric species of *Serapias* (Orchidaceae). *Botanical Journal of the Linnean Society* **169:** 714-724.

Barthlott W, Neinhuis C, Cutler D, Ditsch F, Meusel I, Theisen I, Wilhelmi H. 1998. Classification and terminology of plant epicuticular waxes. *Botanical Journal of the Linnean Society* **126:** 237-260.

Benitez-Vieyra S, Medina AM, Cocucci AA. 2009. Variable selection patterns on the labellum shape of *Geoblasta pennicillata*, a sexually deceptive orchid. *Journal of Evolutionary Biology* **22:** 2354-2362.

Borg-Karlson A-K, Tengö J. 1986. Odor mimetism? Key substances in *Ophrys lutea* - *Andrena* pollination relationship (Orchidaceae: Andrenidae). *Journal of Chemical Ecology* **12:** 1927-1942.

Borg-Karlson A-K. 1990. Chemical and ethological studies of pollination in the genus *Ophrys* (Orchidaceae). *Phytochemistry* **29:** 1359-1387.

Borg-Karlson A-K, Groth I, Ägren L, Kullenberg B. 1993. Form-specific fragrances from *Ophrys insectifera* L. (Orchidaceae) attract species of different pollinator genera. Evidence of sympatric speciation? *Chemoecology* **4:** 39-45.

Borg-Karlson A-K, Tengö J, Valterová I, Unelius CR, Taghizadeh T, Tolasch T, Francke W. 2003. (S)-(+)-Linalool, a mate attractant pheromone component in the bee *Colletes cunicularius*. *Journal of Chemical Ecology* **29:** 1-14.

Bradshaw E, Rudall PJ, Devey DS, Thomas MM, Glover BJ, Bateman RM. 2010. Comparative labellum micromorphology of the sexually deceptive temperate orchid genus *Ophrys*: diverse epidermal cell types and multiple origins of structural colour. *Botanical Journal of the Linnean Society* **162:** 504-540.

Bronner R. 1975. Simultaneous demonstration of lipids and starch in plant tissues. *Stain Technology* **50:** 1-4.

Buschhaus C, Jetter R. 2011. Composition differences between epicuticular and intracuticular wax substructures: How do plants seal their epidermal surfaces? *Journal of Experimental Botany* **62:** 841-853.

Casado CG, Heredia A. 2001. Ultrastructure of the cuticle during growth of the grape berry (*Vitis vinifera*). *Physiologia Plantarum* **111:** 220-224.

Chin S-w, Lutz S, Wen J, Potter D. 2013. The bitter and the sweet: inference of homology and evolution of leaf glands in *Prunus* (Rosaceae) through anatomy, micromorphology, and ancestral–character state reconstruction. *International Journal of Plant Sciences* **174:** 27-46.

Ciotek L, Giorgis P, Benitez-Vieyra S, Cocucci AA. 2006. First confirmed case of pseudocopulation in terrestrial orchids of South America: pollination of *Geoblasta pennicillata* (Orchidaceae) by *Campsomeris bistrimacula* (Hymenoptera, Scoliidae). *Flora* **201:** 365-369.

Correvon H, Pouyanne M. 1916. Un curieux cas de mimétisme chez les Ophrydées. *Journal de la Société Nationale d'Horticulture de France, ser. 4,* **17:** 29-31; 41-47; 84-85.

Cortis P, Vereecken NJ, Schiestl FP, Lumaga MRB, Scrugli A, Cozzolino S. 2009. Pollinator convergence and the nature of species' boundaries in sympatric Sardinian *Ophrys* (Orchidaceae). *Annals of Botany* **104:** 497-506.

Dafni A. 1984. Mimicry and deception in pollination. *Annual Review of Ecology and Systematics* **15:** 259-278.

Darwin C. 1862. *On the various contrivances by which British and foreign orchids are fertilised by insects, and on the good effects of intercrossing.* London: John Murray.

David R, Carde JP. 1964. Coloration diférentielle des inclusions lipidiques et terpeniques des pseudophylles du *Pin maritime* au moyen du reactif Nadi. *Comptes Rendus de l'Académie des Sciences* **258:** 1338-1340.

Delforge P. 2005. *Guide des orchidées d'Europe, d'Afrique du Nord et du Proche-Orient.* 3rd ed. Paris: Delachaux et Niestlé.

Devey DS, Bateman RM, Fay MF, Hawkins JA. 2008. Friends or relatives? Phylogenetics and species delimitation in the controversial European orchid genus *Ophrys*. *Annals of Botany* **101:** 385-402.

Devillers P, Devillers-Terschuren J. 1994. Essai d'analyse systématique du genre *Ophrys*. *Les Naturalistes belges* **75 (Orchidées 7):** 273-400.

Feder N, O'Brien TP. 1968. Plant microtechnique: some principles and new methods. *American Journal of Botany* **55:** 123-142.

Francisco A, Ascensão L. 2013. Structure of the osmophore and labellum micromorphology in the sexually deceptive orchids *Ophrys bombyliflora* and *Ophrys tenthredinifera* (Orchidaceae). *International Journal of Plant Sciences* **174:** 619-636.

Francisco A, Porto M, Ascensão L. 2015. Morphological phylogenetic analysis of *Ophrys* (Orchidaceae): insights from morpho-anatomical floral traits into the interspecific relationships in an unresolved clade. *Botanical Journal of the Linnean Society* **179**: 454-476.

Gaskett AC, Herberstein ME. 2010. Colour mimicry and sexual deception by Tongue orchids (*Cryptostylis*). *Naturwissenschaften* **97:** 97-102.

Gaskett AC. 2011. Orchid pollination by sexual deception: pollinator perspectives. *Biological Reviews* **86:** 33-75.

Gaskett AC. 2012. Floral shape mimicry and variation in sexually deceptive orchids with a shared pollinator. *Biological Journal of the Linnean Society* **106:** 469-481.

Gaskett AC. 2014. Color and sexual deception in orchids: progress toward understanding the functions and pollinator perception of floral color. In: Edens-Meier R, Bernhardt P, eds. *Darwin's orchids: then and now.* Chicago: The University of Chicago Press, 291-309.

Godfery MJ. 1925. The fertilisation of *Ophrys speculum*, *O. lutea* and *O. fusca*. *The Journal of Botany, British and Foreign* **63:** 33-40.

Godfery MJ. 1928. Classification of the genus *Ophrys*. *The Journal of Botany, British and Foreign* **66:** 33-36.

Gögler J, Twele R, Francke W, Ayasse M. 2011. Two phylogenetically distinct species of sexually deceptive orchids mimic the sex pheromone of their single common pollinator, the cuckoo bumblebee *Bombus vestalis*. *Chemoecology* **21:** 243-252.

Gutmann M. 1995. Improved staining procedures for photographic documentation of phenolic deposits in semithin sections of plant tissue. *Journal of Microscopy* **179:** 277-281.

Harborne JB. 1998. *Phytochemical methods: a guide to modern techniques of plant analysis.* 3rd ed. London: Chapman & Hall.

Huber FK, Kaiser R, Sauter W, Schiestl FP. 2005. Floral scent emission and pollinator attraction in two species of *Gymnadenia* (Orchidaceae). *Oecologia* **142:** 564-575.

Inda LA, Pimentel M, Chase MW. 2012. Phylogenetics of tribe Orchideae (Orchidaceae: Orchidoideae) based on combined DNA matrices: inferences regarding timing of diversification and evolution of pollination syndromes. *Annals of Botany* **110:** 71-90.

Jeffree CE. 2006. The fine structure of the plant cuticle. In: Riederer M, Müller C, eds. *Biology of the plant cuticle.* Oxford: Blackwell Publishing Ltd, 11-25.

Jersáková J, Johnson SD, Kindlmann P. 2006. Mechanisms and evolution of deceptive pollination in orchids. *Biological Reviews of the Cambridge Philosophical Society* **81:** 219-235.

Jetter R, Schäffer S, Riederer M. 2000. Leaf cuticular waxes are arranged in chemically and mechanically distinct layers: evidence from *Prunus laurocerasus* L. *Plant, Cell and Environment* **23:** 619-628.

Kay QON, Daoud HS, Stirton CH. 1981. Pigment distribution, light reflection and cell structure in petals. *Botanical Journal of the Linnean Society* **83:** 57-84.

Kearney M, Rieppel O. 2006. Rejecting "the given" in systematics. *Cladistics: The International Journal of the Willi Hennig Society* **22:** 369-377.

Kirk PW. 1970. Neutral red as a lipid fluorochrome. *Stain Technology* **45:** 1-4.

Koch K, Hartmann KD, Schreiber L, Barthlott W, Neinhuis C. 2006. Influences of air humidity during the cultivation of plants on wax chemical composition, morphology and leaf surface wettability. *Environmental and Experimental Botany* **56:** 1-9.

Koch K, Bhushan B, Barthlott W. 2008. Diversity of structure, morphology and wetting of plant surfaces. *Soft Matter* **4:** 1943-1963.

Kowalkowska A, Margońska H, Kozieradzka-Kiszkurno M, Bohdanowicz J. 2012. Studies on the ultrastructure of a three-spurred *fumeauxiana* form of *Anacamptis pyramidalis*. *Plant Systematics and Evolution* **298:** 1025-1035.

Kullenberg B. 1961. Studies in *Ophrys* pollination. *Zoologiska Bidrag fran Uppsala* **34:** 1-340.

Kullenberg B, Bergström G. 1976. Hymenoptera Aculeata males as pollinators of *Ophrys* orchids. *Zoologica Scripta* **5:** 13-23.

Kullenberg B, Borg-Karlson A-K, Kullenberg A-L. 1984. Field studies on the behaviour of the *Eucera nigrilabris* male in the odour flow from flower labellum extract of *Ophrys tenthredinifera*. *Nova Acta Regiae Societatis Scientiarum Upsaliensis, Serie V:C* **3:** 79-110.

Lara Ruiz J. 2010. Polinizadores y visitantes de *Ophrys* L. en la Península Ibérica e Islas Baleares. *Micobotanica-Jaén* **Año V, Nº 3:** http://www.micobotanicajaen.com/Revista/Articulos/JLaraR/Polinizadores/Ophrys.html.

Mant JG, Brändli C, Vereecken NJ, Schulz CM, Francke W, Schiestl FP. 2005. Cuticular hydrocarbons as sex pheromone of *Colletes cunicularius* (Hymenoptera: Colletidae) and the key to its mimicry by the sexually deceptive orchid, *Ophrys exaltata*. *Journal of Chemical Ecology* **31:** 1765-1787.

Melo MC, Borba EL, Paiva EAS. 2010. Morphological and histological characterization of the osmophores and nectaries of four species of *Acianthera* (Orchidaceae: Pleurothallidinae). *Plant Systematics and Evolution* **286:** 141-151.

Mori K. 2010. Pheromones in chemical communication. In: Herrmann A, ed. *The chemistry and biology of volatiles.* Chichester, West Sussex, UK: John Wiley & Sons Ltd., 123-150.

Nixon KC, Carpenter JM. 2012. On homology. *Cladistics: The International Journal of the Willi Hennig Society* **28:** 160-169.

Pansarin LM, Pansarin ER, Sazima M. 2014. Osmophore structure and phylogeny of *Cirrhaea* (Orchidaceae, Stanhopeinae). *Botanical Journal of the Linnean Society* **176:** 369-383.

Parham RA, Kaustinen HM. 1976. Differential staining of tannin in sections of epoxy-embedded plant cells. *Stain Technology* **51:** 237-240.

Paulus HF, Gack C. 1990. Pollinators as prepollinating isolation factors: evolution and speciation in *Ophrys* (Orchidaceae). *Israel Journal of Botany* **39:** 43-79.

Paulus HF. 2006. Deceived males - Pollination biology of the Mediterranean orchid genus *Ophrys* (Orchidaceae). *Journal Europäischer Orchideen* **38:** 303-353.

Peakall R, Ebert D, Poldy J, Barrow RA, Francke W, Bower CC, Schiestl FP. 2010. Pollinator specificity, floral odour chemistry and the phylogeny of Australian sexually deceptive *Chiloglottis* orchids: implications for pollinator-driven speciation. *New Phytologist* **188:** 437-450.

Peakall R, Whitehead MR. 2014. Floral odour chemistry defines species boundaries and underpins strong reproductive isolation in sexually deceptive orchids. *Annals of Botany* **113:** 341-355.

Pearse AGE. 1985. *Histochemistry: theoretical and applied. Volume 2, Analytical technology.* 4th ed. Edinburgh: Churchill-Livingstone.

Pedersen HÆ, Faurholdt N. 2007. *Ophrys, the bee orchids of Europe.* Kew, London: Kew Publishing - Royal Botanic Gardens.

Peter CI, Johnson SD. 2013. Generalized food deception: colour signals and efficient pollen transfer in bee-pollinated species of *Eulophia* (Orchidaceae). *Botanical Journal of the Linnean Society* **171:** 713-729.

Phillips RD, Xu T, Hutchinson MF, Dixon KW, Peakall R. 2013. Convergent specialization - the sharing of pollinators by sympatric genera of sexually deceptive orchids. *Journal of Ecology* **101:** 826-835.

Phillips RD, Scaccabarozzi D, Retter BA, Hayes C, Brown GR, Dixon KW, Peakall R. 2014. Caught in the act: pollination of sexually deceptive trap-flowers by fungus gnats in *Pterostylis* (Orchidaceae). *Annals of Botany* **113:** 629-641.

van der Pijl L, Dodson CH. 1966. *Orchids flowers, their pollination and evolution.* Coral Gables, Florida: University of Miami Press.

Possobom CCF, Guimarães E, Machado SR. 2015. Structure and secretion mechanisms of floral glands in *Diplopterys pubipetala* (Malpighiaceae), a neotropical species. *Flora* **211:** 26-39.

Pouyanne M. 1917. La fécondation des *Ophrys* par les insectes. *Bulletin de la Société d'Histoire Naturelle de l'Afrique du nord* **8:** 6-7.

Pridgeon AM, Stern WL. 1983. Ultrastructure of osmophores in *Restrepia* (Orchidaceae). *American Journal of Botany* **70:** 1233-1243.

Pridgeon AM, Stern WL. 1985. Osmophores of *Scaphosepalum* (Orchidaceae). *Botanical Gazette* **146:** 115-123.

Renner SS. 2005. Rewardless flowers in the angiosperms and the role of insect cognition in their evolution. In: Waser NM, Ollerton J, eds. *Plant-pollinator interactions: from specialization to generalization.* Chicago: University of Chicago Press, 123-144.

Sanguinetti A, Buzatto CR, Pedron M, Davies KL, Ferreira PMdA, Maldonado S, Singer RB. 2012. Floral features, pollination biology and breeding system of *Chloraea membranacea* Lindl. (Orchidaceae: Chloraeinae). *Annals of Botany* **110:** 1607-1621.

Sarrazin M, Vigneron JP, Welch V, Rassart M. 2008. Nanomorphology of the blue iridescent wings of a giant tropical wasp *Megascolia procer javanensis* (Hymenoptera). *Physical Review E* **78:** 051902.

Sattler R. 1994. Homology, homeosis, and process morphology in plants. In: Hall BK, ed. *Homology: the hierarchical basis of comparative biology.* San Diego, CA, USA: Academic Press, 424-476.

Schiestl FP, Ayasse M, Paulus HF, Löfstedt C, Hansson BS, Ibarra F, Francke W. 1999. Orchid pollination by sexual swindle. *Nature* **399:** 421-422.

Schiestl FP. 2005. On the success of a swindle: pollination by deception in orchids. *Naturwissenschaften* **92:** 255-264.

Schiestl FP, Cozzolino S. 2008. Evolution of sexual mimicry in the orchid subtribe Orchidinae: the role of preadaptations in the attraction of male bees as pollinators. *BMC Evolutionary Biology* **8:** 27.

Schiestl FP, Schlüter PM. 2009. Floral isolation, specialized pollination, and pollinator behavior in orchids. *Annual Review of Entomology* **54:** 425-446.

Scopece G, Musacchio A, Widmer A, Cozzolino S. 2007. Patterns of reproductive isolation in mediterranean deceptive orchids. *Evolution* **61:** 2623-2642.

Servettaz O, Bino Maleci L, Grünanger P. 1994. Labellum micromorphology in the *Ophrys bertolinii* agg. and some related taxa (Orchidaceae). *Plant Systematics and Evolution* **189:** 123-131.

Sharma V, Crne M, Park JO, Srinivasarao M. 2009. Structural origin of circularly polarized iridescence in jeweled beetles. *Science* **325:** 449-451.

Soliva M, Kocyan A, Widmer A. 2001. Molecular phylogenetics of the sexually deceptive orchid genus *Ophrys* (Orchidaceae) based on nuclear and chloroplast DNA sequences. *Molecular Phylogenetics and Evolution* **20:** 78-88.

Spaethe J, Moser WH, Paulus HF. 2007. Increase of pollinator attraction by means of a visual signal in the sexually deceptive orchid, *Ophrys heldreichii* (Orchidaceae). *Plant Systematics and Evolution* **264:** 31-40.

Stökl J, Twele R, Erdmann DH, Francke W, Ayasse M. 2008. Comparison of the flower scent of the sexually deceptive orchid *Ophrys iricolor* and the female sex pheromone of its pollinator *Andrena morio*. *Chemoecology* **17:** 231-233.

Stökl J, Schlüter PM, Stuessy TF, Paulus HF, Fraberger R, Erdmann D, Schulz C, Francke W, Assum G, Ayasse M. 2009. Speciation in sexually deceptive orchids: pollinator-driven selection maintains discrete odour phenotypes in hybridizing species. *Biological Journal of the Linnean Society* **98:** 439-451.

Stpiczyńska M. 2001. Osmophores of the fragrant orchid *Gymnadenia conopsea* L. (Orchidaceae). *Acta Societatis Botanicorum Poloniae* **70:** 91-96.

Streinzer M, Paulus HF, Spaethe J. 2009. Floral colour signal increases short-range detectability of a sexually deceptive orchid to its bee pollinator. *The Journal of Experimental Biology* **212:** 1365-1370.

Thomas MM, Rudall PJ, Ellis AG, Savolainen V, Glover BJ. 2009. Development of a complex floral trait: the pollinator-attracting petal spots of the beetle daisy, *Gorteria diffusa* (Asteraceae). *American Journal of Botany* **96:** 2184-2196.

Triponez Y, Arrigo N, Pellissier L, Schatz B, Alvarez N. 2013. Morphological, ecological and genetic aspects associated with endemism in the Fly Orchid group. *Molecular Ecology* **22:** 1431-1446.

Vereecken NJ. 2009. Deceptive behavior in plants. I. Pollination by sexual deception in orchids: a host-parasite perspective. In: Baluška F, ed. *Plant-environment interactions. From sensory plant biology to active plant behavior.* Heidelberg: Springer-Verlag, 203-222.

Vereecken NJ, Cozzolino S, Schiestl FP. 2010. Hybrid floral scent novelty drives pollinator shift in sexually deceptive orchids. *BMC Evolutionary Biology* **10:** 103.

Vereecken NJ, Wilson CA, Hötling S, Schulz S, Banketov SA, Mardulyn P. 2012. Pre-adaptations and the evolution of pollination by sexual deception: Cope's rule of specialization revisited. *Proceedings of the Royal Society B: Biological Sciences* **279:** 4786-4794.

Vereecken NJ, Francisco A. 2014. *Ophrys* pollination: from Darwin to the present day. In: Edens-Meier R, Bernhardt P, eds. *Darwin's orchids: then and now.* Chicago: The University of Chicago Press, 47-67.

Vignolini S, Davey MP, Bateman RM, Rudall PJ, Moyroud E, Tratt J, Malmgren S, Steiner U, Glover BJ. 2012a. The mirror crack'd: both pigment and structure contribute to the glossy blue appearance of the mirror orchid, *Ophrys speculum*. *New Phytologist* **196:** 1038-1047.

Vignolini S, Thomas MM, Kolle M, Wenzel T, Rowland A, Rudall PJ, Baumberg JJ, Glover BJ, Steiner U. 2012b. Directional scattering from the glossy flower of *Ranunculus*: how the buttercup lights up your chin. *Journal of the Royal Society Interface* **9:** 1295-1301.

Vogel S. 1990. *The role of scent glands in pollination: on the structure and function of osmophores.* Rotterdam: A. A. Balkema. [English translation of: Vogel S. 1963. Duftdrüsen im Dienste der Bestäubung: Über Bau und Funktion der Osmophoren. *Akademie der Wissenschaften und der Literatur in Mainz, Abhandlungen der Mathematisch-Naturwissenschaftlichen Klasse* **10**: 600-763].

Vogel S, Hadacek F. 2004. Contributions to the functional anatomy and biology of *Nelumbo nucifera* (Nelumbonaceae) III. An ecological reappraisal of floral organs. *Plant Systematics and Evolution* **249:** 173-189.

Wiemer AP, Moré M, Benitez-Vieyra S, Cocucci AA, Raguso RA, Sérsic AN. 2009. A simple floral fragrance and unusual osmophore structure in *Cyclopogon elatus* (Orchidaceae). *Plant Biology* **11:** 506-514.

Xu S, Schlüter PM, Scopece G, Breitkopf H, Gross K, Cozzolino S, Schiestl FP. 2011. Floral isolation is the main reproductive barrier among closely related sexually deceptive orchids. *Evolution* **65:** 2606–2620.

Xu S, Schlüter PM, Grossniklaus U, Schiestl FP. 2012a. The genetic basis of pollinator adaptation in a sexually deceptive orchid. *PLoS Genetics* **8:** e1002889. doi:10.1371/journal.pgen.1002889.

Xu S, Schlüter PM, Schiestl FP. 2012b. Pollinator-driven speciation in sexually deceptive orchids. *International Journal of Ecology* **2012, Article ID 285081:** 9 pages. doi:10.1155/2012/285081.

CHAPTER 5

MORPHOLOGICAL PHYLOGENETIC ANALYSIS OF *OPHRYS* (ORCHIDACEAE): INSIGHTS FROM MORPHO-ANATOMICAL FLORAL TRAITS INTO THE INTERSPECIFIC RELATIONSHIPS IN AN UNRESOLVED CLADE

This chapter was published in *Botanical Journal of the Linnean Society*:

Francisco A., Porto M. and Ascensão L. 2015. Morphological phylogenetic analysis of *Ophrys* (Orchidaceae): insights from morpho-anatomical floral traits into the interspecific relationships in an unresolved clade. *Botanical Journal of the Linnean Society*, 179: 454-476.

MORPHOLOGICAL PHYLOGENETIC ANALYSIS OF *OPHRYS* (ORCHIDACEAE): INSIGHTS FROM MORPHO-ANATOMICAL FLORAL TRAITS INTO THE INTERSPECIFIC RELATIONSHIPS IN AN UNRESOLVED CLADE

ABSTRACT

Reconstructing the phylogeny of the sexually deceptive orchid genus *Ophrys* is crucial to our understanding of the evolution of its complex floral morphology. Molecular phylogenetic analyses showed that the section *Pseudophrys* forms a well supported clade with *Ophrys bombyliflora*, *O. tenthredinifera* and *O. speculum*, but were unable to elucidate the relationships between these four groups of taxa. Here we conduct a morphological phylogenetic analysis of this unresolved clade of *Ophrys* based on a data matrix of 45 macro- and micromorphological and anatomical floral characters, using maximum parsimony and Bayesian inference. Our cladistic analysis yielded a single most parsimonious tree and a Bayesian 50% majority-rule consensus tree which differed in their overall topology but agreed that *O. tenthredinifera* and *O. bombyliflora* are not sister groups. The phylogenetic placement of *O. tenthredinifera* was ambiguous since it shares six valid synapomorphies each with the cluster of *O. speculum–O. bombyliflora* and with section *Pseudophrys*. In contrast, *O. bombyliflora* is most likely the sister group to *O. speculum*, a finding that rejects an earlier morphological phylogenetic hypothesis and favours the existing molecular trees based on nuclear ITS rather than plastid data.

KEYWORDS: ancestral state reconstruction; Bayesian inference; cladistics; continuous characters; floral character evolution; floral morphology; labellum micromorphology; maximum parsimony; osmophore; sexual deceptive pollination.

INTRODUCTION

An understanding of the evolutionary changes in flower structure that have led to the great diversification of the angiosperms constitutes one of the major scientific challenges, and this understanding can only be achieved within a framework provided by an increasingly accurate reconstruction of the phylogenetic relationships of flowering plants (Endress, 2011). Our knowledge about the phylogeny of diverse groups of angiosperms has benefited unquestionably from the numerous molecular phylogenetic studies that have been conducted at different taxonomic levels over the past two decades (e.g. Chase *et al.*, 1993; Soltis *et al.*, 2000; APG III, 2009; Górniak, Paun & Chase, 2010; Inda, Pimentel & Chase, 2012). Nonetheless, evidence has been accumulating that morphological data remain a valuable source of phylogenetic information which could often be integrated with molecular data in order to improve the accuracy of the phylogenetic tree of several taxonomic groups (Bateman, Hilton & Rudall, 2006; Ronse De Craene & Haston, 2006; Clennett *et al.*, 2012; Cardoso *et al.*, 2013). Cladistic analyses based solely on morphological characters additionally provide morphological synapomorphies which confer support and credibility to the groups recognized in phylogenetic trees (Freudenstein & Rasmussen, 1999; Rudall, 2002; Rudall & Bateman, 2006; Nürk & Blattner, 2010). Moreover, analyzing morphological traits in a phylogenetic context is the only way to understand the evolutionary history of the diverse floral and vegetative characters across taxa (Wagner *et al.*, 2012; Chin *et al.*, 2013; Dong *et al.*, 2013; Roque & Funk, 2013; Sokoloff *et al.*, 2013).

The Euro-Mediterranean terrestrial orchid genus *Ophrys* L. (Orchidaceae: Orchidinae) is remarkable for its extremely diverse insectiform flowers that have evolved a sophisticated way of attracting and deceiving only males of mostly solitary bees (Gaskett, 2011) by means of an almost perfect mimicry of the appearance, texture and sex pheromones of their conspecific females (Kullenberg, 1961; Ågren, Kullenberg & Sensenbaugh, 1984; Schiestl *et al.*, 1999; Vereecken & Schiestl, 2008), guaranteeing the effectiveness of a highly specialized and specific pollination system by sexual deception (Pouyanne, 1917; Schiestl & Schlüter, 2009). Diversification of *Ophrys* is most likely to be driven by the pollinators, through a strong selective pressure on certain floral traits, primarily the floral scent, but also morphological features providing visual and tactile signals (Benitez-Vieyra, Medina & Cocucci, 2009; Streinzer, Paulus & Spaethe, 2009; Ayasse, Stökl & Francke, 2011; Xu, Schlüter & Schiestl, 2012). As a result, morphological similarity in floral features between *Ophrys* spp. may be indicative of convergence instead of common ancestry (Paulus, 2006), which renders floral characters less reliable predictors of phylogenetic relatedness than vegetative characters (e.g. Chase *et al.*, 2009). Because vegetative traits, however, seem to be nearly homogeneous throughout *Ophrys* (Devillers & Devillers-Terschuren, 1994; Stern, 1997; Stern, 2014), floral characters remain the only source of morphological information

that might be useful for phylogenetic inference in *Ophrys*, despite the problems that convergence may pose for phylogenetic reconstruction in this group (Bateman, 2009).

The great morphological floral diversity exhibited by *Ophrys* (see Supporting Information, Fig. S1), associated with a high intraspecific variation of some floral traits (Paulus, 2006), has hindered the reaching of a consensus on the taxonomy in this genus, with the number of species varying enormously between 19 and >250 species, depending on the author (Delforge, 2005; Pedersen & Faurholdt, 2007). The prevailing classification of *Ophrys* until the beginning of the 21st century was the system implemented by Godfery (1928) and upheld by Devillers & Devillers-Terschuren (1994), which divided the genus into two main sections, *Pseudophrys* Godfery and *Ophrys* (synonym: section *Euophrys* Godfery), based on structural differences in the labellum and the stigmatic cavity of the flowers (see Fig. S2). Subsequent molecular phylogenetic analyses, however, have revealed that section *Pseudophrys* is a monophyletic group that is nested in section *Ophrys*, thereby making the latter section paraphyletic (Soliva, Kocyan & Widmer, 2001; Devey *et al.*, 2008; Inda *et al.*, 2012). Species belonging to section *Pseudophrys* were found to consistently form a clade with *O. bombyliflora* Link, *O. tenthredinifera* Willd. and *O. speculum* Link, but the interspecific relationships in this clade remain unresolved (Bateman, Pridgeon & Chase, 1997; Soliva *et al.*, 2001; Devey *et al.*, 2008; Inda *et al.*, 2012; Vereecken *et al.*, 2012). In the most recent molecular phylogenetic study focused on the genus *Ophrys* (Devey *et al.*, 2008), two different topologies were found for this clade. Basically, *O. bombyliflora* was placed as sister to either the *O. speculum* group or the *O. tenthredinifera* group, with equally moderate support, in trees obtained from the analysis of DNA data from the nuclear ITS region or plastid loci, respectively (Devey *et al.*, 2008). This ambiguous placement of *O. bombyliflora* is also evident from the observation of the trees obtained in the other molecular studies performed so far (Bateman *et al.*, 1997; Soliva *et al.*, 2001; Bateman *et al.*, 2003; Inda *et al.*, 2012; Vereecken *et al.*, 2012). The inconclusiveness of existing molecular analyses calls for using other sources of information, particularly morphological data, in an attempt to clarify the phylogeny of this major clade of *Ophrys* further. Moreover, the morphological floral characters that underlie the phylogenetic relatedness of the species that constitute this clade have not been yet identified.

The only cladistic analysis based on morphological data previously performed on the genus *Ophrys* was the study by Devillers & Devillers-Terschuren (1994), which also included a thorough description of the structure of *Ophrys* flowers, proposing credible homologies and new adequate terminology for the complex floral structural details. In the phylogenetic hypothesis suggested by Devillers & Devillers-Terschuren (1994), section *Pseudophrys* was placed at the base of the tree and the group of *O. speculum* was placed as an early diverging group at the base of the remaining part of the genus. Although the trees obtained from molecular phylogenetic studies are usually contrasted with the morphological tree by Devillers & Devillers-Terschuren (1994), it is important to note that this tree is unlikely to

reflect an accurate representation of the relationships between *Ophrys* spp. concerning morphology, as the underlying morphological data matrix contained methodological faults regarding definition and coding of some characters (Bateman *et al.*, 1997). Indeed, the authors themselves admitted that their data matrix did not reflect an objective character analysis (Devillers & Devillers-Terschuren, 1994). Therefore, a phylogenetic analysis of *Ophrys* spp. based on a revised matrix of morphological characters, constructed with explicit criteria for their selection, definition and coding is unquestionably needed.

The great diversity of epidermal cell types occurring in the adaxial surface of the labellum of *Ophrys* species (Bradshaw *et al.*, 2010; Francisco & Ascensão, 2013) is expected to provide informative micromorphological characters to be used in phylogenetic analyses, but its potential has not yet been explored. Although several micromorphological studies have been performed in subtribe Orchidinae (Servettaz, Bino Maleci & Grünanger, 1994; Luo & Chen, 2000; Box *et al.*, 2008; Bell *et al.*, 2009; Bradshaw *et al.*, 2010; Barone Lumaga *et al.*, 2012) and some, particularly those pertaining to pollen and seed ornamentation, have identified features with diagnostic and taxonomic value at the genus level (Barone Lumaga, Cozzolino & Kocyan, 2006; Gamarra *et al.*, 2010; Gamarra *et al.*, 2012), studies that evaluate directly the phylogenetic significance of floral micromorphological traits remain to be done in this subtribe. In previous studies, we have completed detailed micromorphological and anatomical characterization of the labellum and the stigmatic cavity of *Ophrys* spp., which are representative of all four groups that constitute the still unresolved clade formed by the *O. bombyliflora, O. speculum* and *O. tenthredinifera* groups *sensu* Devey *et al.* (2008) and section *Pseudophrys* (Ascensão *et al.*, 2005; Francisco & Ascensão, 2013; A. Francisco & L. Ascensão, unpubl. manuscript). In these studies we have also identified and described in depth the osmophore, the secretory structure that occurs in the labellum of *Ophrys*. Here we use novel micromorphological and anatomical evidence and the solid framework of flower structure terminology established by Devillers & Devillers-Terschuren (1994) as the basis for building a robust morpho-anatomical data matrix, which also included macromorphological data resulting from the current comparative analysis of *Ophrys* flowers.

In the present study we: (1) identify macro-, micro-morphological and anatomical floral characters with potential phylogenetic information in the genus *Ophrys*; (2) help to clarify the phylogenetic relationships between all four well established groups of species that constitute the still unresolved *Ophrys* clade (*O. bombyliflora*, *O. speculum*, *O. tenthredinifera*, and the section *Pseudophrys*) from a morpho-anatomical data matrix; (3) identify the potential synapomorphies which could explain and support the groups found in the phylogenetic tree; and (4) reconstruct the character states for the presumed most recent common ancestor of the investigated clade, contributing to our understanding of the evolution of floral characters in the morphologically diverse *Ophrys* genus.

MATERIAL AND METHODS

TAXON SAMPLING

Inflorescences of seven *Ophrys* taxa (see Fig. S1) were collected between February and April 2005 to 2009, from natural populations occurring in central-western Portugal (in the municipalities of Sesimbra and Loures). The following six taxa constituted the ingroup in the morphological phylogenetic analyses: *O. bombyliflora* Link, *O. fusca* Link subsp. *fusca, O. lutea* Cav., *O. speculum* Link subsp. *lusitanica* O.Danesch & E.Danesch, *O. speculum* Link subsp. *speculum* and *O. tenthredinifera* Willd.. The taxonomic classification adopted here follows Aldasoro & Sáez (2005). Since we are interested in clarifying the interspecific relationships between, rather than within, all four groups that constitute the investigated clade, we have sampled only the most representative taxa of each group occurring in Portugal, excluding similar taxa which share the majority of the floral features with the selected taxa of each group [e.g. *O. fusca* subsp. *dyris* (Maire) Soó]. For the sake of simplicity, hereafter we use the name *O. fusca* to refer to *O. fusca* subsp. *fusca*.

Ophrys scolopax Cav. was selected as the outgroup based on its molecular phylogenetic placement in the other major clade of *Ophrys* that is sister to the investigated clade (Devey *et al.*, 2008). The monophyly of our clade of interest was not intended to be tested here, as it has been well established in previous molecular phylogenetic analyses (Soliva *et al.*, 2001; Devey *et al.*, 2008; Vereecken *et al.*, 2012) and also supported by a karyomorphological study (D'Emerico *et al.*, 2005). Hence, the selection of a single species as outgroup is considered appropriate in this case (Rudall & Bateman, 2006). A voucher specimen of each taxon was deposited in LISU, the Herbarium of the University of Lisbon Botanical Garden in Portugal, and is identified below in the Appendix.

COMPARATIVE MORPHO-ANATOMICAL ANALYSIS

Freshly opened flowers of all seven *Ophrys* taxa were examined and their morphology compared using an Olympus SZH-ILLK stereomicroscope (Olympus Optical, Tokyo). Images were recorded digitally using an Olympus C-7070 Wide Zoom digital camera (Olympus Imaging, Tokyo). A data matrix for phylogenetic inference was built from morphological and anatomical data acquired exclusively by us, in order to ensure comparability in terms of measurements and to allow establishing homology between floral parts. Floral macromorphological data were obtained from our stereomicroscopic observations, field observations and macrographs of *Ophrys* specimens taken in the field. Floral micromorphological and anatomical information was based on four sets of data: (1) the results presented by Ascensão *et al.* (2005) for *O. fusca* and *O. lutea*; (2) the results obtained by Francisco & Ascensão (2013) for *O. bombyliflora* and *O. tenthredinifera*; (3) the results for *O. speculum* subsp. *lusitanica* and *O. speculum* subsp. *speculum* that will be published

elsewhere (A. Francisco & L. Ascensão, unpubl. manuscript); and (4) the results from the present study for *O. scolopax* (see Figs. S3–S6).

For the micromorphological and anatomical characterization of the labellum of *O. scolopax*, flowers at three developmental stages were examined: (1) early bud – buds of 5 x 3 to 8 x 4 mm (length x width), corresponding to 6–11 days before the anthesis; (2) late bud – buds of 8 x 5 to 10 x 8 mm (length x width), corresponding to 1–5 days before the anthesis; (3) freshly opened flower – flowers at the beginning of anthesis. Four open flowers were prepared for scanning electron microscopy, and three flowers in each developmental stage (early bud, late bud and opened flower) were fixed and prepared for the anatomical study under light microscopy, following the procedures described in detail for other *Ophrys* spp. by Francisco & Ascensão (2013). Scanning electron micrographs were recorded on Kodak T-Max 100 professional black-and-white negative film with a MAMIYA 6 x 7 camera coupled with a JEOL T220 scanning electron microscope (JEOL, Tokyo). Light micrographs were obtained digitally with a Leica DFC-420 camera (Leica Microsystems, Heerbrugg, Switzerland) coupled with a Leica DM-2500 microscope (Leica Microsystems, Wetzlar, Germany). Two open flowers were also cleared to allow observing the vasculature of the labellum, two late buds and six freshly opened flowers were immersed in diluted neutral red to indicate the osmophore location and fresh flowers were used for the histochemical characterization of the osmophore, following the procedures reported by Francisco & Ascensão (2013). Additionally, a vanillin–hydrochloric acid test (Gardner, 1975) was used for detection of condensed tannins in historesin sections of flowers.

CHARACTER SELECTION AND CODING

For building the data matrix, explicit and objective criteria were adopted for character selection and state definition, following Wiens (2001) and Sereno (2007). We selected 45 morphological and anatomical floral characters for all seven *Ophrys* taxa according to the following cumulative criteria: (1) their potential for distinguishing taxa across the genus *Ophrys*; (2) the stability of their states among individuals from the same taxon; (3) the feasibility of associated observations; and (4) their independence from each other (Emerson & Hastings, 1998; Sereno, 2007). Out of the 45 characters, one is concerned with the dorsal sepal, four with the lateral petals, one with the gynostemium, six with the stigmatic cavity and 33 with the labellum (Table 1). The stigmatic cavity was defined as the generally concave region in the *Ophrys* flower placed below the gynostemium and contiguous with the basal region of the labellum, which exhibits the stigmatic surface in its upper portion (Devillers & Devillers-Terschuren, 1994; Francisco & Ascensão, 2013). We considered the distal boundary of the stigmatic cavity as being defined by the contrasting epidermal cell type occurring in the adjacent central area of the labellum (typically the basal field). In particular, the stigmatic cavity is always glabrous and mostly composed of flat to lenticular

epidermal cells, whereas the basal field of the labellum has an indumentum consisting of diverse types of trichomes (Francisco & Ascensão, 2013; A. Francisco & L. Ascensão, unpubl. manuscript; present study). In order to accommodate the great amount of information provided by the labellum, we subdivided its characters into four main regions according to their positioning (see Fig. S2), namely: nine characters of the basal region of the labellum, six of the lateral labellum lobes, seven of the speculum, and 11 of the apical region of the labellum (Table 1). The 45 selected characters comprised 18 macromorphological structural characters related to the presence, orientation, position, shape, prominence and extent of floral organs or parts of organs (Fig. 1, see also Figs. S1, S2), 20 micromorphological characters pertaining to the cell types occurring in the different regions of the labellum (see Figs. S3, S7) and seven anatomical characters relative to the osmophore (see Figs. S4, S5C).

This character set is composed of 21 binary (presence-absence), 11 qualitative (non-ordered), and 13 continuous quantitative characters (Table 1). Continuous characters are multistate characters and were expressed in a 0–1 scale in order to allow equal weighting for all types of characters. Of the 13 continuous characters, two correspond to real measurements (characters 17 and 31) and were range-standardized to 0–1, whereas the other 11 describe a given property (e.g. orientation, position, prominence, abundance or extent) of a floral element or organ, by empirically estimating its expression within the observed range. Recognizing certain characters as continuous variables was the simplest assumption about evolutionary change we could make, given the pattern of gradual transition from one character state to another in an ordered manner that we observed for these characters across the *Ophrys* taxa ('transformational pattern'; Sereno, 2007).

PHYLOGENETIC INFERENCE ANALYSES

Phylogenetic analyses were carried out on a morpho-anatomical data matrix consisting of six ingroup *Ophrys* taxa plus an outgroup species (*O. scolopax*), each scored for the 45 characters mentioned above and described in Table 1. Phylogenetic reconstruction was inferred using the methods of maximum parsimony and Bayesian inference.

Maximum parsimony

Maximum parsimony (MP) analyses were conducted in the T.N.T. – Tree Analysis Using New Technology software program, version 1.1 (TNT; Goloboff, Farris & Nixon, 2008). A continuous approach to the data matrix was adopted, in which the 21 binary and the 11 qualitative characters were treated as discrete (numeric) and non-ordered (non-additive) variables and the 13 quantitative continuous characters were treated as continuous variables (Farris, 1970; Goloboff, Mattoni & Quinteros, 2006), in order to improve the accuracy of their states (Wiens, 2001). The scores or codes assigned to the states of each character are provided in Table 1.

All MP analyses were performed using the exhaustive search method (implicit enumeration algorithm; Hendy & Penny, 1982). Two different weighting scenarios based on assumptions about character change rates were applied to characters, one assuming equal weights for all characters and the second using the following prior weights (Table 1): 1 was given to characters related to cells (i.e. all the 27 micromorphological and anatomical characters), based on the assumption that their states change with relative ease along evolutionary time; 2 was assigned to structural characters requiring a specific morphogenesis (16 macromorphological characters); and 3 was given to structural characters requiring a specific morphogenesis that pertain to complex floral structures, such as the gynostemium apex and the apical appendix (two characters), presumably difficult to acquire along evolutionary time. The set of suboptimal trees corresponding to the 5% shortest trees was obtained with three extra steps for the MP analysis under equal character weighting and with four extra steps for that under differential character weighting.

For each tree obtained, group support was assessed by calculating the decay index value (Bremer support; Bremer, 1994) and the percentage obtained from the standard bootstrapping resampling method (Felsenstein, 1985). Bootstrap support was based on 10 000 pseudoreplicates using the exhaustive search method and was measured as the absolute group frequency. To assess homoplasy, the consistency index (CI) and the retention index (RI; Farris, 1989) were computed for every tree. Before computing bootstrap support and CI, the four parsimony-uninformative characters (4, 14, 35, 41; Table 1) were excluded from the data matrix (Carpenter, 1996). In addition, CI and RI were computed for each character in every tree using the CharStats.run macro (Ramírez, 2012), and these CI values were subsequently used to indicate the strong homoplasious characters, which we considered to be those characters with a CI < 0.5.

Additionally, similar MP analyses were performed using a discrete approach to the data matrix in order to be comparable with the results from Bayesian inference analyses, as the software used for the latter is unable to treat continuous characters as such. In the discrete approach, all characters were treated as discrete variables, the 13 quantitative continuous characters being treated as ordered (additive). The continuous characters had to be reclassified accordingly: their states were kept ordered but became scored in a rank (i.e. only their relative positions have significance, not the real distances between them, as occurs in the continuous approach). The score or code assigned to each character state in the discrete approach is provided in Table 1.

From the MP analyses, ancestral character states (i.e. plesiomorphies) were inferred for the presumed most recent common ancestor of all six closely related *Ophrys* taxa investigated and synapomorphies (i.e. derived character states shared by all elements of a group) were reconstructed for each node of every tree.

Bayesian inference

Bayesian inference analyses were performed using the software program MrBayes version 3.2.2 (Ronquist & Huelsenbeck, 2003; Ronquist *et al.*, 2012). The discrete approach to the morpho-anatomical data matrix was adopted, in which all characters were treated as discrete variables, the 13 continuous characters being treated as ordered (Table 1). The model used by MrBayes for morphological (standard) discrete data is based on the Markov k model by Lewis (2001). The state frequencies (and state substitution rates) were allowed to vary over characters according to a symmetric Dirichlet distribution (for multistate characters) or to a beta distribution (for binary characters) with a fixed value in the infinity, in order to achieve equal state frequencies for all characters in the data matrix. To evaluate the influence of character weighting, the prior parameter specifying rate variation across characters was set to either equal (i.e. all characters evolve at the same rate, which is measured in expected state changes per character over the tree) or following a gamma distribution. In the latter scenario, the variation rates were allowed to differ over characters according to a gamma distribution, which was approximated using four rate categories and with its α (shape) parameter set to uniform (varying between 0.001–200), in order to allow the gamma distribution to acquire alternative shapes with equal probability across generations. For each weighting approach, two independent Bayesian Markov Chain Monte Carlo (MCMC) runs were performed, each for 1.5 million generations with four chains, initiated with a random starting tree, and sampled every 100 generations. The first 25% of the sampled trees of each run were excluded as 'burn-in' from the final set of trees used to determine the distribution of the posterior probabilities. To assess MCMC convergence rates, the average standard deviation of split frequencies (ASDSF; Lakner *et al.*, 2008) and the potential scale reduction factor (PSRF; Gelman & Rubin, 1992) for branch lengths and model parameters were recorded (Ronquist *et al.*, 2012).

RESULTS

PHYLOGENETIC RECONSTRUCTION OF THE *OPHRYS* CLADE

The phylogenetic trees obtained by the two alternative methods of inference (MP and Bayesian) of the relationships in our clade of interest were congruent in terms of recovering two strongly supported *Ophrys* groups, namely the group formed by *O. fusca* and *O. lutea* (bootstrap percentage 100, decay value > 16, posterior probability 100) and the group composed of the two subspecies of *O. speculum* (bootstrap percentage 100, decay value > 8, posterior probability 100; Fig. 2). However, these trees differ in the overall topology, since besides those two unequivocal associations they also recognized radically different groups of taxa in two other tree nodes (key nodes A and B in Fig. 2), which appeared consistently with weak to moderate support (Fig. 2).

Table 1. Morpho-anatomical floral characters and their respective states for the six closely related *Ophrys* taxa and the selected outgroup (*Ophrys scolopax*) used in the phylogenetic analyses. Under each character state, the scores or codes used in the continuous (left) and discrete (right) approaches are provided. The 13 continuous characters that were reclassified in the discrete approach (see main text for details) are in bold type. Parsimony-uninformative characters are typed in italic. Figures illustrating each character (Fig.), character types (T), and character weights (W) are provided. Character types comprise binary (B), continuous (C), and qualitative (Q) characters. For characters 22–25 and 35, we considered: (a) flat-lenticular cells as cells that did not protrude from the surface; (b) domed-papillae as rounded protruding cells, either hemispherical or slightly flattened; (c) attenuate trichomes as long protruding cells gradually tapering to a rounded tip; and (d) contorted trichomes as long protruding cells, irregularly sinuate or bent. Cell height classes of characters 14–16 and 27–30 were defined by running a k-means clustering on the height measurements of non-flat epidermal cells occurring in both the basal field (14–16) and the speculum (27–30). These measurements (see Supporting Information, Fig. S7) were taken manually on the scanning electron micrographs. The most adequate number of k-means classes was visually assessed by seeking the best adjustment between the cell height histogram and the class boundaries. Median was used in characters 17 and 31 (instead of the mean) to reduce the influence of extreme points.

Fig.	W	T	Nr	Character	*Ophrys speculum* subsp. *speculum*	*Ophrys speculum* subsp. *lusitanica*	*Ophrys bombyliflora*	*Ophrys tenthredinifera*	*Ophrys fusca* subsp. *fusca*	*Ophrys lutea*	*Ophrys scolopax*
				Dorsal sepal							
1, S1	2	Q	0	dorsal sepal insertion angle (in relation to floral axis)	< 90º 0 / 0	< 90º 0 / 0	~ 90º 1 / 1	~ 90º 1 / 1	< 90º 0 / 0	< 90º 0 / 0	~ 90º 1 / 1
				Lateral petals							
1, S1, S2	2	C	**1**	**petals orientation**	strongly recurved 1.0 / 3	strongly recurved 1.0 / 3	slightly recurved 0.6 / 2	slightly recurved 0.6 / 2	slightly incurved 0.0 / 0	slightly incurved 0.0 / 0	straight 0.3 / 1
1, S1, S2	2	Q	2	petals apex shape	acute 0 / 0	acute 0 / 0	acute 0 / 0	acute 0 / 0	obtuse/ truncate 1 / 1	obtuse/ truncate 1 / 1	acute 0 / 0
1	1	B	3	petals adaxial surface pilosity	pilose 1 / 1	pilose 1 / 1	pilose 1 / 1	pilose 1 / 1	(sub-) glabrous 0 / 0	(sub-) glabrous 0 / 0	pilose 1 / 1
				Gynostemium							
1, S2	3	Q	*4*	*gynostemium apex shape*	obtuse 1 / 1	obtuse 1 / 1	obtuse 1 / 1	obtuse 1 / 1	obtuse 1 / 1	obtuse 1 / 1	acute 0 / 0

				Stigmatic cavity							
1, S3A	2	C	**5**	**floor position**	elevated 1.0 / 2	elevated 1.0 / 2	intermediate 0.6 / 1	elevated 1.0 / 2	in a depression 0.0 / 0	in a depression 0.0 / 0	elevated 1.0 / 2
1	2	C	**6**	**walls (inferior portion) height**	high 1.0 / 2	high 1.0 / 2	high 1.0 / 2	low 0.5 / 1	null 0.0 / 0	null 0.0 / 0	null 0.0 / 0
1, S3A	2	C	**7**	**internal labia prominence**	prominent 0.9 / 2	prominent 1.0 / 2	prominent 0.8 / 2	prominent 0.6 / 2	absent 0.0 / 0	absent 0.0 / 0	reduced to callosities 0.2 / 1
1	2	C	**8**	**external labia prominence**	prominent 1.0 / 2	prominent 1.0 / 2	prominent 0.7 / 2	vestigial 0.3 / 1	absent 0.0 / 0	absent 0.0 / 0	absent 0.0 / 0
1	2	C	**9**	**temporal callosities conspicuousness**	conspicuous 1.0 / 2	conspicuous 1.0 / 2	conspicuous 0.8 / 2	conspicuous 0.6 / 2	absent 0.0 / 0	absent 0.0 / 0	vestigial 0.2 / 1
1	2	C	**10**	**staminodial points conspicuousness**	differentiated into callosities 1.0 / 3	differentiated into callosities 1.0 / 3	differentiated into callosities 0.8 / 3	inconspicuous 0.2 / 1	absent 0.0 / 0	absent 0.0 / 0	visible 0.4 / 2
				Basal region of labellum							
1, S2	1	Q	11	basal field differentiation	evident 1 / 1	evident 1 / 1	evident 1 / 1	evident 1 / 1	undefined 0 / 0	undefined 0 / 0	evident 1 / 1
1	2	Q	12	basal field position (in relation to stigmatic cavity)	internal (confined) 1 / 1	internal (confined) 1 / 1	external 0 / 0	external 0 / 0	external 0 / 0	external 0 / 0	external 0 / 0
1, S2	2	B	13	presence of basal groove	absent 0 / 0	absent 0 / 0	absent 0 / 0	absent 0 / 0	present 1 / 1	present 1 / 1	absent 0 / 0
S3A, C	1	B	*14*	*presence of short-intermediate trichomes (< 95 µm in height)*	present 1 / 1	present 1 / 1	present 1 / 1	present 1 / 1	absent 0 / 0	present 1 / 1	present 1 / 1
--	1	B	15	presence of long trichomes (95-190 µm in height)	present 1 / 1	present 1 / 1	absent 0 / 0	absent 0 / 0	present 1 / 1	present 1 / 1	absent 0 / 0
--	1	B	16	presence of very long trichomes (> 190 µm in height)	absent 0 / 0	absent 0 / 0	absent 0 / 0	absent 0 / 0	present 1 / 1	present 1 / 1	absent 0 / 0
S3A, C	1	C	**17**	**median cell height ***	117.65 µm 0.51 / 1	125.00 µm 0.57 / 1	58.82 µm 0.07 / 0	70.83 µm 0.16 / 0	181.62 µm 1.00 / 1	123.53 µm 0.56 / 1	50.00 µm 0.00 / 0
1	2	B	18	presence of divergent crests and grooves	present 1 / 1	present 1 / 1	absent 0 / 0	absent 0 / 0	absent 0 / 0	absent 0 / 0	absent 0 / 0

1	2	B	19	presence of basal longitudinal crests	absent 0 / 0	absent 0 / 0	absent 0 / 0	absent 0 / 0	present 1 / 1	present 1 / 1	absent 0 / 0
				Lateral labellum lobes							
1, S1, S2	2	C	**20**	**lateral lobes prominence**	flat 0.0 / 0	flat 0.0 / 0	highly prominent 1.0 / 2	moderately prominent 0.7 / 1	flat 0.0 / 0	flat 0.0 / 0	highly prominent 1.0 / 2
1, S1, S5A	1	Q	21	indumentum extent	narrow 0 / 0	narrow 0 / 0	wide 1 / 1	wide 1 / 1	wide 1 / 1	narrow 0 / 0	wide 1 / 1
S3E	1	B	22	presence of flat-lenticular cells	present 1 / 1	present 1 / 1	present 1 / 1	absent 0 / 0	absent 0 / 0	absent 0 / 0	present 1 / 1
--	1	B	23	presence of domed papillae	absent 0 / 0	absent 0 / 0	absent 0 / 0	absent 0 / 0	present 1 / 1	present 1 / 1	absent 0 / 0
--	1	B	24	presence of attenuate trichomes	absent 0 / 0	absent 0 / 0	absent 0 / 0	absent 0 / 0	present 1 / 1	present 1 / 1	absent 0 / 0
S3D	1	B	25	presence of contorted trichomes	present 1 / 1	present 1 / 1	present 1 / 1	present 1 / 1	absent 0 / 0	absent 0 / 0	present 1 / 1
				Speculum							
1, S1, S2	2	Q	26	speculum position	median-apical 1 / 1	median-apical 1 / 1	basal-median 0 / 0	basal-median 0 / 0	basal-median 0 / 0	basal-median 0 / 0	basal-median 0 / 0
--	1	B	27	presence of flat-lenticular cells (≈0 µm in height)	present 1 / 1	present 1 / 1	present 1 / 1	present 1 / 1	absent 0 / 0	absent 0 / 0	absent 0 / 0
S3F, H	1	B	28	presence of papillae (4-20 µm in height)	absent 0 / 0	absent 0 / 0	present 1 / 1	present 1 / 1	absent 0 / 0	absent 0 / 0	present 1 / 1
S3H	1	B	29	presence of short trichomes (21-40 µm in height)	absent 0 / 0	absent 0 / 0	present 1 / 1	present 1 / 1	present 1 / 1	present 1 / 1	present 1 / 1
--	1	B	30	presence of intermediate trichomes (> 40 µm in height)	absent 0 / 0	absent 0 / 0	absent 0 / 0	present 1 / 1	present 1 / 1	present 1 / 1	absent 0 / 0
S3F, H	1	C	**31**	**median non-flat cell height ****	0 µm 0.00 / 0	0 µm 0.00 / 0	8.82 µm 0.19 / 1	27.40 µm 0.59 / 2	37.50 µm 0.81 / 2	46.45 µm 1.00 / 2	17.65 µm 0.38 / 1
S3F, H	1	Q	32	cuticular striations arrangement	parallel arranged striations 1 / 1	parallel arranged striations 1 / 1	radially arranged striations 0 / 0	radially arranged striations 0 / 0	radially arranged striations 0 / 0	radially arranged striations 0 / 0	radially arranged striations 0 / 0

				Apical region of labellum							
S1	1	B	33	presence of submarginal indumentum band	present 1 / 1	present 1 / 1	present 1 / 1	present 1 / 1	absent 0 / 0	absent 0 / 0	present 1 / 1
S2, S5C	1	C	**34**	**glabrous margin extent**	moderate 0.5 / 1	wide 0.7 / 2	wide 0.8 / 2	moderate 0.4 / 1	narrow 0.0 / 0	wide 1.0 / 2	narrow 0.0 / 0
S3K, N	1	Q	*35*	*margin cell type*	domed papillae 1 / 1	domed papillae 1 / 1	flat-lenticular cells 0 / 0	domed papillae 1 / 1	domed papillae 1 / 1	domed papillae 1 / 1	domed papillae 1 / 1
S1, S2	2	B	36	presence of apical notch	present 1 / 1	present 1 / 1	absent 0 / 0	present 1 / 1	present 1 / 1	present 1 / 1	absent 0 / 0
S1, S2, S3L	3	B	37	presence of apical appendix	absent 0 / 0	absent 0 / 0	present 1 / 1	present 1 / 1	absent 0 / 0	absent 0 / 0	present 1 / 1
				Osmophore							
--	1	B	38	osmophore occurrence in lateral petals margin	absent 0 / 0	absent 0 / 0	absent 0 / 0	absent 0 / 0	present 1 / 1	present 1 / 1	absent 0 / 0
S4, S5C	1	C	**39**	**osmophore extent in labellum margin**	apical third 0.5 / 1	apical third 0.5 / 1	apical (only central) 0.0 / 0	apical third 0.5 / 1	full 1.0 / 2	full 1.0 / 2	apical third 0.5 / 1
--	1	B	40	osmophore occurrence in apical labellum surface	absent 0 / 0	absent 0 / 0	absent 0 / 0	present 1 / 1	present 1 / 1	present 1 / 1	absent 0 / 0
S4A-D, H	1	Q	*41*	*abaxial secretory surface extent*	extensive 1 / 1	extensive 1 / 1	limited 0 / 0	extensive 1 / 1	extensive 1 / 1	extensive 1 / 1	extensive 1 / 1
S4B, F, G	1	Q	42	adaxial secretory surface extent	extensive 1 / 1	extensive 1 / 1	extensive 1 / 1	limited 0 / 0	limited 0 / 0	limited 0 / 0	extensive 1 / 1
S4A, B, H	1	B	43	presence of starch in epidermis	absent 0 / 0	absent 0 / 0	absent 0 / 0	absent 0 / 0	present 1 / 1	present 1 / 1	absent 0 / 0
S4A, D, H	1	C	**44**	**abundance of starch in subepidermal parenchyma**	vestigial 0.0 / 0	vestigial 0.0 / 0	abundant 1.0 / 2	abundant 0.8 / 2	rare 0.3 / 1	rare 0.3 / 1	abundant 1.0 / 2

* *Ophrys speculum* subsp. *speculum*: n=39 (4 individuals); *O. speculum* subsp. *lusitanica*: n=30 (3 individuals); *O. bombyliflora*: n=52 (3 individuals); *O. tenthredinifera*: n=33 (3 individuals); *O. fusca* subsp. *fusca*: n=38 (2 individuals); *O. lutea*: n=61 (3 individuals); *O. scolopax*: n=27 (2 individuals).

** *Ophrys speculum* subsp. *speculum*: n=49 (4 individuals); *O. speculum* subsp. *lusitanica*: n=56 (3 individuals); *O. bombyliflora*: n=131 (3 individuals); *O. tenthredinifera*: n=113 (4 individuals); *O. fusca* subsp. *fusca*: n=92 (2 individuals); *O. lutea*: n=72 (2 individuals); *O. scolopax*: n=70 (3 individuals).

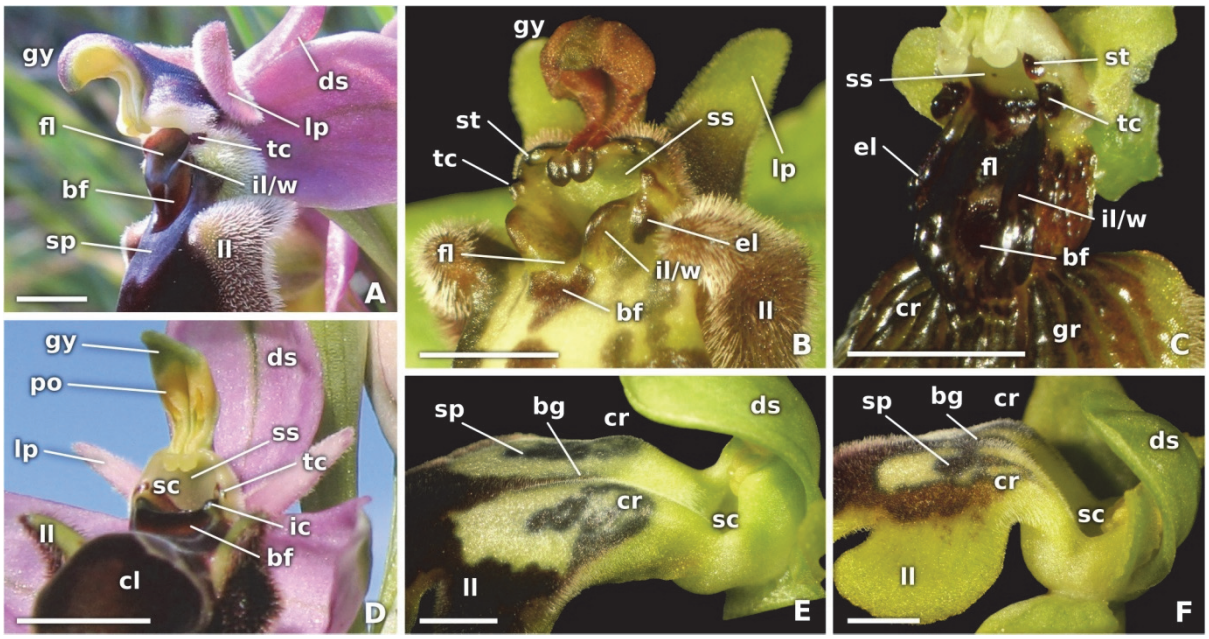

Figure 1. Comparison of the flower structure of *Ophrys* taxa focused on the details of the stigmatic cavity and the basal-median regions of the labellum, illustrating macromorphological characters used for phylogenetic analyses. A, *Ophrys tenthredinifera*. B, *Ophrys bombyliflora*. C, *Ophrys speculum* subsp. *lusitanica*. D, *Ophrys scolopax* (the selected outgroup). E, *Ophrys fusca* subsp. *fusca*. F, *Ophrys lutea*. bf, basal field (11, 12); bg, basal groove (13); cl, central labellum lobe; cr, labellar crest (18, 19); ds, dorsal sepal (0); el, external labium (8); fl, floor of stigmatic cavity (5); gr, labellar groove (18); gy, gynostemium (4); il, internal labium (7); ll, lateral labellum lobe (20, 21); lp, lateral petal (1–3); po, pollinarium; sc, stigmatic cavity (5–10); sp, speculum (26); ss, stigmatic surface; st, staminodial callosity (10); tc, temporal callosity (9); w, wall (inferior portion) of stigmatic cavity (6). Numbers given in brackets correspond to the characters of Table 1. Scale bars: 3 mm.

On the one hand, the two MP analyses using the continuous approach (the core MP analyses hereafter), one performed under equal and the other under unequal character weighting, generated each a single most parsimonious phylogenetic tree with exactly the same topology (tree 1 in Table 2) and nearly the same branch support. The two strongly supported groups of *O. fusca* with *O. lutea* and of subspecies of *O. speculum* were grouped together in node A, and this association was found to constitute the sister group of *O. tenthredinifera* (node B; Fig. 2A, Table 2). The two key nodes were only weakly supported in both MP trees (bootstrap percentages of 52/65 and decay values of 0.7/3.6 for node A, under equal/differential weighting; bootstrap percentages of 61/68 and decay values of 0.7/2.9 for node B, under equal/differential weighting). Similar tree topology and branch support were obtained from the phylogenetic analyses using the neighbour-joining method based on an appropriate distance matrix (see Table S1, Fig. S8).

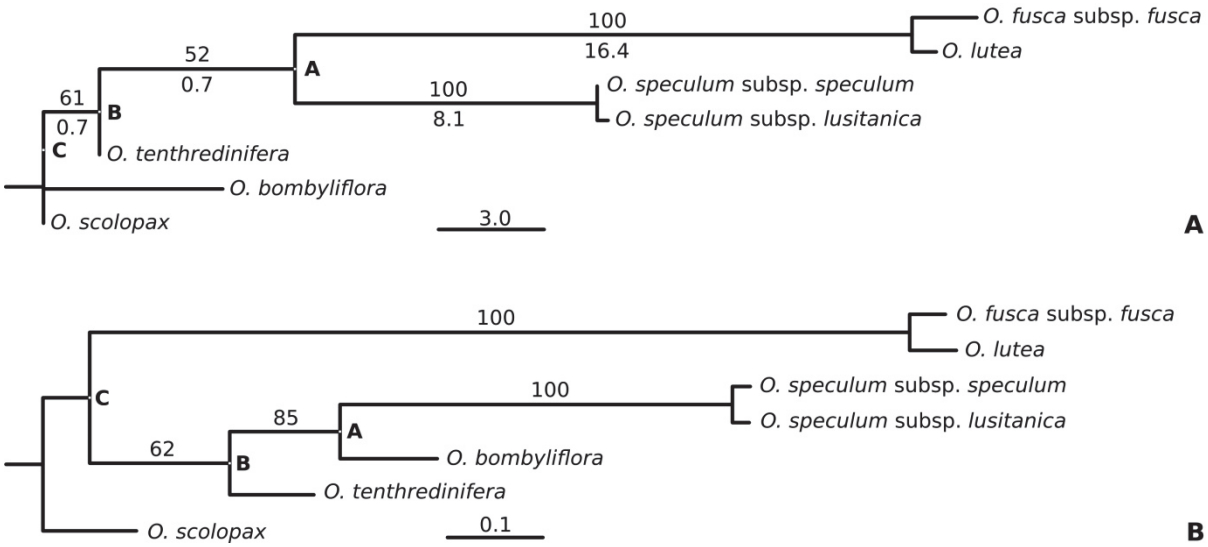

Figure 2. Phylogenetic reconstructions from the data matrix of six closely related *Ophrys* taxa plus one selected outgroup (*Ophrys scolopax*), each scored for 45 morpho-anatomical floral characters. A, The single most parsimonious tree obtained from a parsimony analysis with all characters equally weighted, 13 of which treated as continuous (continuous approach) – tree 1. Bootstrap percentages and decay values are indicated above and below each branch, respectively. B, Fifty-percent majority rule consensus tree obtained from a Bayesian analysis with the 13 continuous characters treated as ordered (discrete approach) and across-character variation rates set to be equal – tree 5. Posterior probability (PP) is indicated above each branch. This analysis also found the association *O. tenthredinifera*–(*O. fusca* subsp. *fusca*–*O. lutea*) with a PP of 34. Key nodes (A and B) and the node representing the presumed most recent common ancestor of taxa that form the ingroup (C) are identified in both trees.

Conversely, the two different Bayesian analyses (assuming equal vs. unequal variation rates across characters) produced each a 50% majority rule consensus tree which recovered consistently the placement of *O. bombyliflora* as sister to the strongly supported group of subspecies of *O. speculum* (node A) with moderate support (posterior probability of 85/71 under equal/unequal across-character variation rates; Fig. 2B; see tree 5 in Table S2). *Ophrys tenthredinifera* was subsequently placed as the sister group of this association (node B) with weak support (posterior probability of 62/49 under equal/unequal across-character variation rates; Fig. 2B, see Table S2). Assuming unequal variation rates across the characters according to a gamma distribution simply decreased the group support of the key nodes A and B, and resulted in the collapse of node B in the consensus tree resulting from this Bayesian analysis (see Table S2). In fact, a contrasting topology (tree 1 vs. tree 5) stands out from the comparison between the Bayesian consensus trees and the most parsimonious tree obtained from the core MP analyses (Table 2, Fig. 2, see also Table S2). However, when the Bayesian consensus trees are compared with the most parsimonious trees obtained from MP analyses under the discrete approach, they mostly agreed on the placement of *O. bombyliflora* as the sister group to the cluster formed by subspecies of *O. speculum* in node A (see Table S2).

Table 2. Most parsimonious and suboptimal trees obtained from the maximum parsimony (MP) analyses under the continuous approach (the core MP analyses) of the morpho-anatomical data matrix of 45 characters for six closely related *Ophrys* taxa (*Ophrys bombyliflora,* OB; *Ophrys fusca* subsp. *fusca,* OF; *Ophrys lutea,* OL; *Ophrys speculum* subsp. *lusitanica,* OSL; *Ophrys speculum* subsp. *speculum,* OSS; and *Ophrys tenthredinifera,* OT) plus one outgroup (*O. scolopax*, which is omitted from trees for the sake of simplicity). Key nodes (A and B) and the node representing the presumed most recent common ancestor of taxa that form the ingroup (C) are identified in selected trees. Consistency index (CI) and retention index (RI) are indicated for each tree. We considered that strongly homoplasious characters are those with CI < 0.5

	Equal character weighting						Unequal character weighting			
	Most parsimonious tree	Suboptimal tree set (5% shortest trees; 3 extra steps)					Most parsimonious tree	Suboptimal tree set (5% shortest trees; 4 extra steps)		
Tree topology (cladogram)	Tree 1 (Fig. 2A) 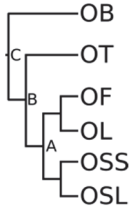	Tree 2 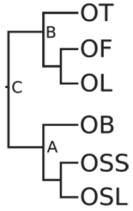	Tree 3 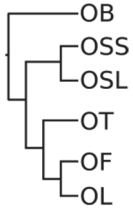	Tree 4 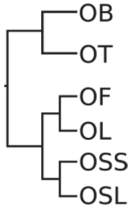	Tree 5 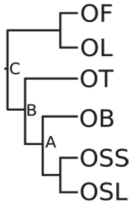	Tree 6 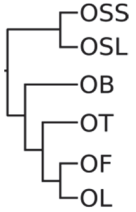	Tree 1 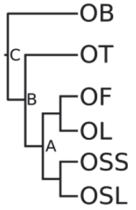	Tree 4 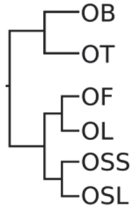	Tree 5 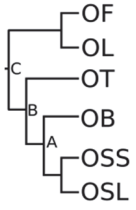	Tree 2 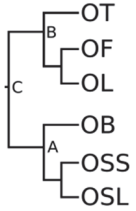
Tree length (steps)	56.76	57.50	57.90	58.35	59.01	59.49	80.96	83.85	84.61	84.80
CI	0.777	0.766	0.761	0.754	0.745	0.739	0.787	0.758	0.751	0.749
RI	0.790	0.777	0.770	0.762	0.750	0.741	0.805	0.770	0.760	0.758
Total nr. of homoplasious characters	16	17	18	19	17	19	26	27	28	27
Nr. of strongly homoplasious characters	1 (char.34)	0	1 (char.34)	1 (char.34)	0	1 (char.34)	9 (chars 1, 5–10, 34, 37)	11 (chars 1, 5–10, 20, 34, 36, 37)	6 (chars 0, 5, 10, 20, 36, 37)	10 (chars 0, 1, 5–9, 20, 36, 37)
Nr. of common homoplasious characters	4 (chars 5, 17, 21, 34)						20 (chars 0–2, 5–10, 12, 13, 17–21, 26, 34, 36, 37)			

Considering the extremely low decay values found for the two key nodes in the most parsimonious trees, the suboptimal tree set corresponding to the 5% shortest trees obtained from each of the core MP analyses was also examined. The suboptimal tree set was composed of five or three trees in the analysis performed under equal or differential character weighting, respectively (Table 2). We found that the tree topology changed considerably with only less than one additional step in the MP analysis under equal weighting. The shortest suboptimal MP tree (tree 2 in Table 2) recognized two clades, one grouping together *O. bombyliflora* and subspecies of *O. speculum* (node A) and the other placing *O. tenthredinifera* as sister to the group of *O. fusca* and *O. lutea* (node B). Furthermore, we observed that the topology of the Bayesian consensus trees was also included in both suboptimal tree sets, being achieved with only 2.25 or 3.65 extra steps (tree 5 in Table 2). Likewise, the examination of the 99% credibility set of trees found during the Bayesian analyses (see Table S3) revealed that, apart from the topology recovered as the 50% majority rule consensus tree, the most likely topology was consistently the one presented by the shortest suboptimal MP tree (tree 2).

Taking into account the entire set of trees obtained from all phylogenetic analyses and all different approaches, we noted that following the two strongly supported nodes (*O. fusca–O. lutea* and subspecies of *O. speculum*), which appeared consistently in all reconstructions, the group recovered more frequently across the trees was that of *O. bombyliflora* placed as sister to the cluster of subspecies of *O. speculum* (Table 2, see also Table S2). Overall, three topologies emerged as the most likely reconstructions, specifically, the topologies presented by the most parsimonious tree (tree 1 in Table 2, Fig. 2A), the shortest suboptimal tree obtained from MP analysis under equal character weighting (tree 2 in Table 2), which also corresponded to the second most likely Bayesian tree (see Table S3), and the Bayesian 50% majority rule consensus tree obtained assuming equal variation rate across characters (tree 5 in Table 2, Fig. 2B). Note that the selected tree topologies correspond precisely to those presented by the three equally most parsimonious trees obtained from MP analyses using the discrete approach under equal character weighting (see Table S2).

Table 3. Reconstruction of the ancestral states of the 45 morpho-anatomical characters for the presumed most recent common ancestor of all the six investigated closely related *Ophrys* taxa (tree node C; Table 2) inferred from the maximum parsimony analyses. The ancestral character states reconstructed from the most parsimonious tree (tree 1) are compared with those inferred from the shortest suboptimal tree obtained under equal character weighting (tree 2) and the suboptimal tree (tree 5) that appeared as the 50% majority rule consensus tree in Bayesian analysis under equal rate variation across characters (see Table 2 for tree topologies). Characters with ambiguous ancestral states are in the lower part of the table. The 24 characters which contain phylogenetic information for all the six *Ophrys* taxa are typed in bold

Character	Tree 1	Tree 2	Tree 5
0 dorsal sepal insertion angle	~ 90°	~ 90°	~ 90°
2 lateral petals apex shape	acute	acute	acute
3 lateral petals adaxial surface pilosity	pilose	pilose	pilose
4 gynostemium apex shape	obtuse	obtuse	obtuse
5 floor position	elevated	elevated	elevated
11 basal field differentiation	evident	evident	evident
12 basal field position	external	external	external
13 basal groove presence	absent	absent	absent
14 basal field short-intermediate trichomes presence	present	present	present
15 basal field long trichomes presence	absent	absent	absent
16 basal field very long trichomes presence	absent	absent	absent
18 basal divergent crests and grooves presence	absent	absent	absent
19 basal longitudinal crests presence	absent	absent	absent
21 lateral labellum lobes indumentum extent	wide	wide	wide
23 lateral labellum lobes domed papillae presence	absent	absent	absent
24 lateral labellum lobes attenuate trichomes presence	absent	absent	absent
25 lateral labellum lobes contorted trichomes presence	present	present	present
26 speculum position	basal-median	basal-median	basal-median
28 speculum papillae presence	present	present	present
29 speculum short trichomes presence	present	present	present
32 speculum cuticular striations arrangement	radially arranged	radially arranged	radially arranged
33 submarginal indumentum band presence	present	present	present
35 margin cell type	domed papillae	domed papillae	domed papillae

37 apical appendix presence	present	present	present
38 osmophore occurrence in lateral petals margin	absent	absent	absent
39 osmophore extent in labellum margin	apical third	apical third	apical third
41 osmophore abaxial secretory surface extent	extensive	extensive	extensive
43 osmophore starch presence in epidermis	absent	absent	absent
44 osmophore starch abundance in subepidermal parenchyma	abundant (1.0)	abundant (0.8-1.0)	abundant (0.8)
1 lateral petals orientation	slightly recurved (0.6)	straight (0.3) or slightly recurved (0.6)	straight (0.3)
6 walls (inferior portion) height	low (0.5)	null (0.0) or low (0.5)	null (0.0)
7 internal labia prominence	prominent (0.6)	reduced to callosities (0.2) or prominent (0.6)	reduced to callosities (0.2)
8 external labia prominence	vestigial (0.3)	absent (0.0) or vestigial (0.3)	absent (0.0)
9 temporal callosities conspicuousness	conspicuous (0.6)	vestigial (0.2) or conspicuous (0.6)	vestigial (0.2)
10 staminodial points conspicuousness	visible (0.4)	visible (0.4)	inconspicuous (0.2) or visible (0.4)
17 basal field median cell height	58.82 µm (0.07)	58.82 µm (0.07) or 70.83 µm (0.16)	70.83 µm (0.16)
20 lateral labellum lobes prominence	highly prominent (1.0)	moderately (0.7) or highly (1.0) prominent	moderately prominent (0.7)
22 lateral labellum lobes flat-lenticular cells presence	present	present	absent or present
27 speculum flat-lenticular cells presence	present	absent or present	absent
30 speculum intermediate trichomes presence	absent	absent	absent or present
31 speculum median non-flat cell height	17.65 µm (0.38)	17.65 µm (0.38)	17.65 µm (0.38) or 27.40 µm (0.59)
34 glabrous margin extent	moderate (0.4-0.5)	moderate (0.4)	narrow (0.0) or moderate (0.4)
36 apical notch presence	absent	absent or present	present
40 osmophore occurrence in apical labellum surface	absent	absent	absent or present
42 osmophore adaxial secretory surface extent	extensive	extensive	limited or extensive

Table 4. Synapomorphies for the two key nodes (A and B) of three selected trees obtained from the maximum parsimony analyses of the data matrix of six closely related *Ophrys* taxa plus one outgroup, each scored for 45 morpho-anatomical floral characters. The trees are the most parsimonious tree (tree 1), the shortest suboptimal tree obtained under equal character weighting (tree 2), and the suboptimal tree (tree 5) that appear as the 50% majority rule consensus tree in the Bayesian analysis under equal variation rate across characters (see Table 2 for tree topologies). Each synapomorphy is identifiable by its respective character number, name, and state, followed by its state score in the case of continuous characters

Tree 1	Tree 2	Tree 5
Node A: **(*O.lutea*-*O.fusca* subsp. *fusca*)-(*O.speculum* subspp.)**	**Node A:** ***O.bombyliflora*-(*O.speculum* subspp.)**	
0 dorsal sepal insertion angle: < 90°		
15 basal field long trichomes presence: present	6 walls (inferior portion) height: high (1.0)	
17 basal field median cell height: 123.53-125.00 µm (0.51-0.56)	8 external labia prominence: prominent (0.7)	
20 lateral labellum lobes prominence: flat (0.0)	10 staminodial points conspicuousness: differentiated into callosities (0.8)	
28 speculum papillae presence: absent	31 speculum median non-flat cell height: 8.82 µm (0.19)	
37 apical appendix presence: absent		
44 osmophore starch abundance in subepidermal parenchyma: rare (0.3)		
Node B: ***O.tenthredinifera*-(*(O.lutea*-*O.fusca* subsp. *fusca*)** **(*O.speculum* subspp.))**	**Node B:** ***O.tenthredinifera*-(*O.lutea*-*O.fusca* subsp. *fusca*)**	**Node B:** ***O.tenthredinifera*-(*O.bombyliflora*(*O.speculum* subspp.))**
20 lateral labellum lobes prominence: moderately prominent (0.7)	10 staminodial points conspicuousness: inconspicuous (0.2)	1 lateral petals orientation: slightly recurved (0.6)
36 apical notch presence: present	22 lateral labellum lobes flat-lenticular cells presence: absent	6 walls (inferior portion) height: low (0.5)
	30 speculum intermediate trichomes presence: present	7 internal labia prominence: prominent (0.6)
	31 speculum median non-flat cell height: 27.4 µm (0.59)	8 external labia prominence: vestigial (0.3)
	40 osmophore occurrence in apical labellum surface: present	9 temporal callosities conspicuousness: conspicuous (0.6)
	42 osmophore adaxial secretory surface extent: limited	27 speculum flat-lenticular cells presence: present

CHARACTER ANALYSIS

Out of the 45 characters of the morpho-anatomical data matrix, 41 were potentially parsimony-informative, representing 91% of the total number of characters, and four (characters 4, 14, 35, 41; Table 1) were found to be autapomorphic (i.e. with a derived character state that is exclusive to a particular taxon) and therefore parsimony-uninformative. Excluding the autapomorphic characters plus the 17 exclusive characters to the taxa grouped in the two strongly supported nodes (those of *O. fusca–O. lutea* and of subspecies of *O. speculum*), we identified 24 characters as providing useful phylogenetic information for all six ingroup *Ophrys* taxa (Table 3).

Parsimony reconstruction of the character states revealed that the three most likely phylogenetic trees (trees 1, 2 and 5; Table 2) agreed about the plesiomorphic state of eight out of the 24 characters inferred for the presumed most recent common ancestor of our clade of interest (node C in trees of Table 2; Table 3). The most notable of these unequivocal plesiomorphies are the presence of a spreading dorsal sepal, an elevated floor in the stigmatic cavity, an apical appendix in the labellum, a speculum provided with papillae (4–21 µm in height), a basal field covered with short-intermediate trichomes (< 95 µm in height) and an osmophore occurring in the apical third of the labellum margin with abundant starch in the subepidermal parenchyma cells (Table 3). In contrast, the other 16 characters present ambiguous plesiomorphic states (Table 3). Likewise, synapomorphies for the key nodes of the trees (nodes A and B) differ according to the tree topology considered (Table 4). As for node A, subspecies of *O. speculum* were placed either as sister to the pair *O. fusca–O. lutea* (in tree 1) or as sister to *O. bombyliflora* (in both tree 2 and tree 5). The former association is supported by seven synapomorphies, of which three are macromorphological and four were micromorphological (Table 4, upper left quarter). On the other hand, the pairing of subspecies of *O. speculum* with *O. bombyliflora* is defined by four synapomorphies mostly concerning the macromorphology of the stigmatic cavity (Table 4, upper right quarter). As for node B, the three different taxa relations that appeared as the most likely always involved *O. tenthredinifera*, which either was placed alternatively as sister to one of the two already mentioned groups found in node A (in tree 1 and tree 5) or formed a group with the pair *O. fusca–O. lutea* alone (in tree 2). Six character states pertaining mostly to the osmophore and the labellum micromorphology supported this latter cluster, whereas another six synapomorphies were reconstructed for the pairing of *O. tenthredinifera* with *O. bombyliflora* – subspecies of *O. speculum*, the most significant being those relative to the stigmatic cavity (Table 4). Lastly, support for *O. tenthredinifera* as sister to the association of the two strongly supported groups of *O. fusca–O. lutea* and subspecies of *O. speculum* reflects mainly their shared presence of an apical notch (Table 4).

Homoplasy affected 36–42% of the characters in the core MP analyses under equal weighting (Table 2). Four characters came out consistently in all MP trees as homoplasious,

i.e. characters that did not fit the tree perfectly inasmuch as some of their states arose independently at least twice on the tree (Felsenstein 2004); specifically, the position of the floor of the stigmatic cavity, the median cell height in the basal field of the labellum, the extent of the indumentum in the lateral labellum lobes and the extent of the glabrous labellum margin, the last being the most homoplasious character in most trees (Table 2). Apart from the most parsimonious tree, the trees that present fewer homoplasious characters were the suboptimal MP trees 2 and 5, which accommodated only one more of these characters than the optimal tree but did not present any strongly homoplasious character (i.e. with a CI < 0.5; Table 2).

DISCUSSION

PHYLOGENETIC RECONSTRUCTION OF THE *OPHRYS* CLADE

The present morphological phylogenetic analysis strongly supports a sister relationship between the two investigated subspecies of *O. speculum* and between *O. fusca* and *O. lutea*, which are the two species representative of section *Pseudophrys* in our study. Since the monophyly of section *Pseudophrys* is well established by molecular evidence (Soliva *et al.*, 2001; Bernardos *et al.*, 2005; Schlüter *et al.*, 2007; Devey *et al.*, 2008), and given the pronounced (micro)morphological similarity found between the taxa belonging to this group (Devillers & Devillers-Terschuren, 1994; Ascensão *et al.*, 2005; Bradshaw *et al.*, 2010), it is reasonable to assume that the phylogenetic placement obtained for the lineage of *O. fusca*–*O. lutea* could be generalized to section *Pseudophrys* as a whole. For the same reason, the placement of the two subspecies of *O. speculum* might likewise be generalized to the so-called *O. speculum* group, which comprises three subspecies that are morphologically similar (Devillers & Devillers-Terschuren, 1994; Delforge, 2005; Devey *et al.*, 2008; Bradshaw *et al.*, 2010; A. Francisco & L. Ascensão, unpubl. manuscript).

For the still unresolved *Ophrys* clade constituted by section *Pseudophrys* and the groups of *O. bombyliflora*, *O. speculum* and *O. tenthredinifera* (Devey *et al.*, 2008) our cladistic analyses found three most likely tree topologies (trees 1, 2 and 5; Table 2, Fig. 2) out of the 15 possible rooted, labelled, bifurcating trees that we could expect to obtain when four operational taxonomic units enter a phylogenetic analysis (Felsenstein, 2004). Although these three phylogenetic trees differ in the taxa that appear grouped in each of the two key nodes (A and B; Tables 2 and 4), all of them concur in that *O. bombyliflora* and *O. tenthredinifera* are not sister groups. Instead, *O. bombyliflora* is most probably placed as sister to *O. speculum*, possibly the most credible relationship found in the present study.

Phylogenetic placement of Ophrys speculum *and* Ophrys bombyliflora

The grouping of *O. speculum* with *O. bombyliflora* appeared in two of the three most plausible phylogenetic topologies that stood out from our analyses and received

consistently a moderate support in the Bayesian consensus trees. This association was also recovered, with comparable levels of support, in the existing molecular trees obtained from the analysis of nuclear ITS data, both separately and in combination with plastid and/or mitochondrial datasets (Bateman *et al.*, 1997; Bateman *et al.*, 2003; Devey *et al.*, 2008; Inda *et al.*, 2012; Vereecken *et al.*, 2012). In contrast, the placement of *O. bombyliflora* as the closest relative of *O. tenthredinifera*, as suggested by the molecular phylogenetic analyses of plastid data alone (Soliva *et al.*, 2001; Devey *et al.*, 2008; Inda *et al.*, 2012), is highly improbable in the light of the present morphological cladistic analysis. Consequently, the present study rejects the previous morphological hypothesis of Devillers & Devillers-Terschuren (1994) in which *O. bombyliflora* was placed in the same group as *O. tenthredinifera* and included in the main assemblage of species of section *Ophrys*, termed *O. bombyliflora–O. fuciflora* (F.W.Schmidt) Moench–*O. sphegodes* Mill., which contained all *Ophrys* spp. apart from those of section *Pseudophrys* and the groups of *O. insectifera* L. and *O. speculum*.

The alternative placement for *O. speculum* was found to be as sister to section *Pseudophrys*, which received only weak support in our most parsimonious trees, obtained using the continuous approach. This grouping was also poorly supported in the plastid tree of Devey *et al.* (2008), the only existing phylogenetic analysis in which it was recovered. The low bootstrap support assigned to the association of *O. speculum–Pseudophrys* indicates that nearly equal proportions of morphological evidence exist in favour and against this relationship (Goloboff *et al.*, 2003). Indeed, comparable low values of bootstrap support were also obtained for the contrasting pairing of *O. speculum–O. bombyliflora* in the trees resulting from the MP analyses under the discrete approach (see Table S2). This fact suggests that a delicate balance seems to occur between the amount of evidence that favours the association *O. speculum–Pseudophrys* and that favouring its alternative, the cluster of *O. speculum–O. bombyliflora*.

However, comparing in detail the morpho-anatomical synapomorphies that confer support for each of these two contrasting scenarios provides a better picture of the most likely associations. We identified seven synapomorphies for the pairing of *O. speculum–Pseudophrys* and four for the grouping of *O. speculum–O. bombyliflora* (Table 4). From these figures we could expect that the former relationship should be more likely than the latter, but in fact the overall evidence provided by the present study points to the opposite. In this judgement, we should take into account: (1) that a mere count of the number of character states in favour and against a particular group may not reflect the amount of evidence that supports the group because of character interaction (Goloboff *et al.*, 2003); and (2) that more importantly than total number, we should critically examine the type of synapomorphies that support each conflicting group and interpret them in the light of the existing knowledge about both character evolution and phylogenetic relationships in the whole genus *Ophrys*.

The pairing of *O. speculum–Pseudophrys* was supported by three out of seven macromorphological synapomorphies, specifically, the presence of an erect dorsal sepal and of flat lateral labellum lobes and the absence of an apical appendix. All these floral features have also evolved in the independent lineage of *O. insectifera* (Devillers & Devillers-Terschuren, 1994; Delforge, 2005; Bradshaw *et al.*, 2010), which was found to either constitute a separate major clade in the genus (Bateman *et al.*, 1997; Devey *et al.*, 2008; Vereecken *et al.*, 2012) or integrate with the other main clade to which our selected outgroup, *O. scolopax*, belongs (Soliva *et al.*, 2001; Inda *et al.*, 2012). These three floral traits are thus homoplasious as they have arisen at least twice in *Ophrys* (Felsenstein, 2004). It is therefore plausible to assume that the loss of the apical appendix and the gain of an erect dorsal sepal and of flat lateral labellum lobes could have evolved on other occasions along the phylogenetic tree and that the link between *O. speculum* and section *Pseudophrys* based on these floral traits could reflect convergence rather than phylogenetic relatedness. The other four synapomorphies shared by these two groups were a scarce amount of starch in the subepidermal parenchyma cells of the osmophore, the occurrence of long trichomes in the basal field, which have a median cell height around 125 μm, and the absence of papillae in the speculum. Although the median cell height in the basal field was found to be strongly homoplasious, the first two characters are unambiguous potential synapomorphies conferring support for this association. Conversely, the shared absence of papillae in the speculum of the pair *O. speculum–Pseudophrys* may raise doubts about the significance of this character state, since it joins two groups with radically different epidermal cell types in the speculum: the former has exclusively flat-lenticular cells, whereas the latter tends to have the longest trichomes within the range observed in this labellum region. As a result, a sister relationship between *O. speculum* and section *Pseudophrys* also seems to be weakly supported in terms of shared derived morphological traits.

Regarding the synapomorphies for the contrasting grouping of *O. speculum–O. bombyliflora*, three out of four pertain to the stigmatic cavity, in particular, the differentiation of staminodial callosities from staminodial points, the occurrence of prominent external labia and the presence of high protrusions of the inferior portion of the cavity walls, the fourth synapomorphy being the low median height of the non-flat cells in the speculum. None of these character states seems to occur in the separate lineage of *O. insectifera* (Devillers & Devillers-Terschuren, 1994; Delforge, 2005; Bradshaw *et al.*, 2010) and all of them are likely to be valid synapomorphies providing support for the link between those groups of species. In this context, the hypothesis of a sister relationship between *O. speculum* and *O. bombyliflora* is better supported in terms of morphological synapomorphies than that supporting the alternative pairing of *O. speculum* with section *Pseudophrys*.

Phylogenetic placement of Ophrys tenthredinifera

The phylogenetic placement of *O. tenthredinifera* is uncertain in the context of the present morphological cladistic analysis, due to the weak support given to all the three alternatives for its position. Our study revealed that *O. tenthredinifera* could be placed as sister to: (1) the pairing of *O. speculum–Pseudophrys* (tree 1); (2) the pairing of *O. speculum–O. bombyliflora* (tree 5); or (3) section *Pseudophrys* alone (tree 2). The second phylogenetic hypothesis agrees with the results from a genome-wide analysis conducted in *Ophrys* (Devey *et al.*, 2008), whereas the third hypothesis closely matches one of the molecular phylogenetic trees obtained for tribe Orchideae by Inda *et al.* (2012), which presented exactly the same topology as our tree 2 for the investigated clade of *Ophrys*. As far as we know, no evidence was found in the literature for the former association. The ambiguous position of *O. tenthredinifera* in the tree for *Ophrys* was also evident in several molecular phylogenetic analyses, where it received similarly weak support (Bateman *et al.*, 1997; Soliva *et al.*, 2001; Bateman *et al.*, 2003; Devey *et al.*, 2008). However, our analyses clearly showed that the sister relationship between *O. tenthredinifera* and *O. bombyliflora* alone, which has been suggested by certain phylogenetic analyses (Devillers & Devillers-Terschuren, 1994; Soliva *et al.*, 2001; Devey *et al.*, 2008; Inda *et al.*, 2012), is extremely unlikely from a morphological point of view, since no synapomorphies were identified for this association. The suborbicular shape of their sepals, who Devillers & Devillers-Terschuren (1994) considered as a floral trait that definitely joins *O. tenthredinifera* and *O. bombyliflora*, is clearly insufficient to justify their phylogenetic proximity. Furthermore, although our distance matrix (see Table S1) shows an overall morphological similarity between these two species, we note that all character states which link them exclusively within the ingroup, such as the presence of apical appendix, papillae in the speculum and abundant starch in the subepidermal parenchyma cells of the osmophore (Francisco & Ascensão, 2013), are also shared with the outgroup taxon (*O. scolopax*), indicating that they are plesiomorphies rather than apomorphies.

The analysis of the synapomorphies supporting each of the three alternatives for the placement of *O. tenthredinifera* showed that only two of these associations present a solid underlying morpho-anatomical basis, namely the grouping of *O. tenthredinifera* with *O. speculum–O. bombyliflora* and that of *O. tenthredinifera* with section *Pseudophrys* alone. Six synapomorphies provide support for each of these two reconstructions, whereas the other association, *O. tenthredinifera* with *O. speculum–Pseudophrys*, is supported by only two synapomorphies, one of them (the presence of an apical notch) being a floral trait also exhibited by the distantly related group of *O. insectifera* (Delforge, 2005; Bradshaw *et al.*, 2010) and the other an intermediate state of a continuous character, in which the concept of synapomorphy must be interpreted with care, due to its dependency on the underlying arbitrary split into discrete states.

Four out of the six synapomorphies that support the cluster of *O. tenthredinifera* with *O. speculum–O. bombyliflora* pertain to the stigmatic cavity, including conspicuous temporal callosities and the extension of the inferior portion of the cavity walls to form prominent internal labia, which are defined as a pair of elongated crests framing the floor on each side (Devillers & Devillers-Terschuren, 1994; Francisco & Ascensão, 2013). Additionally, we recognized here a novel diagnostic feature occurring solely in the stigmatic cavity of this particular cluster, which has not been identified so far: the forward projection of the floor. This floral trait appears to be intimately associated with the extension of the inferior portion of the walls of the stigmatic cavity that results in the formation of the internal labia, and hence it was not included in the phylogenetic analyses to guarantee character independence (Emerson & Hastings, 1998; Sereno, 2007). However, since the floor in the flowers of the outgroup taxon, *O. scolopax*, is clearly not extended, we propose that the presence of a floor projected forward constitute an additional synapomorphy for the cluster formed by *O. tenthredinifera*, *O. speculum* and *O. bombyliflora*. While the occurrence of evident temporal callosities is also shared by the distantly related group of *O. insectifera* (Devillers & Devillers-Terschuren, 1994; Delforge, 2005), the occurrence of prominent internal labia, even though at varying degrees, is a unique synapomorphy for that cluster. Indeed, all the other species that traditionally belong to section *Ophrys*, particularly those of the *O. insectifera* group and the species from the other major clade, i.e. the clade composed of the groups of *O. apifera* Huds., *O. sphegodes*, *O. scolopax*, *O. fuciflora* and *O. umbilicata* Desf. *sensu* Devey *et al.* (2008), seem to exhibit internal callosities instead, which are structures presumably resulting from the reduction of those labia that usually function as pseudoeyes (Devillers & Devillers-Terschuren, 1994; Delforge, 2005).

The other two derived character states shared by the grouping of *O. tenthredinifera* with *O. speculum–O. bombyliflora* were the occurrence of recurved lateral petals and the presence of flat-lenticular epidermal cells in the speculum. The present study corroborates the previous suggestion by Bradshaw *et al.* (2010) that this latter micromorphological feature could constitute a potential synapomorphy for those *Ophrys* taxa. However, contrary to what Bradshaw *et al.* (2010) had found for *O. tenthredinifera*, the predominant cell type in the speculum of this species is not always flat-lenticular cells, but often short, narrow trichomes with flattened bases (Francisco & Ascensão, 2013) roughly similar to those of *O. fusca* and *O. lutea* (Ascensão *et al.*, 2005). This feature was translated into two synapomorphies that favour instead a close relationship between *O. tenthredinifera* and the species in section *Pseudophrys*. Thus, although the occurrence of flat-lenticular cells in the speculum provides support for the close relationship between *O. tenthredinifera*, *O. speculum* and *O. bombyliflora*, the presence of short and intermediate trichomes in the speculum suggests that *O. tenthredinifera* is close to section *Pseudophrys*. This latter relationship is also supported by other four morpho-anatomical synapomorphies, including two features related to the osmophore, notably, the extension of the secretory tissues to

the abaxial surface of the apical region of the labellum (Francisco & Ascensão, 2013). Characters related to the osmophore are presumably good predictors of the phylogenetic relationships, since its secretory cells are apparently not prone to selective pressure by pollinators.

In this context, the nearly equal amount of solid morpho-anatomical evidence in favour of each of the two most supported alternative placements for *O. tenthredinifera* underlies the ambiguity in its position and its 'wild-card' nature in the clade (Rudall, 2002; Goloboff *et al.*, 2003). Accordingly, we conclude that *O. tenthredinifera* most probably constitutes the link taxon between the monophyletic section *Pseudophrys* and the other two taxa of the investigated clade, *O. speculum* and *O. bombyliflora*. The present morphological cladistic analysis points to a close vicinity between these last two species, thus favouring the phylogenetic reconstructions based on nuclear ITS data, alone or combined with datasets of other genomes (Bateman *et al.*, 1997; Bateman *et al.*, 2003; Devey *et al.*, 2008; Inda *et al.*, 2012; Vereecken *et al.*, 2012). However, the hypothesis of hybrid origin, which might be a reason for the phylogenetic conflict between nuclear ITS and plastid DNA-based analyses (Devey *et al.*, 2008), could not be discarded for *O. bombyliflora*, although only improved molecular studies would be able to test such hypothesis.

FLORAL CHARACTER EVOLUTION IN *OPHRYS*

The most parsimonious reconstruction of the ancestral character states for the putative most recent common ancestor of the investigated *Ophrys* clade revealed the evolutionary trend of 29 morphological floral characters for which the plesiomorphic state was found to be unambiguous (Table 3). The ancestral states of the other 16 characters vary according to which phylogenetic hypothesis is considered among the three topologies that have come out as the most likely in the present study. We have argued in the above section that the phylogenetic trees that recovered the grouping of *O. speculum* with *O. bombyliflora* (trees 2 and 5; Table 2) are more plausible reconstructions than the one joining *O. speculum* and section *Pseudophrys* as sister groups. In this context, for the 16 characters with uncertain ancestral state, we have opted to consider as the most plausible plesiomorphic state the one that those trees have in common (Table 3).

Our study revealed that the presence of a gynostemium with an obtuse apex is apparently the only studied floral trait shared by all six taxa of our clade of interest in *Ophrys*. However, an obtuse gynostemium is an ancestral character state in *Ophrys* rather than being a synapomorphy for this clade, as it occurs also in the group of *O. insectifera* (Devillers & Devillers-Terschuren, 1994; Delforge, 2005). An acute gynostemium apex evolved only in the species belonging to the major *Ophrys* clade containing the group of *O. scolopax*, thereby consisting in a unique synapomorphy for all these species (Devillers & Devillers-Terschuren, 1994; Devey *et al.*, 2008; Bradshaw *et al.*, 2010).

The reconstruction of the ancestral states of the stigmatic cavity suggests that the evolution of its morphology in the investigated *Ophrys* clade probably occurred via gradual state transition. For instance, the external labia and the projection of the floor and inferior portion of the walls have probably evolved from a plesiomorphic condition of total absence of these structures towards a derived condition of their maximum conspicuousness, which was achieved in *O. speculum.* Other structures that usually ornament the *Ophrys* stigmatic cavity, namely the internal labia and the temporal callosities, have probably evolved within the clade from an ancestral 'vestigial' state towards two different tendencies, the derived 'null' state (section *Pseudophrys*) and the derived 'prominent' state (*O. tenthredinifera*, *O. speculum* and *O. bombyliflora*).

Regarding labellum characters, the presence of a differentiated basal field is probably the ancestral state from which an undefined basal field subsequently evolved in the lineage of *O. fusca–O. lutea* and, by extension, in the whole of section *Pseudophrys* (Devillers & Devillers-Terschuren, 1994; Ascensão *et al.*, 2005; Bradshaw *et al.*, 2010). In this context, we propose that the basal region of the labellum of *O. fusca–O. lutea* should be considered homologous to the well differentiated basal field of the other *Ophrys* spp., including *O. speculum*, in which the occurrence and position of a basal field have been regarded as controversial (Devillers & Devillers-Terschuren, 1994; Delforge, 2005; Bradshaw *et al.*, 2010). Our most recent study on the labellum micromorphology of *O. speculum* suggests that the flowers of this species also exhibit an evident basal field homologous to that presented by the other *Ophrys* spp., although with some peculiar features (A. Francisco & L. Ascensão, unpubl. manuscript). The present morphological phylogenetic analysis emphasizes that, even though being admittedly difficult to achieve, a correct *a priori* homology assessment of the morphological traits that enter a phylogenetic analysis is crucial to an accurate inference of character evolution based on morphological data (Scotland, Olmstead & Bennett, 2003; Bateman *et al.*, 2006).

As for the epidermal cell types occurring in the adaxial surface of the labellum, our study suggests that the most recent common ancestor of the analysed clade of *Ophrys* had a basal field covered with short-intermediate trichomes, lateral labellum lobes provided with long contorted trichomes (probably accompanied by flat-lenticular cells) and a speculum with papillae and short trichomes. For the speculum of *Ophrys* flowers, which is apparently a major determinant of the success of the pollination mode by sexual deception (Vereecken *et al.*, 2012), two evolutionary trends concerning the epidermal cell height could be inferred from our study. On the one hand, a decrease in the cell height originated flat-lenticular cells (in *O. tenthredinifera*, *O. speculum* and *O. bombyliflora*), a tendency which culminated in a speculum entirely composed of this cell type in *O. speculum* (Bradshaw *et al.*, 2010; Vignolini *et al.*, 2012; A. Francisco & L. Ascensão, unpubl. manuscript). On the other hand, an increase in the cell height gave rise to intermediate trichomes (in *O. tenthredinifera* and *O. fusca–O. lutea*). Both trends have thus evolved in the lineage of *O. tenthredinifera*, a fact

translated into the occurrence of all four different cell types in the speculum of this species, which reinforces its ambiguous position within the clade.

According to the present phylogenetic hypothesis, the plesiomorphic condition in the studied clade of *Ophrys* was the occurrence of an osmophore restricted to the apical third of the labellum margin, which had been either extended to the entire labellum margin in *O. fusca–O. lutea* (Ascensão *et al.*, 2005) or further confined to the apical appendix in *O. bombyliflora* (Francisco & Ascensão, 2013). Also, from a common ancestor exhibiting secretory features in cells occurring in both sides of the labellum, two apomorphic conditions had evolved in the clade, characterized by the nearly complete restriction of the glandular tissues to only one of the surfaces of the labellum (Ascensão *et al.*, 2005; Francisco & Ascensão, 2013). Furthermore, the lineage of *O. fusca–O. lutea* had evolved in a seemingly unique event not only in the genus *Ophrys* but also among the plants provided with osmophores, the occurrence of abundant starch in the secretory epidermal cells (Vogel, 1990; Ascensão *et al.*, 2005), which derived from the plesiomorphic condition of starch accumulation solely in the subepidermal cells. The occurrence of an osmophore appears to be prevalent in subtribe Orchidinae as it was also described in the genera *Himantoglossum* Spreng., *Platanthera* Rich., *Gymnadenia* R.Br. and *Serapias* L. (Vogel, 1990; Stpiczyńska, 2001; Barone Lumaga *et al.*, 2012). However, the homology between the osmophores occurring in these genera and in *Ophrys* should be assessed so that the evolutionary history of the osmophore features across the subtribe could be inferred.

Additionally, our results also suggested that the evolution of certain macromorphological floral characters in the studied clade of *Ophrys* reflects convergence. For instance, the loss of the apical appendix, the modification of the insertion angle that turned the dorsal sepal erect and the change to flat lateral labellum lobes are all apomorphic states which, according to our hypothesis, evolved at least twice independently within this clade, once in *O. speculum* and once in section *Pseudophrys*. All these features are also present in at least one more group of *Ophrys* spp., namely in the *O. insectifera* group (Devillers & Devillers-Terschuren, 1994; Delforge, 2005). Regarding the apical appendix in particular, we note that this is potentially one of the floral traits most liable to be under pollinator-mediated selection, since it is an evident visual and tactile stimulus for male *Eucera* bees performing a cephalic pseudocopulation with *Ophrys* spp. such as *O. tenthredinifera*, *O. bombyliflora* and *O. scolopax* (Kullenberg, 1961; Ågren *et al.*, 1984; Francisco & Ascensão, 2013). The occurrence of an apical appendix in the labellum is, according to our study, the plesiomorphic condition in the clade of interest. However, whether an apical appendix had already been present in the most recent common ancestor of the genus *Ophrys*, playing perhaps an important role in the establishment of the sexually deceptive pollination since its inception remains to be investigated. Only through the addition to the morphological data matrix of information on species of the *O. insectifera* group this issue could be clarified.

LIMITATIONS AND FUTURE DIRECTIONS

An important limitation of our study is the relatively low number of taxa that was sampled per group. This calls for caution when generalizing our conclusions pertaining to the six ingroup taxa, taken as representative, to the whole groups to which they belong, although we believe that the taxa in each group are sufficiently similar to each other to yield the same results in our analysis. In this context, an increase in the taxon sampling is also required in order to fully resolve the phylogenetics relationships in the investigated clade, particularly the still uncertain position of *O. tenthredinifera*. The inclusion of additional taxa of section *Pseudophrys* and of taxa closely related to *O. tenthredinifera* (Delforge, 2005) in the sampled set of the ingroup would especially aid in this purpose. Furthermore, given the great diversity of species included in the other major clade of *Ophrys* to which our selected outgroup belongs, which is composed of five morphologically and genetically distinct groups (*O. apifera*, *O. sphegodes*, *O. scolopax*, *O. fuciflora* and *O. umbilicata* groups *sensu* Devey *et al.*, 2008), it would be important to use a solid morpho-anatomical data matrix like the one presented here as the basis for an expanded morphological cladistic analysis of the whole genus *Ophrys*, integrating data not only from the most representative taxa of each of those groups but also from the *O. insectifera* group. In fact, the phylogenetic placement of *O. insectifera* is still uncertain and weakly supported in previous molecular phylogenetic analyses, being placed either as basally divergent in the genus (Bateman *et al.*, 1997; Devey *et al.*, 2008; Vereecken *et al.*, 2012) or as sister to the major *Ophrys* clade mentioned above (Soliva *et al.*, 2001; Inda *et al.*, 2012). Therefore, such a comprehensive morphological phylogenetic study would help not only clarify the position of *O. insectifera* and *O. tenthredinifera* in the global phylogenetic analysis of the genus but also reconstruct the ancestral character states for the most recent common ancestor of *Ophrys*, hence improving our understanding about the floral trait evolution in this sexually deceptive orchid genus. Ideally, the new morphological data set should be integrated with enhanced molecular data so that an increasing accurate view of the phylogenetic relationships between *Ophrys* spp. could be achieved (Bateman *et al.*, 2006).

CONCLUSIONS

The present morphological phylogenetic analysis sheds some light on the still unresolved interrelationships in the investigated clade of *Ophrys*. According to our cladistic analyses: (1) *O. bombyliflora* and *O. tenthredinifera* are not sister groups; (2) *O. bombyliflora* is most likely the closest relative of *O. speculum*, a finding that favours the existing molecular phylogenetic hypothesis based on nuclear ITS data (alone or combined) but not that based exclusively on plastid data; (3) *O. tenthredinifera* is a ‘wild-card’ species with ambiguous placement which shares different morpho-anatomical character states with section *Pseudophrys* and *O. speculum–O. bombyliflora*; (4) the most solid synapomorphies

that support the groups of taxa found were provided by macromorphological characters from the stigmatic cavity, micromorphological characters from the speculum and anatomical characters pertaining to the osmophore; and (5) the novel diagnostic floral trait which was recognized here for the first time, the forward projection of the floor of the stigmatic cavity, was an important feature shared by *O. tenthredinifera*, *O. speculum* and *O. bombyliflora*. Even considering that it was deliberately focused on only certain *Ophrys* spp., our study represents a significant advance over the single morphological cladistic analysis conducted hitherto in the genus, since our underlying data matrix was built using explicit and objective criteria concerning character selection, coding and state definition.

ACKNOWLEDGEMENTS

We are grateful to I. Duarte (Radboud University Nijmegen, the Netherlands) for advice on phylogenetic methodology and for critically reading the manuscript. We thank R. Magno for valuable discussions and E. Carmo-Silva for providing seven photographs of *Ophrys* in the field (Figs. 1A, D, S1A, B, D, S2B and S5A). We also thank Prof. C. Cruz and Prof. O. Correia (University of Lisbon) for lending us their digital camera for stereomicroscopic image capture. We are grateful to C. Tauleigne Gomes for advice on taxonomic nomenclature and to two anonymous reviewers for helpful comments on the manuscript. The Willi Hennig Society is acknowledged for subsidizing the program TNT and making it freely available. This work was supported by Portuguese funds from Fundação para a Ciência e a Tecnologia (FCT) through the grants SFRH/BD/18823/2004 to A.F. and SFRH/BPD/97025/2013 to M.P., and through the research contracts PEst-OE/EQB/LA0023/2011 and PEst-UID/AMB/50017/2013.

REFERENCES

Ågren L, Kullenberg B, Sensenbaugh T. 1984. Congruences in pilosity between three species of *Ophrys* (Orchidaceae) and their hymenopteran pollinators. *Nova Acta Regiae Societatis Scientiarum Upsaliensis, Serie V:C* **3:** 15-25.

Aldasoro JJ, Sáez L. 2005. *Ophrys* L. In: Aedo C, Herrero A, eds. *Flora Iberica: plantas vasculares da la Península Ibérica e Islas Baleares, Vol. XXI.* Madrid: Real Jardín Botánico, CSIC, 165-195.

APG III. 2009. An update of the Angiosperm Phylogeny Group classification for the orders and families of flowering plants: APG III. *Botanical Journal of the Linnean Society* **161:** 105-121.

Ascensão L, Francisco A, Cotrim H, Pais MS. 2005. Comparative structure of the labellum in *Ophrys fusca* and *O. lutea* (Orchidaceae). *American Journal of Botany* **92:** 1059-1067.

Ayasse M, Stökl J, Francke W. 2011. Chemical ecology and pollinator-driven speciation in sexually deceptive orchids. *Phytochemistry* **72:** 1667-1677.

Barone Lumaga MR, Cozzolino S, Kocyan A. 2006. Exine micromorphology of Orchidinae (Orchidoideae, Orchidaceae): phylogenetic constraints or ecological influences? *Annals of Botany* **98:** 237-244.

Barone Lumaga MR, Pellegrino G, Bellusci F, Perrotta E, Perrotta I, Musacchio A. 2012. Comparative floral micromorphology in four sympatric species of *Serapias* (Orchidaceae). *Botanical Journal of the Linnean Society* **169:** 714-724.

Bateman RM, Pridgeon AM, Chase MW. 1997. Phylogenetics of subtribe Orchidinae (Orchidoideae, Orchidaceae) based on nuclear ITS sequences. 2. Infrageneric relationships and reclassification to achieve monophyly of *Orchis sensu stricto*. *Lindleyana* **12:** 113-141.

Bateman RM, Hollingsworth PM, Preston J, Yi-Bo L, Pridgeon AM, Chase MW. 2003. Molecular phylogenetics and evolution of Orchidinae and selected Habenariinae (Orchidaceae). *Botanical Journal of the Linnean Society* **142:** 1-40.

Bateman RM, Hilton J, Rudall PJ. 2006. Morphological and molecular phylogenetic context of the angiosperms: contrasting the 'top-down' and 'bottom-up' approaches used to infer the likely characteristics of the first flowers. *Journal of Experimental Botany* **57:** 3471-3503.

Bateman RM. 2009. Evolutionary classification of European orchids: the crucial importance of maximising explicit evidence and minimising authoritarian speculation. *Journal Europäischer Orchideen* **41:** 243–318.

Bell AK, Roberts DL, Hawkins JA, Rudall PJ, Box MS, Bateman RM. 2009. Comparative micromorphology of nectariferous and nectarless labellar spurs in selected clades of subtribe Orchidinae (Orchidaceae). *Botanical Journal of the Linnean Society* **160:** 369-387.

Benitez-Vieyra S, Medina AM, Cocucci AA. 2009. Variable selection patterns on the labellum shape of *Geoblasta pennicillata*, a sexually deceptive orchid. *Journal of Evolutionary Biology* **22:** 2354-2362.

Bernardos S, Crespí A, Del Rey F, Amich F. 2005. The section *Pseudophrys* (*Ophrys*, Orchidaceae) in the Iberian Peninsula: a morphometric and molecular analysis. *Botanical Journal of the Linnean Society* **148:** 359-375.

Box MS, Bateman RM, Glover BJ, Rudall PJ. 2008. Floral ontogenetic evidence of repeated speciation via paedomorphosis in subtribe Orchidinae (Orchidaceae). *Botanical Journal of the Linnean Society* **157:** 429-454.

Bradshaw E, Rudall PJ, Devey DS, Thomas MM, Glover BJ, Bateman RM. 2010. Comparative labellum micromorphology of the sexually deceptive temperate orchid genus *Ophrys*: diverse epidermal cell types and multiple origins of structural colour. *Botanical Journal of the Linnean Society* **162:** 504-540.

Bremer K. 1994. Branch support and tree stability. *Cladistics: The International Journal of the Willi Hennig Society* **10:** 295-304.

Cardoso D, de Queiroz LP, de Lima HC, Suganuma E, van den Berg C, Lavin M. 2013. A molecular phylogeny of the vataireoid legumes underscores floral evolvability that is general to many early-branching papilionoid lineages. *American Journal of Botany* **100:** 403-421.

Carpenter JM. 1996. Uninformative bootstrapping. *Cladistics: The International Journal of the Willi Hennig Society* **12:** 177-181.

Chase MW, Soltis DE, Olmstead RG, Morgan D, Les DH, Mishler BD, Duvall MR, Price RA, Hills HG, Qiu Y-L, Kron KA, Rettig JH, Conti E, Palmer JD, Manhart JR, Sytsma KJ, Michaels HJ, Kress WJ, Karol KG, Clark WD, Hédren M, Gaut BS, Jansen RK, Kim K-J, Wimpee CF, Smith JF, Furnier GR, Strauss SH, Xiang Q-Y, Plunkett GM, Soltis PS, Swensen SM, Williams SE, Gadek PA, Quinn CJ, Eguiarte LE, Golenberg E, Learn Jr. GH, Graham SW, Barrett SCH, Dayanandan S, Albert VA. 1993. Phylogenetics of

seed plants: an analysis of nucleotide sequences from the plastid gene *rbc*L. *Annals of the Missouri Botanical Garden* **80:** 528-580.

Chase MW, Williams NH, Faria AD, Neubig KM, Amaral MCE, Whitten WM. 2009. Floral convergence in Oncidiinae (Cymbidieae; Orchidaceae): an expanded concept of *Gomesa* and a new genus *Nohawilliamsia*. *Annals of Botany* **104:** 387-402.

Chin S-w, Lutz S, Wen J, Potter D. 2013. The bitter and the sweet: inference of homology and evolution of leaf glands in *Prunus* (Rosaceae) through anatomy, micromorphology, and ancestral–character state reconstruction. *International Journal of Plant Sciences* **174:** 27-46.

Clennett JCB, Chase MW, Forest F, Maurin O, Wilkin P. 2012. Phylogenetic systematics of *Erythronium* (Liliaceae): morphological and molecular analyses. *Botanical Journal of the Linnean Society* **170:** 504-528.

D'Emerico S, Pignone D, Bartolo G, Pulvirenti S, Terrasi C, Stuto S, Scrugli A. 2005. Karyomorphology, heterochromatin patterns and evolution in the genus *Ophrys* (Orchidaceae). *Botanical Journal of the Linnean Society* **148:** 87-99.

Delforge P. 2005. *Guide des orchidées d'Europe, d'Afrique du Nord et du Proche-Orient.* 3rd ed. Paris: Delachaux et Niestlé.

Devey DS, Bateman RM, Fay MF, Hawkins JA. 2008. Friends or relatives? Phylogenetics and species delimitation in the controversial European orchid genus *Ophrys*. *Annals of Botany* **101:** 385-402.

Devillers P, Devillers-Terschuren J. 1994. Essai d'analyse systématique du genre *Ophrys*. *Les Naturalistes belges* **75 (Orchidées 7):** 273-400.

Dong L-N, Wang H, Wortley AH, Lu L, Li D-Z. 2013. Phylogenetic relationships in the *Pterygiella* complex (Orobanchaceae) inferred from molecular and morphological evidence. *Botanical Journal of the Linnean Society* **171:** 491-507.

Emerson SB, Hastings PA. 1998. Morphological correlations in evolution: consequences for phylogenetic analysis. *The Quarterly Review of Biology* **73:** 141-162.

Endress PK. 2011. Evolutionary diversification of the flowers in angiosperms. *American Journal of Botany* **98:** 370-396.

Farris JS. 1970. Methods for computing Wagner trees. *Systematic Zoology* **19:** 83-92.

Farris JS. 1989. The retention index and the rescaled consistency index. *Cladistics: The International Journal of the Willi Hennig Society* **5:** 417-419.

Felsenstein J. 1985. Confidence limits on phylogenies: an approach using the bootstrap. *Evolution* **39:** 783-791.

Felsenstein J. 2004. *Inferring phylogenies.* Sunderland, Massachusetts: Sinauer Associates, Inc. Publishers.

Francisco A, Ascensão L. 2013. Structure of the osmophore and labellum micromorphology in the sexually deceptive orchids *Ophrys bombyliflora* and *Ophrys tenthredinifera* (Orchidaceae). *International Journal of Plant Sciences* **174:** 619-636.

Freudenstein JV, Rasmussen FN. 1999. What does morphology tell us about orchid relationships? A cladistic analysis. *American Journal of Botany* **86:** 225-248.

Gamarra R, Ortúñez E, Sanz E, Esparza I, Galán P. 2010. Seeds in subtribe Orchidinae (Orchidaceae): the best morphological tool to support molecular analyses. In: Nimis PL, Lebbe RV eds. *Tools for identifying Biodiversity: Progress and Problems. Proceedings of the International Congress. Paris.* EUT - Edizioni Università di Trieste.

Gamarra R, Ortúñez E, Galán Cela P, Guadaño V. 2012. *Anacamptis* versus *Orchis* (Orchidaceae): seed micromorphology and its taxonomic significance. *Plant Systematics and Evolution* **298:** 597-607.

Gardner RO. 1975. Vanillin-hydrochloric acid as a histochemical test for tannin. *Stain Technology* **50:** 315-317.

Gaskett AC. 2011. Orchid pollination by sexual deception: pollinator perspectives. *Biological Reviews* **86:** 33-75.

Gelman A, Rubin D. 1992. Inference from iterative simulation using multiple sequences. *Statistical Science* **7:** 457-472.

Godfery MJ. 1928. Classification of the genus *Ophrys*. *The Journal of Botany, British and Foreign* **66:** 33-36.

Goloboff PA, Farris JS, Källersjö M, Oxelman B, Ramírez MJ, Szumik CA. 2003. Improvements to resampling measures of group support. *Cladistics: The International Journal of the Willi Hennig Society* **19:** 324-332.

Goloboff PA, Mattoni CI, Quinteros AS. 2006. Continuous characters analyzed as such. *Cladistics: The International Journal of the Willi Hennig Society* **22:** 589-601.

Goloboff PA, Farris JS, Nixon KC. 2008. TNT, a free program for phylogenetic analysis. *Cladistics: The International Journal of the Willi Hennig Society* **24:** 774-786.

Górniak M, Paun O, Chase MW. 2010. Phylogenetic relationships within Orchidaceae based on a low-copy nuclear coding gene, *Xdh*: congruence with organellar and nuclear ribosomal DNA results. *Molecular Phylogenetics and Evolution* **56:** 784-795.

Hendy MD, Penny D. 1982. Branch and bound algorithms to determine minimal evolutionary trees. *Mathematical Biosciences* **59:** 277-290.

Inda LA, Pimentel M, Chase MW. 2012. Phylogenetics of tribe Orchideae (Orchidaceae: Orchidoideae) based on combined DNA matrices: inferences regarding timing of diversification and evolution of pollination syndromes. *Annals of Botany* **110:** 71-90.

Kullenberg B. 1961. Studies in *Ophrys* pollination. *Zoologiska Bidrag fran Uppsala* **34:** 1-340.

Lakner C, Van Der Mark P, Huelsenbeck JP, Larget B, Ronquist F. 2008. Efficiency of Markov Chain Monte Carlo tree proposals in Bayesian phylogenetics. *Systematic Biology* **57:** 86-103.

Lewis PO. 2001. A likelihood approach to estimating phylogeny from discrete morphological character data. *Systematic Biology* **50:** 913-925.

Luo Y-B, Chen S-C. 2000. The floral morphology and ontogeny of some Chinese representatives of orchid subtribe Orchidinae. *Botanical Journal of the Linnean Society* **134:** 529-548.

Nürk NM, Blattner FR. 2010. Cladistic analysis of morphological characters in *Hypericum* (Hypericaceae). *Taxon* **59:** 1495-1507.

Paulus HF. 2006. Deceived males - Pollination biology of the Mediterranean orchid genus *Ophrys* (Orchidaceae). *Journal Europäischer Orchideen* **38:** 303-353.

Pedersen HÆ, Faurholdt N. 2007. *Ophrys, the bee orchids of Europe.* Kew, London: Kew Publishing - Royal Botanic Gardens.

Pouyanne M. 1917. La fécondation des *Ophrys* par les insectes. *Bulletin de la Société d'Histoire Naturelle de l'Afrique du nord* **8:** 6-7.

Ramírez M. 2012. Macro CharStats.run, available from https://sites.google.com/site/teosiste/tp/archivos. Posted on 16/02/2012 in 'TNT-Tree Analysis using New Technology' Google Group (https://groups.google.com/forum/?hl=es#!forum/tnt-tree-analysis-using-new-technology). Accessed 02/05/2014.

Ronquist F, Huelsenbeck JP. 2003. MrBayes 3: Bayesian phylogenetic inference under mixed models. *Bioinformatics* **19:** 1572-1574.

Ronquist F, Teslenko M, van der Mark P, Ayres DL, Darling A, Höhna S, Larget B, Liu L, Suchard MA, Huelsenbeck JP. 2012. MrBayes 3.2: efficient Bayesian phylogenetic

inference and model choice across a large model space. *Systematic Biology* **61:** 539-542.

Ronse De Craene LP, Haston E. 2006. The systematic relationships of glucosinolate-producing plants and related families: a cladistic investigation based on morphological and molecular characters. *Botanical Journal of the Linnean Society* **151:** 453-494.

Roque N, Funk VA. 2013. Morphological characters add support for some members of the basal grade of Asteraceae. *Botanical Journal of the Linnean Society* **171:** 568-586.

Rudall P. 2002. Unique floral structures and iterative evolutionary themes in Asparagales: Insights from a morphological cladistic analysis. *The Botanical Review* **68:** 488-509.

Rudall PJ, Bateman RM. 2006. Morphological phylogenetic analysis of Pandanales: testing contrasting hypotheses of floral evolution. *Systematic Botany* **31:** 223-238.

Schiestl FP, Ayasse M, Paulus HF, Löfstedt C, Hansson BS, Ibarra F, Francke W. 1999. Orchid pollination by sexual swindle. *Nature* **399:** 421-422.

Schiestl FP, Schlüter PM. 2009. Floral isolation, specialized pollination, and pollinator behavior in orchids. *Annual Review of Entomology* **54:** 425-446.

Schlüter PM, Kohl G, Stuessy TF, Paulus HF. 2007. A screen of low-copy nuclear genes reveals the *LFY* gene as phylogenetically informative in closely related species of orchids (*Ophrys*). *Taxon* **56** 493-504.

Scotland RW, Olmstead RG, Bennett JR. 2003. Phylogeny reconstruction: the role of morphology. *Systematic Biology* **52:** 539-548.

Sereno PC. 2007. Logical basis for morphological characters in phylogenetics. *Cladistics: The International Journal of the Willi Hennig Society* **23** 565-587.

Servettaz O, Bino Maleci L, Grünanger P. 1994. Labellum micromorphology in the *Ophrys bertolinii* agg. and some related taxa (Orchidaceae). *Plant Systematics and Evolution* **189:** 123-131.

Sokoloff DD, von Mering S, Jacobs SWL, Remizowa MV. 2013. Morphology of *Maundia* supports its isolated phylogenetic position in the early-divergent monocot order Alismatales. *Botanical Journal of the Linnean Society* **173:** 12-45.

Soliva M, Kocyan A, Widmer A. 2001. Molecular phylogenetics of the sexually deceptive orchid genus *Ophrys* (Orchidaceae) based on nuclear and chloroplast DNA sequences. *Molecular Phylogenetics and Evolution* **20:** 78-88.

Soltis DE, Soltis PS, Chase MW, Mort ME, Albach DC, Zanis M, Savolainen V, Hahn WH, Hoot SB, Fay MF, Axtell M, Swensen SM, Prince LM, Kress WJ, Nixon KC, Farris JS. 2000. Angiosperm phylogeny inferred from 18S rDNA, *rbcL*, and *atpB* sequences. *Botanical Journal of the Linnean Society* **133:** 381-461.

Stern WL. 1997. Vegetative anatomy of subtribe Orchidinae (Orchidaceae). *Botanical Journal of the Linnean Society* **124:** 121-136.

Stern WL. 2014. *Anatomy of the Monocotyledons, Volume X: Orchidaceae.* 1st ed. Oxford, UK: Oxford University Press.

Stpiczyńska M. 2001. Osmophores of the fragrant orchid *Gymnadenia conopsea* L. (Orchidaceae). *Acta Societatis Botanicorum Poloniae* **70:** 91-96.

Streinzer M, Paulus HF, Spaethe J. 2009. Floral colour signal increases short-range detectability of a sexually deceptive orchid to its bee pollinator. *The Journal of Experimental Biology* **212:** 1365-1370.

Vereecken NJ, Schiestl FP. 2008. The evolution of imperfect floral mimicry. *Proceedings of the National Academy of Sciences of the United States of America* **105:** 7484-7488.

Vereecken NJ, Wilson CA, Hötling S, Schulz S, Banketov SA, Mardulyn P. 2012. Pre-adaptations and the evolution of pollination by sexual deception: Cope's rule of specialization revisited. *Proceedings of the Royal Society B: Biological Sciences* **279:** 4786-4794.

Vignolini S, Davey MP, Bateman RM, Rudall PJ, Moyroud E, Tratt J, Malmgren S, Steiner U, Glover BJ. 2012. The mirror crack'd: both pigment and structure contribute to the glossy blue appearance of the mirror orchid, *Ophrys speculum*. *New Phytologist* **196:** 1038-1047.

Vogel S. 1990. *The role of scent glands in pollination: on the structure and function of osmophores.* Rotterdam: A. A. Balkema. [English translation of: Vogel S. 1963. Duftdrüsen im Dienste der Bestäubung: Über Bau und Funktion der Osmophoren. *Akademie der Wissenschaften und der Literatur in Mainz, Abhandlungen der Mathematisch-Naturwissenschaftlichen Klasse* **10**: 600-763].

Wagner ST, Isnard S, Rowe NP, Samain M-S, Neinhuis C, Wanke S. 2012. Escaping the lianoid habit: evolution of shrub-like growth forms in *Aristolochia* subgenus *Isotrema* (Aristolochiaceae). *American Journal of Botany* **99:** 1609-1629.

Wiens JJ. 2001. Character analysis in morphological phylogenetics: problems and solutions. *Systematic Biology* **50:** 689-699.

Xu S, Schlüter PM, Schiestl FP. 2012. Pollinator-driven speciation in sexually deceptive orchids. *International Journal of Ecology* **2012, Article ID 285081:** 9 pages. doi:10.1155/2012/285081.

APPENDIX

Taxa examined and their respective herbarium code numbers

Taxon	Herbarium code nr.
Ophrys bombyliflora Link	LISU231243
Ophrys fusca Link subsp. *fusca*	LISU231244
Ophrys lutea Cav.	LISU231505
Ophrys scolopax Cav.	LISU231247
Ophrys speculum Link subsp. *lusitanica* O.Danesch & E.Danesch	LISU231242
Ophrys speculum Link subsp. *speculum*	LISU231246
Ophrys tenthredinifera Willd.	LISU231245

SUPPORTING INFORMATION

Figure S1. Macrographs of *Ophrys* orchids in their natural habitat in Portugal, showing floral macromorphological characters used for phylogenetic analyses.

Figure S2. Macrographs of flowers of *Ophrys lutea* and *Ophrys scolopax*, two species with contrasting floral morphological features belonging to sections *Pseudophrys* and *Ophrys*, respectively, illustrating characters used for phylogenetic analyses.

Figure S3. Scanning electron micrographs of the adaxial surface of the labellum and the stigmatic cavity of *Ophrys scolopax*.

Figure S4. Light micrographs of historesin sections of the labellum of *Ophrys scolopax*, illustrating especially the secretory cells of the osmophore occurring in the apical appendix.

Figure S5. Macrographs of flowers of *Ophrys scolopax* showing the vasculature of the labellum and the areas that appeared stained after immersion in neutral red.

Figure S6. Histochemical characterization of fresh-hand sections of the apical appendix of *Ophrys scolopax*.

Figure S7. Box-plots representing the height of cells in the basal field of the labellum and the height of non-flat cells in the speculum of the labellum of all seven investigated *Ophrys* taxa.

Figure S8. Distance-based phylogenetic tree obtained using the neighbour-joining method.

Table S1. Distance matrix obtained by calculating the Gower distances for each pair of the seven investigated *Ophrys* taxa.

Table S2. Comparison between the results of maximum parsimony analyses under the discrete approach and those of Bayesian analyses for the investigated *Ophrys* taxa.

Table S3. Posterior probability of the trees included in the 99% credibility set of trees found during the Markov Chain Monte Carlo searches of Bayesian analyses.

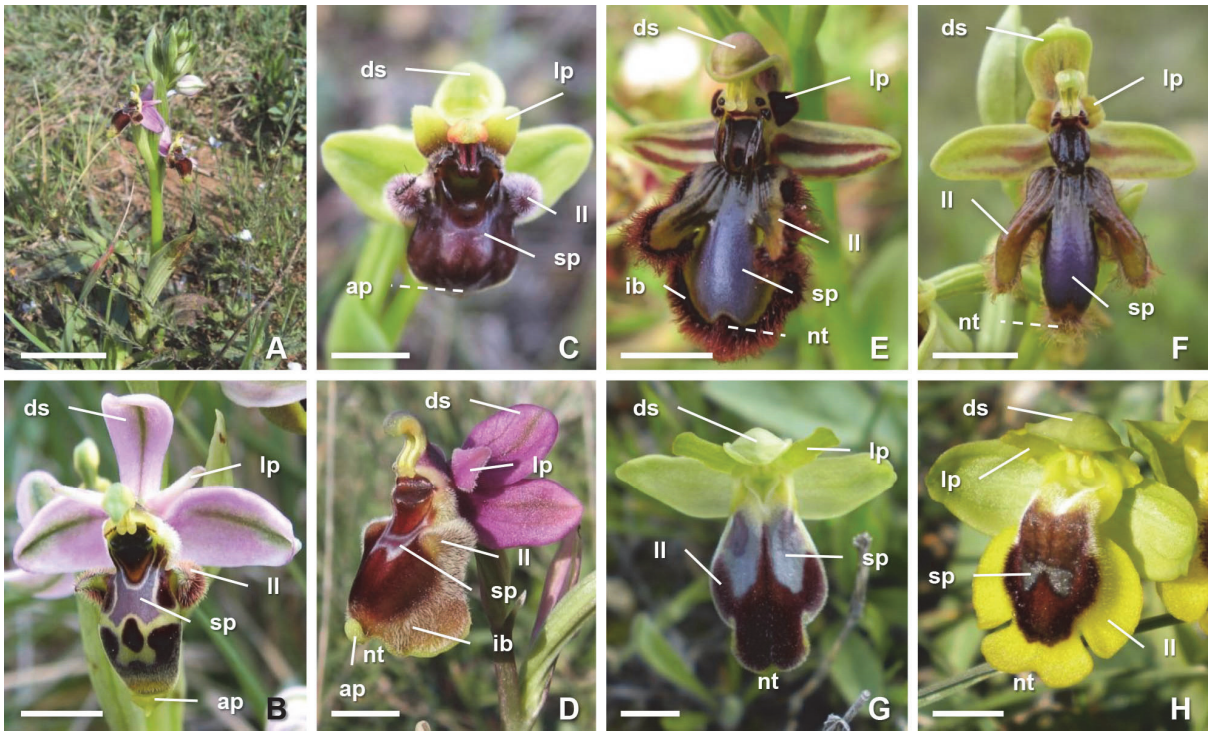

Figure S1. Macrographs of *Ophrys* orchids in their natural habitat in Portugal, showing floral macromorphological characters used for phylogenetic analyses. A, Inflorescence of *Ophrys scolopax*. B–H, Details of *Ophrys* flowers. B, *Ophrys scolopax* (the selected outgroup). C, *Ophrys bombyliflora.* D, *Ophrys tenthredinifera.* E, *Ophrys speculum* subsp. *speculum*. F, *Ophrys speculum* subsp. *lusitanica.* G, *Ophrys fusca* subsp. *fusca.* H, *Ophrys lutea*. ap, apical appendix (37); ds, dorsal sepal (0); ib, submarginal indumentum band (33); ll, lateral labellum lobe (20, 21); lp, lateral petal (1, 2); nt, apical notch (36); sp, speculum (26). Numbers given in brackets correspond to the characters of Table 1. Scale bars: 25 mm (A); 5 mm (B–H).

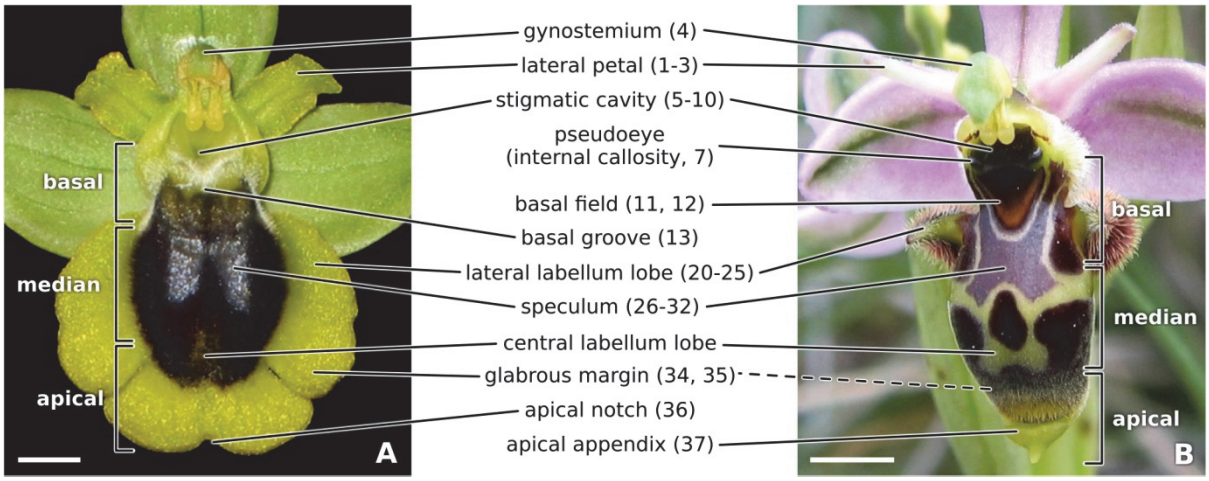

Figure S2. Macrographs of flowers of (A) *Ophrys lutea* and (B) *Ophrys scolopax*, two species with contrasting floral morphological features belonging to the sections *Pseudophrys* and *Ophrys*, respectively. Numbers given in brackets correspond to the characters of Table 1 describing each floral element. Scale bars: 3 mm.

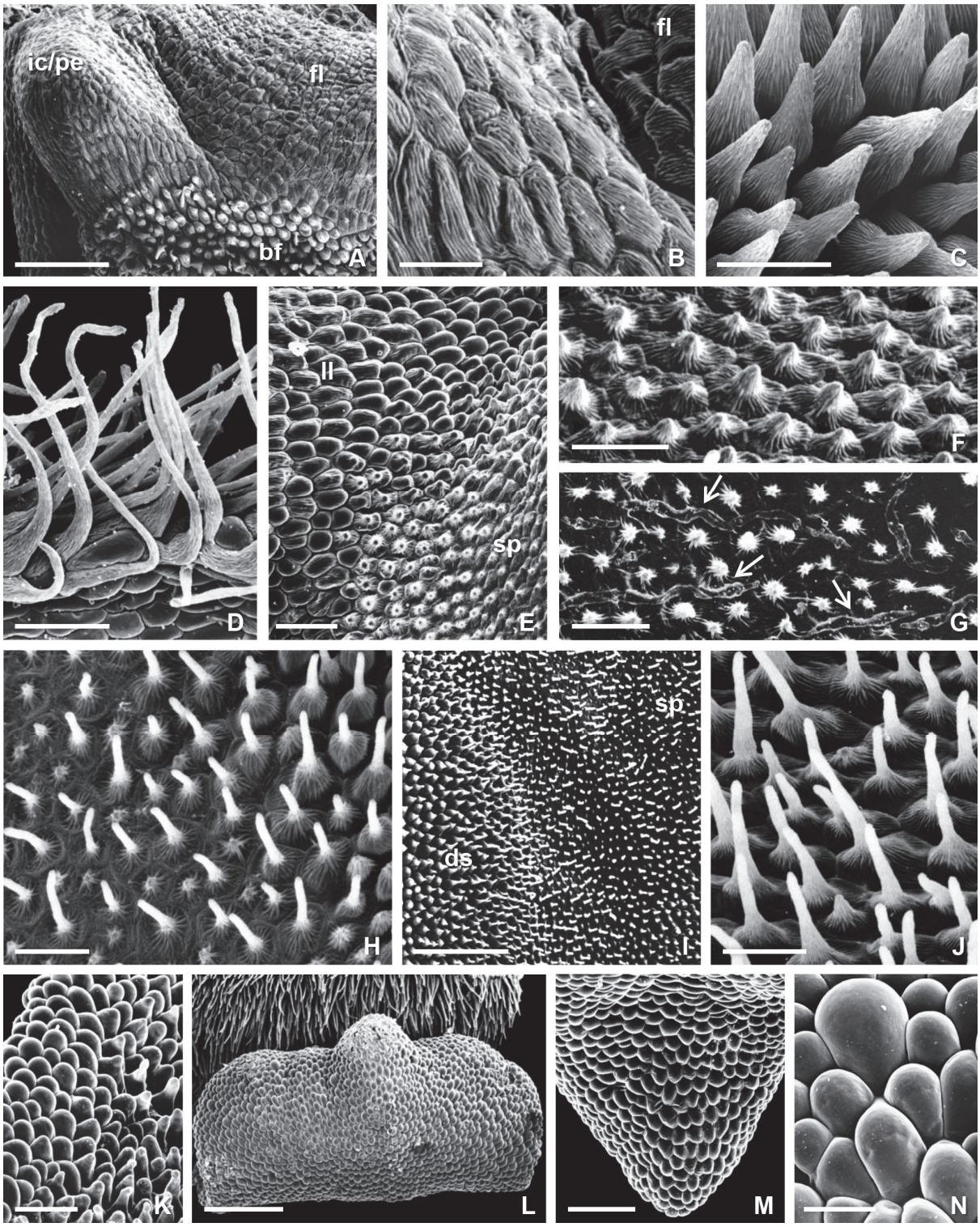

Figure S3. Scanning electron micrographs of the adaxial surface of labellum and stigmatic cavity in *Ophrys scolopax*, showing the eight epidermal cell types that constitute them. A, Glabrous stigmatic cavity in contiguity to the basal region of labellum, showing the internal callosity (7) bearing the pseudoeye in its tip, the floor of stigmatic cavity (5), and the basal field of labellum (14, 17). B, Detail of the striated flat-lenticular cells with polygonal elongated outline occurring in the internal callosity and the floor; the region occupied by the pseudoeyes present cells with a smoother surface (not shown). C, Short sub-conical trichomes of the basal field (14, 17). D, Margin of the hirsute lateral labellum lobe, showing long slightly contorted trichomes (25). E, Glabrous portion of the lateral labellum lobe, near the base (on left), where flat-lenticular cells (22) occur, in contiguity with the lateral area of the speculum (on right). F–H, Different portions of the speculum, which is composed

of both papillae and short trichomes; although trichomes were usually found interspersed with papillae throughout the speculum, they tend to occur more frequently toward its centre. F, Detail of the papillae of the speculum, which have a large, flattened base with polygonal outline and prominent, radially-arranged cuticular striations (28, 31, 32). G, Detail of prominent epicuticular depositions (arrows) laid over some portions of contiguous speculum cells. H, Distal portion of the speculum (on left), showing the short, narrow trichomes with flattened, radially-striated bases (29, 31, 32) occurring among papillae (28, 31, 32). I, Boundary between the distal part of the speculum (on right) and a dark rounded spot (on left) in the median-apical region of labellum. J, Apical indumentum showing long, attenuate trichomes with enlarged bases and a straight tip. K, Glabrous margin of labellum where domed papillae (35) occur. L, Apical appendix (37) near the long, attenuate trichomes with a sinuate tip that form a submarginal indumentum band (33). M, Adaxial surface of the appendix. N, Detail of the domed papillae (35) of the appendix. bf, basal field; ds, dark spot; fl, floor of stigmatic cavity; ic, internal callosity; ll, lateral labellum lobe; pe, pseudoeye; sp, speculum. Numbers in brackets correspond to the characters of Table 1. Scale bars: 500 µm (L); 250 µm (A, I, M); 100 µm (D, E, K); 50 µm (B, C, F–H, J, N).

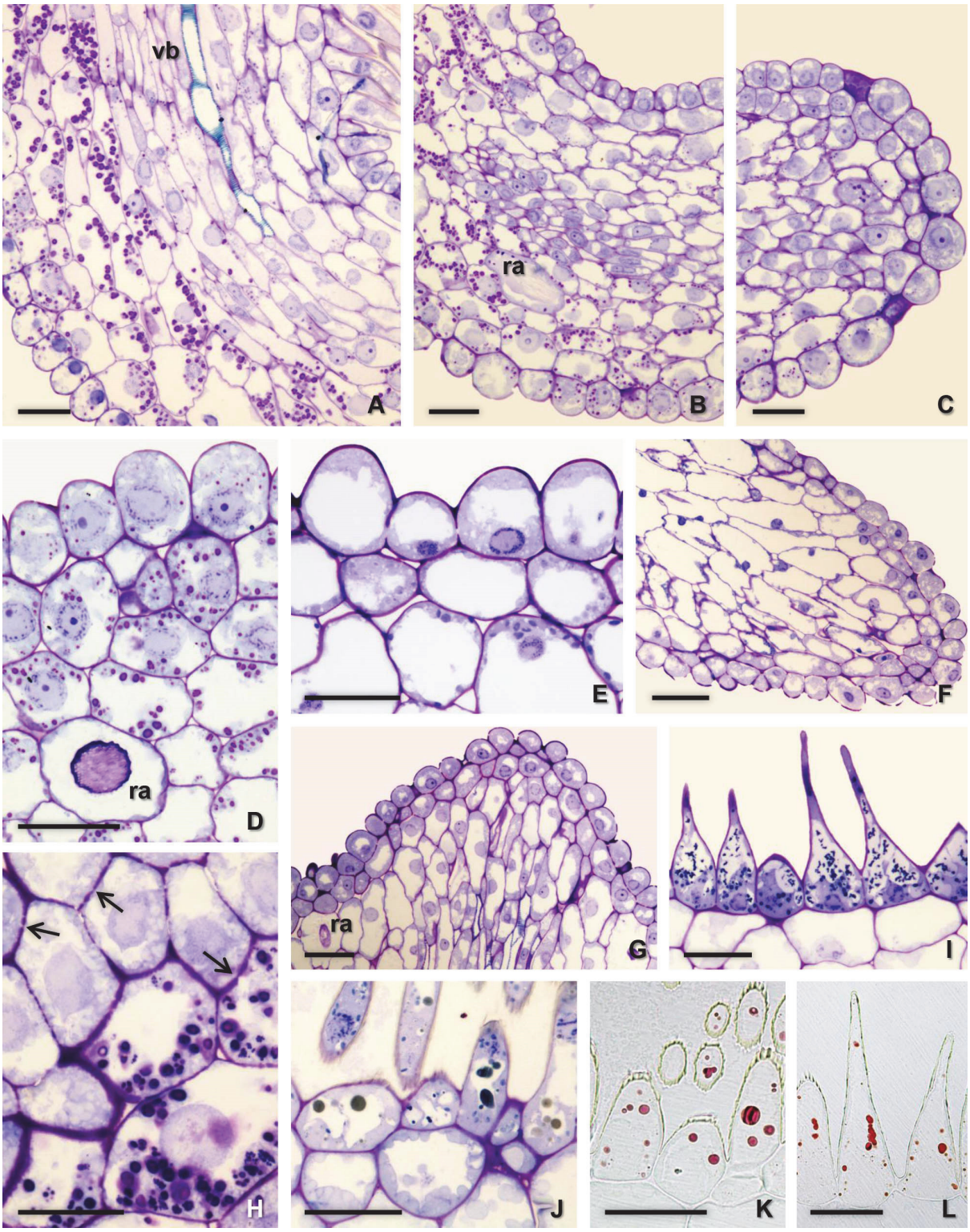

Figure S4. Light micrographs of historesin sections of the labellum of *Ophrys scolopax*, stained with periodic acid–Schiff (PAS) reagent/toluidine blue (A–D, F–I), toluidine blue/dilute Lugol (E, J) or vanillin–hydrochloric acid (K, L). A–H, Sections of the apical region of labellum, illustrating features of the secretory cells of osmophore occurring in the apical appendix; these traits correspond to characters 39 and 41–44 of Table 1. A, Longitudinal section of the apical region of labellum contiguous to the apical appendix of an early bud, showing trichomes on adaxial surface and dome-shaped epidermal papillae and starch-rich parenchyma cells on abaxial surface; note the vasculature of this region. B, C, Longitudinal sections of the apical appendix of an early bud, showing glandular epidermal papillae with a large nucleus and a dense cytoplasm, as well as sub-epidermal parenchyma cells with abundant pink-stained starch-rich plastids, especially on abaxial surface. D, E,

Transverse sections of the secretory tissues on abaxial surface of the appendix of (D) an early bud and (E) an opened flower; note that, from D to E, vacuolization of cells has increased and that the starch content of the subepidermal parenchyma cells was drastically reduced. F, Longitudinal section of the appendix tip of an opened flower; note the increased vacuolization of the subepidermal parenchyma cells as compared with those depicted in C. G, Transverse section of the appendix of an opened flower, showing secretory epidermal cells with dense cytoplasm on the adaxial surface. H, Paradermal section of the secretory tissues on the abaxial surface of the appendix of a late bud, showing abundant starch-rich plastids stained pink with PAS reagent in the subepidermal parenchyma cells; note primary pit fields in the periclinal cell walls (arrows). I–L, Transverse sections of the median-apical region of labellum in a late bud (L) and an opened flower (I–K), showing attenuate trichomes with phenolic vacuolar content. I, J, Phenolic deposits appeared green-stained after general staining with toluidine blue. K, L, Bright red-stained condensed tannins are evident inside vacuoles after treatment with vanillin–hydrochloric acid. ra, raphides; vb, vascular bundles. Scale bars: 100 µm (F, G); 50 µm (A–E, H–L).

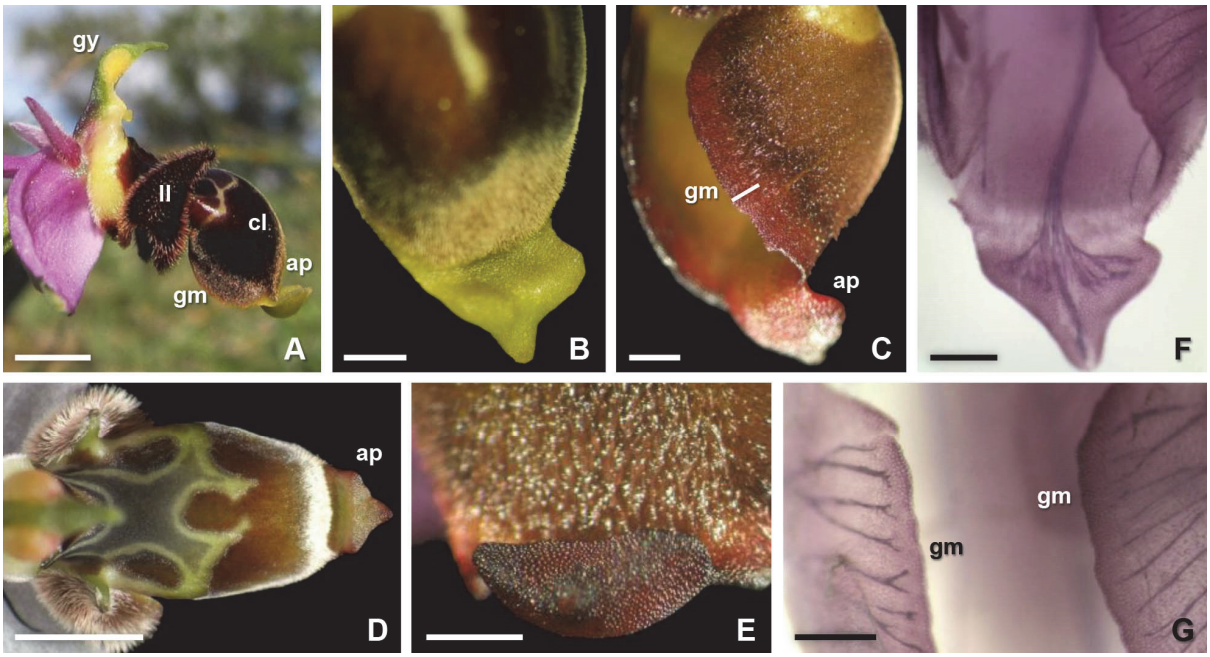

Figure S5. Macrographs of (A–E) fresh flowers and (F, G) cleared flowers of *Ophrys scolopax* stained with safranin. A, Lateral view of a flower in the field, showing the highly convex labellum with recurved margins and the apical appendix. B, Detail of the robust, trilobed appendix. C–E, Flowers after immersion in neutral red. C, E, Freshly opened flower; note that the glabrous labellum margin (in C its width is marked with a full line) and the appendix stained intense red, indicating their presumed secretory nature. D, Opening floral bud; note that the appendix appears only light-red-stained. E, Detail of the intensely red-stained appendix. F, G, Vasculature of the labellum, showing (F) the intense branched venation of the appendix and (G) the branched pattern of veins towards the glabrous margin of labellum. ap, apical appendix; cl, central labellum lobe; gm, glabrous margin of labellum; gy, gynostemium; ll, lateral labellum lobe. Scale bars: 4 mm (A, D); 1 mm (B, C, E–G).

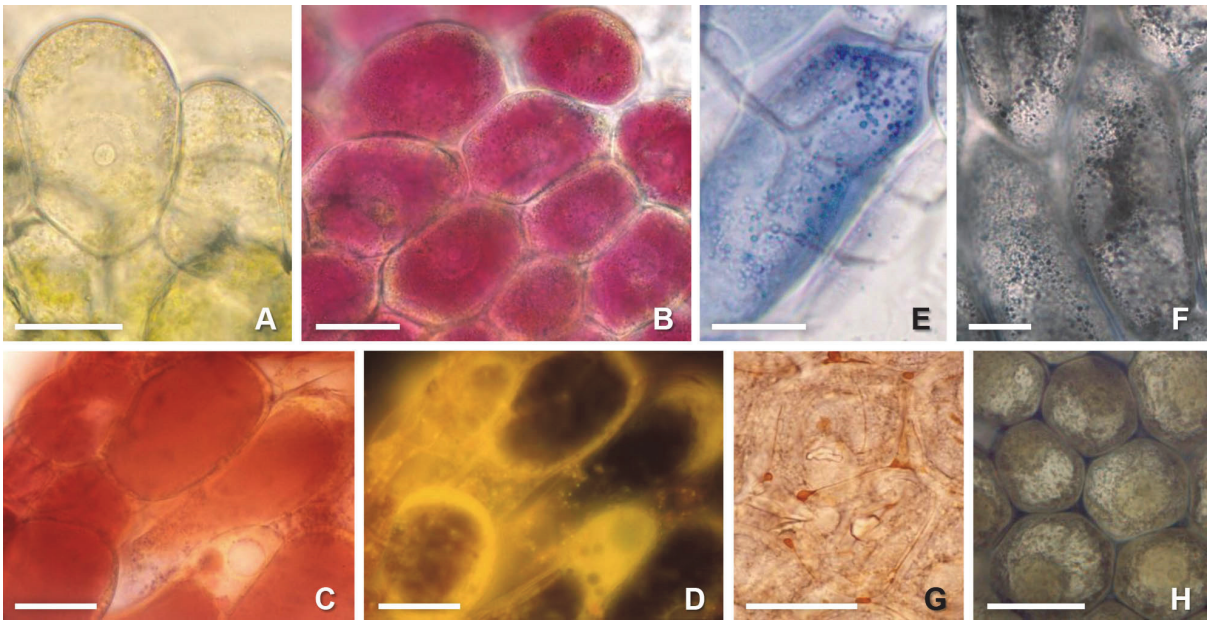

Figure S6. Histochemical characterization of fresh-hand sections of the apical appendix of *Ophrys scolopax*. A, Dome-shaped epidermal cells without any treatment (control). B, Paradermal section stained with diluted neural red, showing epidermal cells of the osmophore with bright pink-stained vacuoles. C, D, Transverse section of the appendix stained with neutral red seen under (C) visible light and (D) blue light; note the golden-yellow secondary fluorescence of the cytoplasm under blue

light, which seems to contain lipophilic content. E, F, Paradermal sections of the appendix stained with (E) Nadi reagent and (F) Sudan Black B, showing blue- and black-stained droplets of a terpene-rich lipophilic secretion in the cytoplasm of epidermal cells. G, H, Paradermal sections of the appendix tip stained with (G) Sudan IV and (H) osmium tetroxide, showing red- and black-stained lipophilic secretion outside epidermal cell walls. Scale bars: 40 µm (A–D, G, H); 20 µm (E, F).

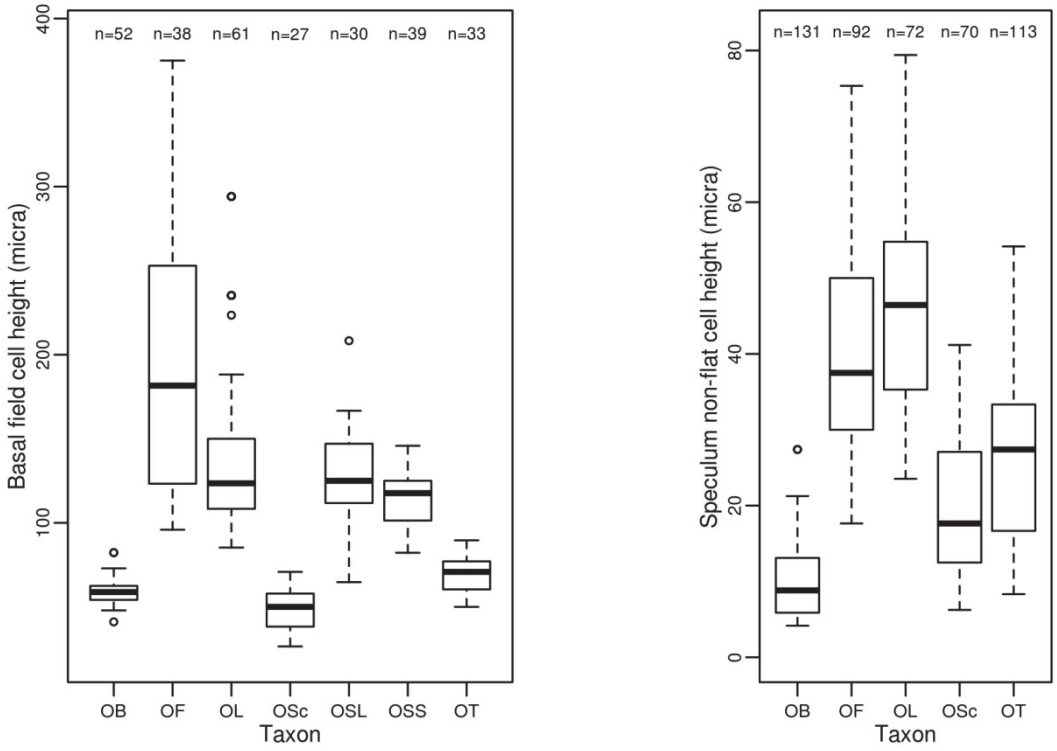

Figure S7. Box-plots representing (A) the height of cells in the basal field of the labellum and (B) the height of non-flat cells in the speculum of the labellum of the seven *Ophrys* taxa: *Ophrys bombyliflora* (OB, 3 individuals), *Ophrys fusca* subsp. *fusca* (OF, 2 individuals), *Ophrys lutea* (OL, 3 individuals – A; 2 individuals – B), *Ophrys scolopax* (OSc, 2 individuals – A; 3 individuals – B), *Ophrys speculum* subsp. *lusitanica* (OSL, 3 individuals), *Ophrys speculum* subsp. *speculum* (OSS, 4 individuals), and *Ophrys tenthredinifera* (OT, 3 individuals – A; 4 individuals – B). These measurements were used for defining characters 14–17 and 27–31 (Table 1). OSL and OSS are not represented in B because the speculum in these two taxa is entirely composed of flat-lenticular cells. Boxes represent the central 50% of measurements, the black line is the median, and the whiskers extend to the point which is no more than 1.5 times the length of the box away from the box.

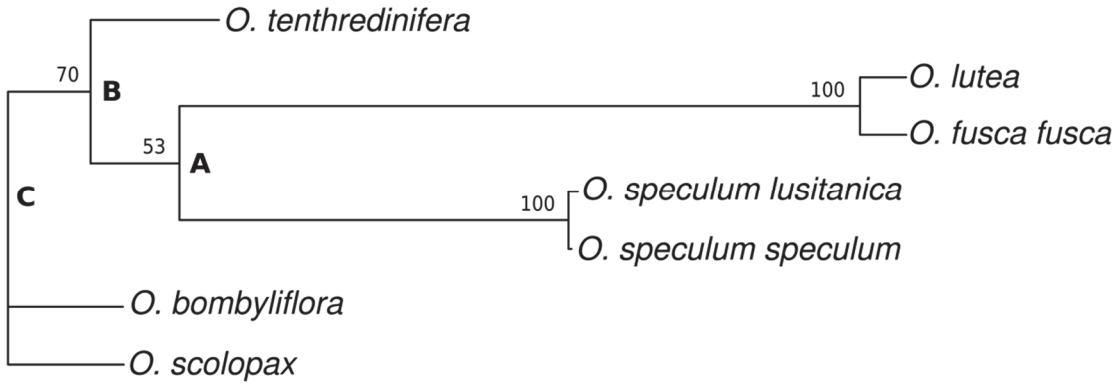

Figure S8. Distance-based phylogenetic tree obtained from the distance matrix of Table S1 using the neighbour-joining method (Saitou & Nei, 1987). The distance matrix was obtained by calculating the Gower distances in the data matrix consisting of six ingroup *Ophrys* taxa plus one outgroup (*Ophrys scolopax*), each scored for 45 morpho-anatomical floral characters, 13 of which being treated as continuous (like in the maximum parsimony analysis under continuous approach) and all equal-weighted. Bootstrap percentages, which were obtained with 10000 replications after removing the four parsimony-uninformative characters (4, 14, 35, 41; Table 1) from the data matrix, are indicated above each branch. Key nodes (A and B) and the node representing the presumed common ancestor of taxa that form the ingroup (C) are also identified. Distance analyses were performed with the function “nj” of package "ape" version 3.1-4 (Paradis, Claude & Strimmer, 2004) under the R environment (R Core Team, 2014).

REFERENCES

Paradis E, Claude J, Strimmer K. 2004. APE: Analyses of Phylogenetics and Evolution in R language. *Bioinformatics* **20:** 289-290.

R Core Team. 2014. R: a language and environment for statistical computing. Vienna, Austria: R Foundation for Statistical Computing. http://www.R-project.org.

Saitou N, Nei M. 1987. The neighbor-joining method: a new method for reconstructing phylogenetic trees. *Molecular Biology and Evolution* **4:** 406-425.

Table S1. Distance matrix obtained by calculating the Gower distances (Legendre & Legendre, 1998) for each pair of taxa of the morpho-anatomical data matrix consisting of six ingroup *Ophrys* taxa plus one outgroup (*Ophrys scolopax*), each scored for 45 morpho-anatomical floral characters, 13 of which being treated as continuous (like in the maximum parsimony analyses under continuous approach) and all equal-weighted. The Gower distance (Gower, 1971) was used because it allows mixing different types of variables (binary, qualitative, and continuous characters) in the distance computation, being commonly used in studies of functional (trait) diversity (Botta-Dukát, 2005; Laliberté & Legendre, 2010). The distance matrix was obtained using the function "gowdis" of package "FD" (Laliberté & Legendre, 2010; Laliberté, Legendre & Shipley, 2014) under the R environment (R Core Team, 2014).

		Taxon						
Nr.	Taxon	0	1	2	3	4	5	6
0	*Ophrys scolopax* (outgroup)	-						
1	*Ophrys speculum* subsp. *speculum*	0.49	-					
2	*Ophrys speculum* subsp. *lusitanica*	0.50	0.09	-				
3	*Ophrys bombyliflora*	0.16	0.39	0.39	-			
4	*Ophrys tenthredinifera*	0.23	0.48	0.49	0.22	-		
5	*Ophrys fusca* subsp. *fusca*	0.65	0.79	0.80	0.79	0.58	-	
6	*Ophrys lutea*	0.69	0.76	0.76	0.79	0.61	0.06	-

REFERENCES

Botta-Dukát Z. 2005. Rao's quadratic entropy as a measure of functional diversity based on multiple traits. *Journal of Vegetation Science* **16:** 533-540.

Gower JC. 1971. A general coefficient of similarity and some of its properties. *Biometrics* **27:** 857-871.

Laliberté E, Legendre P. 2010. A distance-based framework for measuring functional diversity from multiple traits. *Ecology* **91:** 299-305.

Laliberté E, Legendre P, Shipley B. 2014. FD: measuring functional diversity from multiple traits, and other tools for functional ecology. R package version 1.0-12.

Legendre P, Legendre L. 1998. *Numerical Ecology.* Amsterdam: Elsevier Science B.V.

R Core Team. 2014. R: a language and environment for statistical computing. Vienna, Austria: R Foundation for Statistical Computing. http://www.R-project.org.

Table S2. Comparison between the results of maximum parsimony (MP) analyses under the discrete approach and those of Bayesian analyses of the morpho-anatomical data matrix of 45 characters for six closely related *Ophrys* taxa (*Ophrys bombyliflora,* OB; *Ophrys fusca* subsp. *fusca,* OF; *Ophrys lutea,* OL; *Ophrys speculum* subsp. *lusitanica,* OSL; *Ophrys speculum* subsp. *speculum,* OSS; and *Ophrys tenthredinifera,* OT) plus one outgroup (*O. scolopax*, which is omitted from trees for the sake of simplicity). For each MP tree, consistency index (CI) and retention index (RI) are presented, and bootstrap percentages are given above each branch. For each Bayesian analysis, average standard deviation of split frequencies (ASDSF) and potential scale reduction factor (PSRF) are given, and posterior probability (PP) values are presented above tree branches; PP values of the groups of taxa that did not appear in the 50% majority rule consensus trees are also given. Key nodes (A and B) and the node representing the presumed most recent common ancestor of taxa that form the ingroup (C) are identified in each tree.

	Maximum parsimony (discrete approach)					**Bayesian inference**	
	Equal character weights				Unequal weights	Equal variation rate	Unequal variation rate
	Most parsimonious trees			50% Majority rule consensus tree	Most parsimonious tree	50% Majority rule consensus tree	50% Majority rule consensus tree
Tree topology (cladogram)	Tree 1 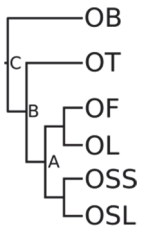	Tree 2 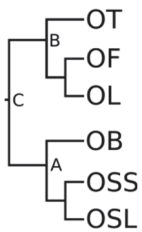	Tree 5 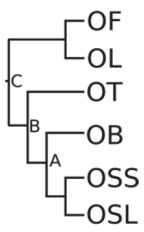	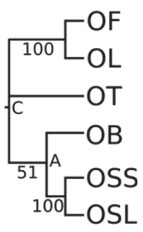	Tree 5 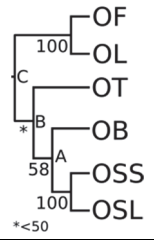	Tree 5 (Fig. 2B) 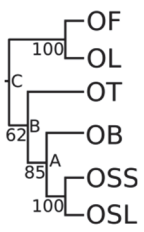	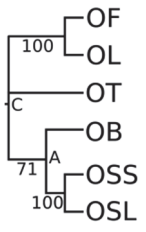
Tree length (steps)	79			-	117	**PP values of additional groups**	OT-(OF-OL): 34	OT-OB-(OSS-OSL): 49 OT-(OF-OL): 38 OT-(OF-OL)-(OSS-OSL): 10
CI	0.733			-	0.748	**ASDSF**	0.00377	0.00305
RI	0.747			-	0.769	**PSRF**	1.000	1.000

Table S3. Posterior probability (PP) of the trees included in the 99% credibility set of trees found during the Markov Chain Monte Carlo searches of Bayesian analyses, using equal and unequal [gamma distribution, α uniform (0.001–200)] variation rate across characters. The trees are sorted by their PP and those whose topology is found within the suboptimal tree set (5% shortest trees) obtained from maximum parsimony analyses (Table 2) are identified. The three most likely trees (considering the results of all the analyses conducted) are typed in bold.

Equal variation rate	Unequal variation rate
p = 0.539 (**tree 5**)	p = 0.404 (**tree 5**)
p = 0.293 (**tree 2**)	p = 0.288 (**tree 2**)
p = 0.056	p = 0.060 (tree 3)
p = 0.037 (tree 3)	p = 0.057
p = 0.025	p = 0.036
p = 0.015 (tree 6)	p = 0.036 (**tree 1**)
p = 0.014	p = 0.030
p = 0.008 (**tree 1**)	p = 0.029 (tree 6)
p = 0.006	p = 0.027
	p = 0.013 (tree 4)
	p = 0.006
	p = 0.005

CHAPTER 6

GENERAL DISCUSSION

GENERAL DISCUSSION

The present thesis represents a substantial contribution to the fields of floral biology and pollination of the sexually deceptive orchid genus *Ophrys*, focusing on three major topics: (1) osmophore structure and function; (2) labellum micromorphology; and (3) phylogenetic reconstruction and floral trait evolution. First, this work constitutes a significant advance in our knowledge of *Ophrys* osmophores, giving continuity to the work initiated by Stefan Vogel in the early 1960s, who provided the first anatomical description of the osmophores of *O. fusca*, *O. lutea* and *O. fuciflora* (Vogel, 1990). Through our detailed anatomical and histochemical study on the labellum of seven *Ophrys* taxa, at three different stages of flower development, we were able to confirm the findings of Vogel for *O. fusca* and *O. lutea* (Chapter 2) and to demonstrate that an osmophore also occurs in *O. bombyliflora* and *O. tenthredinifera* (Chapter 3), in the two subspecies of *O. speculum* occurring in Portugal (Chapter 4) and in *O. scolopax* (Chapter 5). A thorough characterization of the location, structure and secretion of the osmophore was provided for each taxon in Chapters 2–5 and supplementary data were obtained for the osmophores of *O. fusca* and *O. lutea* as the study proceeded (Appendix A). Additionally, a chemical analysis of the volatile organic compounds emitted by the flowers of *O. fusca* and *O. lutea* was conducted by gas chromatography coupled with flame ionization detection (GC-FID) using a semi-dynamic headspace sampling method (Appendix B).

Second, our detailed comparative micromorphological characterization of the labellum and the stigmatic cavity revealed a great diversity of epidermal cell types in the adaxial surface of the flower in each *Ophrys* species and established putative homologies between the different floral parts of all investigated taxa (Chapters 2–5). Most remarkably, homologies were hypothesised to exist between the distinctive apical appendix of *O. bombyliflora*, which was described here for the first time (Chapter 3), and the appendixes of the other *Ophrys* species and between the uncommon basal field of *O. speculum*, which is confined to the cupuliform concavity occurring between the stigmatic cavity's labia (Chapter 4), and the basal fields of the other species. Furthermore, some novel micromorphological features were described in *Ophrys* flowers (Chapters 2–4), and those found in flowers of *O. speculum* constitute new evidences of visual and tactile mimicry of the female of their specific wasp pollinator (Chapter 4).

Lastly, the comparative micromorphological and anatomical analysis of the features of the labellum and the osmophore in the seven studied taxa allowed us to build a data matrix of 45 characters, which was subsequently used for the phylogenetic reconstruction of the interspecific relationships in the investigated clade of *Ophrys* and for inferring its ancestral floral character states (Chapter 5). Our cladistic analysis showed that *O. tenthredinifera* and *O. bombyliflora* are not sister groups, rejecting the existing morphological cladistic hypothesis, and pointed to a sister relationship between *O. bombyliflora* and *O. speculum*,

which was supported by four synapomorphies concerning the stigmatic cavity and the speculum, favouring the existing molecular trees based on nuclear ITS data (alone or combined) but not on plastid data alone (Chapter 5).

A COMPARATIVE ANALYSIS OF *OPHRYS* OSMOPHORES

Our study revealed that *Ophrys* flowers present consistently an osmophore in the apical region of the labellum (Chapters 2–5, Appendix A), a location that fits well with the primary function assigned to a scent-producing gland, i.e. synthesizing and emitting volatile organic compounds for long-range attraction of insect pollinators (Vogel, 1990). Most osmophores are located in exposed portions of the flowers, mainly at the margin or the tip of sepals and/or petals, which facilitates a more rapid dispersion of the volatile secretion into the atmosphere, further assisted by the wind (Pridgeon & Stern, 1983; Vogel, 1990; Sanguinetti *et al.*, 2012; Pansarin, Pansarin & Sazima, 2014; Possobom, Guimarães & Machado, 2015). The osmophores of *Ophrys*, however, have histological and cytological features which vary according to the species (Chapters 2–5, Appendix A).

Concerning the extent of the osmophore tissues in the labellum, the investigated *Ophrys* species could be divided into two groups: (1) those provided with an apical appendix, i.e. *O. bombyliflora*, *O. tenthredinifera* and *O. scolopax*; and (2) those without an apical appendix and with a central notch in the apical region of the labellum, i.e. *O. fusca*, *O. lutea* and *O. speculum*. In the species of the former group, the osmophore occurs in the apical appendix, but while that of *O. bombyliflora* is restricted to it, the osmophore in *O. scolopax* and *O. tenthredinifera* also extends to the apical labellum margin, and in this latter species, it occupies the abaxial surface of the apical region of the labellum as well (Chapters 3 and 5). On the other hand, in the second group of species, the osmophore of *O. speculum* is confined to the apical margin of the labellum (Chapter 4), whereas that of *O. fusca* and *O. lutea* extends to the entire labellum margin and to the abaxial surface of the apical region of the labellum (Chapter 2, Appendix A), as in *O. tenthredinifera* (Chapter 3). In addition, the osmophore in *O. fusca* and *O. lutea* also includes the margin of the lateral petals (Appendix A), like in other genera of the subtribe Orchidinae, such as *Platanthera* and *Gymnadenia* (Vogel, 1990; Stpiczyńska, 2001).

As for the osmophore structure, all species display a morphologically undifferentiated osmophore composed of a secretory layer of epidermal cells, which are dome-shaped papillae except for *O. bombyliflora* (where they are lenticular cells instead), and two to three subepidermal parenchyma cell layers (Chapters 2–5, Appendix A). The parenchyma tissue underlying the osmophore presents always several crystal idioblasts containing calcium oxalate raphides, which are particularly abundant in the appendix of *O. bombyliflora* (Chapter 3). The formation of raphide crystals in *Ophrys* tissues could be a way of regulating intracellular calcium levels (Franceschi & Nakata, 2005; Paiva & Machado,

2005) in an orchid genus that occurs mainly in calcareous soils. The central vein of the labellum was found to branch towards the labellum margin and the apical appendix of *Ophrys* flowers (Chapters 3 and 5, Appendix A), and hence the parenchyma tissue of the osmophores in *Ophrys* is supplied with vascular bundles, like occurs in other scent-producing glands (Vogel, 1990). The intense venation of the osmophore tissues could provide an additional supply of water and sugars for the metabolic activity of secretory cells, and certainly assures a high turgor pressure in cells of the apical appendixes, which act as an important tactile signal for male insect pollinators (Chapter 3).

The great majority of osmophores is located in the adaxial surface of the floral organ that bears them (Pridgeon & Stern, 1983; Pridgeon & Stern, 1985; Stern, Curry & Pridgeon, 1987; Stpiczyńska, 2001; Bolin, Maass & Musselman, 2009; Melo, Borba & Paiva, 2010; Sanguinetti *et al.*, 2012), as in the apical appendix of *O. bombyliflora* (Chapter 3). Besides the osmophores of *O. fusca*, *O. lutea* and *O. tenthredinifera* (Chapters 2 and 3, Appendix A), the other few exceptions to this rule were also found in Orchidaceae, mainly in the terrestrial orchid tribe Cranichideae, which present the abaxial surface with secretory features (Vogel, 1990; Pansarin, de Moraes Castro & Sazima, 2009; Wiemer *et al.*, 2009; Borba *et al.*, 2014). In the other two studied *Ophrys* species, *O. speculum* and *O. scolopax*, both surfaces of the labellum margin and the appendix are involved in the secretory process (Chapters 4 and 5).

A high starch content was found in the osmophores of the investigated *Ophrys* species, in flowers prior to the anthesis (especially at the stage of early bud), like in most of the other osmophore-containing species (Pridgeon & Stern, 1983; Stern *et al.*, 1987; Vogel, 1990; Skubatz, Kunkel & Meeuse, 1993; Vogel & Hadacek, 2004). This high starch content sharply decreased – but did not disappear completely – in open flowers (Chapters 2, 3 and 5, Appendix A). However, such pattern was not found in *O. speculum* (Chapter 4), which presented only vestigial starch content at the earliest stage of floral development, and no detectable starch thereafter. Abundant starch-rich plastids were observed in the subepidermal parenchyma cells of the osmophores of *O. bombyliflora*, *O. tenthredinifera* and *O. scolopax* (Chapters 3 and 5), whereas in *O. fusca* and *O. lutea* the bulk of starch occurred in the plastids of the domed papillae of the secretory epidermis, an exclusive quality of the osmophore of these two species (Chapter 2, Appendix A), in clear contrast to the common location of starch reserve in the parenchyma tissue of all the other described osmophores (e.g. Pridgeon & Stern, 1983; Vogel, 1990; Skubatz *et al.*, 1993; Vogel & Hadacek, 2004). The typical accumulation of large amounts of reserve materials like starch in the fragrance-producing tissues is assumed to be neccessary to meet the need for energy and/or carbon to synthesise a great amount of a volatile secretion within a short period of time (Stern *et al.*, 1987; Vogel, 1990). High energy requirements are needed for the synthesis of the volatile organic compounds that are generally produced in the osmophores, which are mostly terpenes, phenylpropanoid compounds and amines, but also aliphatic or

cyclic short-chained aldehydes, ketones, alcohols, esters, among others (Vogel, 1990). The glandular cells of the osmophores of *Ophrys* spp. synthesise a terpene-rich lipophilic secretion with a phenolic fraction, which was found consistently in small quantity and temporarily accumulated in the periplasmic space, loose cell walls, vacuoles and/or cortical cytoplasm, and sometimes it also appeared on the surface of the epidermal cells, particularly in *O. fusca* and *O. speculum* (Chapters 2–5, Appendix A). The low amount of secretion detected by histochemical tests in the osmophore cells of all studied species may be caused by the high volatility of its components. An intense and continued activity of the osmophore is thus required to assure that the high volatile secretion is emitted to the atmosphere in sufficient amount to be detected by insect pollinators at long distances (Vogel, 1990). Therefore, the starch reserve observed in *Ophrys* spp. (Chapters 2, 3 and 5, Appendix A) is probably used as a source of both energy and structural material for the synthesis of the volatile terpene-rich lipophilic secretion. Since a starch depletion occurs after the cessation of the secretory period of the osmophores (Pridgeon & Stern, 1983; Stern *et al.*, 1987; Vogel, 1990; Skubatz *et al.*, 1993; Vogel & Hadacek, 2004; Melo *et al.*, 2010), changes in the starch content along flower development give us an indication of the osmophore period of activity (Chapter 3).

The investigated *Ophrys* taxa present a prolonged period of anthesis that lasts a minimum of 6 days (in *O. bombyliflora*) or 14 days (in *O. scolopax*) and that can reach 21 days in some flowers of *O. lutea* (Appendix C). The flowers of all studied species emit a faint to moderate scent in the stage of freshly opened flower, which corresponds to the largest part of the period of anthesis (Appendix C). In effect, headspace sorption analyses of flowers of *O. fusca* and *O. lutea*, which are the two most scented *Ophrys* species among those studied, revealed that the emission rate of volatile organic compounds from flowers was extremely low varying into the nanogram range (Appendix B), which agrees with those previously estimated for *Ophrys* flowers (Borg-Karlson, 1990; Schiestl *et al.*, 1997). Odour emission varies considerably from flower to flower and it appears to be influenced by environmental factors such as temperature and radiation (Kaiser, 1993). Notwithstanding, in all studied *Ophrys* species, the fragrance seems to be more intense in the first days of anthesis, corresponding to the peak of activity of the osmophore, an observation that fits well the evident decrease in the starch content of osmophore tissues from late buds to open flowers (Chapters 3 and 5, Appendix A). Considering that a faint scent is continuously emanated from freshly opened flowers of *Ophrys* spp. and some starch persists in the osmophore tissues at this stage, we suggest that the osmophores remain active throughout the largest portion of the period of anthesis (Chapter 3).

THE ROLE OF THE OSMOPHORES IN THE ATTRACTION OF *OPHRYS* POLLINATORS

The occurrence of an osmophore synthesizing a terpene-rich lipophilic secretion in the labellum of all investigated *Ophrys* species leads us to question its relevance to the highly specific pollination by sexual deception that has evolved in these orchids. The high specificity of this pollination system, in which one *Ophrys* species is pollinated by a single or a few related insect species (Kullenberg, 1961; Paulus & Gack, 1990), is achieved by the chemical mimicry occurring between certain compounds of the odour bouquet of each *Ophrys* species and the sex pheromone used by the females of its specific pollinator to attract conspecific males for reproduction (Schiestl *et al.*, 1999; Schiestl *et al.*, 2000; Ayasse *et al.*, 2003; Mant *et al.*, 2005; Stökl *et al.*, 2005; Stökl *et al.*, 2008), which is usually highly species-specific (Ayasse, Paxton & Tengö, 2001; Wyatt, 2010). In terms of chemical structure, insect pheromones are molecules of hydrocarbons and other fatty acid derivatives such as aliphatic alcohols, aldehydes, esters and ketones, lactones and terpenoid compounds, which are usually combined in certain proportions in more or less complex mixtures to assure a species-specific signal (Ayasse *et al.*, 2001; Mant *et al.*, 2005; Stökl *et al.*, 2008; Mori, 2010). Although some pheromones are considered to be non-volatile compounds, such as contact pheromones of some insects which due to their chemical structure and high molecular mass exert their action through touching, all pheromones should be more or less volatile compounds (Mori, 2010).

In most *Ophrys*-pollinator interactions hitherto investigated, namely those involving species pollinated by solitary bees of genus *Andrena*, such as *O. sphegodes*, *O. fusca*, *O. bilunulata* and *O. iricolor*, and by the *Colletes cunicularius* solitary bee, such as *O. exaltata*, the semiochemicals considered key to elicit mating behaviour in male insects (i.e. the behaviourally active compounds that mimic the female sex pheromone) were found to be mainly a series of long-straight-chained unsaturated hydrocarbons (n-alkenes; Schiestl *et al.*, 1999; Schiestl *et al.*, 2000; Schiestl & Ayasse, 2002; Mant *et al.*, 2005; Stökl *et al.*, 2005; Stökl *et al.*, 2008; Stökl *et al.*, 2009; Xu *et al.*, 2011; Xu *et al.*, 2012) occurring in the cuticle of the insect body and in the cuticular waxes of the epidermal cell walls at the adaxial surface of the labellum (Ayasse *et al.*, 2001; Blomquist & Bagnères, 2010; Schlüter *et al.*, 2011). These long-chained hydrocarbons, because of their high molecular mass and low vapour pressure, are low volatile compounds that presumably are detected by patrolling-male pollinators only at short distances from the labellum (Ayasse, Stökl & Francke, 2011). Therefore, they are unlikely synthesised in the osmophore, which typically produces diverse compounds with high volatility for long-range attraction of pollinators (Vogel, 1990).

Notwithstanding, a functional osmophore was found in the labellum of all investigated *Ophrys* species (Chapters 2–5). Osmophores are secretory structures assumed to have evolved from the diffuse fragrance-producing epidermis in the flowers towards a specialization in pollination interactions through the attraction of specific groups of

pollinators in diverse pollination systems (Stern *et al.*, 1987; Vogel, 1990; Sazima *et al.*, 1993; Skubatz *et al.*, 1996; Stpiczyńska, 2001; Teixeira, Borba & Semir, 2004; Peter *et al.*, 2009; Wiemer *et al.*, 2009; Heiduk *et al.*, 2010; Melo *et al.*, 2010; van der Niet, Hansen & Johnson, 2011). Hence, the mere occurrence of an osmophore suggests that it should play an important role in the pollination of all studied *Ophrys* species. One possible explanatory model for the pollination process in these species is a model that predicts complementary functions of the highly volatile organic compounds synthesised in the osmophore and the cuticular waxes enriched in low volatile hydrocarbons and other fatty-acid derivatives spread over the labellum surface: the osmophore compounds act as long range pollinator attractants whereas the cuticular waxes act at close distance and upon contact, playing the key role of triggering the mating behaviour in male insects that is crucial for an effective pollination (Chapter 3), in agreement with other models previously suggested by Kullenberg & Bergström (1976) and Steiger, Schmitt & Schaefer (2011). The fact that an osmophore exists in all studied species (Chapters 2–5) confers more support to our hypothesis (Chapter 3), as opposed to the usual view that cuticular waxes enriched in hydrocarbons are sufficient for the success of pollination (Bateman *et al.*, 2011; Vereecken *et al.*, 2011).

The osmophore of *O. speculum* presents, however, only a vestigial starch content and hence is presumably less active than those of the other *Ophrys* species (Chapter 4), an hypothesis that is in accordance with the existing knowledge about the semiochemicals involved in the specific attraction of its wasp pollinator, *Dasyscolia ciliata*. The highly specific signal used in the reproduction of this wasp consists predominantly in three uncommon (w-1)-hydroxy and (w-1)-oxo carboxylic acids, which also occur in the cuticle of the epidermal cells of the labellum and have a higher volatility than the key long-chained n-alkenes commonly used by other species (Ayasse *et al.*, 2003; Ayasse *et al.*, 2011). In this case, the osmophore seems to have lost functional importance but most likely constitutes a reservoir of semiochemicals that represents evolutionary potential for adaptation to new pollinators (Chapter 4). This is particularly relevant in a species that maintains a highly specific interaction with a single insect pollinator, and hence is exposed to a high extinction risk, associated with a higher probability of extinction of that pollinator species.

The proposed model of complementary roles for the osmophore compounds and the cuticular waxes in the pollination process of *Ophrys* orchids requires, however, empirical confirmation in the field. In order to test the importance of the osmophore in the pollinator attraction, we need to: (1) know if all species in genus *Ophrys* present an osmophore; (2) identify the compounds effectively synthesised in this scent-producing gland; (3) find out whether the volatility of compounds influences the distance reached by them under real conditions in natural habitats, since the evaporation and the transport of the odour molecules from the labellum are influenced by several factors such as air temperature, humidity, turbulence and wind velocity (Kullenberg, Borg-Karlson & Kullenberg, 1984); and

(4) test whether the compound volatility impacts on the effective attraction of insect pollinators in the field.

COMPARATIVE LABELLUM MICROMORPHOLOGY AND ITS SIGNIFICANCE FOR *OPHRYS* POLLINATION

A great diversity of epidermal cell types was found in the adaxial surface of the labellum in each investigated *Ophrys* species, which varied between 3 different cell types in *O. fusca* and *O. lutea* and 11 cell types in *O. bombyliflora* (Chapters 2–5), following three criteria, i.e. the curvature of the outer cell wall, the cell outline and the cuticular sculpture (Koch, Bhushan & Barthlott, 2008). In total, 18 different types of epidermal cells have been distinguished in the labella of *Ophrys* species, which represents a cell diversity that largely surpasses that occurring in the labellum of other orchids of the same subtribe Orchidinae (Box *et al.*, 2008; Barone Lumaga *et al.*, 2012; Bateman *et al.*, 2013). Epidermal cells were found to vary between four major groups in terms of general shape, i.e. flat-lenticular cells, domed-shaped papillae, short trichomes and long trichomes, which present either a smooth or striated cell surface (Chapters 2–5). Through a detailed comparative micromorphological analysis of the seven studied taxa we were able to distinguish objectively not only the labellum from the contiguous stigmatic cavity (Chapters 3 and 5) but also the major areas occurring in the adaxial surface of the labellum and the stigmatic cavity (Chapters 2–5), which allowed the establishment of homology between the floral parts based on three criteria of homology assessment, i.e. similarity in relative position, sharing a common special feature and/or the occurrence of intermediate forms (Sattler, 1994; Chin *et al.*, 2013).

The stigmatic cavity of *Ophrys* flowers is generally hemispherical, comprising a flat floor flanked by the cavity walls, whose inferior portion was found to extend to form prominent labia in *O. bombyliflora*, *O. tenthredinifera* and *O. speculum* (Chapter 5). It is typically glabrous and ornamented with temporal and staminodial callosities besides pseudoeyes, which exhibit flat-lenticular cells with a smooth cell wall surface or a finely diffuse cuticular pattern (Chapters 2–5). The floor of the stigmatic cavity presents consistently densely-striated flat-lenticular cells with an elongated polygonal outline in all studied species apart from *O. fusca* and *O. lutea* (section *Pseudophrys*), two species that present a contrasting spherical stigmatic cavity with no pseudoeyes, callosities or labia, besides the floor is placed in a depression (Chapters 2 and 5).

The labellum of the studied *Ophrys* species comprises two flat or prominent lateral lobes and a central lobe, which ends with an apical appendix in three species and is provided with an apical notch, except in *O. bombyliflora* and *O. scolopax* (Chapters 3 and 5). The labellum can also be divided into three main regions, i.e. basal (which is contiguous to the stigmatic cavity), median and apical regions (Chapters 2–5). Six major areas were

generally recognized in the labellum of each *Ophrys* species: (1) the basal field, which is clearly differentiated in all studied species except *O. fusca* and *O. lutea* (Chapters 2, 3 and 5), although in *O. speculum* it presents a singular position and configuration (Chapter 4); (2) the speculum, which presents flat-lenticular cells, papillae and/or short to intermediate narrow trichomes, depending on the species, but that have a flattened polygonal base in common (Chapters 2–5), a feature that might be related to a better reflection of incident light (Kay, Daoud & Stirton, 1981); (3) the lateral lobes, which are mostly covered with a dense indumentum of long trichomes, either attenuate (in *O. fusca* and *O. lutea*) or contorted (Chapters 2–5); (4) the median-apical indumentum, composed of long attenuate trichomes in all species, although in *O. bombyliflora* and *O. tenthredinifera* it also includes short conical trichomes (Chapter 3); (5) the glabrous margin, occurring consistently in all *Ophrys* species, although its extent differs from species to species (Chapter 5), which is composed of dome-shaped papillae, except in *O. bombyliflora*, the species that presents the widest glabrous labellum margin consisting entirely of flat-lenticular cells (Chapter 3); and (6) the apical appendix, which is only present in *O. bombyliflora*, *O. tenthredinifera* and *O. scolopax* (Chapters 3 and 5).

Such comparative study provided hence accurate micromorphological information which was incorporated into a morpho-anatomical data matrix that was subsequently used as the basis for reconstructing the phylogenetic interspecific relationships and the ancestral states of floral characters in the unresolved clade of *Ophrys* under analysis (Chapter 5). However, we are aware that the homology between two structures or areas of the flower, as well as the precise delimitation of the stigmatic cavity, could only be definitely established by means of ontogenetic studies (Luo & Chen, 2000; Vaes *et al.*, 2006; Box *et al.*, 2008; Thomas *et al.*, 2009). Considering that the assessment of homology is the basis of any character definition (Kearney & Rieppel, 2006; Nixon & Carpenter, 2012), phylogenetic inferences based on truly homologous characters would be comparatively more robust and reliable.

On the other hand, the great diversity of epidermal cell types found in the adaxial surface of the labellum of *Ophrys* species, which contrasts deeply with the homogeneous abaxial labellum surface composed of pavement cells across nearly all its extent (Chapters 2 and 3), leads us to suppose that the specific arrangement of the different cell types in the adaxial labellum surface should play a significant role in pollination by providing the crucial tactile stimulus for insect pollinators to accomplish the necessary copulatory attempts with the labellum that assure the effectiveness of pollination, in accordance with the findings of previous field experiments (Kullenberg, 1961; Kullenberg & Bergström, 1976; Kullenberg *et al.*, 1984). Indeed, the key combination of certain types of trichomes (or special papillae) arranged into a particular pattern with a robust, three-dimensional structure of appropriate size that tactilely simulates the body of a female insect is shared apparently by all species pollinated by sexual deception described so far (Ågren, Kullenberg & Sensenbaugh, 1984;

Singer *et al.*, 2004; Blanco & Barboza, 2005; Ciotek *et al.*, 2006; Davies & Stpiczyńska, 2006; Thomas *et al.*, 2009; Ellis & Johnson, 2010; Gaskett & Herberstein, 2010; Vereecken *et al.*, 2012; Phillips *et al.*, 2013; Phillips *et al.*, 2014). The tactile signal provided by the contrasting configuration of the labellum and the stigmatic cavity in some sympatric *Ophrys* species that share the same insect pollinator, as is the case of *O. fusca* and *O. sphegodes*, determines the different positioning of the insect upon the labellum so that an abdominal or cephalic pseudocopulation could take place (Chapters 2 and 3), hence providing an effective mechanical reproductive isolation barrier which prevents hybridization (Stökl *et al.*, 2005; Schiestl & Schlüter, 2009), although a few exceptions have been reported (Cortis *et al.*, 2009; Vereecken, Cozzolino & Schiestl, 2010).

Furthermore, some floral features in the studied *Ophrys* species were found to present a remarkable similarity to certain parts of the body of female insects and could thus constitute new evidences of visual mimicry, like several details of the stigmatic cavity, basal labellum region and speculum of *O. speculum*, which mimic the macro- and microstructure of the crossed wings of the female of its specific pollinator, the *Dasyscolia ciliata* wasp (Chapter 4). The speculum of this *Ophrys* species, especially its strong UV-reflectance, seems to play a decisive role in the short-range attraction of male insect pollinators to the flower (Kullenberg, 1961; Paulus, 2006). The role of visual signals in pollinator attraction and in reproductive success of *Ophrys* orchids has been tested only for a few species and hence requires further investigation (Kullenberg, 1961; Paulus, 2006; Spaethe, Moser & Paulus, 2007; Streinzer, Paulus & Spaethe, 2009; Vereecken & Schiestl, 2009; Spaethe, Streinzer & Paulus, 2010; Streinzer *et al.*, 2010; Rakosy *et al.*, 2012). It has become apparent that the importance of visual cues differs among insect genera and seems to be related to the sensory system and mate searching behaviour of each insect genus (Spaethe *et al.*, 2010). For instance, males of solitary bees of genus *Eucera*, which are regular pollinators of *O. bombyliflora*, *O. tenthredinifera* and *O. scolopax* among others, rely strongly on visual signals to recognize their females, and therefore are able to use the typical coloured perianth of these *Ophrys* species as a stimulus that increases the flower detectability at short distances (Streinzer *et al.*, 2009; Spaethe *et al.*, 2010). In contrast, for males of solitary bees of genus *Andrena*, which pollinate most species of the section *Pseudophrys*, such as *O. fusca* and *O. lutea*, the vision seems to be of little importance during the mate search and detection, which is clearly dominated by olfaction, even at close distances from the female and *Ophrys* flower (Kullenberg, 1961; Vereecken & Schiestl, 2009; Spaethe *et al.*, 2010).

Therefore, the three-dimensional configuration and extraordinary complexity of the labellum of *Ophrys* flowers, reflected in the great number of different epidermal cell types arranged into specific patterns which originate well-defined areas throughout the adaxial surface of the labellum and the contiguous stigmatic cavity of each species, should provide both visual and tactile stimuli for their pollinators, which reinforce the key odour signal and

contribute decisively towards the success of pollination by sexual deception of *Ophrys* species (Kullenberg & Bergström, 1976).

OPHRYS PHYLOGENY AND FLORAL TRAIT EVOLUTION

Our morphological phylogenetic analysis of the clade of *Ophrys* formed by *O. bombyliflora*, *O. tenthredinifera*, *O. speculum* and the section *Pseudophrys* (which includes *O. fusca* and *O. lutea*) provided some insights into the phylogenetic relationships between these species (Chapter 5). Two tree topologies were found as the most likely reconstructions of the investigated clade of *Ophrys*, which concur in the placement of *O. speculum* as sister to *O. bombyliflora* but differ in the position of *O. tenthredinifera*, which was placed alternatively as sister to the pairing of *O. speculum* with *O. bombyliflora* or as sister to section *Pseudophrys* (Chapter 5). One of the major contributions of our morphological cladistic analysis was the disclosure of the floral character states (synapomorphies) that confer support to the groups found in the phylogenetic trees, which constitutes an advantage that no molecular phylogenetic analysis is able to present (Freudenstein & Rasmussen, 1999; Rudall, 2002; Rudall & Bateman, 2006; Nürk & Blattner, 2010; Ronse De Craene & Wanntorp, 2011). The sister relationship between *O. speculum* and *O. bombyliflora*, which received a moderate support level in our Bayesian analyses, was found to be supported by four synapomorphies pertaining mainly to the stigmatic cavity, namely the differentiation of staminodial callosities from staminodial points, the occurrence of prominent external labia, the presence of high protrusions of the inferior portion of the cavity walls, and the low median height of the non-flat cells in the speculum (Chapter 5). The ambiguous placement of *O. tenthredinifera* in the tree, however, is due to the fact that six valid synapomorphies support the cluster of *O. tenthredinifera* with *O. speculum–O. bombyliflora* and other six synapomorphies confer support to the alternative pairing of *O. tenthredinifera* with section *Pseudophrys* (Chapter 5). Four out of the six synapomorphies that favour the former association pertain again to the stigmatic cavity, and a seventh novel diagnostic feature, i.e. the forward projection of the floor of the stigmatic cavity, which is intimately associated with extension of the inferior portion of the cavity walls to form prominent internal labia, was also proposed as an additional synapomorphy for this particular cluster (Chapter 5). In contrast, the alternative placement of *O. tenthredinifera* as sister to section *Pseudophrys* was supported by two derived character states pertaining to the speculum (the presence of intermediate trichomes with more than 40 μm in height and a median non-flat cell height of 27.4 μm), two features connected with the osmophore (the nearly complete restriction of the secretory tissues to the abaxial side and their extension to the apical labellum surface), the absence of flat-lenticular cells in the lateral labellum lobes, besides the occurrence of inconspicuous staminodial points in the stigmatic cavity (Chapter 5).

The most likely phylogenetic trees obtained from our analysis (trees 2 and 5; Chapter 5) favour the existing molecular trees based on the analysis of nuclear ITS data, separately or combined with plastid and/or mitochondrial datasets (Bateman, Pridgeon & Chase, 1997; Bateman *et al.*, 2003; Devey *et al.*, 2008; Inda, Pimentel & Chase, 2012; Vereecken *et al.*, 2012), and rejects both the single existing morphological cladistic hypothesis (Devillers & Devillers-Terschuren, 1994) and the molecular phylogenetic trees based exclusively on plastid data (Soliva, Kocyan & Widmer, 2001; Devey *et al.*, 2008; Inda *et al.*, 2012). Furthermore, our hypothesis is also relatively congruent with a recent molecular phylogenetic analysis performed with 37 species of genus *Ophrys*, based on six nuclear loci, which found a comparatively better resolution and stronger support levels for the relationships in the major clades of *Ophrys* (Breitkopf *et al.*, 2015). According to this recent molecular phylogenetic tree, which presented exactly the same topology as our suboptimal tree 6 for the investigated clade of *Ophrys* (Chapter 5), *O. speculum* was placed as basally divergent in the clade and was followed by *O. bombyliflora* which in turn was sister to the cluster of *O. tenthredinifera* and section *Pseudophrys*, all nodes receiving strong support level (Breitkopf *et al.*, 2015). Two major aspects emerge thus from the comparison of this molecular tree with our morphological phylogenetic hypothesis. On the one hand, the sister relationship between *O. tenthredinifera* and section *Pseudophrys* was favoured, which resolved the ambiguity in the position of *O. tenthredinifera* found in our analyses (Chapter 5) and in previous molecular phylogenetic analyses (Bateman *et al.*, 1997; Soliva *et al.*, 2001; Bateman *et al.*, 2003; Devey *et al.*, 2008). Our cladistic analysis revealed that this association has a solid underlying morpho-anatomical basis of six valid synapomorphies, as mentioned above. On the other hand, the molecular tree by Breitkopf *et al.* (2015) suggests that *O. speculum* is an early-diverging lineage placed at the base of the clade, whereas section *Pseudophrys* is the most recent divergent group of species of this clade of *Ophrys*, which represents the reverse of the branching sequence of our tree 5 but that is not totally incompatible with the topology of the other most plausible tree (tree 2) found in our analyses (Chapter 5). In fact, our tree 2 recovered two groups, namely *O. tenthredinifera*–section *Pseudophrys* and *O. speculum–O. bombyliflora*, whose divergence time was impossible to determine using our inference methods (Chapter 5).

Another benefit of our morphological phylogenetic analysis was the reconstruction of the ancestral character states for the putative most recent common ancestor of the investigated clade of *Ophrys*, which revealed the most parsimonious evolutionary trend of 29 morpho-anatomical floral characters, whose plesiomorphic states were found to be unambiguous (Chapter 5). For instance, an apical appendix and an osmophore occurring in the apical third of the labellum margin with abundant starch in the subepidermal parenchyma tissue have been already unequivocally present in the ancestor of our clade of interest. An osmophore was observed in the labellum of all investigated *Ophrys* taxa, including the distantly related *O. scolopax* used here as outgroup (Chapters 2–5), and also in

the labellum of a few species of five genera of the subtribe Orchidinae (Vogel, 1990; Stpiczyńska, 2001; Barone Lumaga *et al.*, 2012; Kowalkowska *et al.*, 2012). Therefore, the occurrence of an osmophore in the labellum is a putative plesiomorphic feature that may have been already present in the most recent common ancestor of genus *Ophrys*, an hypothesis that could only be tested if morpho-anatomical information on *O. insectifera*, a distantly related species whose phylogenetic placement in the tree is still uncertain (Bateman *et al.*, 1997; Soliva *et al.*, 2001; Devey *et al.*, 2008; Inda *et al.*, 2012; Vereecken *et al.*, 2012; Breitkopf *et al.*, 2015), is added to the data matrix.

For the other 16 floral characters that were found to have an ambiguous plesiomorphic state, we have considered as the most plausible the ancestral state that the two most likely tree topologies obtained in our cladistic analysis (trees 2 and 5) have in common, in order to trace their evolutionary trend (Chapter 5). When we contrast these ancestral character states with those reconstructed for our suboptimal tree 6, which presents the same topology as the molecular tree by Breitkopf *et al.* (2015), we notice that the majority of them differs among trees, in particular those pertaining to the stigmatic cavity, which were synapomorphies for the groups recovered in our tree 5 (Chapter 5) and plesiomorphies for the clade in the suboptimal tree 6, because of the reverse sequence of divergence episodes that the molecular tree represents.

Therefore, it would be important to perform an expanded morphological analysis of the whole genus *Ophrys* by incorporating data of additional taxa, particularly *O. insectifera*, and to combine morphological and molecular data in future phylogenetic studies so that an increasing accurate picture of the phylogenetics and floral character evolution in genus *Ophrys* could be traced (Bateman, Hilton & Rudall, 2006).

CONCLUSIONS

The major conclusions of the present thesis can be summarized as follows:

1. A secretory structure specialized in the synthesis and emission of a volatile fragrance – an osmophore – occurs consistently in the apical region of the labellum in the seven investigated *Ophrys* taxa. More specifically, the osmophore is located at the labellum margin and/or in the apical appendix, extending to the abaxial surface of the apical region of the labellum in *O. tenthredinifera*, *O. fusca* and *O. lutea*, and also occupying the entire margins of the labellum and the lateral petals in these two latter species.
2. The occurrence of a functional osmophore in all investigated species indicates that it should play an important role in *Ophrys* pollination. We propose that the osmophore synthesizes highly volatile long-range pollinator attractants, which are

complementary to the cuticular waxes spread over the labellum surface for the success of pollination by sexual deception.

3. A great diversity of epidermal cell types occurs in the adaxial surface of the labellum of each studied *Ophrys* taxa, and the specific arrangement of the different cell types probably provides a significant tactile stimulus for insect pollinators to accomplish the necessary copulatory attempts with the labellum that assure the effectiveness of pollination.
4. A detailed comparative micromorphological analysis allowed us to distinguish objectively different regions in the labellum and in the contiguous stigmatic cavity of *Ophrys* flowers, and thus establish potential homologies between floral parts of the seven studied taxa.
5. The morphological phylogenetic analysis of the investigated clade of *Ophrys*, based on a data matrix built using objective and explicit criteria for character selection, coding and state definition, showed that *O. tenthredinifera* and *O. bombyliflora* are not sister groups and pointed to a sister relationship between *O. speculum* and *O. bombyliflora*, which rejects an earlier morphological cladistic hypothesis and favours the existing molecular phylogenetic trees based on nuclear ITS data (alone or combined), but not those based exclusively on plastid data.

FUTURE DIRECTIONS

The present thesis represents a significant step towards a better understanding of the flower structure, pollinator attraction, phylogenetic relationships and floral trait evolution in a group of closely related species of the orchid genus *Ophrys*. However, our study also highlighted some important points that require further investigation at four fundamental levels.

At the cellular level, an ultrastructural study is needed to elucidate the mode of biosynthesis, transport and elimination of the terpene-rich lipophilic secretion in the osmophores of *Ophrys*, in particular by finding evidences for the cell compartments involved in the secretory pathways, which we predict that are mainly smooth endoplasmic reticulum intimately associated with plastids and mitochondria (Croteau, Kutchan & Lewis, 2000; Dudareva *et al.*, 2006; Lichtenthaler, 2010), and for sites of intracellular secretion accumulation.

At the micromorphological level, it would be fundamental to perform ontogenetic studies of the *Ophrys* flowers to demonstrate definitively the homology between the different regions and structures of the labellum and the stigmatic cavity, in order to confer robustness to phylogenetic inferences. Also, micromorphological information of the flowers of both an increased number of *Ophrys* taxa and a larger number of individuals sampled per taxon is needed as a basis for improving our morpho-anatomical data matrix and for evaluating intraspecific variation.

At the evolutionary level, a better understanding of both the phylogenetic relationships in all major clades of genus *Ophrys* and the evolutionary trends of floral features would be achieved with an integrated phylogenetic analysis combining molecular data from nuclear loci and morpho-anatomical data from a solid data matrix like the one presented here, but that incorporates information of the most representative taxa of each group of species of the whole genus *Ophrys*.

At the chemo-ecological level, several lines of future research could be implemented in order to improve our knowledge about pollination by sexual deception in *Ophrys* orchids. First, it would be crucial to identify the insect pollinators of *Ophrys* species in Portugal and to discover the specific pollinator of the Iberian endemic *O. speculum* subsp. *lusitanica*, which remains unknown. Second, it would be needed to characterize the female sex pheromone used by *Ophrys* male pollinators for reproduction, especially that which is used by species of solitary bees of genus *Eucera* (not yet identified), and compare it with the odour compounds released by *Ophrys* flowers, in order to identify the key semiochemicals involved in the attraction of male pollinators. Third, the labellum margin and/or the appendix, on the one hand, and the labellum surface, on the other, of each *Ophrys* species should be analyzed separately by solvent extraction, to find out differences in the compounds occurring in the cuticle of each of these two labellum regions. Fourth, behavioural tests with insect pollinators of *Ophrys* are required to test if the volatility of compounds influences not only their dispersion under natural conditions, but also the effective attraction of specific pollinators in the field. Lastly, it would be important to test if intraspecific variation in some morphological floral features (e.g. labellum size, speculum colouration and configuration) among *Ophrys* populations is linked with the attraction of different pollinators and affects the reproductive success of each *Ophrys* population.

REFERENCES

Ågren L, Kullenberg B, Sensenbaugh T. 1984. Congruences in pilosity between three species of *Ophrys* (Orchidaceae) and their hymenopteran pollinators. *Nova Acta Regiae Societatis Scientiarum Upsaliensis, Serie V:C* **3:** 15-25.

Ayasse M, Paxton RJ, Tengö J. 2001. Mating behavior and chemical communication in the order Hymenoptera. *Annual Review of Entomology* **46:** 31-78.

Ayasse M, Schiestl FP, Paulus HF, Ibarra F, Francke W. 2003. Pollinator attraction in a sexually deceptive orchid by means of unconventional chemicals. *Proceedings of the Royal Society B: Biological Sciences* **270:** 517-522.

Ayasse M, Stökl J, Francke W. 2011. Chemical ecology and pollinator-driven speciation in sexually deceptive orchids. *Phytochemistry* **72:** 1667-1677.

Barone Lumaga MR, Pellegrino G, Bellusci F, Perrotta E, Perrotta I, Musacchio A. 2012. Comparative floral micromorphology in four sympatric species of *Serapias* (Orchidaceae). *Botanical Journal of the Linnean Society* **169:** 714-724.

Bateman RM, Pridgeon AM, Chase MW. 1997. Phylogenetics of subtribe Orchidinae (Orchidoideae, Orchidaceae) based on nuclear ITS sequences. 2. Infrageneric

relationships and reclassification to achieve monophyly of *Orchis sensu stricto*. *Lindleyana* **12:** 113-141.

Bateman RM, Hollingsworth PM, Preston J, Yi-Bo L, Pridgeon AM, Chase MW. 2003. Molecular phylogenetics and evolution of Orchidinae and selected Habenariinae (Orchidaceae). *Botanical Journal of the Linnean Society* **142:** 1-40.

Bateman RM, Hilton J, Rudall PJ. 2006. Morphological and molecular phylogenetic context of the angiosperms: contrasting the 'top-down' and 'bottom-up' approaches used to infer the likely characteristics of the first flowers. *Journal of Experimental Botany* **57:** 3471-3503.

Bateman RM, Bradshaw E, Devey DS, Glover BJ, Malmgren S, Sramkó G, Thomas MM, Rudall PJ. 2011. Species arguments: clarifying competing concepts of species delimitation in the pseudo-copulatory orchid genus *Ophrys*. *Botanical Journal of the Linnean Society* **165:** 336-347.

Bateman RM, Rudall PJ, Hawkins JA, Sramkó G. 2013. *Himantoglossum hircinum* (Lizard Orchid) reviewed in the light of new morphological and molecular observations. *New Journal of Botany* **3:** 122-140.

Blanco MA, Barboza G. 2005. Pseudocopulatory pollination in *Lepanthes* (Orchidaceae: Pleurothallidinae) by fungus gnats. *Annals of Botany* **95:** 763-772.

Blomquist GJ, Bagnères A-G. 2010. Introduction: history and overview of insect hydrocarbons. In: Blomquist GJ, Bagnères A-G, eds. *Insect hydrocarbons. Biology, biochemistry, and chemical ecology.* Cambridge: Cambridge University Press, 3-18.

Bolin JF, Maass E, Musselman LJ. 2009. Pollination biology of *Hydnora africana* Thunb. (Hydnoraceae) in Namibia: brood-site mimicry with insect imprisonment. *International Journal of Plant Sciences* **170:** 157-163.

Borba EL, Salazar GA, Mazzoni-Viveiros S, Batista JAN. 2014. Phylogenetic position and floral morphology of the Brazilian endemic, monospecific genus *Cotylolabium*: a sister group for the remaining Spiranthinae (Orchidaceae). *Botanical Journal of the Linnean Society* **175:** 29-46.

Borg-Karlson A-K. 1990. Chemical and ethological studies of pollination in the genus *Ophrys* (Orchidaceae). *Phytochemistry* **29:** 1359-1387.

Box MS, Bateman RM, Glover BJ, Rudall PJ. 2008. Floral ontogenetic evidence of repeated speciation via paedomorphosis in subtribe Orchidinae (Orchidaceae). *Botanical Journal of the Linnean Society* **157:** 429-454.

Breitkopf H, Onstein RE, Cafasso D, Schlüter PM, Cozzolino S. 2015. Multiple shifts to different pollinators fuelled rapid diversification in sexually deceptive *Ophrys* orchids. *New Phytologist* **207:** 377-389.

Chin S-w, Lutz S, Wen J, Potter D. 2013. The bitter and the sweet: inference of homology and evolution of leaf glands in *Prunus* (Rosaceae) through anatomy, micromorphology, and ancestral–character state reconstruction. *International Journal of Plant Sciences* **174:** 27-46.

Ciotek L, Giorgis P, Benitez-Vieyra S, Cocucci AA. 2006. First confirmed case of pseudocopulation in terrestrial orchids of South America: pollination of *Geoblasta pennicillata* (Orchidaceae) by *Campsomeris bistrimacula* (Hymenoptera, Scoliidae). *Flora* **201:** 365-369.

Cortis P, Vereecken NJ, Schiestl FP, Lumaga MRB, Scrugli A, Cozzolino S. 2009. Pollinator convergence and the nature of species' boundaries in sympatric Sardinian *Ophrys* (Orchidaceae). *Annals of Botany* **104:** 497-506.

Croteau R, Kutchan TM, Lewis NG. 2000. Natural products (secondary metabolites). In: Buchanan BB, Gruissem W, Jones RL, eds. *Biochemistry and molecular biology of plants.* Rockville, Maryland: American Society of Plant Biologists, 1250-1318.

Davies KL, Stpiczyńska M. 2006. Labellar micromorphology of Bifrenariinae Dressler (Orchidaceae). *Annals of Botany* **98:** 1215-1231.

Devey DS, Bateman RM, Fay MF, Hawkins JA. 2008. Friends or relatives? Phylogenetics and species delimitation in the controversial European orchid genus *Ophrys*. *Annals of Botany* **101:** 385-402.

Devillers P, Devillers-Terschuren J. 1994. Essai d'analyse systématique du genre *Ophrys*. *Les Naturalistes belges* **75 (Orchidées 7):** 273-400.

Dudareva N, Negre F, Nagegowda DA, Orlova I. 2006. Plant volatiles: recent advances and future perspectives. *Critical Reviews in Plant Sciences* **25:** 417-440.

Ellis AG, Johnson SD. 2010. Floral mimicry enhances pollen export: the evolution of pollination by sexual deceit outside of the Orchidaceae. *The American Naturalist* **176:** E143–E151.

Franceschi VR, Nakata PA. 2005. Calcium oxalate in plants: formation and function. *Annual Review of Plant Biology* **56:** 41-71.

Freudenstein JV, Rasmussen FN. 1999. What does morphology tell us about orchid relationships? A cladistic analysis. *American Journal of Botany* **86:** 225-248.

Gaskett AC, Herberstein ME. 2010. Colour mimicry and sexual deception by Tongue orchids (*Cryptostylis*). *Naturwissenschaften* **97:** 97-102.

Heiduk A, Brake I, Tolasch T, Frank J, Jürgens A, Meve U, Dötterl S. 2010. Scent chemistry and pollinator attraction in the deceptive trap flowers of *Ceropegia dolichophylla*. *South African Journal of Botany* **76:** 762-769.

Inda LA, Pimentel M, Chase MW. 2012. Phylogenetics of tribe Orchideae (Orchidaceae: Orchidoideae) based on combined DNA matrices: inferences regarding timing of diversification and evolution of pollination syndromes. *Annals of Botany* **110:** 71-90.

Kaiser R. 1993. *The scent of orchids - olfactory and chemical investigations.* Amsterdam: Elsevier Science Publishers B.V.

Kay QON, Daoud HS, Stirton CH. 1981. Pigment distribution, light reflection and cell structure in petals. *Botanical Journal of the Linnean Society* **83:** 57-84.

Kearney M, Rieppel O. 2006. Rejecting "the given" in systematics. *Cladistics: The International Journal of the Willi Hennig Society* **22:** 369-377.

Koch K, Bhushan B, Barthlott W. 2008. Diversity of structure, morphology and wetting of plant surfaces. *Soft Matter* **4:** 1943-1963.

Kowalkowska A, Margońska H, Kozieradzka-Kiszkurno M, Bohdanowicz J. 2012. Studies on the ultrastructure of a three-spurred *fumeauxiana* form of *Anacamptis pyramidalis*. *Plant Systematics and Evolution* **298:** 1025-1035.

Kullenberg B. 1961. Studies in *Ophrys* pollination. *Zoologiska Bidrag fran Uppsala* **34:** 1-340.

Kullenberg B, Bergström G. 1976. Hymenoptera Aculeata males as pollinators of *Ophrys* orchids. *Zoologica Scripta* **5:** 13-23.

Kullenberg B, Borg-Karlson A-K, Kullenberg A-L. 1984. Field studies on the behaviour of the *Eucera nigrilabris* male in the odour flow from flower labellum extract of *Ophrys tenthredinifera*. *Nova Acta Regiae Societatis Scientiarum Upsaliensis, Serie V:C* **3:** 79-110.

Lichtenthaler HK. 2010. Biosynthesis and emission of isoprene, methylbutanol and other volatile plant isoprenoids. In: Herrmann A, ed. *The chemistry and biology of volatiles.* Chichester, West Sussex, UK: John Wiley & Sons Ltd., 11-48.

Luo Y-B, Chen S-C. 2000. The floral morphology and ontogeny of some Chinese representatives of orchid subtribe Orchidinae. *Botanical Journal of the Linnean Society* **134:** 529-548.

Mant JG, Brändli C, Vereecken NJ, Schulz CM, Francke W, Schiestl FP. 2005. Cuticular hydrocarbons as sex pheromone of *Colletes cunicularius* (Hymenoptera: Colletidae) and the key to its mimicry by the sexually deceptive orchid, *Ophrys exaltata*. *Journal of Chemical Ecology* **31:** 1765-1787.

Melo MC, Borba EL, Paiva EAS. 2010. Morphological and histological characterization of the osmophores and nectaries of four species of *Acianthera* (Orchidaceae: Pleurothallidinae). *Plant Systematics and Evolution* **286:** 141-151.

Mori K. 2010. Pheromones in chemical communication. In: Herrmann A, ed. *The chemistry and biology of volatiles.* Chichester, West Sussex, UK: John Wiley & Sons Ltd., 123-150.

van der Niet T, Hansen DM, Johnson SD. 2011. Carrion mimicry in a South African orchid: flowers attract a narrow subset of the fly assemblage on animal carcasses. *Annals of Botany* **107:** 981-992.

Nixon KC, Carpenter JM. 2012. On homology. *Cladistics: The International Journal of the Willi Hennig Society* **28:** 160-169.

Nürk NM, Blattner FR. 2010. Cladistic analysis of morphological characters in *Hypericum* (Hypericaceae). *Taxon* **59:** 1495-1507.

Paiva EAS, Machado SR. 2005. Role of intermediary cells in *Peltodon radicans* (Lamiaceae) in the transfer of calcium and formation of calcium oxalate crystals. *Brazilian Archives of Biology and Technology* **48:** 147-153.

Pansarin LM, de Moraes Castro M, Sazima M. 2009. Osmophore and elaiophores of *Grobya amherstiae* (Catasetinae, Orchidaceae) and their relation to pollination. *Botanical Journal of the Linnean Society* **159:** 408-415.

Pansarin LM, Pansarin ER, Sazima M. 2014. Osmophore structure and phylogeny of *Cirrhaea* (Orchidaceae, Stanhopeinae). *Botanical Journal of the Linnean Society* **176:** 369-383.

Paulus HF, Gack C. 1990. Pollinators as prepollinating isolation factors: evolution and speciation in *Ophrys* (Orchidaceae). *Israel Journal of Botany* **39:** 43-79.

Paulus HF. 2006. Deceived males - Pollination biology of the Mediterranean orchid genus *Ophrys* (Orchidaceae). *Journal Europäischer Orchideen* **38:** 303-353.

Peter CI, Coombs G, Huchzermeyer CF, Venter N, Winkler AC, Hutton D, Papier LA, Dold AP, Johnson SD. 2009. Confirmation of hawkmoth pollination in *Habenaria epipactidea*: leg placement of pollinaria and crepuscular scent emission. *South African Journal of Botany* **75:** 744-750.

Phillips RD, Xu T, Hutchinson MF, Dixon KW, Peakall R. 2013. Convergent specialization - the sharing of pollinators by sympatric genera of sexually deceptive orchids. *Journal of Ecology* **101:** 826-835.

Phillips RD, Scaccabarozzi D, Retter BA, Hayes C, Brown GR, Dixon KW, Peakall R. 2014. Caught in the act: pollination of sexually deceptive trap-flowers by fungus gnats in *Pterostylis* (Orchidaceae). *Annals of Botany* **113:** 629-641.

Possobom CCF, Guimarães E, Machado SR. 2015. Structure and secretion mechanisms of floral glands in *Diplopterys pubipetala* (Malpighiaceae), a neotropical species. *Flora* **211:** 26-39.

Pridgeon AM, Stern WL. 1983. Ultrastructure of osmophores in *Restrepia* (Orchidaceae). *American Journal of Botany* **70:** 1233-1243.

Pridgeon AM, Stern WL. 1985. Osmophores of *Scaphosepalum* (Orchidaceae). *Botanical Gazette* **146:** 115-123.

Rakosy D, Streinzer M, Paulus H, Spaethe J. 2012. Floral visual signal increases reproductive success in a sexually deceptive orchid. *Arthropod-Plant Interactions* **6:** 671-681.

Ronse De Craene LP, Wanntorp L. 2011. Introduction: establishing the state of the art - the role of morphology in plant systematics. In: Wanntorp L, Ronse De Craene LP, eds. *Flowers on the tree of life. Systematics Association Special Volume Series, vol. 80.* New York, USA: Cambridge University Press, 1-7.

Rudall P. 2002. Unique floral structures and iterative evolutionary themes in Asparagales: Insights from a morphological cladistic analysis. *The Botanical Review* **68:** 488-509.

Rudall PJ, Bateman RM. 2006. Morphological phylogenetic analysis of Pandanales: testing contrasting hypotheses of floral evolution. *Systematic Botany* **31:** 223-238.

Sanguinetti A, Buzatto CR, Pedron M, Davies KL, Ferreira PMdA, Maldonado S, Singer RB. 2012. Floral features, pollination biology and breeding system of *Chloraea membranacea* Lindl. (Orchidaceae: Chloraeinae). *Annals of Botany* **110:** 1607-1621.

Sattler R. 1994. Homology, homeosis, and process morphology in plants. In: Hall BK, ed. *Homology: the hierarchical basis of comparative biology.* San Diego, CA, USA: Academic Press, 424-476.

Sazima M, Vogel S, Cocucci AA, Hausner G. 1993. The perfume flowers of *Cyphomandra* (Solanaceae): pollination by euglossine bees, bellows mechanism, osmophores, and volatiles. *Plant Systematics and Evolution* **187:** 51-88.

Schiestl FP, Ayasse M, Paulus HF, Erdmann D, Francke W. 1997. Variation of floral scent emission and postpollination changes in individual flowers of *Ophrys sphegodes* subsp. *sphegodes*. *Journal of Chemical Ecology* **23:** 2881-2895.

Schiestl FP, Ayasse M, Paulus HF, Löfstedt C, Hansson BS, Ibarra F, Francke W. 1999. Orchid pollination by sexual swindle. *Nature* **399:** 421-422.

Schiestl FP, Ayasse M, Paulus HF, Löfstedt C, Hansson BS, Ibarra F, Francke W. 2000. Sex pheromone mimicry in the early spider orchid (*Ophrys sphegodes*): patterns of hydrocarbons as the key mechanism for pollination by sexual deception. *Journal of Comparative Physiology A* **186:** 567-574.

Schiestl FP, Ayasse M. 2002. Do changes in floral odor cause speciation in sexually deceptive orchids? *Plant Systematics and Evolution* **234:** 111-119.

Schiestl FP, Schlüter PM. 2009. Floral isolation, specialized pollination, and pollinator behavior in orchids. *Annual Review of Entomology* **54:** 425-446.

Schlüter PM, Xu S, Gagliardini V, Whittle E, Shanklin J, Grossniklaus U, Schiestl FP. 2011. Stearoyl-acyl carrier protein desaturases are associated with floral isolation in sexually deceptive orchids. *Proceedings of the National Academy of Sciences of the United States of America* **108:** 5696-5701.

Singer RB, Flach A, Koehler S, Marsaioli AJ, Amaral MCE. 2004. Sexual mimicry in *Mormolyca ringens* (Lindl.) Schltr. (Orchidaceae: Maxillariinae). *Annals of Botany* **93:** 755-762.

Skubatz H, Kunkel DD, Meeuse BJD. 1993. Ultrastructural changes in the appendix of the *Sauromatum guttatum* inflorescence during anthesis. *Sexual Plant Reproduction* **6:** 153-170.

Skubatz H, Kunkel DD, Howald WN, Trenkle R, Mookherjee B. 1996. The *Sauromatum guttatum* appendix as an osmophore: excretory pathways, composition of volatiles and attractiveness to insects. *New Phytologist* **134:** 631-640.

Soliva M, Kocyan A, Widmer A. 2001. Molecular phylogenetics of the sexually deceptive orchid genus *Ophrys* (Orchidaceae) based on nuclear and chloroplast DNA sequences. *Molecular Phylogenetics and Evolution* **20:** 78-88.

Spaethe J, Moser WH, Paulus HF. 2007. Increase of pollinator attraction by means of a visual signal in the sexually deceptive orchid, *Ophrys heldreichii* (Orchidaceae). *Plant Systematics and Evolution* **264:** 31-40.

Spaethe J, Streinzer M, Paulus HF. 2010. Why sexually deceptive orchids have colored flowers. *Communicative and Integrative Biology* **3:** 139-141.

Steiger S, Schmitt T, Schaefer HM. 2011. The origin and dynamic evolution of chemical information transfer. *Proceedings of the Royal Society B: Biological Sciences* **278:** 970-979.

Stern WL, Curry KJ, Pridgeon AM. 1987. Osmophores of *Stanhopea* (Orchidaceae). *American Journal of Botany* **74:** 1323-1331.

Stökl J, Paulus HF, Dafni A, Schulz C, Francke W, Ayasse M. 2005. Pollinator attracting odour signals in sexually deceptive orchids of the *Ophrys fusca* group. *Plant Systematics and Evolution* **254:** 105-120.

Stökl J, Twele R, Erdmann DH, Francke W, Ayasse M. 2008. Comparison of the flower scent of the sexually deceptive orchid *Ophrys iricolor* and the female sex pheromone of its pollinator *Andrena morio*. *Chemoecology* **17:** 231-233.

Stökl J, Schlüter PM, Stuessy TF, Paulus HF, Fraberger R, Erdmann D, Schulz C, Francke W, Assum G, Ayasse M. 2009. Speciation in sexually deceptive orchids: pollinator-driven selection maintains discrete odour phenotypes in hybridizing species. *Biological Journal of the Linnean Society* **98:** 439-451.

Stpiczyńska M. 2001. Osmophores of the fragrant orchid *Gymnadenia conopsea* L. (Orchidaceae). *Acta Societatis Botanicorum Poloniae* **70:** 91-96.

Streinzer M, Paulus HF, Spaethe J. 2009. Floral colour signal increases short-range detectability of a sexually deceptive orchid to its bee pollinator. *The Journal of Experimental Biology* **212:** 1365-1370.

Streinzer M, Ellis T, Paulus HF, Spaethe J. 2010. Visual discrimination between two sexually deceptive *Ophrys* species by a bee pollinator. *Arthropod-Plant Interactions* **4:** 141-148.

Teixeira SP, Borba EL, Semir J. 2004. Lip anatomy and its implications for the pollination mechanisms of *Bulbophyllum* species (Orchidaceae). *Annals of Botany* **93:** 499-505.

Thomas MM, Rudall PJ, Ellis AG, Savolainen V, Glover BJ. 2009. Development of a complex floral trait: the pollinator-attracting petal spots of the beetle daisy, *Gorteria diffusa* (Asteraceae). *American Journal of Botany* **96:** 2184-2196.

Vaes E, Vrijdaghs A, Smets EF, Dessein S. 2006. Elaborate petals in Australian *Spermacoce* (Rubiaceae) species: morphology, ontogeny and function. *Annals of Botany* **98:** 1167-1178.

Vereecken NJ, Schiestl FP. 2009. On the roles of colour and scent in a specialized floral mimicry system. *Annals of Botany* **104:** 1077-1084.

Vereecken NJ, Cozzolino S, Schiestl FP. 2010. Hybrid floral scent novelty drives pollinator shift in sexually deceptive orchids. *BMC Evolutionary Biology* **10:** 103.

Vereecken NJ, Streinzer M, Ayasse M, Spaethe J, Paulus HF, Stökl J, Cortis P, Schiestl FP. 2011. Integrating past and present studies on *Ophrys* pollination – a comment on Bradshaw *et al*. *Botanical Journal of the Linnean Society* **165:** 329-335.

Vereecken NJ, Wilson CA, Hötling S, Schulz S, Banketov SA, Mardulyn P. 2012. Pre-adaptations and the evolution of pollination by sexual deception: Cope's rule of

specialization revisited. *Proceedings of the Royal Society B: Biological Sciences* **279:** 4786-4794.

Vogel S. 1990. *The role of scent glands in pollination: on the structure and function of osmophores.* Rotterdam: A. A. Balkema. [English translation of: Vogel S. 1963. Duftdrüsen im Dienste der Bestäubung: Über Bau und Funktion der Osmophoren. *Akademie der Wissenschaften und der Literatur in Mainz, Abhandlungen der Mathematisch-Naturwissenschaftlichen Klasse* **10**: 600-763].

Vogel S, Hadacek F. 2004. Contributions to the functional anatomy and biology of *Nelumbo nucifera* (Nelumbonaceae) III. An ecological reappraisal of floral organs. *Plant Systematics and Evolution* **249:** 173-189.

Wiemer AP, Moré M, Benitez-Vieyra S, Cocucci AA, Raguso RA, Sérsic AN. 2009. A simple floral fragrance and unusual osmophore structure in *Cyclopogon elatus* (Orchidaceae). *Plant Biology* **11:** 506-514.

Wyatt T. 2010. Pheromones and signature mixtures: defining species-wide signals and variable cues for identity in both invertebrates and vertebrates. *Journal of Comparative Physiology A* **196:** 685-700.

Xu S, Schlüter PM, Scopece G, Breitkopf H, Gross K, Cozzolino S, Schiestl FP. 2011. Floral isolation is the main reproductive barrier among closely related sexually deceptive orchids. *Evolution* **65:** 2606–2620.

Xu S, Schlüter PM, Grossniklaus U, Schiestl FP. 2012. The genetic basis of pollinator adaptation in a sexually deceptive orchid. *PLoS Genetics* **8:** e1002889. doi:10.1371/journal.pgen.1002889.

APPENDIX A

SUPPLEMENTARY DATA ON THE LABELLUM AND THE OSMOPHORE IN *OPHRYS FUSCA* AND *O. LUTEA*

APPENDIX A: SUPPLEMENTARY DATA ON THE LABELLUM AND THE OSMOPHORE IN *OPHRYS FUSCA* AND *O. LUTEA*

MATERIAL AND METHODS

PLANT MATERIAL

Inflorescences of *Ophrys fusca* Link subsp. *fusca* and *Ophrys lutea* Cav. were collected in February and March, between 2005 and 2009, from natural populations occurring throughout the central-western region of Portugal. A voucher specimen of each species was deposited in LISU, the Herbarium of the University of Lisbon Botanical Garden, Portugal (LISU 231244 and LISU 231505). The taxonomic classification adopted here follows Aldasoro & Sáez (2005). For the sake of simplicity, hereafter we use the name *O. fusca* to refer to *O. fusca* subsp. *fusca*.

Three different developmental stages of the flower were investigated: (1) early bud, buds with dimensions of 7 x 4 to 8 x 5 mm (length x width) in *O. fusca* and 5 x 4 to 7 x 5 mm in *O. lutea,* corresponding to 7–12 and 5–9 days before the anthesis, respectively; (2) late bud, buds with dimensions of 8 x 6 to 11 x 8 mm (length x width) in *O. fusca* and 7 x 6 to 10 x 8 mm in *O. lutea*, corresponding to 1–6 and 1–4 days before anthesis, respectively; and (3) freshly opened flower, flowers at the beginning of anthesis.

LABELLUM VASCULATURE

Two opened flowers of each species, fixed with FAA (formaldehyde : glacial acetic acid : 50% ethanol, 1:1:18, v/v) under vacuum at room temperature for 24 h, were cleared by the method of diaphanization described by Shobe & Lersten (1967). Cleared flowers were stained with 1% ethanol solution of safranin O (w/v) for 30 min. After a washing in ethanol, the flowers were kept immersed in this alcohol and observed using an Olympus SZH-ILLK stereomicroscope (Olympus Optical, Tokyo). Images were recorded digitally with an Olympus C-7070 Wide Zoom digital camera (Olympus Imaging, Tokyo).

OSMOPHORE LOCATION

For the macroscopic identification of fragrance-producing areas in the flowers, elective vital staining with diluted neutral red (Vogel, 1990) was used. Two late buds and seven freshly opened flowers of each species were immersed in 0.01% neutral red for 2–5 h. After staining, flowers were rinsed in tap water and examined under the stereomicroscope. Images were recorded digitally.

LABELLUM ANATOMY

To follow the histological and cytological changes during the flower development, pieces of labellum taken from early buds, late buds, and freshly opened flowers of the two *Ophrys* species were processed for anatomical study under light microscopy. Samples were fixed as described for SEM, but after the washing in the fixative buffer and dehydration through an ethanol series, they were infiltrated with and embedded in Leica Historesin. Sections 2 µm thick were cut with a Leica RM-2155 microtome (Leica Microsystems, Nussloch, Germany). Sections were sequentially stained with periodic acid–Schiff (PAS) reagent/toluidine blue O (Feder & O'Brien, 1968) or toluidine blue O with pretreatment with sodium hypochlorite plus post-staining with dilute Lugol (Gutmann, 1995), for general histology and for total polysaccharides and starch. Sudan black B was used for detection of lipids and tannins (Bronner, 1975; Parham & Kaustinen, 1976), with appropriate controls.

Portions of the apical margin of the labellum taken from flowers of *O. lutea* at all three developmental stages were also fixed with 2.5% glutaraldehyde in 0.1 M sodium phosphate buffer at pH 7.2 for 12–16 h at 4^{o}C and post-fixed with 2% osmium tetroxide for 1 h at room temperature. After dehydration in a graded acetone series, samples were embedded in Epon-Araldite resin (Electron Microscopy Sciences, Fort Washington, PA). Semithin sections (approximately 0.5 µm thick) were obtained on a Sorvall MT-1 ultramicrotome (Sorvall, Norwalk, CT) and stained with Sudan black B for lipids and tannins (Bronner, 1975; Parham & Kaustinen, 1976). Observations were made with a Leica DM-2500 microscope (Leica Microsystems, Wetzlar, Germany), and images were recorded digitally with a Leica DFC-420 camera (Leica Microsystems, Heerbrugg, Switzerland) and the Leica Application Suite software (ver. 2.8.1).

HISTOCHEMISTRY

For the histochemical characterization of the osmophore, transverse and longitudinal hand-cut sections of the apical margin of the labellum were made in fresh late buds and opened flowers from both species. Neutral red was used as a vital stain to locate glandular cells (Vogel, 1990) and as a lipid fluorochrome for detection of lipids under UV and blue light (Kirk, 1970). Sections were tested for total lipids with Sudan IV (Pearse, 1985). Phenolic compounds were detected by their autofluorescence under UV and blue light (Harborne, 1998). Observations under UV and blue wavelengths were made with a Leitz SM-LUX epifluorescence microscope (Leitz-Wetzlar, Wetzlar, Germany) equipped with an HBO 50-W mercury vapor lamp, filter block A (excitation filter BP 340-380, dichroic mirror 450, and barrier filter LP-430), and filter block I2 (excitation filter BP 450-490 and barrier filter LP-515). Images were recorded on Kodak Ultra Gold 400 ASA color slide film with a Leica Wild MPS-52 camera (Leica, Vienna). Otherwise, observations were made with the Leica DM-2500 microscope, and images were recorded digitally.

RESULTS

The present results constitute supplementary data concerning the location, structure and secretion of the osmophores of *Ophrys fusca* and *O. lutea* (Chapter 2), which were obtained during the anatomical and histochemical study of flowers at the stages of early bud, late bud and flower at anthesis.

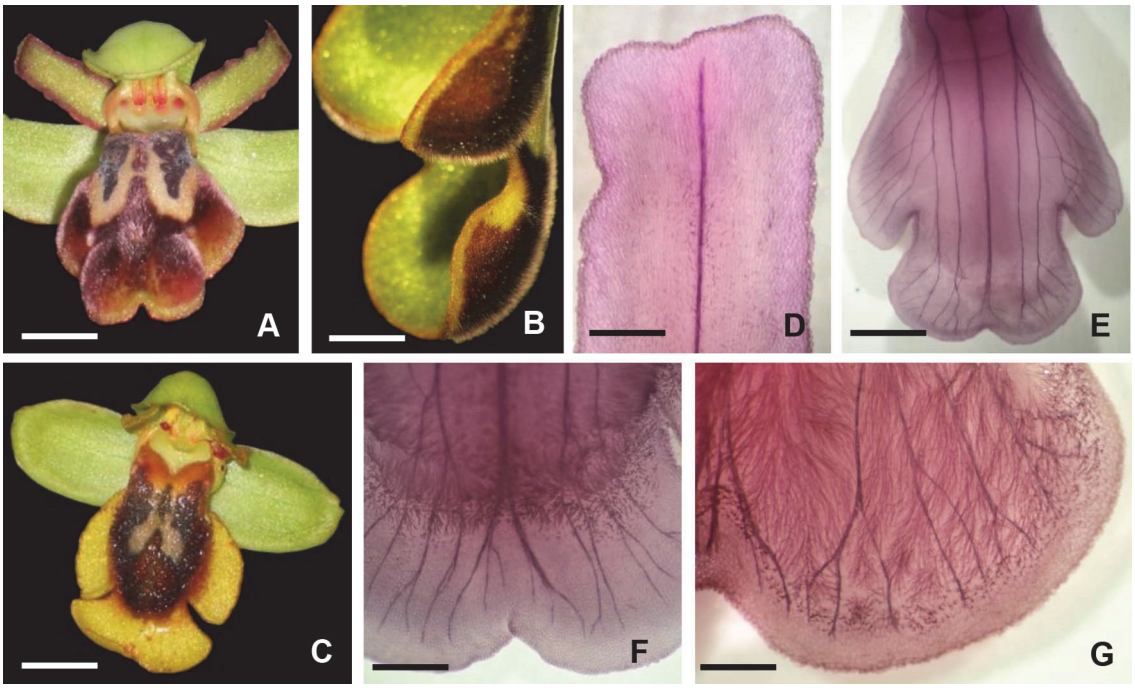

Figure I. Stereomicrographs of fresh flowers (A–C) and cleared flowers stained with safranin (D–G) of *Ophrys fusca* (A, B, E, G) and *Ophrys lutea* (C, D, F). A–C, Flowers after immersion in diluted neutral red. A, B, *Ophrys fusca* – note the red-staining of the margins of lateral petals and of the entire margin of the labellum. C, *Ophrys lutea* – note that the broad yellow margin of the labellum remains unstained. D–G, Vasculature of floral organs. D, Lateral petal, showing the unbranched central vein. E–G, Labellum, showing the branched pattern of veins. F, G, Enlarged view of the labellum margins in *O. lutea* (F) and *O. fusca* (G). Scale bars: 5 mm (A, C); 3 mm (B, E); 1 mm (D, F, G).

As for the macroscopic identification of fragrance-producing areas in the flower, using a diluted neutral red solution in a concentration of 0.01% for immersion of flowers (Vogel, 1990), instead of the initially used concentration of 0.1% (Chapter 2), resulted in a red-staining of the entire margin of the labellum and the lateral petals in freshly opened flowers of *O. fusca* (Fig. IA, B). However, the broad yellow margin of the labellum of freshly opened flowers of *O. lutea* did not practically stain (Fig. IC), but this fact does not mean that this floral area is not involved in scent production, since this elective vital staining with diluted neutral red proposed by Vogel (1990) is not specific for the secretory cells of the osmophores. In fact, the diluted neutral red is usually used as indicative of fragrance-producing cells in the flowers, but only if the colour hue and the anatomy of the stained floral parts are taken into account (Vogel & Hadacek, 2004). This applies not only to the immersion of entire flowers in the diluted neutral red but also to the hand-cut fresh

sections placed in the same diluted stain (Vogel 1990). The diagnostic colour hue of the vacuole content of secretory cells involved in scent production is a deep bluish or magenta staining, like that found in the vacuoles of the domed epidermal papillae of the labellum margin of freshly opened flowers of *O. lutea*, which contrasts to the orange to brick-red staining of the underlying parenchyma cells (Fig. IID).

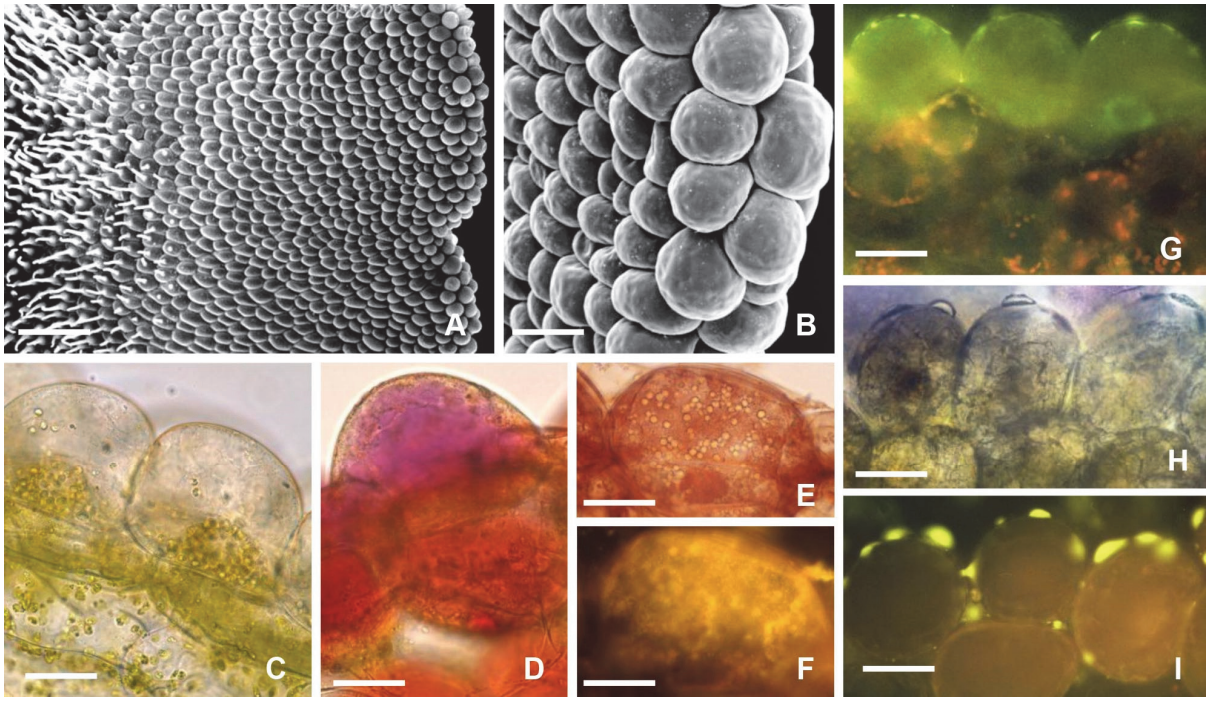

Figure II. Secretory cells of the osmophore of *Ophrys lutea* (A, B, D–G) and *Ophrys fusca* (C, H, I). A, B, Scanning electron micrographs of flowers of *O. lutea*. A. Lateral labellum lobe, showing the broad glabrous margin contiguous to the attenuate trichomes of the central indumentum. B, Margin of the lateral petal with enlarged dome-shaped papillae. C–I, Light micrographs of transverse fresh-hand sections of the apical margin of the labellum. C, Without any treatment. D–F, Sections stained with neutral red. D, Dome-shaped epidermal cells with pink-stained vacuoles. E, F, Sections stained with neutral red, in bright field (E) and under blue light (F) – note the golden-yellow secondary fluorescence of the cytoplasm under blue light. G, Autofluorescence of the labellum margin of *O. lutea* – note the green autofluorescence detected near the outer cell walls of the domed papillae and the red-autofluorescence of the chloroplasts in the subepidermal parenchyma cells. H, I, Section of the labellum margin of *O. fusca* observed in bright field (H) and under blue light (I) – note the yellowish-green autofluorescence of droplets on the surface of the epidermal cells. Scale bars: 250 µm (A); 100 µm (B); 75 µm (G–I); 50 µm (C–F).

The anatomical study corroborated the first indication given by the elective vital staining test that the entire margin of the labellum and the lateral petals of *O. fusca* and *O. lutea* are composed of secretory cells involved in the synthesis of fragrance compounds (Fig. III). Indeed, the osmophore in *O. fusca* and *O. lutea* is not restricted to the labellum, as initially suggested in Chapter 2, but also includes the enlarged dome-shaped papillae occurring at the margin of the lateral petals (Figs. IIB, IIIK, L). In the labellum, the osmophore of both species occurs in the margin of the whole labellum, more specifically at the margin itself and on the abaxial labellum surface adjacent to the margin, from the apical region

near the central notch (Fig. IIIA, B) to the basal region, and also extends to the abaxial surface of the apical region of the labellum (Fig. IIIC–F). In the apical region of the labellum near the central notch, both the adaxial and the abaxial surfaces of the labellum margin are glandular (Fig. IIIA, B). The osmophore is composed of the domed epidermal papillae, which acquire often a reniform shape near the central notch especially in *O. fusca* (Fig. IIIB, H), and the two to three layers of subepidermal parenchyma cells. The secretory epidermal cells have a dense cytoplasm with a large nucleus at the base of the cell surrounded by numerous starch-rich plastids, several small vacuoles occupying the cell apex and thin cell walls where primary pit fields were occasionally observed (Chapter 2; Fig. IIIG–J). Such secretory epidermal cells with starch-rich plastids occur in the abaxial surface of the labellum of both species from the apical margin until the area of the apical region of the labellum where the parenchyma reaches a maximum of four-to-five layers of cells in width in *O. fusca* (Fig. IIIC, D) and five-to-six cell layers in width in *O. lutea* (Fig. IIIE, F). The osmophores of both species present thus a nearly identical extent in the labellum, although that of *O. lutea* extends a little further upwards, occupying practically all the extent of the abaxial surface of the broad yellow glabrous apical labellum margin.

Considerably less starch was found in the osmophore of *O. fusca* than in that of *O. lutea* (Fig. IIIA, B, G–J). Although some starch was also observed in the subepidermal parenchyma, the bulk of the starch in the osmophores of *O. fusca* and *O. lutea* occurs in the secretory epidermis (Chapter 2; Fig. IIIA, G–J), a fact that is unique among osmophore-containing plants, already mentioned by Vogel (1990). Abundant starch is present in the early bud stage throughout the entire labellum, especially on the abaxial surface (Chapter 2), which disappears totally from the non-glandular areas and continues to exist in the secretory epidermal cells of the osmophore, even though in less amount, in flowers at anthesis (Fig. IIIA–F). Such decrease in starch content is particularly evident in *O. lutea* (Fig. IIIA, E, F). Along with starch depletion, an increase in cell vacuolization also occurs in the osmophore tissues during flower development (Fig. IIIA–F). Additionally, the branched vasculature exhibited by the labellum of both species towards the margins (Fig. IIIE–G) contrasts strongly with the single central vein that typically occurs in the other petals (Fig. IIID).

Furthermore, a Sudan-positive lipophilic secretion was found in the small vacuoles of the epidermal cells of the apical labellum margin (Chapter 2) and the lateral petal margin in *O. lutea* (Fig. IIIJ, L). Some lipophilic inclusions were also detected by their golden-yellow secondary fluorescence under blue light, after staining with neutral red, in the cytoplasm of these domed papillae (Fig. IIE, F). Translucent droplets were often observed on the surface of the domed papillae occurring at the labellum margin in fresh flowers *O. fusca*, which appeared to exhibit a yellowish green autofluorescence, usually assigned to phenolic compounds (Fig. IIH, I). A green autofluorescence was also detected near the outer cell walls of the domed papillae in *O. lutea* (Fig. IIG). As a result, a lipophilic secretion with a phenolic

fraction seems to be synthesized by the dome-shaped papillae of the osmophore in both species.

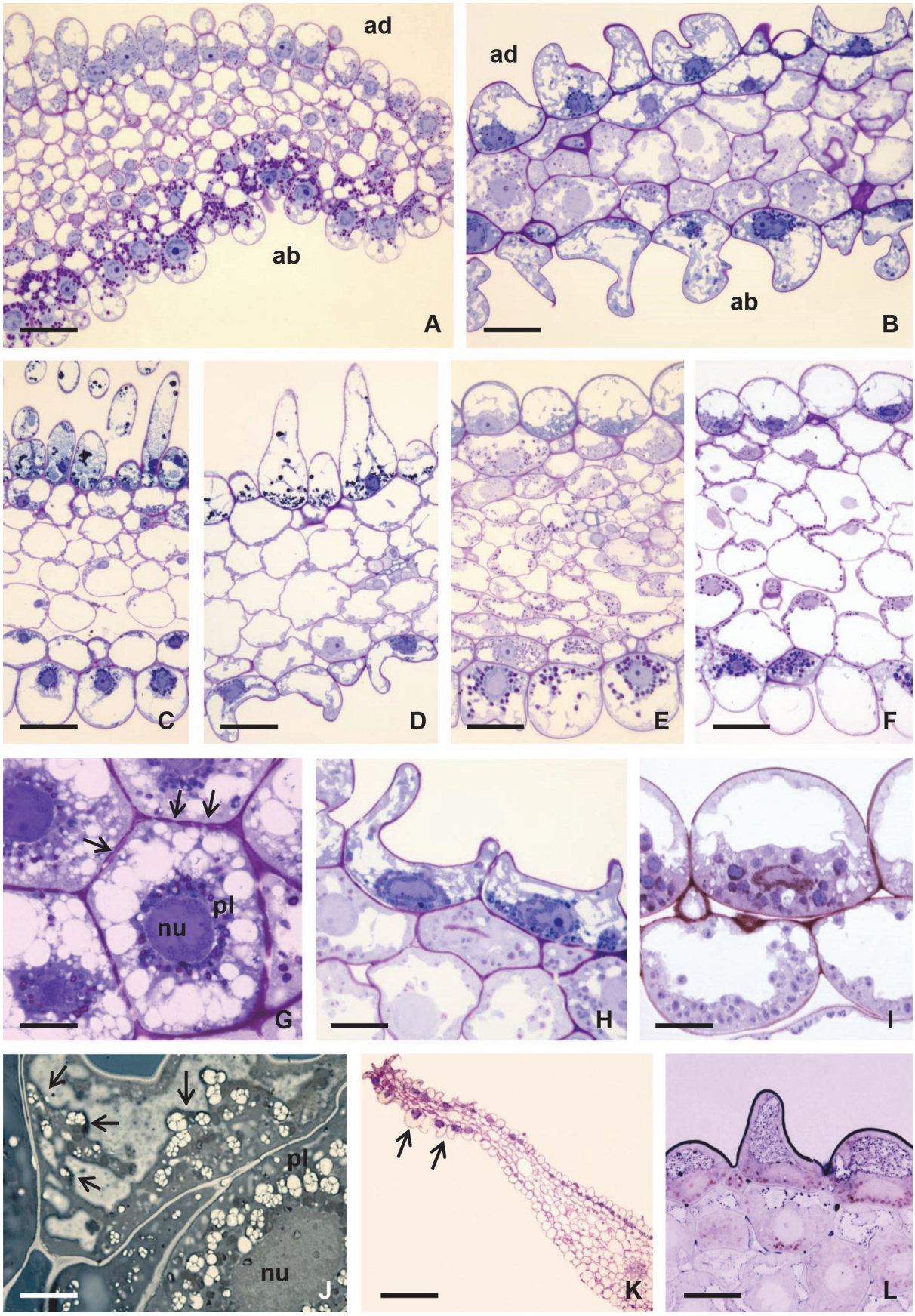

Figure III. Light micrographs of historesin sections (A–I, K, L) and epoxy section (J) of the secretory tissues of the osmophore in *Ophrys lutea* (A, E, F, I–L) and *Ophrys fusca* (B–D, G, H). Sections were stained with PAS/toluidine blue (A–H, K), toluidine blue/Lugol (I) and Sudan black B (J, L). A, B, Transverse sections of the apical margin of the labellum near the central notch in an early bud of *O.*

lutea (A) and in an opened flower of *O. fusca* (B), showing the secretory tissues – note that PAS-positive magenta-stained starch grains accumulate especially in plastids of epidermal cells on the abaxial surface of the labellum. C, D, Transverse sections of the apical region of the labellum in a late bud (C) and an open flower (D) of *O. fusca*, showing attenuate trichomes on the adaxial surface and dome-shaped to reniform papillae with secretory features on the abaxial surface. E, F, Transverse sections of the apical region of the labellum in a late bud (E) and an open flower (F) of *O. lutea*, showing domed papillae on both labellum surfaces, but PAS-positive starch-rich plastids occurring especially in the epidermal cells on the abaxial surface – note the increased cell vacuolization and the decreased starch content as flower develops. G, Paradermal section of the secretory epidermal cells on the abaxial surface of the labellum in an early bud of *O. fusca*, showing a large nucleus surrounded by plastids with some starch, several small vacuoles and primary pit fields (arrows) along the cell walls. H, I, Transverse sections of the secretory cells at the labellum margin in open flowers of *O. fusca* (H) and *O. lutea* (I) – note that the starch content in the plastids of epidermal cells in *O. fusca* is lower than that in *O. lutea*. J, Paradermal epoxy section of the secretory epidermal cells in a late bud of *O. lutea*, showing plastids with several starch grains (unstained) around the nucleus and a Sudan-positive black-stained lipophilic secretion at the periphery of vacuoles (arrows). K, L, Transverse sections of a lateral petal in a late bud of *O. lutea*. K, General view of the lateral petal, showing enlarged dome-shaped papillae at the margin (arrows). L, Detail of secretory cells at the petal margin, showing Sudan-positive droplets of lipophilic secretion inside vacuoles besides black-stained cuticle. ab, abaxial surface; ad, adaxial surface; nu, nucleus; pl, plastids. Scale bars: 500 µm (K); 150 µm (A); 75 µm (B–F, L); 25 µm (G–I); 10 µm (J).

REFERENCES

Aldasoro JJ, Sáez L. 2005. *Ophrys* L. In: Aedo C, Herrero A, eds. *Flora Iberica: plantas vasculares da la Península Ibérica e Islas Baleares, Vol. XXI.* Madrid: Real Jardín Botánico, CSIC, 165-195.

Bronner R. 1975. Simultaneous demonstration of lipids and starch in plant tissues. *Stain Technology* **50:** 1-4.

Feder N, O'Brien TP. 1968. Plant microtechnique: some principles and new methods. *American Journal of Botany* **55:** 123-142.

Gutmann M. 1995. Improved staining procedures for photographic documentation of phenolic deposits in semithin sections of plant tissue. *Journal of Microscopy* **179:** 277-281.

Harborne JB. 1998. *Phytochemical methods: a guide to modern techniques of plant analysis.* 3rd ed. London: Chapman & Hall.

Kirk PW. 1970. Neutral red as a lipid fluorochrome. *Stain Technology* **45:** 1-4.

Parham RA, Kaustinen HM. 1976. Differential staining of tannin in sections of epoxy-embedded plant cells. *Stain Technology* **51:** 237-240.

Pearse AGE. 1985. *Histochemistry: theoretical and applied. Volume 2, Analytical technology.* 4th ed. Edinburgh: Churchill-Livingstone.

Shobe WR, Lersten NR. 1967. A technique for clearing and staining gymnosperm leaves. *Botanical Gazette* **128:** 150-152.

Vogel S. 1990. *The role of scent glands in pollination: on the structure and function of osmophores.* Rotterdam: A. A. Balkema. [English translation of: Vogel S. 1963. Duftdrüsen im Dienste der Bestäubung: Über Bau und Funktion der Osmophoren. *Akademie der Wissenschaften und der Literatur in Mainz, Abhandlungen der Mathematisch-Naturwissenschaftlichen Klasse* **10**: 600-763].

Vogel S, Hadacek F. 2004. Contributions to the functional anatomy and biology of *Nelumbo nucifera* (Nelumbonaceae) III. An ecological reappraisal of floral organs. *Plant Systematics and Evolution* **249:** 173-189.

APPENDIX B

CHEMICAL ANALYSIS OF VOLATILE ORGANIC COMPOUNDS IN *OPHRYS FUSCA* AND *O. LUTEA*

APPENDIX B: CHEMICAL ANALYSIS OF VOLATILE ORGANIC COMPOUNDS IN *OPHRYS FUSCA* AND *O. LUTEA*

MATERIAL AND METHODS

Inflorescences of *Ophrys fusca* Link subsp. *fusca* (hereafter referred to as *O. fusca*, for the sake of simplicity) and *Ophrys lutea* Cav., collected in April and May 2007 from natural populations, were put into gas-washing flasks sealed with two three-way PTFE (Teflon) stopcocks, which contained some distilled water at the bottom. Several inflorescences of the same *Ophrys* species were placed on each flask, in a number that varied between 3 to 9 for *O. fusca* and between 9 to 19 for *O. lutea*. Flasks remained closed for 24 h in ambient conditions of light and temperature, near a window with direct sunlight during the morning. Identical flasks with distilled water but without plants were placed in the same conditions and were used as controls.

A semi-dynamic headspace technique was used for sampling the volatile organic compounds (VOCs) of the scent emitted by *Ophrys* inflorescences. Headspace samples were obtained in two moments: the first after 7 h and the second after 24 h from the time when inflorescences have been closed into the sampling flasks. After the first sampling time, the flasks were opened for 1 min to be fulfilled with renewed ambient air before being closed again for more 17 h, when the second sampling time occurred. At the end, fresh mass of the inflorescences enclosed in each flask was determined, and then they were dried in an oven at 80^{o}C for 24 h for dry mass determination.

At each sampling time, a flow of N50 nitrogen gas at a flow rate of 100 ml.min^{-1} was allowed to pass through the inflorescences for 3 min, in order to remove completely the volatile enriched air (headspace) contained in each flask and to capture it into a polymer trap. Volatile organic compounds were adsorbed in polymers of Tenax-TA and Carbopack-B (60-80 mesh, 150 mg of each) enclosed into steel tubes (160 mm x 5 mm). Before being trapped, VOCs passed over a Teflon tube fulfilled with potassium carbonate in order to remove most of water vapour.

Prior to sampling, the Tenax-Carbopack tubes were thermally cleaned at 270^{o}C under a flow of helium (14 ml.min^{-1} for 5 h) and stored in individual glass containers. After sampling, each tube was placed into the glass container and stored in a freezer until analysis. Cleaned Tenax-Carbopack tubes immediately after thermal regeneration were also analysed and used as blanks.

The analysis of the VOCs was carried out on a Chrompack CP-9001 gas chromatograph (Chrompack, Middleburg, The Netherlands) equipped with a flame ionization detector (GC-FID) and a Chrompack TCT injector, using a DB-1 fused silica capillary column (60 m x 0.32 mm, film thickness of 1 µm, J&W Scientific, Folsom, California, USA). The compounds adsorbed on polymers contained into the steel tubes were thermally desorbed at 270^{o}C

under helium flow and, through a process of cryogenic concentration, directly concentrated in a Tenax-filled silica capillary tube at -100^{o}C for 10 min. Following a rapid rise of temperature until 220^{o}C in 3 min, the compounds were injected on the chromatographic column and analyzed using the next temperature program: 3 min at 40^{o}C, then rise of 4^{o}C.min^{-1} until attain 200^{o}C for 43 min, followed by a 4-min rise at a rate of 20^{o}C.min^{-1} and a final period of 3 min at 280^{o}C.

The identification of VOCs was possible whenever the retention time of their peaks in the GC column matches those of authentic standards. Methanol solutions of a single standard compound and mixtures of authentic standards (16 different monoterpenes and oxygenated terpenoid derivatives obtained from Fluka-Chemika and Sigma-Aldrich Chemical Company) were prepared. Tenax-Carbopack tubes identical to sampling tubes were injected with 5 µl of each methanol solution of standard compounds and the solvent was removed under a helium flow at a rate of 50 ml.min^{-1} for 5 min. Following thermal desorption of standards compounds into the GC system, their retention times and peak areas were determined for quantification purposes. Data were analysed and compared using the CP-Maitre Chromatography Data System software (version 2.5, Chrompack International).

RESULTS

Table IV. Comparison of the volatile organic compounds (VOCs) emitted by inflorescences of *Ophrys lutea* and *Ophrys fusca* sampled by semi-dynamic headspace technique and analysed by gas chromatography with flame ionization detection (GC-FID). **Classes of estimated mass of VOCs (m)**: **trace** = m ≤ 1,5 ng; **I** = 1,5 ng < m ≤ 3 ng; **II** = 3 ng < m ≤ 6 ng; **III** = 6 ng < m ≤ 12 ng; **IV** = 12 ng < m ≤ 30 ng; **V** = 30 ng < m ≤ 60 ng; **VI** = 60 ng < m ≤ 120 ng; **VII** = 120 ng < m ≤ 300 ng; **VIII** = m > 300 ng. *Vestigial* refers to a relative amount of a compound that was also emitted by the corresponding controls. Additionally, the term *vestigial* was used when a residual emission of a compound was detected, i.e. when the peak area of a compound in the chromatogram was between 1 and 2 times the standard deviation of the peak areas of that compound found in the control. For the VOCs with largest peak areas found in the controls (i.e. VOCs nº 91, 123, and 131, typed in grey), the term vestigial was applied only when the peak area of those compounds was between 3 and 5 times the standard deviation of the corresponding peak areas in the controls. The two samples whose chromatograms were contrasted in Figures V and VI are highlighted in dark grey. The main 42 emitted VOCs are highlighted in light grey and detailed in Table VII.

***Ophrys* species**	***O. lutea***							***O. fusca***					
Samples	OL7-7h	OL8-7h	OL9-7h	OL10-7h	OL10-17h	OL11-7h	OL11-17h	OF4-17h	OF5-7h	OF5-17h	OF6-7h	OF6-17h	OF7-17h
Number of Inflorescences	9	11	10	11		19		3	7		7		9
Nr. of Flowers (young/mature + senescent)	19 (19+0)	21 (15+6)	20 (16+4)	26 (21+5)		32 (26+6)		8 (8+0)	18 (10+8)		14 (11+3)		19 (13+6)
Total Dry Mass of Inflorescences (g)	0.7798	0.6860	0.5762	1.0077		1.0579		0.5741	0.7960		0.9267		1.0054
Total Mass of Emitted VOCs (ng)	413.1	2885.9	65.4	986.7	57.3	68.4	110.2	20.6	20.4	633.4	680.1	179.9	34.4
Total Mass of VOCs/Total Dry Mass (ng/g)	529.8	4206.8	113.6	979.2	56.9	64.7	104.1	35.8	25.6	795.7	733.8	194.1	34.3
Total Mass of VOCs (ng)/Flower	21.7	137.4	3.3	38.0	2.2	2.1	3.4	2.6	1.1	35.2	48.6	12.8	1.8
Emission rate of VOCs (ng/h)	59.0	412.3	9.3	141.0	5.7	9.8	11.0	2.1	2.9	63.3	97.2	18.0	3.4
Emission rate of VOCs (ng/h/flower)	3.1	19.6	0.5	5.4	0.2	0.3	0.3	0.3	0.2	3.5	6.9	1.3	0.2
Emitted VOCs													
1		III											
2		II											
3				II							trace		
4		I											
5										V		V	
6		VII											
7		vestigial											
8				II							III		
9		V											
10		IV	II	II						trace	trace	II	
11	vestigial	II		III	V	trace	V				IV		
12		III							I			I	
13													I
14	III					vestigial		vestigial					

15	II				trace	II	trace		trace		III		II	
16														I
17	IV				I	I	I		I		II		I	I
18	II					I	trace							
19														I
20														trace
21		IV												
22		I												
23		vestigial												
24		IV									I	II		
25	III													
26	vestigial	III		III								III		
27		V		III							III			
28											II		I	
29	I		I											
30	II				II		I							
31	III				II	II	II		trace					trace
32														II
33		II												
34		vestigial												
35		III												
36		II												
37		II	III							II	III	IV	II	
38		IV		IV										
39		vestigial												
40	II			I										
41		II		vestigial							vestigial			
42	II	trace												
43											vestigial	VI		
44		IV												
45	II	trace		I		trace			II					II
46				VI			trace					VI		
47		vestigial												
48		IV	I	II							I	II	trace	
49	V	IV												
50		vestigial												
51		vestigial		II										
52	III													
53		vestigial												
54		III		II			trace			I	V	V	IV	trace

55		IV												
56		II												
57		VIII												
58											VII			
59		III												
60		vestigial												
61		II												
62	III	IV												
63		IV												
64		IV		III						IV	III			
65	vestigial	vestigial									vestigial			
66	IV	V		IV			trace			IV	IV			
67		III		II						vestigial	vestigial			
68		III									IV			
69		II												
70		IV		II			trace		vestigial	IV	IV	III	trace	
71				I										
72		IV												
73											vestigial			
74. Thujene		V		III		II					III			
75		vestigial												
76. α-Pinene		VII		IV					III	V	V	IV		
77	V				II			III					III	
78		V												
79		III												
80. Camphene				II										
81		vestigial												
82. Sabinene	V	VII		IV							IV		I	
83											II			
84. β-Pinene	V	VI	vestigial	VII		II	I			IV	VI	vestigial		
85	IV	trace											I	
86. Benzaldehyde		VIII								VI				
87	IV													
88											II			
89. α-Phellandrene	II	IV	I	II	trace		trace							
90											vestigial			
91											vestigial			
92											V			
93		II		vestigial		trace	trace				III			
94. Limonene		IV	I	IV						II	III			

95. Eucalyptol	vestigial													
96	V	IV	IV	V		IV	V				II	III	III	
97		II										I		
98		V												
99		IV												
100				V		trace						IV	III	
101. γ-Terpinene		vestigial		vestigial							II			
102											I			
103		III									trace	II		
104	vestigial	vestigial				vestigial	vestigial					II		
105	IV	IV	III	VI		II	II				VI	V	IV	
106				VII										
107. Linalool				trace								trace	II	
108		V												
109													III	
110		III		III						trace	III	III	II	
111			I	I		trace	trace				trace	I		
112	II													
113				I							II	I		
114		I												
115		vestigial										IV		
116		IV												
117		I	trace	trace										
118	III	vestigial										II		
119		VI												
120		VI												
121				vestigial										
122		II												
123		vestigial									vestigial			
124		trace	II	trace	trace	trace							II	
125		II		II										
126		I		IV										
127		III		IV								III		
128		III		IV										
129		III		IV							III			
130		III	vestigial	IV						vestigial	I			
131				vestigial										
132		II		III										
133. Myrtenol	vestigial	IV	vestigial	IV		I	trace					vestigial		
134		III		V		I								

135. β-Citronellol				I										
136		vestigial		IV		I					vestigial			
137				I							II		III	
138		trace		I										
139		I	I	III										
140		III		II		II					III	vestigial		
141		III		I							I	I		
142. Geraniol		II		vestigial							II			
143						I		trace						
144		III												
145			I	IV		I								
146				vestigial										
147	IV	vestigial												
148		II									II			
149	III													
150		III									vestigial	II		
151	III													

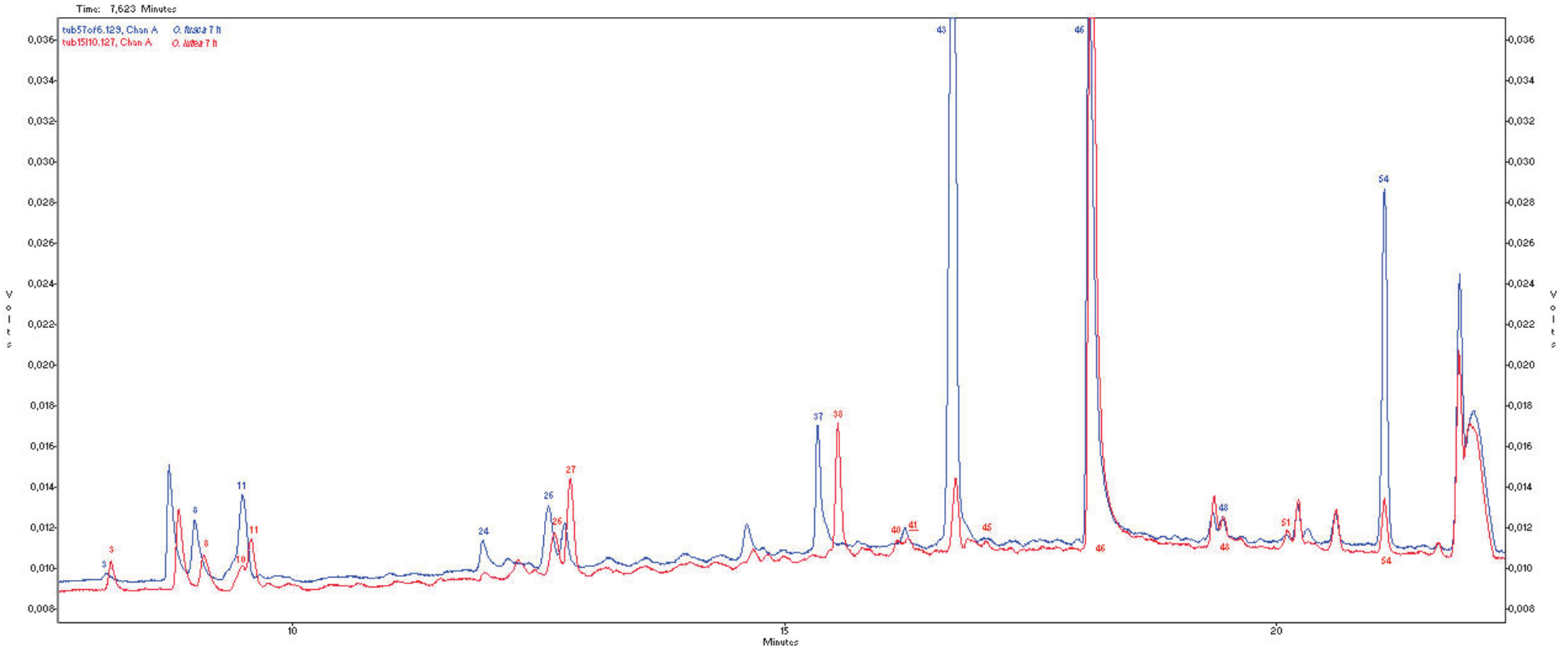

Figure V. Comparison between the chromatograms (7–23 min elution time) of the volatile organic compounds found in the headspace samples of inflorescences of *Ophrys fusca* (blue) and *Ophrys lutea* (red). Labelled peaks correspond to the compounds effectively emitted by the inflorescences to the headspace, enumerated in Table IV.

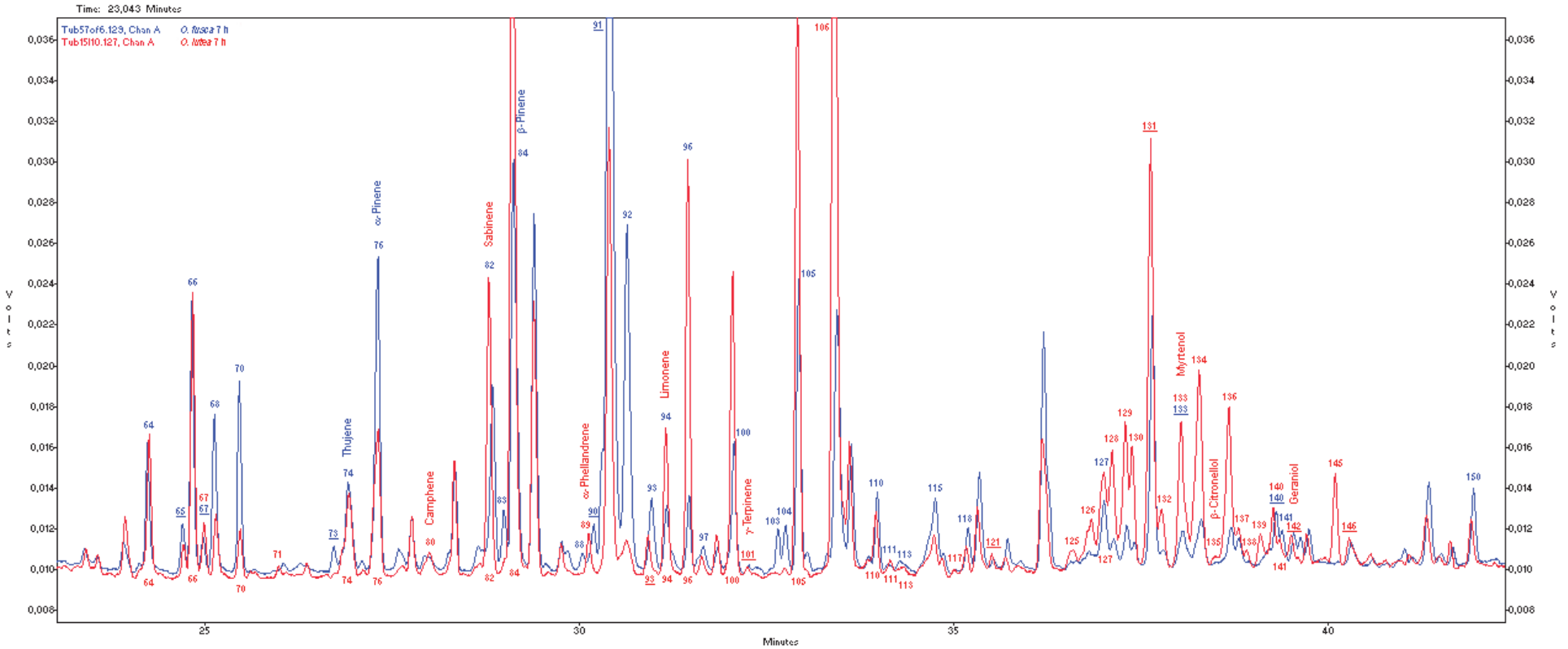

Figure VI. Comparison between the chromatograms (23–43 min elution time) of the volatile organic compounds found in the headspace samples of inflorescences of *Ophrys fusca* (blue) and *Ophrys lutea* (red). Labelled peaks correspond to the compounds effectively emitted by the inflorescences to the headspace, enumerated in Table IV.

Table VII. Comparison of the main volatile organic compounds (VOCs) emitted by inflorescences of *Ophrys lutea* and *Ophrys fusca* expressed in percentage of mass relative to the total mass emitted. *Vestigial* refers to a relative amount of a compound that was also emitted by the corresponding controls. Additionally, the term *vestigial* was used when a residual emission of a compound was detected, i.e. when the peak area of a compound in the chromatogram was between 1 and 2 times the standard deviation of the peak areas of that compound found in the control. n.d.: not detected.

***Ophrys* species**	***Ophrys lutea***		***Ophrys fusca***	
Total number of emitted VOCs	118	Emitting samples	72	Emitting samples
Nr. VOCs exclusively emitted by	60		14	
Main emitted VOCs (42)				
5	n.d.	0	10%-25%	1/3
10	< 5%	3/7	< 2.5%	1/2
11	vestigial-65%	6/7	2.5%	1/6
15	1%-7%	4/7	1%-5%	1/2
17	2%-5%	4/7	0.5%-10%	2/3
18	1%-3%	3/7	n.d.	0
26	< 1%	3/7	1.5%	1/6
30	0.5%-7%	3/7	n.d.	0
31	3%-7%	4/7	4%-5%	1/3
37	0.5%-11%	2/7	1.5%-30%	2/3
38	< 1.5%	2/7	n.d.	0
43	n.d.	0	vestigial-7%	1/3
45	< 2%	4/7	9%-16%	1/3
48	< 3%	3/7	< 1%	1/2
49	0.7%-8%	2/7	n.d.	0
54	< 1%	3/7	4%-13%	5/6
62	< 2.5%	2/7	n.d.	0
66	1%-4%	4/7	2%-4%	1/3
70	< 1%	3/7	vestigial-4%	5/6
74. Thujene	1%-5%	3/7	2%	1/6
76. α-Pinene	3%-5%	2/7	5%-45%	2/3
77	9%-10%	2/7	25%-56%	1/3
82. Sabinene	3%-10%	3/7	2.5%-7%	1/3
84. β-Pinene	vestigial-15%	6/7	vestigial-9%	1/2
89. α-Phellandrene	< 3%	6/7	n.d.	0
93	vestigial-1.5%	4/7	1.5%	1/6
94. Limonene	1%-4%	3/7	< 1.5%	1/3
96	0.5%-40%	6/7	1%-3%	1/2
100	2%-4%	2/7	2%-5%	1/3
104	vestigial	4/7	0.5%	1/6
105	1%-18%	6/7	4%-17%	1/2
110	< 1%	2/7	1.5%-6%	2/3
111	< 4%	4/7	< 0.5%	1/3

117	< 1.5%	3/7	n.d.	0
124	1.5%-6%	5/7	2%	1/6
130	< 1.5%	3/7	< 0.5%	1/3
133. Myrtenol	vestigial-3%	6/7	vestigial	1/6
134	< 3%	3/7	n.d.	0
136	vestigial-3%	3/7	vestigial	1/6
139	< 3%	3/7	n.d.	0
140	< 5%	3/7	< 2%	1/3
145	1.5%-3%	3/7	n.d.	0

APPENDIX C

FLOWER LONGEVITY IN *OPHRYS*

APPENDIX C: FLOWER LONGEVITY IN *OPHRYS*

Table VIII. Dimensions of *Ophrys* flowers at three developmental stages and duration of the period of anthesis (flower longevity). For conducting the measurements, some individuals of the seven investigated *Ophrys* taxa were potted in the field and carried to the laboratory. Pots were placed near a window with direct sunlight during the morning and were watered whenever necessary. Flower longevity, i.e. the duration of the period of anthesis, was determined for each species following daily observations of the development of flowers of each species for one month. The number of days elapsed from opening to senescence was counted for each flower. At the end, all plants were carried back to their natural habitat.

Stage	**Feature**	***Ophrys speculum* subsp. *speculum***		***Ophrys speculum* subsp. *lusitanica***		***Ophrys bombyliflora***		***Ophrys tenthredinifera***		***Ophrys fusca* subsp. *fusca***		***Ophrys lutea***		***Ophrys scolopax***	
Early Bud	Dimensions (length x width; mm)	5x3 to 7x3	n=44	5x3 to 6x4	n=24	5x3 to 6x4	n=26	7x4 to 8x5	n=40	7x4 to 8x5	n=31	5x4 to 7x5	n=61	5x3 to 8x4	n=43
	Age (nr. days before anthesis)	3 to 7		4 to 6		3 to 7		4 to 9		7 to 12		5 to 9		6 to 11	
Late Bud	Dimensions (length x width; mm)	7x4 to 9x6		7x4 to 8x6		7x4 to 8x6		8x6 to 10x7		8x6 to 11x8		7x6 to 10x8		8x5 to 10x8	
	Age (nr. days before anthesis)	1 to 2		1 to 3		1 to 2		1 to 3		1 to 6		1 to 4		1 to 5	
Freshly Opened Flower	Mean (SD) dimensions of labellum (length x width; mm)	13(2)x11(2)	n=20	13(2)x10(1)	n=13	8(1)x7(1)	n=7	13(3)x12(2)	n=10	17(3)x11(1)	n=6	15(3)x12(2)	n=10	11(2)x7(2)	n=6
	Age (nr. days of anthesis)	5 to 12	n=26	6 to 10	n=14	5 to 7	n=14	6 to 9	n=28	6 to 10	n=17	7 to 14	n=25	8 to 13	n=14
	Period of anthesis (nr. days)	**12 to 17**		**12 to 16**		**6 to 8**		**9 to 12**		**10 to 17**		**10 to 21**		**14 to 19**	

APPENDIX D

EXPERIMENTAL PROTOCOLS

APPENDIX D: EXPERIMENTAL PROTOCOLS

SCANNING ELECTRON MICROSCOPY

1. Fixation with 2.5% glutaraldehyde in 0.1 M sodium phosphate buffer, pH 7.2, under vacuum at room temperature for 20 min, followed by 48–72 h at 4^0C.
2. Rinsing in the fixative buffer, 3x20 min.
3. Dehydration in a graded acetone series: 30%, 50%, 70%, 80%, 90%, 15 min. each.
4. Absolute acetone, 3x20 min.
5. Critical-point drying with carbon dioxide.
6. Mounting in object-holders.
7. Coating with a thin layer of gold.
8. Examination using a scanning electron microscope at an accelerating voltage of 15/20 kV.

STEREOMICROSCOPY

I. Macroscopic detection of fragrance-producing areas by elective vital staining (Vogel, 1990)

1. Immersion of the flowers in 0.01% Neutral Red in tap water, 2–6 h.
2. Washing in tap water.
3. Examination using a stereomicroscope.

II. Diafanization I (after Shobe & Lersten, 1967)

1. Fixation with FAA (formaldehyde p.a. : glacial acetic acid : 50% ethanol, 1:1:18, v/v), 24 h, under vacuum, at room temperature.
2. Rinsing in 50% ethanol. Storing in this solution overnight (o.n.)
3. Hydration through an ethanol series: 50%, 20%, 10%, 30 min each.
4. Distilled water, 30 min.
5. Clearing with 5% sodium hydroxide, 2 h (maximum).
6. Washing in distilled water, 3x30 min.
7. Clearing with 5% sodium hypochlorite, 10 min.
8. Washing in distilled water, 4x30 min.
9. Dehydration through an ethanol series: 10%, 20%, 30%, 50%, 1 h each.
10. 70% ethanol, o.n.
11. 95% ethanol, 30 min.
12. Absolute ethanol, 2x20 min.
13. Staining with 1% ethanol solution of Safranin *O* (w/v), 30 min.
14. Washing in absolute ethanol, 4x10 min.

15. Immersion of floral organs in ethanol for examination and image recording using a stereomicroscope.
16. Making of semi-permanent preparations with Kaiser's glycerol gelatin on an electric heating plate at 60°C. Then, let it dry completely at room temperature for 30 min.

III. Diafanization II (after Fuchs, 1963)

1. 50% ethanol, 8 h, at room temperature.
2. 70% ethanol, 72–80 h, under vacuum.
3. 95% ethanol, 72 h.
4. Staining with 1% Fuchsin in 95% ethanol, 10 min.
5. Washing in distilled water, 3x10 min.
6. Clearing with 15% sodium hydroxide, 2 h (maximum).
7. Washing in distilled water, 6x30 min.
8. Dehydration through an ethanol series: 10%, 30%, 50%, 70%, 90%, 15 min each.
9. Absolute ethanol, 3x20 min.
10. Ethanol : hydrochloric acid (1:1), 15 min.
11. Washing in absolute ethanol, 3x30 min.
12. Immersion of floral organs in glycerin : distilled water (1:1)
13. Making of semi-permanent preparations with Kaiser's glycerol gelatin on an electric heating plate at 60°C. Then, let it dry completely at room temperature for 30 min.

LIGHT MICROSCOPY

A. FREE-HAND SECTIONS IN FRESH FLOWERS

I. Vital staining of osmophores (Vogel, 1990)

1. Staining with 0.01% Neutral Red in tap water, 20 min.
2. Examination using a bright field light microscope.

Expected results – Vacuoles from odor-producing cells are electively stained showing a vivid pink or pale lilac color.

II. Neutral Red as a lipid fluorochrome (Kirk, 1970)

1. Staining with 0.1% Neutral Red in 0.1 M sodium phosphate buffer, pH 6.5, 20 min.
2. Examination under ultraviolet light (and blue light) using an epifluorescence microscope.

Expected results – Lipids fluoresce in either bright lemon yellow or blue-green, apparently dependent upon their composition.

III. Sudan IV (Pearse, 1985) for detection of lipids

1. Staining with 0.3% Sudan IV in 70% ethanol, at room temperature and/or in an oven at 60°C, 30 min.
2. Rapid washing with 70% ethanol
3. Washing in distilled water.

Expected results – Lipids stain red.

IV. Sudan Black B (Pearse, 1985) for detection of lipids

1. Staining with 0.3% Sudan Black B (w/v) in 70% ethanol*, in an oven at 60°C, 10 min.
2. Rapid washing in 70% ethanol.
3. Washing in distilled water.

* The saturated alcoholic solution of the fat-solvent dye must be placed into a pre-heated oven at 60°C for 24 h. Next day, the solution (while still hot) must be filtrated before it could be used.

Expected results – Lipids stain black or bluish black.

V. Osmium tetroxide (Ganter & Jollès, 1969) for detection of unsaturated lipids

1. Staining with 0.2% osmium tetroxide, at room temperature, 2 h.
2. Rinsing in distilled water.

Expected results – Unsaturated lipids stain black.

VI. Nadi Reagent (David & Carde, 1964) for detection of terpenoids

1. Staining with Nadi Reagent (solution prepared at the moment of use), 1 h, at room temperature, in darkness.

0.1% α-naphtol in 40% ethanol	0.5 ml
1% hydrochloride dimethyl *p*-phenylenediamine	0.5 ml
0.05 M sodium phosphate buffer, pH 7.2	49 ml

2. Rinsing in 0.1 M sodium phosphate buffer, pH 7.2, 2 min.
3. Rapid washing in distilled water.

Expected results – By oxidation, the mixture of α-naphtol and *p*-phenylenediamine produces nascent indophenol blue that changes its colour by variation in pH. Essences appear blue stained, lipid inclusions stain purple-red and the colour of oleoresins varies

between indigo and violet accordingly to the relative proportions of essential oil and resinic acids in the mixture.

VII. Ruthenium Red (Johansen, 1940) for detection of pectins

1. Staining with 1000 p.p.m. of Ruthenium Red (prepared at the moment of use), 30–45 min.
2. Washing in distilled water.

Expected results – Pectins stain intensely pink.

VIII. Autofluorescence under blue and UV light (Harborne, 1998) for detection of phenolic compounds

1. Examination of fresh sections under blue ultraviolet light, using an epifluorescence microscope equipped with a high-pressure mercury vapour arc-discharge lamp and filter blocks for UV light and blue light excitation.

Expected results – Phenolic compounds autofluoresce in intense yellow-green under blue light and in blue under UV light.

IX. Iron (III) chloride (Johansen, 1940) for detection of phenolic compounds

1. Staining with 10% ferric trichloride, 15–30 min.
2. Rapid washing in water.

Expected results – Phenolic compounds stain intense green, purple, deep blue or black accordingly to their composition.

X. Potassium dichromate (Gabe, 1968) for detection of phenolic compounds

1. Staining with 10% ferric trichloride, 30 min.
2. Rapid washing in water.

Expected results – Phenolic compounds stain brown to reddish brown.

B. HISTORESIN SECTIONS IN FIXED FLOWERS

I. Specimens processing

1. Fixation with 2.5% glutaraldehyde in 0.1 M sodium phosphate buffer, pH 7.2, under vacuum at room temperature for 20 min, followed by 48–72 h at 4^{o}C.
2. Rinsing in the fixative buffer, 3x20 min.

3. Dehydration in a graded ethanol series: 30%, 50%, 70%, 80%, 90%, 15 min each.
4. Absolute ethanol, 3x20 min.
5. Infiltration with ethanol : activated Leica basic historesin (3:1, 1:1 and 1:3), 16-24 h each at 4°C.
6. Pure activated historesin, 3x16-24 h at 4°C.
7. Embedding in pure activated historesin with hardener, at the proportion 15:1, on an electric heating plate at 40°C, for 24 h.
8. Sectioning using a Leica rotary microtome (sections 2 µm thick).

II. Leica Basic Historesin (Leica Microsystems)

For infiltration:

Basic resin liquid (2-hydroxyethyl methacrylate)	100 ml
Activator (dibenzoyl peroxide)	1 g (equivalent to 2 activator bags)

For embedding:

Infiltration solution	15 ml
Hardener (dimetyl sulfoxide)	1 ml (added with magnetic agitation, 1 min)

III. Periodic acid–Schiff (PAS) Stain (after Feder & O'Brien, 1968) for detection of polysaccharides

1. Aldehyde blockade: saturated solution of 2,4-dinitrophenylhydrazine (2,4-DNPH) in 15% acetic acid, 10 min.

   Add 0.5 g of 2,4-DNPH to 100 ml of 15% acetic acid.

   Stir the solution by magnetic agitation for 1 h, and filter before use.
2. Thorough rinse with running water, 20 min.
3. Drying in an oven at 60°C, 20 min.
4. 1% periodic acid, 10 min.
5. Washing in running water, 5 min.
6. Drying in an oven at 60°C, 20 min.
7. Staining with Schiff's reagent, 30 min, in darkness.

   Dissolve 2 g of sodium metabisulfite in 300 ml of distilled water.

   Dissolve 2 g of hydrochloride parafuchsin in 60 ml of 1 N hydrochloric acid.

   Mix both solutions and let mixture stand for 24 h at 4°C into a sealed flask, in darkness.

   Add 1.2 g of activated carbon (active charcoal) in magnetic agitation for 2–10 min, until a colourless solution is obtained (repeat this step if necessary).

Filter the solution (in conditions of low luminosity) and keep it colourless at 4°C, in darkness, for 6 months.

8. Transfer quickly and directly to three successive baths of 0.5% sodium metabisulfite in 0.05N hydrochloric acid, 2 min in each.
9. Rinse in running water, 5 min.
10. Drying at room temperature.

Negative control – omission of the treatment with periodic acid.

Expected results – Starch and some complex polysaccharides, especially in the compound middle lamella of the cell wall, are stained vivid pink. Cellulose is generally not stained.

Historesin sections stained with PAS were counterstained with two different solutions of Toluidine Blue *O*, as described below.

IV. Toluidine Blue *O* (after Feder & O'Brien, 1968)

11. Staining with 0.05% Toluidine Blue *O* in an oven at 60°C, 15–20 min.
12. Rinse in running water.
13. Shake the slides vigorously once or twice to remove excess water and let the sections dry at room temperature.

Expected results (O'Brien, Feder & McCully, 1964; Feder & Wolf, 1965) – RNA (e.g. nucleolus) stains purple, DNA stains blue or blue-green. Some polyphosphates, polysulfates, and polycarboxylic acids, including alginic acid and pectic acids (e.g. middle lamella) stain red. Collenchyma, parenchyma, sieve tubes and companion cells stain red or reddish purple. Lignin and some polyphenols (e.g. lignified walls of the tracheary elements and sclerenchyma) are stained green or bluish green. Callose and starch remains unstained.

V. Toluidine Blue *O* in McIlvaine's buffer (Kraus & Arduin, 1997)

11. Staining with 0.05% Toluidine Blue *O* in McIlvaine's buffer, pH 4.4, at room temperature, 30 min.

McIlvaine´s buffer, pH 4.4:

Solution A – 0.1 M citric acid (dissolve 4.2 g in 200 ml of distilled water).

Solution B – 0.2 M disodium hydrogen phosphate (dissolve 5.68 g in 200 ml of distilled water).

Stir 55.9 ml of solution A in 44.1 ml of solution B and adjust pH to 4.4.

12. Rinse in running water.
13. Drying at room temperature.

VI. Toluidine Blue *O* with pre-treatment with sodium hypochloride (Gutmann, 1995) for general histology

1. Pre-treatment with a commercial solution of sodium hypochlorite, 10 s.
2. Rinse thoroughly with distilled water.
3. Staining with 0.05% Toluidine Blue *O*, 15 min.
4. Rinse thoroughly with distilled water.
5. Blow dry immediately with a brief blast of clean air.
6. Allow to dry in an oven at 50–60^{o}C, 10 min.

Expected results – Phenolic vacuolar inclusions lose their characteristic green metachromasy and stain orthochromatically blue. Pre-treatment with sodium hypochlorite produces an overall enhancement of staining intensity.

VII. Toluidine Blue *O* with pre-treatment with sodium hypochloride plus post-staining with dilute Lugol's stain (Gutmann, 1995) for general histology and detection of starch

1. Pre-treatment with a commercial solution of sodium hypochlorite, 10 s.
2. Rinse thoroughly with distilled water.
3. Staining with 0.05% Toluidine Blue *O*, 15 min.
4. Rinse thoroughly with distilled water.
5. Post-staining treatment with Lugol's stain (iodine/potassium iodide) diluted with distilled water 1:3 (v/v), 1 min.
6. Blow dry immediately with a brief blast of clean air.
7. Rinse briefly with distilled water.
8. Blow dry immediately with a brief blast of clean air.
9. Allow to dry at room temperature, 5 min.

Expected results – Phenolic droplets stain deep blue black. Cellulose walls and cytoplasm exhibit a brownish colour. Starch grains are displayed in blue-violet.

VIII. Sudan Black B (Bronner, 1975; Parham & Kaustinen, 1976) for detection of lipids and tannins

1. Staining with 0.3% Sudan Black B (w/v) in 70% ethanol*, in an oven at 60^{o}C, 1 h.
2. Rapid washing in 70% ethanol.
3. Washing in distilled water.

* The saturated alcoholic solution of the fat-solvent dye must be placed into a pre-heated oven at 60^{o}C for 24 h. Next day, the solution (while still hot) must be filtrated before it could be used.

Expected results – Lipids stain dark blue to black, tannin deposits stain brownish-orange and starch grains remain unstained.

IX. Vanillin – Hydrochloric Acid (Gardner, 1975) for detection of condensed tannins

1. Staining with 0.5% vanillin in 9% hydrochloric acid*, 10 min.
2. Examination using a light microscope putting a drop of 9% hydrochloric acid on the glass slide containing the sections.

* The staining solution must be prepared at the moment of use under magnetic agitation.

Expected results – Condensed tannins (leucoanthocyanins and catechins) appear cherry-red stained.

Negative control – Examination of preparations mounted with a drop of 9% hydrochloric acid.

X. DMB Reagent (adapted from Mace & Howell, 1974) for detection of condensed tannins

1. Staining with DMB reagent: 1% 2,4-dimethoxybenzaldehyde in 95% ethanol : 18% hydrochloric acid (1:1)*, 10 min.
2. Examination using a light microscope in a drop of the DMB reagent on the glass slide containing the sections.

* The staining solution must be prepared at the moment of use.

Expected results – Condensed tannins (leucoanthocyanins and catechins) appear pink stained.

XI. Iron (III) chloride (adapted from Johansen, 1940) for detection of phenolic compounds

1. Staining with 10% ferric trichloride, 1 h.
2. Washing in running water.

Expected results – Phenolic compounds stain intense green, purple, deep blue or black accordingly to their composition.

C. SEMI-THIN EPOXY RESIN SECTIONS OF FIXED FLOWERS

I. Specimens processing

1. Fixation with 2.5% glutaraldehyde in 0.1 M sodium phosphate buffer, pH 7.2, 12–16 h at 4^{o}C.
2. Rinsing in the fixative buffer, 3x20 min.

3. Post-fixation with 2% osmium tetroxide in 0.1 M sodium phosphate buffer, pH 7.2, 1 h at room temperature.
4. Washing in distilled water, 3x20 min.
5. 2% tannic acid in ultrapure water : 0.1 M sodium phosphate buffer, pH 7.2 (1:1), 30 min.
6. Washing in distilled water, 3x10 min.
7. Dehydration in a graded acetone series: 30%, 50%, 70%, 80%, 90%, 15 min each.
8. Absolute acetone, 3x20 min.
9. Propylene oxide, 3x20 min.
10. Infiltration with propylene oxide : Epon-Araldite Resin (3:1, 1:1 and 1:3), 12–16 h each.
11. Pure Epon-Araldite Resin, 3x1 h.
12. Embedding in pure Epon-Araldite Resin, 72 h in an oven at 60^{o}C.
13. Sectioning using an ultramicrotome (sections roughly 0.5 μm thick).

II. Epon-Araldite Resin (epoxy resin; Mollenhauer, 1964)

DDSA, dodecenyl succinic anhydride	50 ml
Embed-812 (Epon-812 substitute)	20 ml
Araldite 502	12 ml
BDMA, benzyldimethylamine	2.46 ml (equivalent to 3% added to the final volume at the moment of use the resin)

III. Sudan Black B (Bronner, 1975; Parham & Kaustinen, 1976) for detection of lipids and tannins

1. Staining with 0.3% Sudan Black B (w/v) in 70% ethanol*, in an oven at 60^{o}C, 60–90 min.
2. Rapid washing in 70% ethanol.
3. Washing in distilled water.

* The saturated alcoholic solution of the fat-solvent dye must be placed into a pre-heated oven at 60^{o}C for 24 h. Next day, the solution (while still hot) must be filtrated before it could be used.

Expected results – Lipids stain dark blue to black, tannin deposits stain brownish-orange and starch grains remain unstained.

TRANSMISSION ELECTRON MICROSCOPY

ULTRA-THIN EPOXY RESIN SECTIONS OF FIXED FLOWERS

I. Specimens processing

We used seven protocols of fixation/post-fixation (A, B, C, D, E, F, G) in order to achieve the most appropriate method for preservation of secretion in the osmophore.

A.

1. Fixation with 2.5% glutaraldehyde in 0.1 M sodium phosphate buffer, pH 7.2, 12–16 h at 4^{o}C.
2. Rinsing in the fixative buffer, 3x20 min.

B.

1. Fixation with 2.5% glutaraldehyde and 2% paraformaldehyde in 0.1 M sodium phosphate buffer, pH 7.2 (modified Karnovsky's fixative) 12–16 h at 4^{o}C.
2. Rinsing in the fixative buffer, 3x20 min.

C.

1. Fixation with 2.5% glutaraldehyde in 0.1 M sodium phosphate buffer, pH 7.2, 12–16 h at 4^{o}C.
2. Rinsing in the fixative buffer, 3x20 min.
3. Post-fixation with 2% osmium tetroxide in 0.1 M sodium phosphate buffer, pH 7.2, 1 h at room temperature.
4. Washing in distilled water, 3x20 min.

D.

1. Fixation with 2.5% glutaraldehyde in 0.1 M sodium phosphate buffer, pH 7.2, 12–16 h at 4^{o}C.
2. Rinsing in the fixative buffer, 3x20 min.
3. Post-fixation with 2% osmium tetroxide in 0.1 M sodium phosphate buffer, pH 7.2, with 0.1% caffeine (added to the final volume), 1 h at room temperature.
4. Washing in distilled water, 3x20 min.

E.

1. Fixation with 2.5% glutaraldehyde in 0.05 M sodium phosphate buffer, pH 7.2, 12–16 h at 4^{o}C.
2. Rinsing in the fixative buffer, 3x20 min.
3. Post-fixation with 1% osmium tetroxide in 0.05 M sodium phosphate buffer, pH 7.2, with 0.8% potassium ferricyanide (added to the final volume; Robards & Wilson, 1993), 2 h at room temperature.
4. Washing in distilled water, 3x20 min.

Following fixation (and post-fixation, when appropriate), the small portions of the *Ophrys* osmophores were processed as described below.

5. 2% tannic acid in ultrapure water : 0.1 M sodium phosphate buffer, pH 7.2 (1:1), 30 min.
6. Washing in distilled water, 3x10 min.
7. Dehydration in a graded acetone series: 30%, 50%, 70%, 80%, 90%, 15 min each.
8. Absolute acetone, 3x20 min.
9. Propylene oxide, 3x20 min.
10. Infiltration with propylene oxide : Epon-Araldite Resin (3:1, 1:1 and 1:3), 12–16 h each.
11. Pure Epon-Araldite Resin, 3x1 h.
12. Embedding in pure Epon-Araldite Resin, 72 h in an oven at 60^{o}C.
13. Sectioning using an ultramicrotome (sections 50–70 nm thick).

The next two protocols of fixation/post-fixation were used in combination with a slower impregnation procedure. Both were found to be the most appropriate methodology for preserving and embedding the osmophore tissues of *Ophrys* flowers.

F.

1. Fixation with 2% glutaraldehyde in 0.1 M cacodilate buffer, pH 7.2, 1–2 h under vacuum at room temperature followed by 16–20 h at 4^{o}C.
2. Rinsing in the fixative buffer, 3x20 min.
3. Post-fixation with 1% osmium tetroxide in the respective buffer, 1 h at room temperature.
4. Rinsing in the fixative buffer, 3x20 min.

G.

1. Fixation with 2.5% glutaraldehyde and 2% paraformaldehyde in 0.1 M sodium phosphate buffer, pH 7.2 (modified Karnovsky's fixative), 1–2 h under vacuum at room temperature followed by 16–20 h at 4^{o}C.
2. Rinsing in the fixative buffer, 3x20 min.
3. Post-fixation with 1% osmium tetroxide in the respective buffer, 1 h at room temperature.
4. Rinsing in the fixative buffer, 3x20 min.

Following fixation and post-fixation, the small portions of the *Ophrys* osmophores were processed as described below.

5. Dehydration in a graded acetone series: 30%, 50%, 70%, 80%, 90%, 15 min each.
6. Absolute acetone, 3x20 min.

7. Propylene oxide, 3x20 min.
8. Infiltration with propylene oxide : Epon-Araldite Resin (3:1, 1:1 and 1:3), 12–16 h each.
9. Pure epoxy resin, 10–12 h under vacuum, at 4°C.
10. Pure epoxy resin, 12–16 h, at 4°C.
11. Pure epoxy resin, 4 h, at room temperature.
12. Embedding in pure epoxy resin, 72–96 h in an oven at 60°C.
13. Sectioning using an ultramicrotome (sections 50–70 nm thick).

II. Epon-Araldite Resin (epoxy resin; Mollenhauer, 1964)

DDSA, dodecenyl succinic anhydride	50 ml
Embed-812 (Epon-812 substitute)	20 ml
Araldite 502	12 ml
BDMA, benzyldimethylamine	2.46 ml (equivalent to 3% added to the final volume at the moment of use the resin)

III. Formvar (after Robards & Wilson, 1993)

1. Shed 200 ml of chloroform (trichloromethane) into a very-well dehydrated large-mouth glass flask.
2. Add 0.77 g of formvar (polyvinyl formal) and let the powder dissolve slowly in the solvent for 3–4 days without any agitation, in the darkness.
3. Coat cupper grids with membranes made of this solution of 0.385% (w/v) formvar in chloroform.

IV. Positive staining of ultra-thin sections

1. Filter and centrifuge staining solutions for 15 min at high speed immediately before use them.
2. Submerge grids with ultra-thin sections in a saturated absolute methanolic solution of uranyl acetate (Stempak & Ward, 1964), 8–10 min.
3. Rapidly dip each grid several times in 2 changes of absolute methanol, then in 50% methanol in CO_2-free water.
4. Wash the grids with jets of CO_2-free water from a plastic wash bottle.
5. Allow grids to dry on a filter paper for some minutes.
6. Place single drops of 0.4% lead citrate in CO_2-free water with 1% sodium hydroxide 10N on a Petri dish containing a dental wax-coated bottom and an amount of sodium hidroxide pellets sufficient to scavenge any carbon dioxide from the air of the staining chamber.
7. Float each grid, section side down, on each single drop of lead citrate stain for 15–17 min.
8. Wash immediately the grids with jets of CO_2-free water.

9. Place the grids on a filter paper and allow them to dry prior to examination in a transmission electron microscope.

V. Developing of the film

1. Introduction of the unprocessed black-and-white negative film (6.5 x 9 cm) into the film-holders, inside a darkroom, in total darkness.
2. Development of the film with the D-19 Kodak professional developer for 5 min, with continuous agitation during the first 30 s and intermittent agitation of 5 s every 30 s, keeping temperature around 18–24^{o}C.
3. Rinsing of the film in a stop bath for 1 min, with vigorous agitation during the first 15 s.
4. Fixation of the film with a fixer for 30 min, with frequent agitation.
5. Washing of the film in running water for 30 min. Add some droplets of detergent at the end of the washing period and continue washing until removing most part of the foam.
6. Drying of the film in a dust-free dryer for 30 min.

REFERENCES

Bronner R. 1975. Simultaneous demonstration of lipids and starch in plant tissues. *Stain Technology* **50:** 1-4.

David R, Carde JP. 1964. Coloration diférentielle des inclusions lipidiques et terpeniques des pseudophylles du *Pin maritime* au moyen du reactif Nadi. *Comptes Rendus de l'Académie des Sciences* **258:** 1338-1340.

Feder N, Wolf MK. 1965. Studies on nucleic acid metachromasy. II. Metachromatic and orthochromatic staining by toluidine blue of nucleic acids in tissue sections. *The Journal of Cell Biology* **27:** 327-336.

Feder N, O'Brien TP. 1968. Plant microtechnique: some principles and new methods. *American Journal of Botany* **55:** 123-142.

Fuchs C. 1963. Fuchsin staining with NaOH clearing for lignified elements of whole plants or plant organs. *Stain Technology* **38:** 141-144.

Gabe M. 1968. *Techniques histologiques.* Paris: Masson & Cie.

Ganter P, Jollès G. 1969. *Histologie normale et pathologique. Volume 1.* Paris: Gauthier-Villars.

Gardner RO. 1975. Vanillin-hydrochloric acid as a histochemical test for tannin. *Stain Technology* **50:** 315-317.

Gutmann M. 1995. Improved staining procedures for photographic documentation of phenolic deposits in semithin sections of plant tissue. *Journal of Microscopy* **179:** 277-281.

Harborne JB. 1998. *Phytochemical methods: a guide to modern techniques of plant analysis.* 3rd ed. London: Chapman & Hall.

Johansen DA. 1940. *Plant microtechnique.* New York: McGraw-Hill.

Kirk PW. 1970. Neutral red as a lipid fluorochrome. *Stain Technology* **45:** 1-4.

Kraus JE, Arduin M. 1997. *Manual básico de métodos em morfologia vegetal.* Rio de Janeiro: Editora da Universidade Rural.

Mace ME, Howell CR. 1974. Histochemistry and identification of condensed tannin precursors in roots of cotton seedlings. *Canadian Journal of Botany* **52:** 2423-2426.

Mollenhauer HH. 1964. Plastic embedding mixtures for use in electron microscopy. *Stain Technology* **39:** 111-114.

O'Brien TP, Feder N, McCully ME. 1964. Polychromatic staining of plant cell walls by toluidine blue *O*. *Protoplasma* **59:** 368-373.

Parham RA, Kaustinen HM. 1976. Differential staining of tannin in sections of epoxy-embedded plant cells. *Stain Technology* **51:** 237-240.

Pearse AGE. 1985. *Histochemistry: theoretical and applied. Volume 2, Analytical technology.* 4th ed. Edinburgh: Churchill-Livingstone.

Robards AW, Wilson AJ. 1993. Procedures in electron microscopy. Chichester, West Sussex, England: John Wiley & Sons Ltd.

Shobe WR, Lersten NR. 1967. A technique for clearing and staining gymnosperm leaves. *Botanical Gazette* **128:** 150-152.

Stempak JG, Ward RT. 1964. An improved staining method for electron microscopy. *The Journal of Cell Biology* **22:** 697-701.

Vogel S. 1990. *The role of scent glands in pollination: on the structure and function of osmophores.* Rotterdam: A. A. Balkema. [English translation of: Vogel S. 1963. Duftdrüsen im Dienste der Bestäubung: Über Bau und Funktion der Osmophoren. *Akademie der Wissenschaften und der Literatur in Mainz, Abhandlungen der Mathematisch-Naturwissenschaftlichen Klasse* **10**: 600-763].